Undergraduate Lecture Notes in Physics

Ken'iti Kido

Digital Fourier Analysis: Fundamentals

Springer

Undergraduate Lecture Notes in Physics

For further volumes:
http://www.springer.com/series/8917

Undergraduate Lecture Notes in Physics (ULNP) publishes authoritative texts covering topics throughout pure and applied physics. Each title in the series is suitable as a basis for undergraduate instruction, typically containing practice problems, worked examples, chapter summaries, and suggestions for further reading.

ULNP titles must provide at least one of the following:

- An exceptionally clear and concise treatment of a standard undergraduate subject.
- A solid undergraduate-level introduction to a graduate, advanced, or non-standard subject.
- A novel perspective or an unusual approach to teaching a subject.

ULNP especially encourages new, original, and idiosyncratic approaches to physics teaching at the undergraduate level.

The purpose of ULNP is to provide intriguing, absorbing books that will continue to be the reader's preferred reference throughout their academic career.

Series editors

Ken'iti Kido

Digital Fourier Analysis: Fundamentals

Springer

Ken'iti Kido
Yokohama-shi
Japan

Additional material to this book can be downloaded from http://extras.springer.com/

ISSN 2192-4791 ISSN 2192-4805 (electronic)
ISBN 978-1-4614-9259-7 ISBN 978-1-4614-9260-3 (eBook)
DOI 10.1007/978-1-4614-9260-3
Springer New York Heidelberg Dordrecht London

Library of Congress Control Number: 2014940159

Title of the Japanese edition: ディジタルフーリエ解析 1 基礎編—published by CORONA PUBLISHING CO., LTD—Copyright 2007

Printed on acid-free paper

Springer is part of Springer Science+Business Media (www.springer.com)

Preface

Fourier analysis is one method of investigating the origin of functions and their properties by using Fourier series and Fourier transform(s). The Fourier series and Fourier transforms were introduced by the mathematician Jean Baptiste Joseph Fourier at the beginning of the nineteenth century; they are widely applied in the engineering and science fields. One-dimensional waveforms (as functions of time or position) and two-dimensional images (as functions of two positional axes) are the main subjects studied nowadays using Fourier analysis. Fourier analysis is an important method used to analyze complex sound waveforms in the field of acoustical engineering. This is the reason why this book was originally listed in the series of books published by the Acoustical Society of Japan. However, since Fourier analysis is also applicable in many other engineering sciences, these two books, *Digital Fourier Analysis: Fundamentals, and Digital Fourier Analysis: Advanced Techniques*, are useful to readers in broader fields.

The Fourier transform itself does not fit well with analog processing because it requires too much numerical processing, such as multiplications and summations. That is the reason waveform analysis during the analog age could not make full use of the Fourier method of analysis. Fourier analysis was more valuable as the basis of theoretical analysis than for its practical applications during the analog era. However, the digitally processed Fourier transform became a reality with the emergence of the digital computer in the middle of the twentieth century. The later development of the Fast Fourier transform (FFT) algorithm in 1965 and the subsequent inventions of microchips for signal processing accelerated the application of Fourier analysis based signal processing.

In the twenty-first century, Fourier analysis technology is widely used in our daily activities, and as a natural consequence, the technology is "hidden in a black box" in most of its applications. Even experts in the field use this technology without knowing details of how Fourier techniques are implemented. However, engineers, who wish to play important roles in developing future technologies, must do more than just deal with black boxes. Engineers must understand the basis of the present Fourier technology in order to create and build up new technologies based on it.

This book is intended so that high-school graduates or first or second grade college students with the basic knowledge of mathematics can learn the Fourier analysis without too much difficulty. In order to do that, explanations of equations

start from the very beginning and details of derivation steps are also described. This is very rare for this kind specialized book.

This book also deals with advanced topics so that engineers who are presently involved in signal processing work can get hints to solve their own specific problems. Ways of thinking that lie behind or lead to theories are also described, that are a must to apply theories to practical problems.

This work comprises two volumes. Seven chapters are included in Volume I, titled "Digital Fourier Analysis: Fundamentals." Volume II, titled "Digital Fourier Analysis: Advanced Techniques" contains six chapters. As the titles indicate, more advanced topics are included in Volume II. In this sense, the former may be classified as a text for undergraduate course and the latter for graduate course. Notice, however, that Volume I includes some advanced topics, whereas Volume II contains necessary items needed for a better understanding of Volume I.

Following are a brief explanation of each chapter. First, the contents of Volume I are briefly described.

Chapter 1 commences with an explanation of the impulse as being the limit of the summation of cosine waves with ascending frequencies. This chapter shows that all waveforms can be synthesized by the use of Fourier series, i.e. that sine and cosine waves are the basis of waveform analysis. It then gives a geometric image to Euler's formula by explaining that the projections of a constantly rotating vector around the origin of the rectangular coordinate system onto their real and imaginary axes are the cosine and sine functions, i.e. the real and imaginary parts of a complex exponential function, respectively. The reader will be naturally guided to the concepts of instantaneous phases and instantaneous frequencies through this learning.

Chapter 2 starts with the theory on how to determine coefficients of the Fourier series of a periodic function. It investigates the properties of the Fourier series, showing why high order coefficients are needed for the waveform synthesis and what kind of properties the Fourier series of even and odd function waveforms have. Then, it shows that the Fourier series expansion becomes the Fourier transform pair when the period is made infinitely large.

Chapter 3 deals with the problems encountered when one tries to express a continuous waveform by a sequence of numbers in order to numerically compute the Fourier transform. For that purpose, it investigates the most important issue in digitization: how to handle the sampling time based on the knowledge of the Fourier series; and guides the reader automatically to the sampling theorem. Then the relation between a continuous waveform and the discrete numerical sequence, which is the sampled version of the waveform, is discussed.

Chapter 4 guides you to the definition of the discrete Fourier transform (DFT) and the inverse Discrete Fourier transform (IDFT). The DFT transforms a numerical sequence with a finite length to another numerical sequence with the same length, and the IDFT transforms the latter sequence back to the former sequence. Then this chapter clarifies that these sequences are periodic and they have the length (data number) of the sequence as their periodicity. For later applications, the Discrete Cosine transform (DCT) is derived from basic concepts.

The DCT describes the relationship between time domain and frequency domain functions using only cosine functions.

Chapter 5 explains a principle of the FFT which drastically decreases the number of multiplications and summations required in the computation of the DFT. The FFT is an innovative numerical calculation method which has greatly expanded the range of application of Fourier analysis.

Chapter 6 discusses several items such as: (1) properties of the spectrum given by the DFT of a *N*-sample sequence (waveform) taken from a long chain of data; (2) its relation with the spectrum of the original data; (3) the relationship between sampling time and frequency resolution, and (4) a reason why new frequency components that do not exist in the original waveform are produced by the DFT; and so on.

Chapter 7 studies details of various weighting functions (time windows) applied to waveforms in order to obtain stable and accurate spectra (frequencies and amplitudes) by the DFT approach.

The explanation of Volume I ends here. But, as recognized by readers, the description is much insufficient for the use of Fourier Analysis in the practical applications. More knowledge described in Volume II will be required for deep understanding the descriptions of Volume I and for the application of Fourier analysis to wide area.

Chapter 1 of Volume II guides the reader through the use of a convolution of two sequences to be calculated from an input and the system's impulse response. It becomes clear that the Fourier transform of a convolution can be expressed as the multiplication of the two respective Fourier transforms, and this leads to the exploration of a new way that a convolution in the time domain can be calculated in the frequency domain. Since an issue based on DFT periodicity is raised at this time, this chapter discusses the issue and explains in detail how to obtain the correct result.

In Chap. 2, the correlation function that quantitatively expresses the degree of similarity between two time sequences is derived. The difference between the correlation and convolution functions is that the directions of the time axes of one of two time sequences in the process of multiplication and summation calculation are opposite with each other. The Fourier transform of the correlation function of two time sequences is given as a cross-spectrum of the two functions in the frequency domain, which will be discussed in the next chapter.

Chapter 3 introduces a Cross-spectrum method that uses multiplication of spectra. The Cross-spectrum technique is a powerful method for uncovering an original function as an inverse process based on the convolution or the correlation function. This is a good example of the DFT's usefulness. DFT periodicity is the most important factor. This chapter illustrates the kind of problems related to Cross-spectrum analysis, and discusses how to avoid errors, by taking advantage of periodicity.

Chapter 4 introduces the concept of a Cepstrum which is defined as a Fourier transform of the logarithm of a spectrum. This useful method of analysis is based on a little quirky idea. Cepstrum analysis is a powerful method of signal analysis

for detecting hidden information that is not visible from the Fourier transform of a time domain signal.

Chapter 5, at first, analyzes the problem that occurs when a waveform is depicted as a rotating vector in order to obtain its envelope. Since an orthogonal waveform of the original waveform is needed to get a rotating vector, the question of how to derive the orthogonal function in the frequency region is discussed. The calculation of the orthogonal function in the time region by applying the inverse Fourier transform to the orthogonal function in the frequency region results in the Hilbert transform. While the Hilbert transform is a demodulation of the amplitude-modulated wave to get an envelope as a length of rotating vector, it is, also, a demodulation of the frequency-modulated wave, producing an instantaneous frequency which is the rotating speed of the vector.

Chapter 6 touches upon two-dimensional DFT and DCT methods. At first, a definition of the two-dimensional DFT is given. When the reader tries to obtain two-dimensional spectra of images with basic patterns, one can easily guess its output from the relation between the one-dimensional waveform and its spectrum. The reader will understand that one-dimensional Fourier transform procedure is an important base. By showing definitions of DCT and samples of two-dimensional DCT spectra of simple images, the concept of how the information compression by DCT takes place will be explained with concrete examples.

One of the features of this book is that it contains a number of figures that have an interactive supplement. (The supplementary files can be downloaded from http://extras.springer.com). Figures with this feature are indicated by their caption, which includes the file name of the corresponding animation file. To view the animation, click the corresponding exe file to start the program, and then click the green "start" button after data input and/or selection of conditions. Then the program starts the calculation based on the theory, input data, and conditions. The reader may see unexpected results occasionally. As they have their own causes or reasons, it will be worthwhile for the reader to think of them for a deeper understanding. Note that the programs are written in Visual Basic and may not work on all computers.

I would like to emphasize the following through my long experience as a writer of this book and also as a user of this book in my classes and other lectures. The reader will lose more than he/she earns if he/she prematurely thinks that he/she has understood one topic after running a related program and briefly looking at the result. The reader must run programs with various data and conditions and look at the corresponding results and then he/she must think how they are related with each other. With the attached programs, the reader can do these easily while having some fun.

Very few references are listed at the end of this book compared to the contents of this book. This is because most of the theories are described from the beginning, and as a result this book became self-contained. Theory-oriented readers should refer to books such as [4]–[9] in Reference. Since the Fourier analysis techniques are developing day by day, the readers should refer to current journals in the related area.

Finally, although I would like to express my sincere appreciation to all those who gave me tremendous encouragement and cooperation to write this book, I must apologize that I cannot list up all of their names. My excuse is that so many people assisted me in writing this book.

This book, originally published in Japanese, was translated first by Dr. Hideo Suzuki, a former professor of Chiba Institute of Technology, Mr. Jin Yamagishi, a technology management consultant of JINY Consultant Inc., and myself, and then, very carefully checked and corrected by Dr. Harold A. Evensen of Michigan Technological University in USA and Dr. Leonard L. Koss of Monash University in Australia.

I would like to express my sincere appreciation to all of those who contributed to publishing this book.

February 2013 Ken'iti Kido

Contents

Chapter 1
Sine and Cosine Waves

All time waveforms that occur can be synthesized by sine and/or cosine waves.* Even the ideal impulse function, which is an idealized time history, can be expressed in a mathematical limit as the sum of sine and/or cosine waves. Waveforms that can be observed are approximated by the sum of a finite number of the sine and/or cosine waves and the accuracy of the approximation is improved as the number of sine and/or cosine waves increases. Thus, understanding of the role of sine and cosine waves is of great importance as the basis of the waveform (signal) analysis. First, it will be demonstrated that various waveforms are synthesized by the sum of sine and/or cosine waves. Then, the property of sine and cosine waves will be examined.

The terms given by $\sin(2\pi ft)$ and $\cos(2\pi ft)$ are defined as sine and cosine waves (or functions), respectively, where f is frequency. Hz, and t is time, s. Occasionally, the term "sine wave" is used to imply both sine and cosine waves.

1.1 Synthesis of an Impulse by Cosine Waves

All real waveforms are composed by adding sine and/or cosine waves; this will be demonstrated using the case of an impulse time history.

The left-hand side chart of Fig. 1.1 shows cosine waves with $t = 0$ at the center of the horizontal time axis. All waveforms take the value 1 at $t = 0$ except for the dc (direct current) component, which is equal to 0.5. The first ac (alternating current) or fluctuating component has the frequency f, the second component $2f$, the third $3f$, and so on. The n-th curve from the top of the right-hand side chart shows the synthesized waveforms using up to the n-th component starting from the dc (0-th order). The value of the synthesized waveform at $t = 0$ increases monotonically as the number of the components increases. At times other than $t = 0$ and its vicinity, the values alternate between 1 and -1. Since always the higher frequency (i.e., shorter time period) components are added one by one, the amplitude cannot increase except in the vicinity of $t = 0$. As a result, as the number of added

K. Kido, *Digital Fourier Analysis: Fundamentals*,
Undergraduate Lecture Notes in Physics, DOI: 10.1007/978-1-4614-9260-3_1,

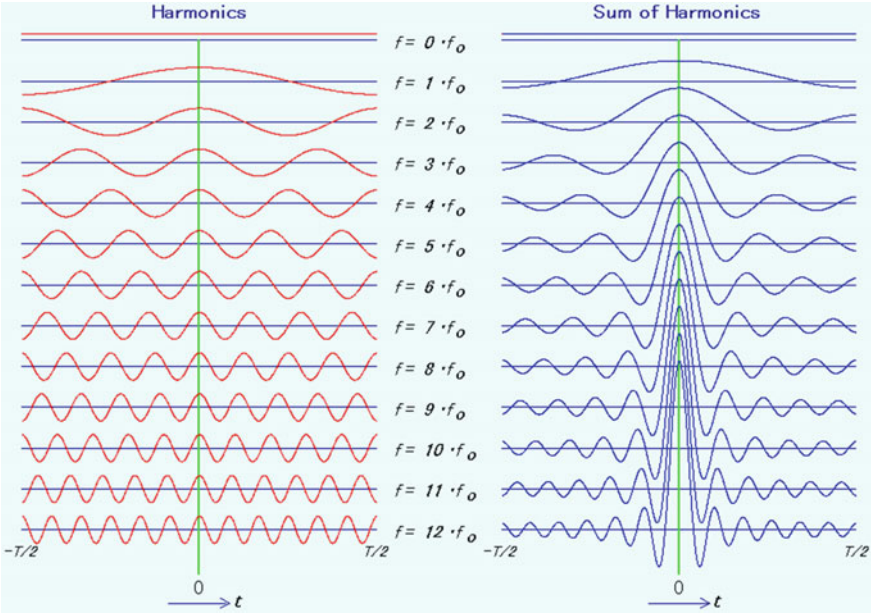

Fig. 1.1 Synthesis of an impulse by adding cosine harmonics with matched phases (zero initial phases). Animation available in supplementary files under filename E1-01_PP.exe

components increases, the values around $t = 0$ get larger and larger, and the width of the "spike" gets narrower and narrower.

From the above discussion, we can say that the synthesized waveform composed of an infinite number of cosine waves (components) becomes an impulse, which has an infinitely large height and an infinitesimally narrow width.

1.2 Synthesis of Rectangular Waveforms by Sine and Cosine Waves

Since a waveform such as the impulse function can be synthesized by sine and cosine functions, it is natural to consider that other waveforms can be synthesized in a similar manner.

The accuracy of a synthesized rectangular wave increases as the number of cosine waves increases in the summation and this is shown in Fig. 1.2. The left-hand side chart shows added waveforms from the 1st component, up to the 9th order component. Figure 1.2 shows that the synthesized waveform (thick line) approaches the target waveform (thin line) as the number of the added components increases. The period of the "1st" order cosine wave is the same as the period of the rectangular wave. The 2nd, 3rd, …, and n-th order cosine waves have the

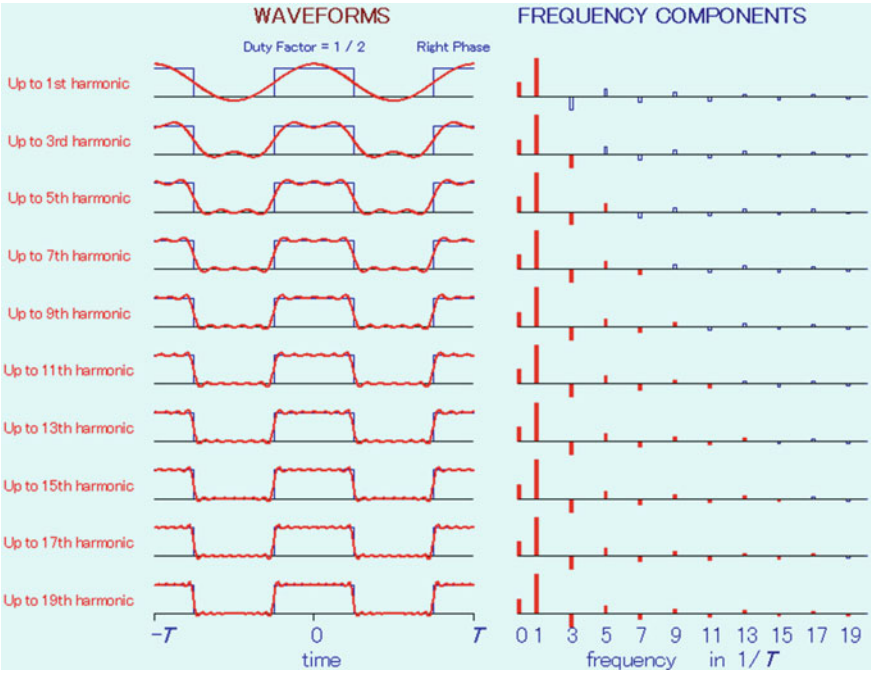

Fig. 1.2 Process of synthesizing a rectangular wave by adding cosine waves with matched phases (zero initial phases). Animation available in supplementary files under filename E1-02_Rectangle.exe

periods of 1/2, 1/3, …, and 1/*n* of the 1st order component. The 0th order is the dc component. Figure 1.2 clearly shows that the rectangular wave can be synthesized by cosine waves.

The right-hand chart shows the size of the individual components that are necessary to compose the rectangular wave. The filled bars represent the added components and the empty bars represent un-added components. The upward and downward bars indicate positive and negative amplitudes of the components, respectively. The positions of the bars on the horizontal axis correspond to their frequencies. Note that the even order frequency components are not necessary in order to compose the rectangular wave shown in Fig. 1.2.

The third row of the left-hand side chart shows the waveform that contains components up to the 5th harmonic of the square wave as can be seen from the same row of the right-hand-side chart. As the order of the added components (indicated by the filled bars) increases, the synthesized waveform approaches that of the rectangular waveform. Each component of a waveform is called a "*spectrum*." In the present case, the spectrum is not continuous and has an infinitely narrow band and, therefore, it is called a "*line spectrum*." If the waveform is periodic, the wave consists of only line spectra. If the waveform is symmetric with

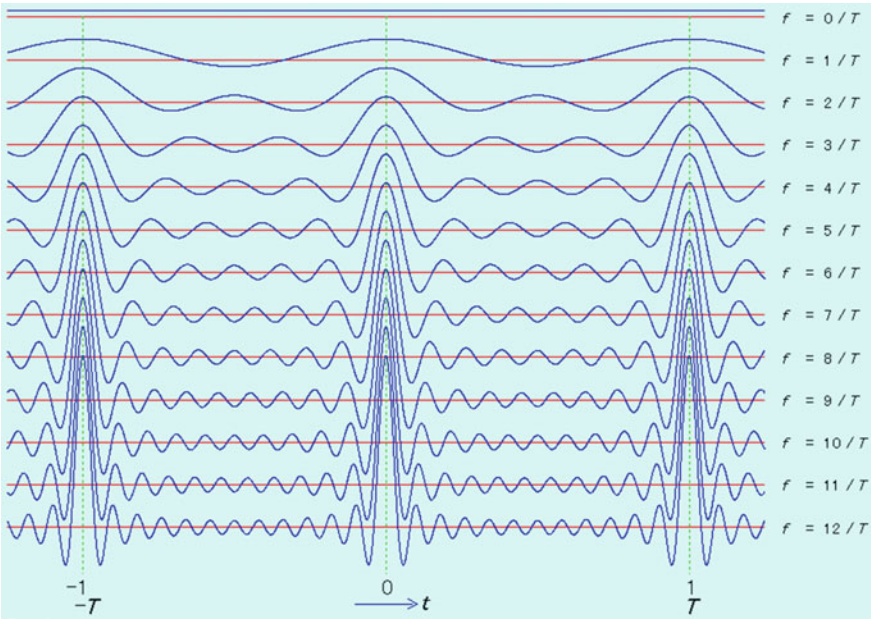

Fig. 1.3 Synthesis of series of impulses with period T by adding cosine waves with period T and its harmonics with matched phases (zero initial phases). Animation available in supplementary files under filename E1-03_PeriodicImpulse.exe

respect to the origin of the time axis, it comprises only cosine waves. If the waveform is rotationally symmetric, it comprises only sine waves. In general, any waveform consists of sine and/or cosine waves.

1.3 Time Period

In Fig. 1.2, one half of a rectangle appears on either side of the wave. This indicates that an infinite number of rectangles may appear with the period T on the time axis. Other impulses in Fig. 1.1 are not observed simply because only the range of the time axis from $-T/2$ to $T/2$ is shown, where T is the time period of the cosine wave of the lowest order. Figure 1.3 shows the time axis in the range slightly larger than the twice the period of the lowest order cosine wave. Now, three impulses are visible, with the separation between them equal to the period of the lowest order cosine wave.

From the above discussion, we can say that any wave that comprises the 1st and higher order components is periodic with the period equal to the period of the 1st order component. For this reason, the sine and/or cosine waves with the period equal to that of the periodic wave is called the *fundamental* (component) and other

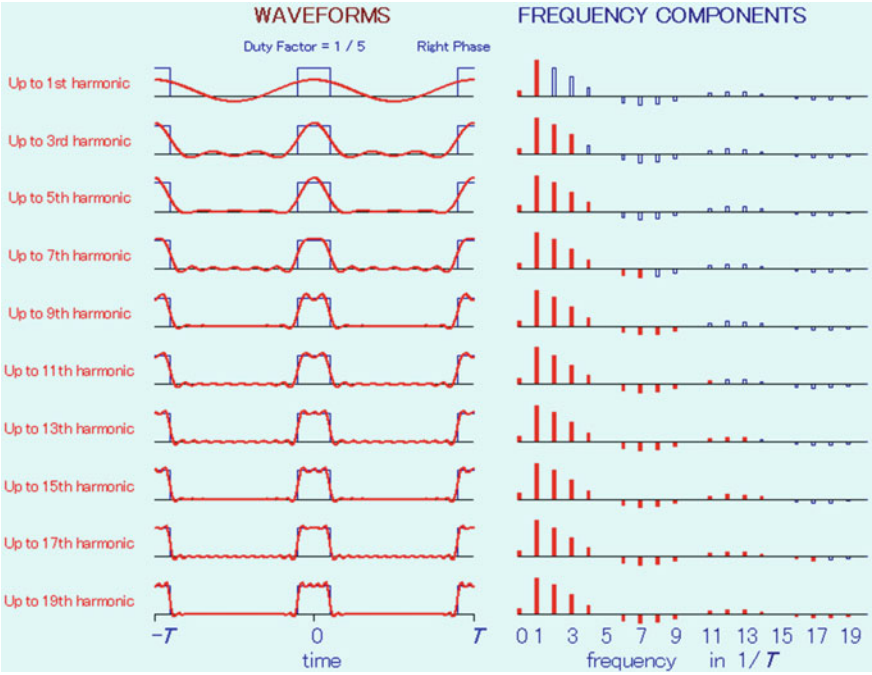

Fig. 1.4 Process of synthesizing a rectangular pulse with a short duration by adding harmonic cosine waves. Animation available in supplementary files under filename E1-04_Rectangle.exe

components with frequencies equal to the integer multiples of the fundamental are called *harmonics.*

In order to synthesize a wave with only one impulse in the infinite time length, T (the period of the fundamental component) must be made infinite. However, it is not necessary to deal with an infinitely long wave for practical applications. A single event wave such as an impulse can be analyzed by assuming that the wave is periodic, with period long enough to separate the events so that they do not interact with each other.

1.4 Harmonics and Waveforms

The rectangular wave shown in Fig. 1.2, which is 1 during half of the period and 0 during the other half of the period, with the center of the rectangle on the origin of the time axis, is composed only of odd order harmonics. If the durations are not equal, even-order harmonics are also necessary. The rectangular wave in Fig. 1.4, which is 1 only during 1/5 of the period, requires more harmonics than the one in Fig. 1.2. The graphical representation of Fig. 1.4 is the same as the one in Fig. 1.2.

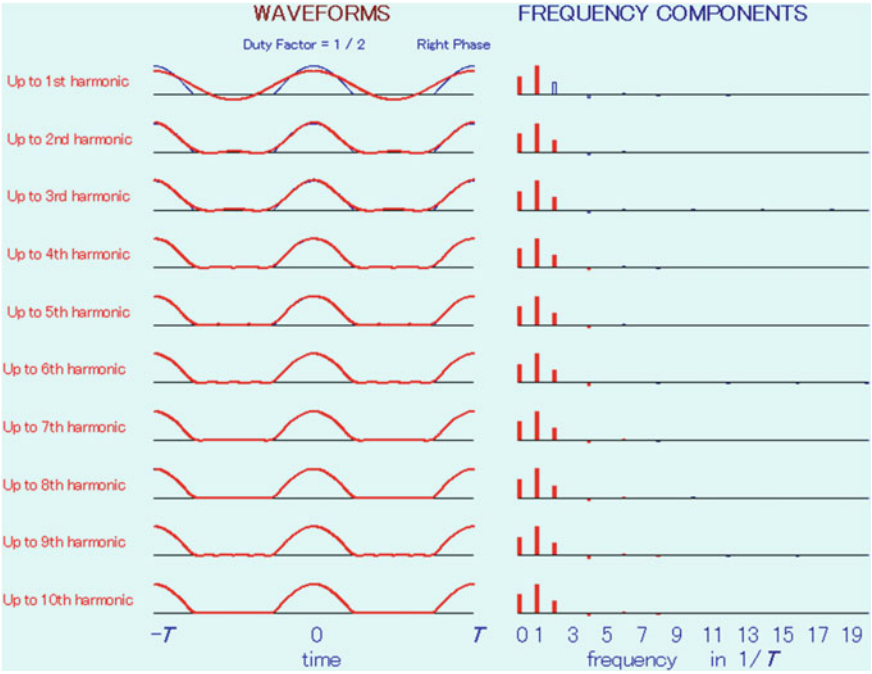

Fig. 1.5 Synthesis of a half-wave rectified sine wave. Note the rapid approach to the target waveform. Animation available in supplementary files under filename E1-05_HalfSine.exe

However, it looks quite different in the way that the harmonics up to 4th are positive, and those from the 6th to 9th are negative. The pulses in Fig. 1.4 are shorter than in Fig. 1.2, indicating that the former changes more rapidly than the latter. A wave that changes rapidly contains more harmonics than a wave that changes more slowly.

The extreme case of the short pulse is the impulse. In this case, the amplitudes of harmonics are frequency independent as seen in Fig. 1.1. On the contrary, a half-sine wave shown in Fig. 1.5 is approximated well with a small number of low-order harmonics. As the second waveform from the top shows, the difference between the thin line (half-sine wave) and the thick line (approximation) is very small. Even when the third harmonic is added, the thick line does not change much (see the third waveform from the top).

Figure 1.6 shows one example of a saw-tooth waves which has a vertical sharp edge indicating that it needs a lot of harmonics for a good approximation. This is a general property of the waveform synthesis.

The waveform shown in Fig. 1.6 is different from those shown in Figs. 1.1, 1.2, 1.3, 1.4 and 1.5. The saw-tooth wave shown in Fig. 1.6 is anti-symmetric with respect to $t = 0$ (magnitudes at $t = -t_0$ and t_0 are equal but their signs are opposite), while the waveforms shown in Figs. 1.1, 1.2, 1.3, 1.4 and 1.5 are symmetric (values at $t = -t_0$ and t_0 are equal). The symmetric waveforms can be synthesized

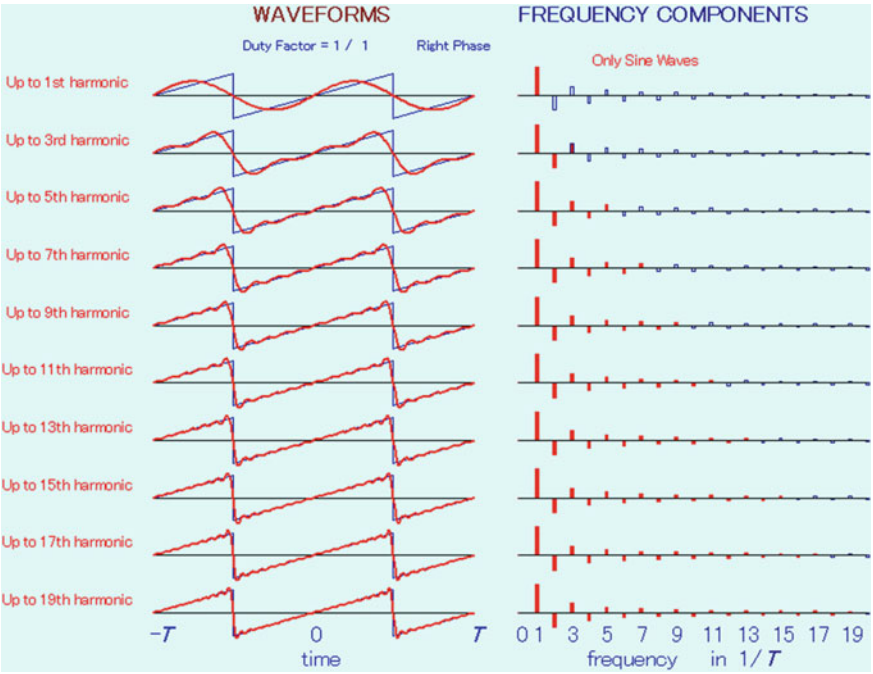

Fig. 1.6 Process of synthesis of a saw-tooth wave by adding only sine harmonics. Animation available in supplementary files under filename E1-06_SawTooth.exe

with only symmetric cosine waves, whereas the anti-symmetric waveforms can be synthesized only with anti-symmetric sine waves.

The programs used to draw Figs. 1.1, 1.2, 1.3, 1.4, 1.5 and 1.6 are attached to this book. Each program will run if the user clicks the figures in the PowerPoint slides. Conditions of the waveform synthesis can be varied and their effects on the waveform can be observed. Experience of synthesizing various waveforms will help the reader to better understand the relations between the waveforms and their spectra.

Let us summarize the terminology used thus far. The waveforms in Figs. 1.1, 1.2, 1.3, 1.4, 1.5 and 1.6 are periodic with *period T*, and their components are sine and cosine waves. Among them, the sine and cosine waves with period *T,* i.e., with frequency f_0 (= 1/*T*) are the *fundamental* waves. The frequency f_0 is the *fundamental frequency*. The waves with integer multiples of the fundamental frequency f_0 are the 2nd, 3rd, … *harmonics*. Every periodic waveform is synthesized by a combination of the fundamental and the harmonics. Higher harmonics are necessary in order to compose waveforms with sharper edges. Since the fundamental wave and harmonics are sine and cosine waves of the corresponding frequencies, they are also referred to as *frequency components* or *frequency spectra*. The periodic waves are composed only with harmonics with multiple integers of the fundamental frequency. They are indicated by lines as shown in the right-hand side chart of Fig. 1.2. These components are called *line spectra*.

1.5 Fourier Series

So far, we have used only figures to explain the synthesis concept so that the readers can grasp intuitive physical images of waves and their constituents. It is now necessary to use equations for further development.

Figures 1.1 and 1.3 show that the impulse is synthesized by adding an infinite number of cosine waves with equal amplitudes. This is expressed by the following equation:

$$\delta(t) = 0.5 + \cos(2\pi\frac{1}{T}t) + \cos(2\pi\frac{2}{T}t) + \cos(2\pi\frac{3}{T}t) + \cdots \tag{1.1}$$

The constant 0.5 on the right-hand side can be considered a cosine wave with frequency 0. The second term is the fundamental component with the period T. Therefore, if T is made large, the distances between impulses become large and the fundamental frequency becomes small. At the limit of T going to infinity, the fundamental frequency becomes zero and there exists only one impulse in the infinite time span.

Expressing a periodic waveform by the fundamental and harmonics is referred to as *a Fourier series expansion*. The coefficient (amplitude) of each component is referred to as a *Fourier coefficient*. The line spectra introduced at the end of Sect. 1.2 are one example of Fourier coefficients.

In general, a periodic wave $x(t)$ with the period T can be expressed by the summation of cosine and sine waves with frequencies that are integer multiples of the fundamental frequency $1/T$.

$$\begin{aligned} x(t) &= A_0 + A_1\cos(2\pi\frac{1}{T}t) + A_2\cos(2\pi\frac{2}{T}t) + A_3\cos(2\pi\frac{3}{T}t) + \cdots \\ &\quad + B_1\sin(2\pi\frac{1}{T}t) + B_2\sin(2\pi\frac{2}{T}t) + B_3\sin(2\pi\frac{3}{T}t) + \cdots \\ &= A_0 + A_1\cos(2\pi f_0 t) + A_2\cos(4\pi f_0 t) + A_3\cos(6\pi f_0 t) + \cdots \\ &\quad + B_1\sin(2\pi f_0 t) + B_2\sin(4\pi f_0 t) + B_3\sin(6\pi f_0 t) + \cdots \end{aligned} \tag{1.2}$$

where A_n and B_n (n = 1, 2, 3, …) are the Fourier coefficients. The component A_0 with zero frequency is a constant and therefore it is referred to as the *DC* (*direct current*) component; it represents the average value of the waveform over the period. The method of Fourier expansion will be introduced in Chap. 2.

The fundamental frequency f_0 (= $1/T$) becomes infinitely small as the period T becomes infinitely large as a limit value. In this case, the components are distributed continuously on the frequency axis, and the spectrum is called a *continuous spectrum*.

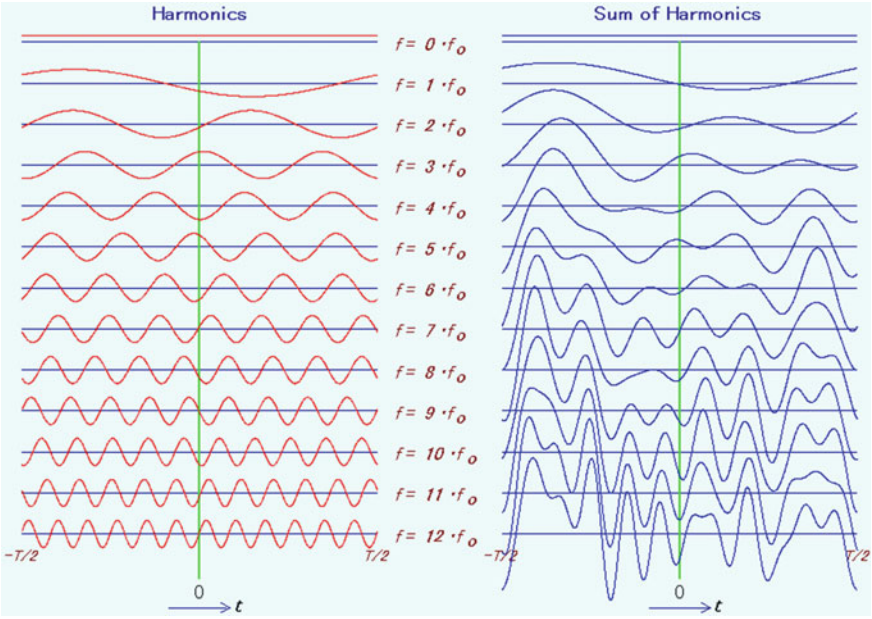

Fig. 1.7 Impulse waveform change due to random phase of harmonics used to synthesize the waveform. Cosine waves have the same magnitudes as those given in Fig. 1.1, but they are randomly shifted on the time axis. Animation available in supplementary files under filename E1-07_PP.exe

1.6 Shift of Harmonics on the Time Axis

We considered only the amplitudes of harmonics in the previous sections. However, if the harmonics are each shifted on the time axis, the synthesized waveform is changed.

For example, as shown in Fig. 1.7, if we shift the harmonics randomly (within $\pm$ $T/2$) on the time axis, the composed waveform becomes quite different from the impulse shown in Fig. 1.1.

The composed waveform always changes if the harmonics are shifted on the time axis. Fig. 1.8 shows the case when the harmonics in Fig. 1.2 are shifted randomly within $\pm$ $0.2T$. As these two cases show, the waveform is always affected by the relative time shifts of harmonics from the fundamental component.

The waveforms shown in Figs. 1.1, 1.2, 1.3, 1.4 and 1.5 are symmetric with respect to t, i.e., $x(t) = x(-t)$, and therefore, they are composed only by cosine waves. In contrast, the anti-symmetric waveforms, which have the property $x(t) = -x(-t)$, are composed only of sine waves. In general, any waveform can be expressed by the summation of sine and cosine waves as shown by Eq. (1.2). Now, let us look at the contributions of sine and cosine components to a rectangular wave whose center is shifted in time from $t = 0$.

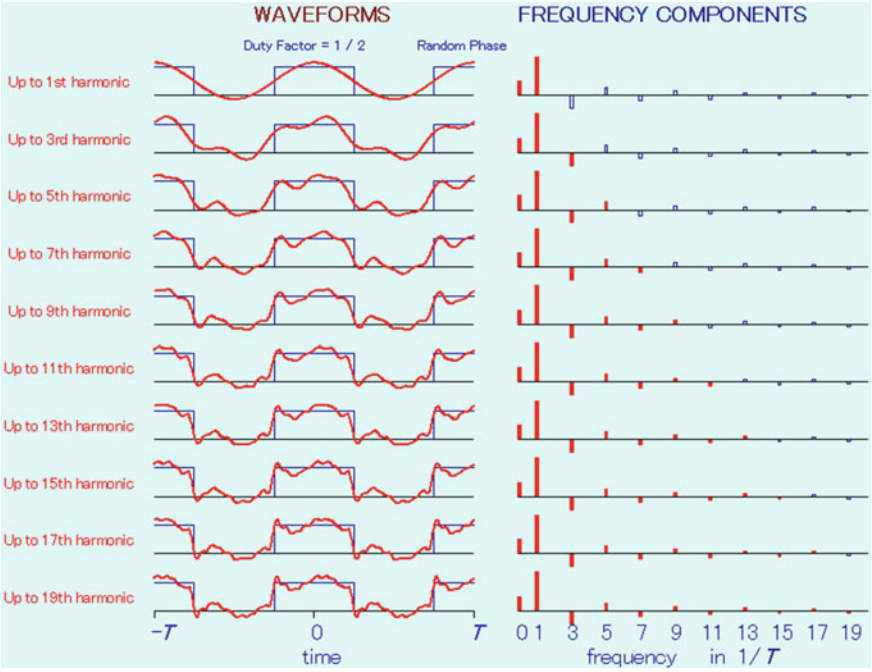

Fig. 1.8 Process of synthesizing a rectangular wave by adding cosine waves. Cosine waves have the same magnitudes as those in Fig. 1.2, but they are randomly shifted on the time axis within $\pm$ 0.2T. Animation available in supplementary files under filename E1-08_Rectangle.exe

The two center columns of Fig. 1.9 are the Fourier cosine (left) and sine (right) coefficients of each order (A_n and B_n in Eq. 1.2). Those of the 0th order (dc component) are 0.692 and 0, respectively. Those of the 1st order (fundamental) component are 1 and 0.509, respectively. The left-hand side of Fig. 1.9 shows the waveforms of the cosine (solid lines) and sine (dotted lines) components added up to 0th, 1st, 2nd, … to 15th orders. The solid lines are always symmetric and the dotted lines are always anti-symmetric. The right-hand side of Fig. 1.9 shows the added waveforms of the cosine and sine components. It is the same rectangular waveform as that shown in Fig. 1.2 except that the waveform in Fig. 1.9 is shifted on the time axis. In the program attached to this book, the reader can change the starting and ending times (τ_1 and τ_2) of the waveform.

Another way of understanding the roles of sine and cosine waves is that the original rectangular wave can be divided into two rectangular waves, one is symmetric and the other is anti-symmetric. The Fourier series of the former can be represented only by cosine waves (*even functions*) and that of the latter only by sine waves (*odd functions*). Running the program for various waveforms will help the reader understand the necessities and roles of the sine and cosine waves for the Fourier series expansion.

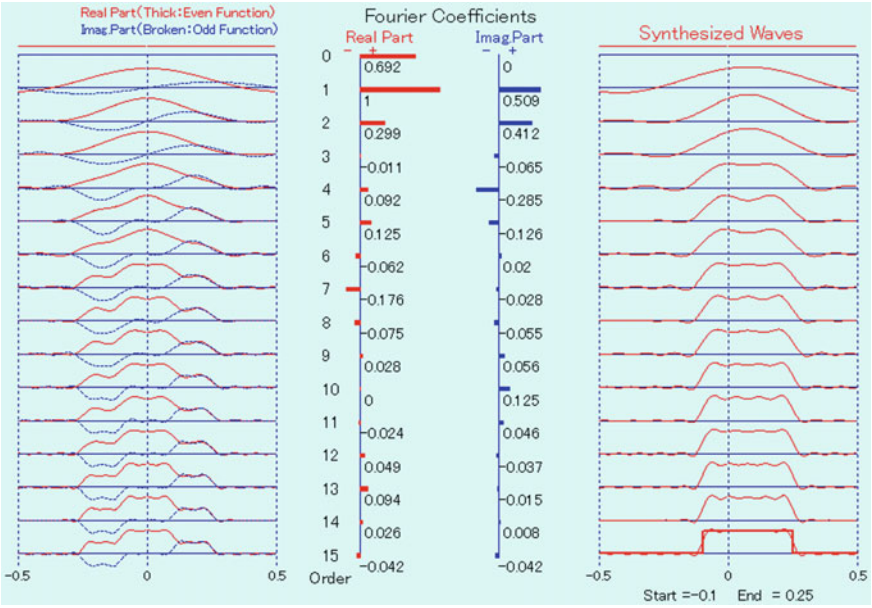

Fig. 1.9 Cosine (*real*) and sine (*imaginary*) components that comprise a non-symmetric rectangular wave. Animation available in supplementary files under filename E1-09_Synthesis.exe

It has been mentioned that, for correct synthesis of the original waveform, the sine and cosine components should not be shifted in time. A shift of a wave on the time axis is equivalent to the phase change of the wave. In order to properly understand the phase, the relation between complex exponential functions and real sine and cosine functions must be made clear.

1.7 Complex Exponential Functions and Sine and Cosine Functions

A complex exponential function is an exponential function with a complex power. Since this book deals with signals, an exponential function e^{st} is treated, where s is a complex number with $s- = \sigma + j\omega$ (σ and ω are real numbers, j is the imaginary unit, i.e. $\sqrt{-1}$, and t is time. The case with $s- = j\omega$ (purely imaginary) is the most important. The function $e^{j\omega t}$ has a cosine function as its real part and a sine function as its imaginary part.

$$e^{j\omega t} = \cos \omega t + j \sin \omega t \tag{1.3}$$

Equation (1.3) is referred to as Euler's formula. In this book, ω represents an *angular frequency*, radians/second, which is related to the *frequency f,* Hz, by

$$\omega = 2\pi f \tag{1.4}$$

In most theoretical books, ω is used instead of f. But since f is intuitively easy to understand, it will be used throughout this book. The Euler's formula is rewritten as

$$e^{j2\pi ft} = \cos 2\pi ft + j \sin 2\pi ft \tag{1.5}$$

The plane defined by the rectangular coordinate system with the horizontal axis (or real axis) representing real numbers and the vertical axis (or imaginary axis) representing imaginary numbers is referred to as the *complex plane*. Any complex number can be given its own point on the complex plane. The complex number defined by Eq. (1.5) has its real value $\cos 2\pi ft$ and imaginary value $\sin 2\pi ft$ on the complex plane. As time t increases, the point on the complex plane moves along the circle with radius 1. This is because the radius is given by $|e^{j2\pi ft}| = \sqrt{(\cos 2\pi ft)^2 + (\sin 2\pi ft)^2}$, which is equal to 1. In order to better represent the point $(\cos 2\pi ft, \sin 2\pi ft)$, a *vector* (an arrow) with its starting point at the origin (0,0) and its ending point at $(\cos 2\pi ft, \sin 2\pi ft)$ is considered. At $t = 0$ the front end of the vector is on the horizontal axis (1,0), and as t increases, the vector rotates counterclockwise with the angular speed of $2\pi f$. For this reason, the vector defined by Eq. (1.5) is referred to as a *rotating vector*. In general, the *counterclockwise* and *clockwise rotations* are considered as positive and negative rotations, respectively. The frequency, f, is considered as the number of rotations per second. If it is positive, the rotation is counterclockwise.

The projection on the horizontal axis of the vector rotating in the positive direction is the real part of Eq. (1.5). The trajectory of the projection of this point on the horizontal axis is the cosine wave shown in Fig. 1.10, where the vertical axis is used as the time axis with the positive direction downward. In the same way, the trajectory of the projection of the point on the vertical axis is the sine wave shown in Fig. 1.10, where the horizontal axis is used as its time axis. By comparing Fig. 1.10 with Eq. (1.5), the meaning of the Euler's formula will become clear. The reader should refer to the program attached to this book. If the reader runs the program, he/she can see the rotating vector, which will help him understand the practical use of Euler's formula.

The first term of the right-hand side of Eq. (1.5) is the cosine wave and the second term is the sine wave. If they are taken as real and imaginary parts, respectively, the exponential function $e^{j2\pi ft}$ can be considered as a vector which rotates f times per second around the origin. One period of a wave corresponds to one rotation of the vector. The function $e^{j2\pi ft}$ is referred to as the *complex exponential* (*or sinusoidal*) *function*.

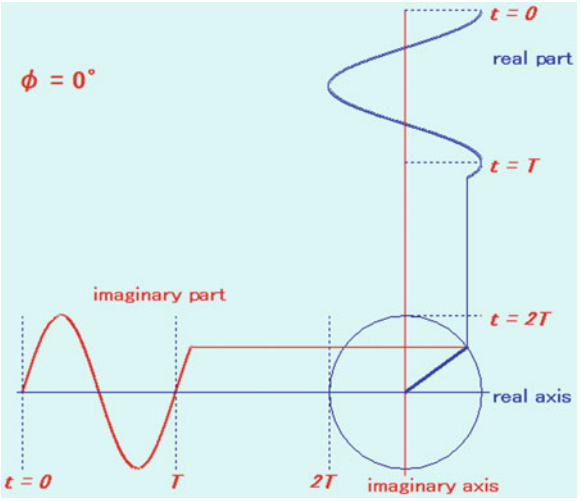

Fig. 1.10 Trajectory of a unit vector rotating around the origin of the complex plane with a positive constant angular velocity. Animation available in supplementary files under filename E1-10_RotVector.exe

So far counterclockwise rotating vectors have been considered. What would happen if the vector rotates clockwise? Time can never go in reverse. Thus, the frequency f must be negative to represent the vector rotating clockwise. If we consider that f is the number of waves in one second, it is not easy to understand negative frequency. However, considering vectors rotating in positive (counter-clock wise) and negative (clock wise) directions, the concept of the *negative frequency* can be understood as well as the concept of *positive frequency*.

From the above discussion, it can be concluded that the complex exponential function with negative frequency, $e^{-j2\pi ft}$, is a vector rotating in the negative direction, i.e., clockwise. Its projection on the real axis (horizontal axis) is the same as $e^{j2\pi ft}$, but the projection on the imaginary axis (vertical axis) is $-\sin(2\pi ft)$. It is expressed by the equation:

$$e^{-j2\pi ft} = \cos 2\pi ft - j \sin 2\pi ft \tag{1.6}$$

Figure 1.11 shows the rotating vector in the negative (clockwise) direction and its projections. The cosine wave is the same as that in Fig. 1.10 and the sine wave has the opposite sign.

Figure 1.12 shows two vectors rotating in opposite directions. If we add the two vectors, the cosine wave amplitude is doubled and the sine wave amplitudes cancel with each other. This concept is expressed by

$$e^{j2\pi ft} + e^{-j2\pi ft} = 2 \cos 2\pi ft \tag{1.7}$$

Equation (1.7) is simply obtained by adding Eqs. (1.5) and (1.6). Figure 1.12 will help the reader understand the physical meaning of Eq. (1.7).

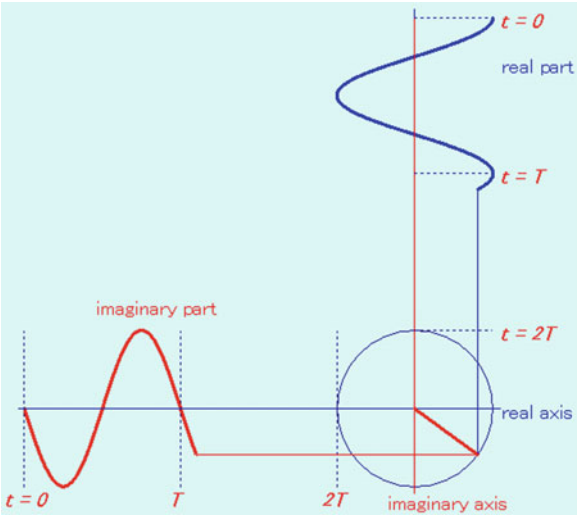

Fig. 1.11 Trajectory of a unit vector rotating around the origin of the complex plane with a negative constant angular velocity. Animation available in supplementary files under filename E1-11_RotVector.exe

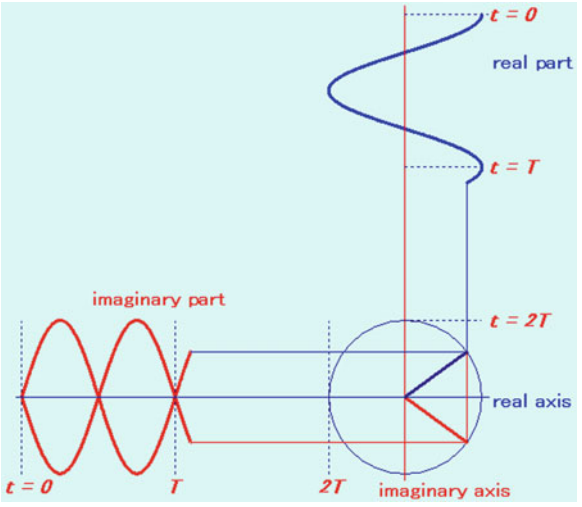

Fig. 1.12 Trajectories of two vectors rotating around the origin of the complex plane with identical positive and negative constant angular velocities. Animation available in supplementary files under filename E1-12_RotVector.exe

From Eq. (1.7), the cosine wave can be expressed by positive and negative frequency components.

$$\cos 2\pi ft = (e^{j2\pi ft} + e^{-j2\pi ft})/2 \tag{1.8}$$

Similarly,

$$\sin 2\pi ft = (e^{j2\pi ft} - e^{-j2\pi ft})/2j \tag{1.9}$$

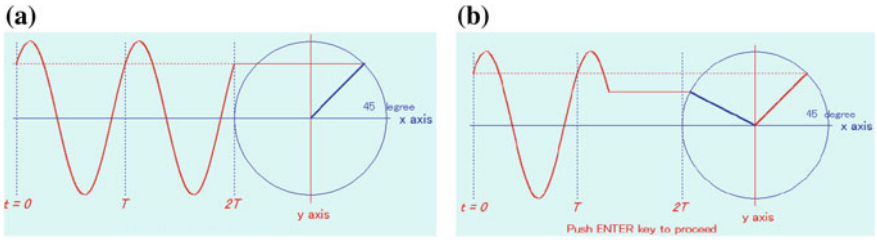

Fig. 1.13 Phases of a sine wave shown by projections of rotating vectors on the imaginary-axis (a:0°, b: 40°). Animation available in supplementary files under filename E1-13_a_VsinPhase.exe and E1-13_b_VsinPhase.exe. **a** $\sin(2\pi ft)$. **b** $\sin(2\pi ft+\phi)$ ϕ=40°

1.8 Phases of Cosine and Sine Functions

In Sect. 1.7, the sine wave (function) is expressed as the projection of the rotating vector on the imaginary (vertical) axis. If the vector at $t = 0$, is tilted from the horizontal axis, the sine function is shifted on the time axis. The shift is proportional to the initial angle of rotation from the horizontal axis. Let ϕ be the initial angle at zero time. Then, the projection of the rotating vector with the initial angle ϕ on the vertical axis is given by

$$\sin(2\pi ft + \phi). \tag{1.10}$$

The angle ϕ is referred to as the *initial phase* and $\sin(2\pi ft + \phi)$ is referred to as a *sine wave with the initial phase* (*shift*) ϕ. If $\phi = 0$, the initial vector lies on the positive horizontal axis, and the sine wave has 0 time shift as shown in Fig. 1.13a. Figure 1.13b shows the case with $\phi = 40°$. The sine wave has the *positive* (*or leading*) *phase* since it starts from $\phi = 40°$. If the vector starts with an angle below the positive real axis, it is said that the wave has a *negative phase* (*or phase delay*).

The phase is expressed by the angle of the vector. The phase of 90° is the right angle and the phase of 360° is one rotation. Since one rotation is 2π radians, the phase can be expressed in radians as well as degrees. The radian expression is used most often in theoretical equations, the reason will be made clear soon.

Waves with different initial phases will now be examined. Figure 1.14 shows the sine waves with 0°, ±30°, ±60°, and ±90° initial phases. The waves in Fig. 1.14 are drawn from the top to the bottom in the order of the phase advance. Note that the peaks of the waves shift from the left to the right as the initial phase reduces (from the top to the bottom). This means that the peaks of a wave with a more delayed phase comes later than those of a wave with a more advanced phase (remember that the time progresses from the left to the right on the horizontal axis). On the right-hand side of Fig. 1.14 the initial vectors are also shown. If the vectors are compared with the corresponding waveforms, it will be understood that the upper waves in the figure are more advanced in their phases than the lower ones.

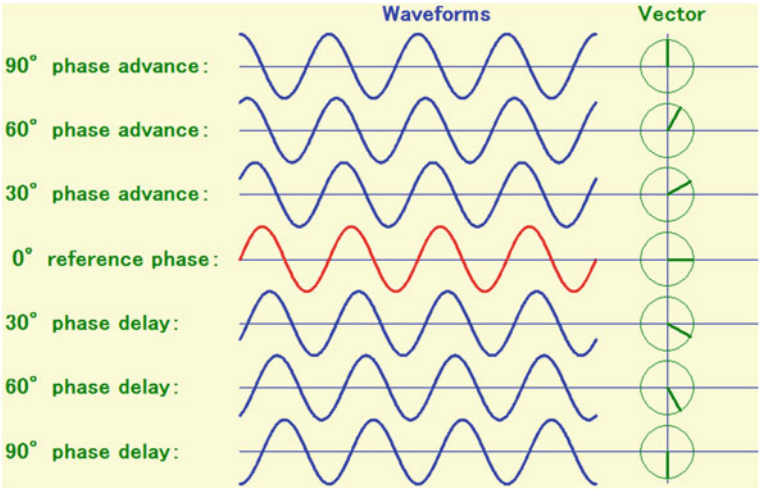

Fig. 1.14 Reference sine wave (*middle*) and sine waves with phase-lead (*above*) and with phase delay (*below*). Animation available in supplementary files under filename E1-14_Sin7phase.exe

The cosine and sine waves have a 90° or $\pi/2$ radian phase difference with each other. In other words, they are the same wave except that they are 1/4 wavelength shifted on the time axis. This is expressed by the trigonometric equation

$$\cos(2\pi ft) = \sin(2\pi ft + \pi/2) \tag{1.11}$$

This can also be corroborated by running the program of Fig. 1.10 or 1.13.

Now, Fig. 1.13 will be reviewed by using simple equations. Assume that two sine waves are expressed by

$$x_1(t) = \sin(2\pi ft) \tag{1.12}$$

and

$$x_2(t) = \sin(2\pi ft + \varphi) \tag{1.13}$$

In this case, $x_2(t)$ leads $x_1(t)$ by the angle ϕ (assuming that $\phi > 0$) in phase. On the other hand, the wave

$$x_3(t) = \sin(2\pi ft - \phi) \tag{1.14}$$

is a sine wave with a phase delay of ϕ compared to the wave $x_1(t)$.

Two types of "*phase angle of a signal*," are considered. One is the total phase $(2\pi ft + \phi)$ within the parenthesis of the sine or the cosine function, and the other is the phase difference ϕ (or the *initial phase* at $t = 0$). The latter is used very often

because there are many cases when only the phase differences between waves, or the initial phase of a single wave, is of importance.

The unit of phase angle is the radian, and one rotation in the complex plane is equivalent to 2π radians. It can also be expressed as 360° (degrees) of rotation. The degree is more familiar than the radian in engineering practice. However, in computer software, the values of sine and cosine are calculated using radians. Therefore, it is recommended that the reader use radians in the computer program or at least make sure which unit (radian or degree) is employed in the specific function being used. If necessary, change degrees to radians, or vice versa, beforehand.

1.9 Synthesis of Sine Wave with Arbitrary Phase

Formulae of the trigonometric functions, sine and cosine, with initial phase ϕ are expressed as

$$\begin{aligned} \sin(2\pi ft + \phi) &= \cos(\phi)\sin(2\pi ft) + \sin(\phi)\cos(2\pi ft) \\ \cos(2\pi ft + \phi) &= \cos(\phi)\cos(2\pi ft) - \sin(\phi)\sin(2\pi ft) \end{aligned} \tag{1.14}$$

As these equations show, by adding sine and cosine functions (with the same frequency and zero initial phases), a new sine or cosine wave with a different phase is produced. In Fig. 1.15, an example of producing a sine wave which leads in phase by 30° is shown. Another approach will be given below.

Let the amplitudes of sine and cosine waves be A_s and A_c, respectively. The summation of the two waves gives one sine wave that has a positive or negative phase depending on the relation between A_s and A_c:

$$\begin{aligned} &A_s \sin(2\pi ft) + A_c \cos(2\pi ft) \\ &= \sqrt{A_s^2 + A_c^2}\left(\frac{A_s}{\sqrt{A_s^2 + A_c^2}}\sin(2\pi ft) + \frac{A_s}{\sqrt{A_s^2 + A_c^2}}\cos(2\pi ft)\right) \\ &= \sqrt{A_s^2 + A_c^2}(\cos\phi \sin(2\pi ft) + \sin\phi \cos(2\pi ft)) = \sqrt{A_s^2 + A_c^2}\sin(2\pi ft + \phi) \end{aligned} \tag{1.15}$$

where

$$\phi = \arccos\left(\frac{A_s}{\sqrt{A_s^2 + A_c^2}}\right) = \arcsin\left(\frac{A_c}{\sqrt{A_s^2 + A_c^2}}\right) = \arctan\left(\frac{A_c}{A_s}\right) \tag{1.16}$$

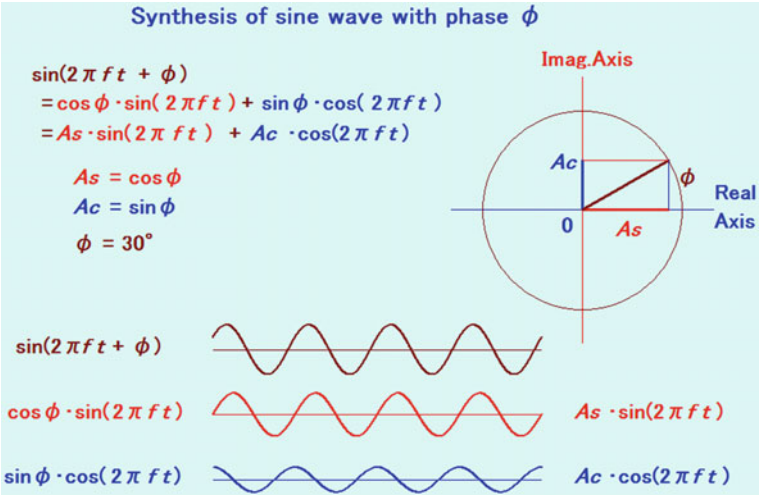

Fig. 1.15 Addition of sine and cosine waves to synthesize sine wave with phase φ. Animation available in supplementary files under filename E1-15_PhaseSynthesis_1.exe

The dependence of the phase ϕ given by Eq. (1.16) on A_s and A_c are shown by the upper right chart in Fig. 1.15. If we assume that $\sqrt{A_s^2 + A_c^2} = 1$, A_s and A_c are given by

$$A_s = \cos(\phi), \quad A_c = \sin(\phi) \tag{1.17}$$

In the chart, A_s is the vector on the real axis and the A_c is the vector on the imaginary axis, both shown by thick lines. The resultant vector has the angle (= phase) ϕ, which is considered positive if the vector is on the upper half plane.

In the explanations up to now, the term "leading in phase" is equivalent to "shifting the wave towards the negative time direction." This concept is correct for a wave at any frequency. The point is that the equivalent time shift corresponding to a particular phase difference is dependent on the frequency. Then a question arises, "When a wave with multiple frequency components is shifted in time without changing its waveform, what occurs to the phases of each component?" An answer is easily obtained if phase shifts of individual components of an impulse for a given time shift are considered.

Figure 1.16 shows a composition of an impulse which is shifted by τ on the time axis. In this case all harmonics as well as the fundamental must be shifted by τ. As the left-hand side chart shows, the same amount of time delay causes a smaller amount of phase change for a lower frequency component and a larger amount of phase change for a higher frequency component. The phase change equivalent to the time delay is proportional to the frequency of the component. This can be understood by the following way.

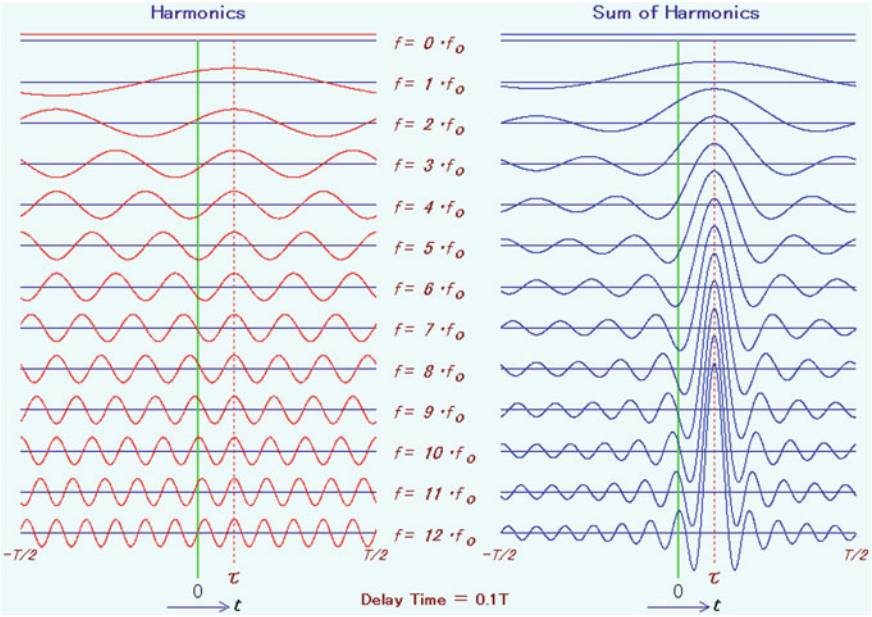

Fig. 1.16 Components that comprise the impulse with time delay τ. The phase delay of each component is proportional to its frequency. Animation available in supplementary files under filename E1-16_PP.exe

A cosine wave with time shift τ is expressed as

$$f(t) = \cos\{2\pi f(t-\tau)\} = \cos(2\pi ft - 2\pi f\tau) \tag{1.18}$$

The above equation shows that the phase shift is given by

$$\theta = -2\pi f\tau \tag{1.19}$$

If there is a time delay τ, then a component with frequency f that comprises the impulse has a phase shift $-2\pi f\tau$. This indicates that the time delay (or lead) of a waveform is caused by the phase delays (leads) of individual components that are proportional to their frequencies.

The impulse expressed by Eq. (1.1) is an impulse located at $t = 0$. The impulse located at $t = \tau$, as shown in Fig. 1.16 is expressed by the equation below.

$$\delta(t-\tau) = 0.5 + \cos(2\pi\frac{t-\tau}{T}) + \cos(2\pi\frac{2t-2\tau}{T}) + \cos(2\pi\frac{3t-3\tau}{T}) + \cdot\ \cdot\ \cdot \tag{1.20}$$

which can be rewritten as

$$\begin{aligned}\delta(t-\tau) &= 0.5 + \cos(2\pi\frac{t}{T} - 2\pi\frac{\tau}{T}) + \cos(2\pi\frac{2t}{T} - 2\pi\frac{2\tau}{T}) + \cos(2\pi\frac{3t}{T} - 2\pi\frac{3\tau}{T}) + \cdots \\ &= 0.5 + \cos(2\pi\frac{t}{T} - \phi_1) + \cos(2\pi\frac{2t}{T} - \phi_2) + \cos(2\pi\frac{3t}{T} - \phi_3) + \cdots\end{aligned} \tag{1.21}$$

Equation (1.21) shows that the k-th order harmonic has the same amount of phase delay (given by the product of the frequency (k/T) and the time delay τ) as that given by Eq. (1.19).

Equation (1.21) can also be written using Eq. (1.11) as

$$\delta(t-\tau) = 0.5 + \sin(2\pi\frac{t}{T} + \frac{\pi}{2} - \phi_1) + \sin(2\pi\frac{2t}{T} + \frac{\pi}{2} - \phi_2) + \sin 2\pi\frac{3t}{T} + \frac{\pi}{2} - \phi_3) + \cdots \tag{1.22}$$

As has been already shown in Figs. 1.7 and 1.8, a waveform drastically changes as the phases of the harmonics change with respect to the phase of the fundamental. Normally, it is impossible to guess orders and phases of harmonics contained in the signal. However, it is not so difficult to distinguish between two signals which contain only the even and odd order harmonics if the orders of harmonics are low.

Figure 1.17 shows two waveforms; one is at the fundamental ($x_1(t) = A_1 \cos 2\pi f_1 t$) and 2nd order harmonic ($x_2(t) = A_2 \cos(2\pi f_2 t + \theta)$) and the other is with the fundamental and the 3rd harmonic ($x_3(t) = A_3 \cos(2\pi f_3 t + \theta)$). The phases of the harmonics are varied from 0 to $6\pi/4$ within steps of $\pi/4$ radians. The program attached enables the reader to change the order of harmonics. The reader should try various cases to gain an understanding of the general trend of the differences between the signals with even and odd components.

1.10 Instantaneous Phase and Frequency

From the previous explanations, we understand that the cosine wave $\cos(2\pi ft + \phi)$ is the projection of the rotating vector on the real axis that has the angle ϕ from the real axis at $t = 0$. The angle of the rotating vector$(2\pi ft + \phi)$, when measured counterclockwise from the positive real axis, monotonically increases with time. Based on this understanding, we call the time-dependent angle $(2\pi ft + \phi)$ *the instantaneous phase* of the cosine wavecos$(2\pi ft + \phi)$, which can be expressed as a function of time.

$$\theta(t) = 2\pi ft + \phi \tag{1.23}$$

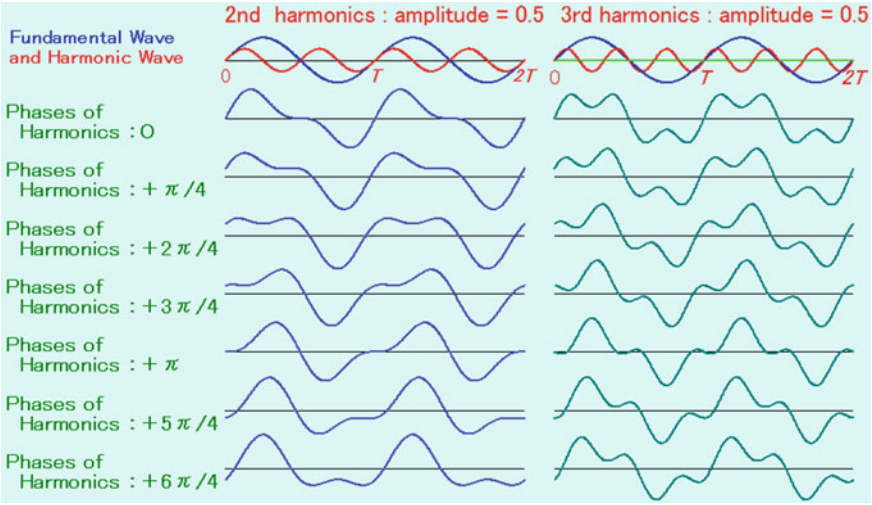

Fig. 1.17 Superposition of the fundamental and the 2nd harmonic waves (*left*) and the fundamental and the 3rd harmonic waves (*right*). Phases from 0 to $6\pi/4$ using $\pi/4$ radian steps and are given to the 2nd and 3rd harmonics. Animation available in supplementary files under filename E1-17_PhaseofHarmonic.exe

After defining the instantaneous phase, we consider the relation between the phase and the frequency. In general, the frequency is defined as the number of repetitions of a cyclic wave in one second. Referring to Fig. 1.10, the cosine and the sine waves are the projection of the rotating vector on the real-axis and imaginary-axis, respectively. The frequency is actually the number of the rotation of the vector in one second. After the vector rotates f times in one second, the phase increases by $2\pi f$ since one rotation is equivalent to 2π. This is also obvious from Eq. (1.23) since

$$\theta(1) - \theta(0) = 2\pi f \tag{1.24}$$

Then the frequency can be obtained as the phase change in one second divided by 2π.

$$f = \frac{1}{2\pi}\frac{[\theta(1) - \theta(0)]}{1 - 0} \tag{1.25}$$

Equation (1.25) indicates that, if the rotation speed of the vector is constant, the frequency is obtained by dividing the phase increase in every one second (which is always equal to $2\pi f$) by 2π. However, if the rotation speed changes, the following definition must be applied instead of Eq. (1.25):

$$f(t) = \frac{1}{2\pi}\frac{\theta(t) - \theta(t - \Delta t)}{t - (t - \Delta t)}\bigg|_{\Delta t \to 0} = \frac{1}{2\pi}\frac{d\theta(t)}{dt} \tag{1.26}$$

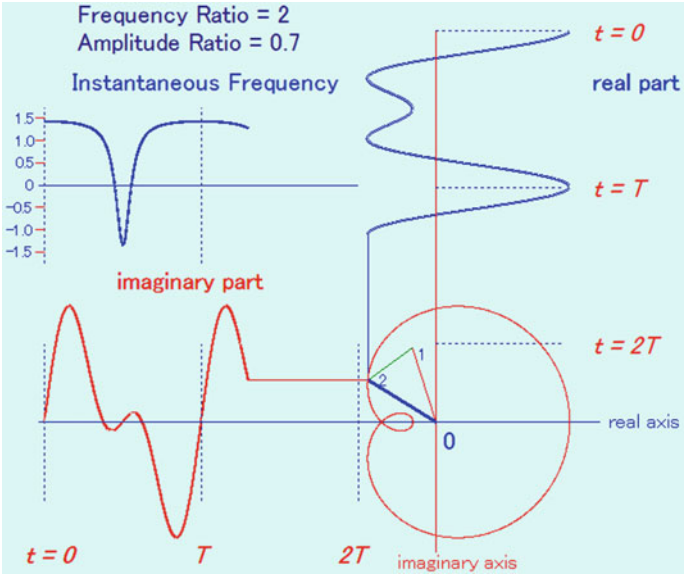

Fig. 1.18 Rotating vector, whose projection on the real axis is equal to $2[\cos 2\pi ft + 0.6\cos 2\pi(2f)t]$, and the instantaneous frequency obtained from the angular velocity of the vector. Animation available in supplementary files under filename E1-18_InstF.exe

This is the *instantaneous frequency* of any signal at any given time, where $\theta(t) = 2\pi ft + \varphi$ is the instantaneous phase. Instead of the instantaneous frequency, the *instantaneous angular frequency* can be defined using the relation given by Eq. (1.4).

$$\omega(t) = 2\pi f(t) = \frac{d\theta(t)}{dt} \tag{1.27}$$

The angular frequency is the rotational angle per second of the vector rotating in the positive direction, which has the unit of rad/s (radian per second). From Eqs. (1.23) and (1.26), it is concluded that the instantaneous frequency of a single sine or cosine wave is constant (time-independent).

If a signal has multiple frequency components, then the speed of the rotating vector is not always constant. As an example, consider a signal with two frequency components, one component has a frequency of 1 and amplitude of 1, and the other has a frequency of 2 and amplitude of 0.6, respectively. The locus of the rotating vector is shown in Fig. 1.18. The vector of the first component rotates around the origin with radius 1 and at a constant rotating speed (1 revolution per 1 s), which is shown by the vector $\overrightarrow{01}$. The second component vector is drawn from the front end of the vector $\overrightarrow{01}$, which is indicated by $\overrightarrow{12}$ in the figure. Considering that the second vector rotates with twice the speed of the first vector, it is understood that the locus of the added vector 02 (shown by the thick line) becomes just like a

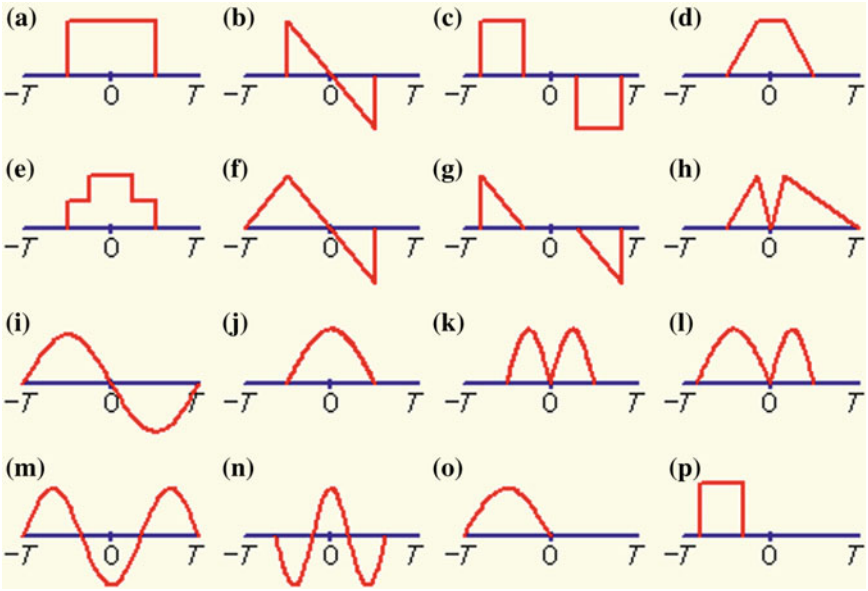

Fig. 1.19 Examples of waveforms (The maximum value is one for every figure)

"cardioid figure." When the added vector is around the negative axis, it rotates in the clockwise direction for a short period of time, resulting in the negative instantaneous frequency. The instantaneous frequency is shown by the upper left chart in Fig. 1.18. The details of instantaneous frequency are discussed in Chap. 12.

If the reader runs the program, he will gain a better understanding of the generating mechanism of the negative instantaneous frequency.

1.11 Exercise

1. What kind of wave is obtained if the phase of a sine wave is advanced by $\pi/2$?
2. What kind of wave is obtained if the phase of a sine wave is delayed by $\pi/2$?
3. What kind of wave is obtained if the phase of a cosine wave is advanced by $\pi/2$?
4. What kind of wave is obtained if the phase of a cosine wave is delayed by $\pi/2$?
5. What kind of wave is obtained if a sine wave and a cosine wave with the same amplitude, frequency, and phase are added?
6. Show how to obtain a sine wave with a 30° initial phase from a sine wave with 0° initial phase?
7. Draw examples of waveforms of even functions.
8. Draw examples of waveforms of odd functions.

9. Two waveforms are at hand: one is made of a fundamental and its 2nd harmonic and the other is made of the fundamental and the 3rd order harmonic. How are the two distinguished?
10. If phase delays are introduced to all harmonics (including the 1st order) of a periodic signal, with the property that they are each proportional to their individual orders, how does the signal change?
11. Which waveforms in Fig. 1.19 can be synthesized using only sine waves?
12. Which waveforms in Fig. 1.19 can be synthesized using only cosine waves?
13. Which waveforms in Fig. 1.19 must be synthesized using both sine and cosine waves?
14. The Fourier series expansion of (o) in Fig. 1.19 whose period is 2T is composed of the cosine series and the sine series.

    (a) Draw the waveform synthesized only by the cosine series.
    (b) Draw the waveform synthesized only by the sine series.

15. The Fourier series expansion of (*p*) in Fig. 1.19 whose period is 2T is composed of the cosine series and the sine series.

    (a) Draw the waveform synthesized only by the cosine series.
    (b) Draw the waveform synthesized only by the sine series.

Chapter 2
Fourier Series Expansion

In Chap. 1, it was shown, mostly by using graphics, that various waves can be expressed by a summation of sine and cosine functions, i.e., by the Fourier series (see Eq. 1.5). In this chapter, first, a method of determining coefficients of Fourier series will be given. A key idea is the integral of the products of sine and cosine functions. It was shown that an addition of sine and cosine functions with the same frequency can be combined into one sine or cosine function by introducing a phase term (see Eq. 1.5). It is also possible to express an arbitrary function by a combination of even and odd functions. The former and the latter can be expressed by cosine and sine functions, respectively. The next step is the expression of a Fourier series by complex exponential functions. The coefficients in this case are also complex, but since the mathematical manipulations are simpler, this method will be used most of the time hereafter.

The steps will be given one by one in this chapter and the reader should understand that the same thing is dealt with from different angles. A derivation of the Fourier transform pair as the extreme case of the Fourier series is the last subject in this chapter.

2.1 Integrals of Sine and Cosine Functions

As the starting point of this chapter, Eq. (1.2) is shown here again. It states that a waveform $x(t)$ with period T can be expressed by sine and cosine functions with frequencies $kf_0 = k/T$ $(k = 0, 1, 2, \ldots)$.

$$\begin{aligned} x(t) = A_0 &+ A_1 \cos 2\pi \frac{1}{T} t + A_2 \cos 2\pi \frac{2}{T} t + A_3 \cos 2\pi \frac{3}{T} t + \cdots \\ &+ B_1 \sin 2\pi \frac{1}{T} t + B_2 \sin 2\pi \frac{2}{T} t + B_3 \sin 2\pi \frac{3}{T} t + \cdots \end{aligned} \tag{2.1}$$

The first task is to find a way of determining the Fourier coefficients A_k and B_k assuming that a periodic function can be represented in the form of Eq. (2.1). In

K. Kido, *Digital Fourier Analysis: Fundamentals*,
Undergraduate Lecture Notes in Physics, DOI: 10.1007/978-1-4614-9260-3_2,

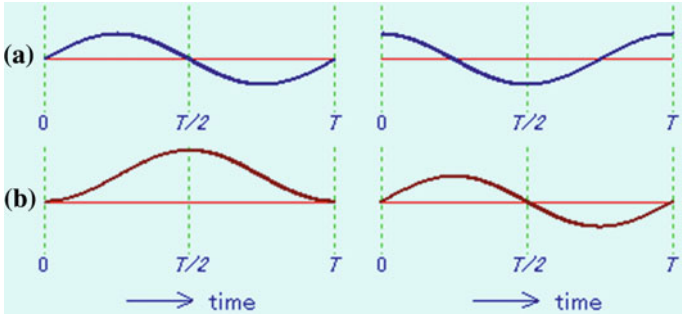

Fig. 2.1 Sine and cosine functions (*top*) and their integrations (*bottom*) starting from $t = 0$ and ending at $t = T$. Animation available in supplementary files under filename E2-01_SinCos.exe

order to determine the Fourier coefficients, both sides of Eq. (2.1) are multiplied by $\cos\{2\pi(k/T)t\}$ or $\sin\{2\pi(k/T)t\}$ and integrated over one period T. Since the integration can be carried out term by term, the basic problem is how to integrate the sine, cosine, and their products over one period (T).

With regard to the first term A_0, we need to integrate $1 \cdot \cos\{2\pi(k/T)t\}$ or $1 \cdot \sin\{2\pi(k/T)t\}$. For $k = 0$, $\cos\{2\pi(k/T)t\} = 1$ and $\sin\{2\pi(k/T)t\} = 0$. Therefore, their integration over period T is T and zero, respectively. It is obvious that the integrations of sine and cosine functions over multiples of their fundamental period are zero if $k \geq 1$. Figure 2.1a shows $\sin\{2\pi(1/T)t\}$ and $\cos\{2\pi(1/T)t\}$, and Fig. 2.1b shows how the integrations vary as the integration time is increased from t = 0 to T. Since the positive and negative areas are the same, the integration over one period becomes zero for both cases. It should be clear that the results are the same for higher orders ($k \geq 2$).

With regard to the higher order terms A_n ($n \geq 1$), it is necessary to investigate the integration of $\cos\{2\pi(k/T)t\}$ and $\sin\{2\pi(k/T)t\}$ multiplied by either $\cos\{2\pi(m/T)t\}$ or $\sin\{2\pi(m/T)t\}$. It should be remembered that both k and m are integers. The situation varies depending on the two cases: $k = m$ and $k \neq m$. Since equations of integration of products of sine and cosine functions are shown in many books, an emphasis will be put on gaining a physical image of these integrations.

Figure 2.2 shows integrations of cosine (a) and sine (b) functions multiplied by themselves. In this figure (a), $x_1(t)$ and $x_2(t)$ are the same cosine functions with the period T. The product of these two functions is shown by the curve $W_{12}(t)$ (thin line). This function never takes negative values and it has the period of $T/2$ (twice of the original frequency). The integration of $W_{12}(t)$ is shown by $E_{12}(t)$ (thick line), which is a monotonically increasing function. The integration of $W_{12}(t)$ over period T takes a finite value. A formula (equation) is needed to obtain this value, which will be discussed in Sect. 2.2. In the case of the sine function, the integration takes a different path but the final value at $t = T$ is the same as that of the cosine function.

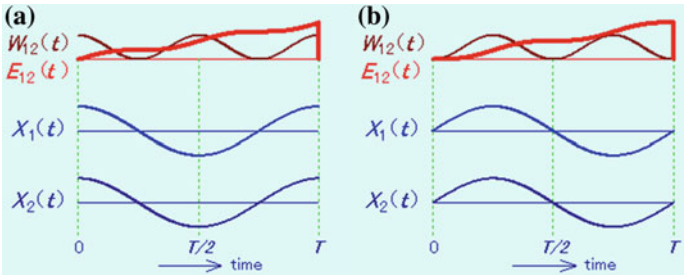

Fig. 2.2 Integration of $\cos^2\{2\pi(1/T)t\}$ and $\sin^2\{2\pi(1/T)t\}$. Animation available in supplementary files under filename E2-02_SCIntegral.exe

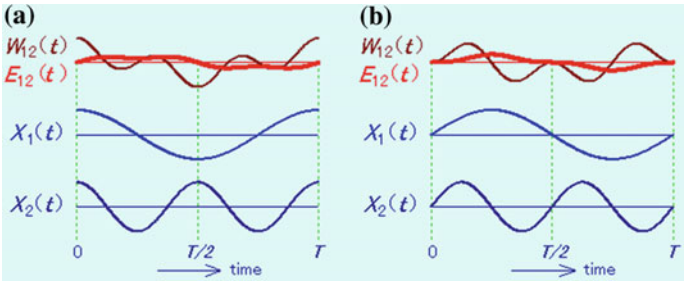

Fig. 2.3 Integration of **a** $\cos\{2\pi(1/T)t\} \times \cos\{2\pi(2/T)t\}$ and **b** $\sin\{2\pi(1/T)t\} \times \sin s\{2\pi(2/T)t\}$. Animation available in supplementary files under filename E2-03_SCIntegral.exe

Even if the functions $x_1(t)$ and $x_2(t)$ are both sine or cosine functions, if $k \neq m$, the integration becomes zero. This is shown in Fig. 2.3 for the case with the frequency ratio of 1:2 (Fig. 2.3a: cosine functions, Fig. 2.3b: sine functions). The validity can be checked for any ratio of two integers (k and m) by running the program.

If $x_1(t)$ is a cosine function and $x_2(t)$ is a sine function, the integration becomes zero regardless of the values of k and m. Fig. 2.4 shows these cases.

In summary, it is concluded that the integrals of products of two sine or two cosine functions are zero except for the cases when the frequencies of the two sine or two cosine functions are identical (i.e., $k = m$). This statement is also valid for the cases of integration of $\cos\{2\pi(k/T)t\}$ and $\sin\{2\pi(k/T)t\}$. Each of these functions is considered as the product of itself with the cosine function of zero frequency ($m = 0$) since $\cos\{2\pi(0/T)t\} = 1$. A set of functions with the property that the integration of a product of any two of its functions over the same fixed range is zero unless the functions are identical is called an "orthogonal system." A set of sine and cosine functions that have integer multiples of a fundamental frequency has this "orthogonality" property.

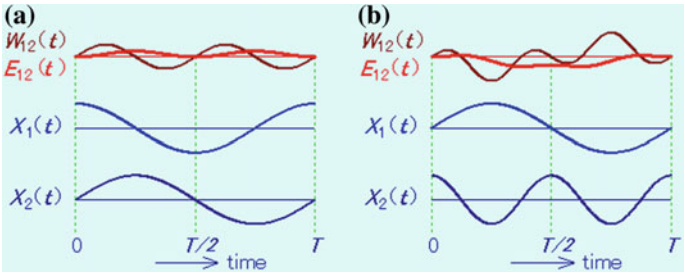

Fig. 2.4 Integration of **a** $\cos\{2\pi(1/T)t\} \times \sin\{2\pi(1/T)t\}$ and **b** $\sin\{2\pi(1/T)t\} \times \cos\{2\pi(2/T)t\}$. Animation available in supplementary files under filename E2-04_SCIntegral.exe

It has been made clear from the above discussion that, if the right-hand side is multiplied by $\cos\{2\pi(k/T)t\}$ or $\sin\{2\pi(k/T)t\}$ and integrated from $t = 0$ to T, only the k-th term of the cosine or sine series remains. This is the means by which the coefficients A_k and B_k can be determined. Since we cannot determine the values of integration from the charts, we must use equations, which will be developed in the next section.

2.2 Calculations of Fourier Coefficients

In order to derive formulae to determine the coefficients of the Fourier series, explanations given in Sect. 2.1 will be followed using equations.

First, what kinds of results are obtained if we integrate both sides of Eq. (2.1)?

$$\int_0^T x(t)dt = \int_0^T [A_0 + A_1 \cos 2\pi \frac{1}{T}t + A_2 \cos 2\pi \frac{2}{T}t + A_3 \cos 2\pi \frac{3}{T}t + \cdots + B_1 \sin 2\pi \frac{1}{T}t + B_2 \sin 2\pi \frac{2}{T}t + B_3 \sin 2\pi \frac{3}{T}t + \cdots]dt$$

The integration of the right-hand side will be done term by term. The first term with A_0, is given by

$$\int_0^T A_0 dt = TA_0 \tag{2.2}$$

The integrations of the following terms with coefficients A_k, $k = 1, 2,\ldots$ are all equal to zero.

$$\int_0^T A_k \cos 2\pi \frac{k}{T}tdt = A_k \frac{T}{2\pi} \sin 2\pi \frac{k}{T}t \Big|_0^T = 0 \tag{2.3}$$

It is the same for the coefficients B_k, $k = 1, 2, \ldots$

$$\int_0^T B_k \sin 2\pi \frac{k}{T} t dt = -B_n \frac{T}{2\pi} \cos 2\pi \frac{k}{T} t \Big|_0^T = 0 \tag{2.4}$$

Equation (2.2) is rewritten, giving an equation to determine A_0.

$$A_0 = \frac{1}{T} \int_0^T x(t) dt \tag{2.5}$$

Next, we will multiply $\cos\{2\pi(k/T)t\}$ on both sides of Eq. (2.1).

$$\begin{aligned} \int_0^T x(t) \cos\left(2\pi \frac{k}{T} t\right) dt = \int_0^T [A_0 \cos\left(2\pi \frac{k}{T} t\right) + A_1 \cos\left(2\pi \frac{1}{T} k\right) \cos\left(2\pi \frac{k}{T} t\right) \\ + A_2 \cos\left(2\pi \frac{2}{T} t\right) \cos\left(2\pi \frac{k}{T} t\right) + \cdots + A_n \cos^2\left(2\pi \frac{k}{T} t\right) + \cdots \\ + B_1 \sin\left(2\pi \frac{1}{T} t\right) \cos\left(2\pi \frac{k}{T} t\right) + \cdots + B_k \sin\left(2\pi \frac{k}{T} t\right) \cos\left(2\pi \frac{k}{T} t\right) + \cdots] dt \end{aligned} \tag{2.6}$$

Let's check this integration term by term. The first term becomes zero as shown by Eq. (2.3). The second and higher order terms are the integrations of products of cosine functions with different frequencies or the products of sine and cosine functions. The discussion in Sect. 2.1 showed that there is only one nonzero term, which is the product of cosine functions with the same frequency.

The product of $\cos\{2\pi(k/T)t\}$ and $\sin\{2\pi(k/T)t\}$ is rewritten as

$$\cos\left(2\pi \frac{k}{T} t\right) \cos\left(2\pi \frac{m}{T} t\right) = \frac{1}{2} \left\{ \cos\left(2\pi \frac{k+m}{T} t\right) + \cos\left(2\pi \frac{k-m}{T} t\right) \right\}.$$

The integration of this product from $t = 0$ to T is zero if $k \neq m$. If $k = m$, the second term of the right-hand side is $T/2$ since $\cos\{2\pi(0/T)t\} = 1$. Similarly, the product of $\cos\{2\pi(k/T)t\}$ and $\sin\{2\pi(m/T)t\}$ is rewritten as

$$\cos\left(2\pi \frac{k}{T} t\right) \sin\left(2\pi \frac{m}{T} t\right) = \frac{1}{2} \left\{ \sin\left(2\pi \frac{k+m}{T} t\right) - \sin\left(2\pi \frac{k-m}{T} t\right) \right\}.$$

The integration of this product from $t = 0$ to T becomes zero for both cases: $k \neq m$ and $k = m$.

Finally, only one nonzero term remains, which is

$$\int_0^T x(t) \cos\left(2\pi \frac{k}{T} t\right) dt = A_k \frac{T}{2}.$$

This gives the equation to determine A_k,

$$A_k = \frac{2}{T}\int_0^T x(t)\cos\left(2\pi\frac{k}{T}t\right)dt. \tag{2.7}$$

Similarly, the equation to determine B_k is given by

$$B_k = \frac{2}{T}\int_0^T x(t)\sin\left(2\pi\frac{k}{T}t\right)dt. \tag{2.8}$$

The range of integration need not be from $t = 0$ to T. It can be over any range from $t = T_1$ to T_2 as long as $T_2 - T_1 = T$. Then the equations to determine Fourier coefficients are given as

$$A_0 = \frac{1}{T}\int_{T_1}^{T_1+T} x(t)dt \tag{2.9}$$

$$A_k = \frac{2}{T}\int_{T_1}^{T_1+T} x(t)\cos\left(2\pi\frac{k}{T}t\right)dt \tag{2.10}$$

$$B_k = \frac{2}{T}\int_{T_1}^{T_1+T} x(t)\sin\left(2\pi\frac{k}{T}t\right)dt. \tag{2.11}$$

If a symmetrical expression is preferred, the equations will be

$$A_0 = \frac{1}{T}\int_{-T/2}^{T/2} x(t)dt \tag{2.12}$$

$$A_k = \frac{2}{T}\int_{-T/2}^{T/2} x(t)\cos\left(2\pi\frac{k}{T}t\right)dt \tag{2.13}$$

$$B_k = \frac{2}{T}\int_{-T/2}^{T/2} x(t)\sin\left(2\pi\frac{k}{T}t\right)dt. \tag{2.14}$$

The three sets of equations to calculate Fourier coefficients have been presented (Eqs. (2.5), (2.7)–(2.14)). The most general expression is the second set. Each set will give different values of A_k and B_k. This is due to the phase difference caused by the change of starting point of each harmonic of the waveform. However, the magnitude of each harmonic $\sqrt{A_k^2 + B_k^2}$ is independent of the starting point.

A reason why a waveform is expanded into a series of sine and cosine functions is because each coefficient can be determined using the orthogonality property of sine and cosine functions. There are other types of orthogonal functions that could be used to expand the same waveform. However, there is no reason here to seek other orthogonal functions since the sine and cosine functions constitute one of the most elegant sets of orthogonal systems.

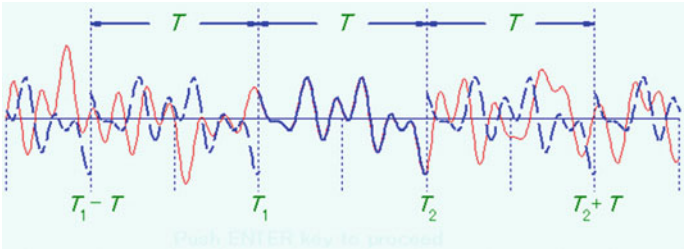

Fig. 2.5 An infinitely long waveform (*thin line*) and its Fourier expansion in the range $T_1 \leq t < T_2$ (*thick line*). The Fourier series expansion repeats the same (extracted) waveform outside the range $T_1 \leq t < T_2$, as shown by the dotted line. Animation available in supplementary files under filename E2-05_AnalysisRange.exe

Until now, we have not paid much attention to the region outside of the range $0 \leq t < T$, $T_1 \leq t < T_2$, or $-T/2 \leq t < T/2$, within which the function is defined. However, since the fundamental component of the Fourier series has the periodicity T and its k-th harmonic has the periodicity T/k, any waveform expressed by use of the Fourier series will exhibit the periodicity T. Therefore, as shown in Fig. 2.5, if the portion of a waveform between $T_1 \leq t < T_2$ is expressed by a Fourier series, the Fourier series expansion of that waveform repeats the waveform with period T (thick line) within the range $T_1 \leq t < T_2$. Note that the original waveform (thin line) and the Fourier series expansion extended outside the range $T_1 \leq t < T_2$ (dotted line) may be different.

Since selecting a portion of a continuous waveform is analogous to looking at the waveform through a window, it is called *time-windowing* in the field of signal processing. The period T or $T_2 \sim T_1$ is the length of the *time window*. The waveform expressed by the Fourier series repeats the extracted waveform within that time window, with the period of the window length.

As shown by Eq. (2.1), the Fourier series is expressed by the series of cosine functions with coefficients A_k and the series of sine functions with coefficients B_k. Once A_k and B_k are obtained, each cosine and sine combination can be combined into one cosine or one sine function as shown by Eqs. (1.23) and (1.25). Only the results will be shown here.

The expression using only cosine functions is given by

$$x(t) = C_0 + C_1 \cos\left(2\pi \frac{1}{T} t - \phi_1\right) + C_2 \cos\left(2\pi \frac{2}{T} t - \phi_2\right) + \cdots \tag{2.15}$$

where

$$C_0 = A_0,\ C_k = \sqrt{A_k^2 + B_k^2},\ \phi_k = \arctan(B_k/A_k) \tag{2.16}$$

A similar expression using only sine functions is given by

$$x(t) = C_0 + C_1 \sin\left(2\pi \frac{1}{T} t + \theta_1\right) + C_2 \sin\left(2\pi \frac{2}{T} t + \theta_2\right) + \cdots \tag{2.17}$$

where C_0, C_k are given by Eq. (2.16) and θ_k is given by

$$\theta_k = \arctan(A_k / B_k) \tag{2.18}$$

The coefficient $C_k = \sqrt{A_k^2 + B_k^2}$, which is common for Eqs. (2.15) and (2.17), is the amplitude of the combined component of the cosine and sine functions with frequency k/T. Therefore, the set of amplitudes C_k is called the *amplitude spectrum*, which is expressed as a function of k (order) or the real frequency (k/T). On the other hand, a set of squares C_k^2 is called the *power spectrum*, since, for example, the square of the amplitude of the voltage or the current is proportional to the (electrical) power. The frequencies of the spectra given as components of the Fourier series are integer multiples of $1/T$. The spectra are distributed at discrete points on the frequency axis and their magnitudes are expressed by vertical thin lines. Therefore, they are called *line spectra*.

2.3 Expressing Waveforms by Even Functions

The Fourier coefficients, or Fourier spectra, obtained using an extracted waveform with length T have cosine and sine components as shown in Fig. 2.6. The time windowed (extracted) waveform repeats itself with period T, and the spacing between the adjacent spectra is $1/T$. Each spectrum is actually composed of two components, the cosine ("real") and sine ("imaginary") components, A_k and B_k, respectively. These two can be combined into single cosine or sine components while introducing the phase terms as shown by Eq. (2.15) or (2.17). The introduction of phase may make the situation more complex, rather than making it simpler. Then, a question arises, "Is there a way of expressing a waveform by cosine or sine functions without using phase terms?"

As we have learned in Chap. 1, an even function, which is symmetric with respect to the origin of time $t = 0$, is expressed only by cosine functions, and an odd function, which is anti-symmetric with respect to the origin of time $t = 0$, is expressed only by sine functions. Then, if a waveform that is symmetric with $x(t)$ is introduced into the time range, $-T \leq t < 0$, as shown in Fig. 2.7, and if the combined waveform (A_{2TE}) is expressed by the Fourier series with period $2T$, the series will contain only the cosine terms.

Figure 2.7 shows exactly what we expect. Figures 2.6 and 2.7 are the spectra of waveform constructed from the same portion of another waveform. Figure 2.6 shows Fourier coefficients of a periodic waveform A_T with a single period T and Fig. 2.7 shows Fourier coefficients of a periodic waveform (A_{2TE}) with period $2T$. Therefore, the frequency spacing (resolution) of the former figure is $1/T$ and

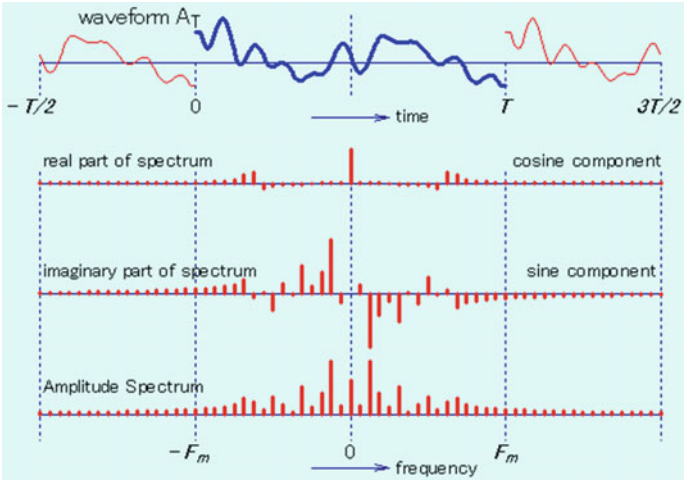

Fig. 2.6 Fourier coefficients (real and imaginary parts of the spectrum) and amplitude spectra obtained when the extracted waveform A_T is assumed to be periodic. Animation available in supplementary files under filename E2-06_F-Coeff_A.exe

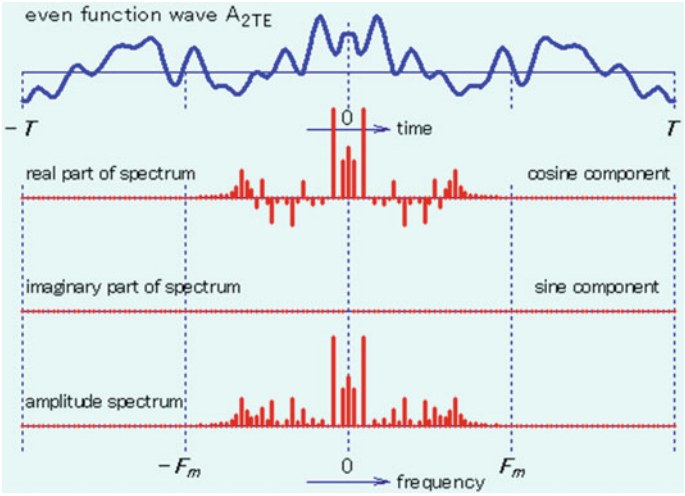

Fig. 2.7 Even waveform A_{2TE} with period $2T$ and its spectra obtained by adding a symmetric waveform of A_T (see Fig. 2.6) in the region $-T \leq t < 0$. Animation available in supplementary files under filename E2-07_EvenF_A.exe

that of the latter figure is $1/2T$ (one half of the former). In order to make this clear, the horizontal axis is scaled by frequency (instead of integer k) and vertical dotted lines are inserted at every F_m frequency. Following charts are shown using the same format so that the charts may be compared more easily.

The waveform shown in Fig. 2.6 has many spectral components outside of $\pm F_m$. A reason why so many spectral lines are necessary is that the constructed waveform has a large discontinuity at the connections when the portion of the waveform with the period T is repeated. The constructed waveform in Fig. 2.7, has a smaller degree of discontinuity and, therefore, more of the harmonics are kept within $\pm F_m$. As shown in Fig. 2.7, if a symmetric waveform is introduced into the time range, $-T \leq t < 0$, the constructed waveform becomes an even function and the whole range from $-T$ to T must be taken into account when applying the Fourier series expansion. In this case, the waveform in the range from 0 to T is completely recovered and the series has only cosine terms. This may seem to be an advantage to be able to avoid the use of the phase terms. However, since the period is doubled (in other words, the frequency spacing is one half), two times the number of spectra are necessary to cover the same frequency range. The number of spectral lines of the waveforms shown in Figs 2.6 and 2.7 are the same since the latter needs only the cosine terms even though the spectral density is twice.

For later use, what was explained above will be described using equations. In order to express the waveform $x(t)$ in $0 \leq t < T$ using only cosine terms, the symmetric waveform $x(-t)$ is added to the range $-T \leq t < 0$. The combined waveform is of course symmetric (even), which will be named $z(t)$. The k-th order Fourier coefficients defined in the range $-T \leq t < T$, is given by

$$A_k = \frac{1}{T}\int_{-T}^{T} z(t)\cos\left(2\pi\frac{k}{2T}t\right)dt$$

Since $z(t)$ and cosine functions are both even functions, the integration from t = -T to 0 is the same with the integration from 0 to T. Therefore, the above integration can be given by

$$A_k = \frac{2}{T}\int_{0}^{T} z(t)\cos\left(2\pi\frac{k}{2T}t\right)dt.$$

Since $x(t) = z(t)$ in the range from 0 to T, it is given by

$$A_k = \frac{2}{T}\int_{0}^{T} x(t)\cos\left(2\pi\frac{k}{2T}t\right)dt. \tag{2.19}$$

The coefficient A_0 can be obtained by the same way.

$$A_0 = \frac{1}{T}\int_{0}^{T} x(t)dt \tag{2.20}$$

With these coefficients, the waveform $x(t)$ in $0 \leq t < T$ can be expressed by

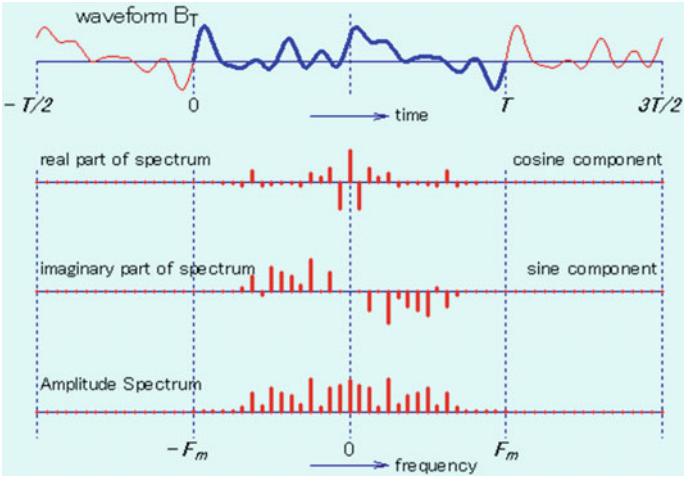

Fig. 2.8 Fourier series obtained when the extracted waveform B_T is assumed to be periodic. Animation available in supplementary files under filename E2-08_F-Coeff_B.exe

$$x(t) = A_0 + A_1 \cos\left(2\pi \frac{1}{2T} t\right) + A_2 \cos\left(2\pi \frac{2}{2T} t\right) + A_3 \cos\left(2\pi \frac{3}{2T} t\right) + \cdots \tag{2.21}$$

This is called the "cosine Fourier series." By expressing the waveform in Fig 2.6 using the cosine Fourier series, the frequency components higher than F_m are not visible and it seems possible to approximate $x(t)$ with relatively low frequency components. At first glance, this method seems to be a good idea, but it is necessary to make sure if this is always the case.

Let's take an example ("waveform B_T") shown in Fig. 2.8. As shown in the figure, there are very few spectral lines in the range outside of $\pm F_m$. One reason is that the original waveform itself contains small levels of high frequency components. Another reason is that the waveform in $0 \leq t < T$ is connected smoothly at the joint to the preceding and following repetitive waveforms, which are shown by the dotted lines in the figure. The reader can check this by running the program Fig. 2.8.

Figure 2.9 shows an even function, "waveform B_{2TE}" with period $2T$ produced by adding the time-reversed waveform of B_T in the region $-T \leq t < 0$ and its spectra. Since waveform B_T increases sharply at $t = 0$, the symmetric waveform B_{2TE} has a large discontinuity at $t = 0$. Since it is an even function, the Fourier series is composed of cosine functions only. A comparison of Fig. 2.9 with Fig. 2.8 shows that waveform B_{2TE} has a larger distribution of spectra in the high frequency region. A reason for this is that there is a large trough (discontinuity) around $t = 0$. Since, the more abrupt the waveform change is, the larger the high frequency components are, Fig. 2.9 has larger high frequency components. This is necessary not to produce the waveform in $0 \leq t < T$, but to produce the symmetric

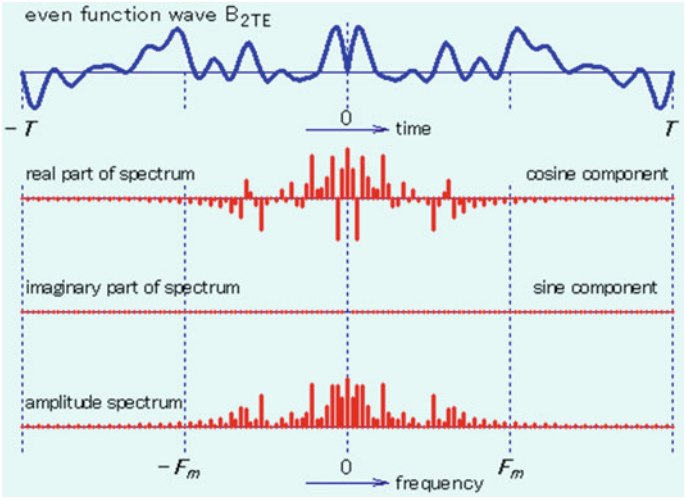

Fig. 2.9 Even waveform B_{2TE} with period $2T$ obtained by adding a symmetric waveform of B_T in the region $-T \leq t < 0$ and its spectra. Animation available in supplementary files under filename E2-09_EvenF_B.exe

waveform in the negative time range. If more components are necessary, the benefit of expressing the waveform only by the cosine series is lost. What can be done to avoid this?

2.4 Expressing Waveforms by Odd Functions

The even function B_{2TE} with period $2T$ produced by adding the time-reversed waveform of B_T into the region $-T \leq t < 0$ has more higher frequency components than B_T. Another way of connecting B_T in the region $-T \leq t < 0$ is to reverse B_T in time and also to reverse its sign, resulting in an *odd function* as shown in Fig. 2.10.

Figure 2.10 clearly shows that the connection at $t = 0$ is now smooth and the spectral distribution is narrower than Fig. 2.9. Since the waveform is an odd function, its Fourier series contains only sine components. It became possible to express the series only by sine functions with lower levels of the high frequency components. The reason why the levels of the high frequency components are kept low is that the connected waveform has no abrupt change at $t = 0$ and at $\pm T$. This assures smooth connections at $t = 0$, and $\pm T$. On the other hand, if an odd waveform A_{2TO} is made from A_T, levels of the high frequency components are increased. This can be checked by running the program in the CD

Let's write down the Fourier coefficients for the case of odd functions. Since the waveform is made anti-symmetric, the coefficients are all sine waves. If a time-

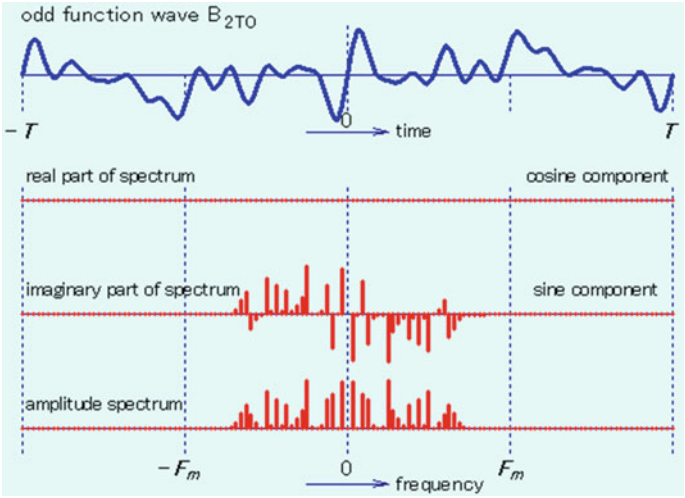

Fig. 2.10 Odd waveform B_{2TO} with period $2T$ produced by adding the time-reversed and sign-reversed waveform of B_T in the region $-T \leq t < 0$, and its spectra. Animation available in supplementary files under filename E2-10_OddF_B.exe

reversed and sign-reversed signal $-x(-t)$ of the original waveform $x(t)$ $(0 \leq t < T)$ is introduced into the time range $-T \leq t < 0$, an odd function with period $2T$ is produced, which will be referred to as $z(t)$. The Fourier coefficients of $z(t)$ is given by changing the region of integration as

$$B_k = \frac{1}{T}\int_{-T}^{T} z(t)\sin\left(2\pi\frac{k}{2T}t\right)dt.$$

Since $z(t)$ and the sine functions are both odd functions, their products are even functions, and the above integral can be obtained by doubling the integration in the region $0 \leq t < T$.

$$B_k = \frac{2}{T}\int_{0}^{T} x(t)\sin\left(2\pi\frac{k}{2T}t\right)dt \tag{2.22}$$

By the use of these coefficients, the waveform $x(t)$ $(0 \leq t < T)$ is given only by sine terms.

$$x(t) = B_1\sin\left(2\pi\frac{1}{2T}t\right) + B_2\sin\left(2\pi\frac{2}{2T}t\right) + B_3\sin\left(2\pi\frac{3}{2T}t\right) + \cdots \tag{2.23}$$

This is called the *sine Fourier series*.

In the Fourier series expansion of a portion of a waveform, both sine and cosine terms are necessary. In the discussion in Sects. 2.3 and 2.4, it was made clear that,

depending on the way of combining the same waveform and making a new waveform with period $2T$, it can be expressed solely by sine or cosine terms. Which one to choose may depend on the property of the waveform as well as signal processing needed later. However, it is clear that the choice of methods is dependent on the waveform.

2.5 Expressing Waveforms by Complex Exponential Functions

In Sect. 1.7, it was shown that the sine and cosine waves can be replaced by a complex exponential function, of which the real part is the cosine function and the imaginary part is the sine function. A geometrical expression of the complex exponential function by a rotating vector on the complex plane led to the idea of phase "lead" or phase "delay", which corresponds to the positive or negative angle of the rotating vector at $t = 0$ measured counter-clockwise from the positive real axis. More benefits, such as the simpler expression of the series and convenient mathematical handling tools, are gained by the introduction of the complex exponential functions into the Fourier series expansion.

In order to introduce the Fourier series expansion expressed by complex exponential functions, some of the equations that have been shown before will be listed here.

$$a_0 = A_0 T = \int_{-T/2}^{T/2} x(t)dt \tag{2.24}$$

$$a_k = \frac{A_k}{2} T = \int_{-T/2}^{T/2} x(t) \cos\left(2\pi \frac{k}{T} t\right) dt \tag{2.25}$$

$$b_k = \frac{B_k}{2} T = \int_{-T/2}^{T/2} x(t) \sin\left(2\pi \frac{k}{T} t\right) dt \tag{2.26}$$

Using the above equations, Eq. (2.1) can be rewritten as Eq. (2.27)

$$\begin{aligned} x(t) =& \frac{1}{T}\left[a_0 + 2a_1 \cos\left(2\pi \frac{1}{T} t\right) + 2a_2 \cos\left(2\pi \frac{2}{T} t\right) + 2a_3 \cos\left(2\pi \frac{3}{T} t\right) + \cdots \right. \\ & \left. + 2b_1 \sin\left(2\pi \frac{1}{T} t\right) + 2b_2 \sin\left(2\pi \frac{2}{T} t\right) + 2b_3 \sin\left(2\pi \frac{3}{T} t\right) + \cdots\right] \\ =& \frac{1}{T} a_0 + \frac{2}{T} \sum_{k=1}^{\infty} \left[a_k \cos\left(2\pi \frac{k}{T} t\right) + b_k \sin\left(2\pi \frac{k}{T} t\right)\right]. \end{aligned} \tag{2.27}$$

The use of Euler's formula (Eq. 1.3) enables us to express the cosine and sine functions using complex exponential functions.

$$x(t) = \frac{1}{T}a_0 + \frac{2}{T}\sum_{k=1}^{\infty}\frac{1}{2}[(a_k - jb_k)\exp(j2\pi\frac{k}{T}t) + (a_k + jb_k)\exp(-j2\pi\frac{k}{T}t)]$$

By introducing new coefficients X_k, and defining $X_{-k} = X_k^*$, Eq. (2.28) can be derived.

$$x(t) = \frac{1}{T}\sum_{k=-\infty}^{\infty} X_k \exp\left(j2\pi\frac{k}{T}t\right) \tag{2.28}$$

Now let's get an expression for the coefficient X_k. Multiplying both sides of Eq. (2.28) by $\exp\{-j2\pi(m/T)\}$ and integrating from $-T/2$ to $T/2$:

$$\int_{-T/2}^{T/2} x(t)\exp\left(-j2\pi\frac{m}{T}t\right)dt = \frac{1}{T}\sum_{k=-\infty}^{\infty} X_k \int_{-T/2}^{T/2}\exp\left(j2\pi\frac{k}{T}t\right)\exp\left(-j2\pi\frac{m}{T}t\right)dt$$

The integration on the right-hand side becomes

$$\int_{-T/2}^{T/2}\exp\left(j2\pi\frac{m}{T}t\right)\exp\left(-j2\pi\frac{m}{T}t\right)dt = \int_{-T/2}^{T/2} dt = T$$

for $k = m$, and

$$\int_{-T/2}^{T/2}\exp\left(j2\pi\frac{k-m}{T}t\right)dt = 0$$

for $k \neq m$. Then Eq. (2.29) is obtained.

$$X_k = \int_{-T/2}^{T/2} x(t)\exp\left(-j2\pi\frac{k}{T}t\right)dt \tag{2.29}$$

Equation (2.28) is the Fourier series expressed by the use of complex exponential functions and Eq. (2.29) is the equation used to obtain the coefficients. The coefficient X_k is referred to as the "amplitude" of the complex wave componentexp$\{-j2\pi(k/T)\}$, in the same way that A_k and B_k are the amplitudes of cosine and sine waves, respectively. However, since X_k is complex, it is referred to as the *complex amplitude*". The situation may seem to be more complicated but it is not. There is the same number of coefficients A_k's for positive and negative k's and the real and imaginary parts are even and odd, respectively. Since $\exp\{-j2\pi(k/T)\}$

has a real (even) part and an imaginary (odd) part, the expression of the Fourier series becomes simpler than using sine and cosine functions. In following sections, describing digital processing carried out using computers, the complex exponential functions will be used most of the time.

Equation (2.28) is the equation that gives a waveform from the complex coefficients when the Fourier series is expressed by the complex exponential functions. On the other hand, Eq. (2.29) gives a complex amplitude of the coefficients from the waveform. These are the pairs of expressions that exist between the waveform and the complex amplitude of each harmonic. If a waveform is given, its complex coefficients are obtained by Eq. (2.29); if the complex coefficients are given, the waveform is recovered by Eq. (2.28).

The waveform $x(t)$ is the time-dependent function and the Fourier coefficient X_k is dependent on the order k of each frequency component. Therefore, X_k is considered a frequency-dependent function. In this sense, $x(t)$ and X_k are referred to as *time domain* and *frequency domain functions*, respectively. The terms X_k are referred to as *complex Fourier coefficients* or *complex spectra*.

Let's check the similarities and differences between Eqs. (2.28) and (2.29). Equation (2.28) gives a waveform of time domain function obtained by multiplying the Fourier coefficients, i.e., the complex spectra, by complex exponential functions whose exponents are purely imaginary with positive sign. Equation (2.29) gives Fourier coefficients (complex spectra) of the frequency domain function, which is obtained by multiplying the waveform in the time domain by the complex exponential functions, whose exponents are purely imaginary with negative sign. There is much similarity between the two equations except that the exponents have opposite signs and Eq. (2.28) is composed of summations and Eq. (2.29) is composed of integrations. The latter may seem to be a major difference. This is caused by the fact that the frequency spectra exist at discrete points on the frequency axis (because the waveform is periodic). In this case, the integration on the frequency domain becomes a summation (with multiplication) at its extremity. The opposite sign of the exponent will be discussed in the next section. Thus far, the region of integration has been from $-T/2$ to $T/2$. As has been discussed before, this is not a necessary condition. It can be from T_1 to T_2 as long as $T = T_2 - T_1$. Then Eq. (2.29) becomes

$$X_k = \int_{T_1}^{T_1+T} x(t) \exp\left(-j2\pi \frac{k}{T} t\right) dt. \tag{2.30}$$

The equation for obtaining the time function is still the same (Eq. 2.28). The difference is that the integration interval is from T_1 to T_2. The property that the cosine function is even and the sine function is odd is inherent in the property of X_k in that the real and imaginary parts are the even and odd functions of k.

The property of periodicity remains the same when Eq. (2.28) is applied to the region outside of $T_1 \leq t < T_2$. This can be checked by substituting t by $t + pT$ (p: integer).

$$x(t+pT) = \frac{1}{T}\sum_{k=-\infty}^{\infty} X_k \exp\left\{j2\pi\frac{k}{T}(t+pT)\right\}$$
$$= \frac{1}{T}\sum_{k=-\infty}^{\infty} X_k \exp\left(j2\pi\frac{k}{T}t\right)\exp(j2\pi kp)$$

Since k and p are both integers,

$$\exp(j2\pi kp) = 1.$$

Therefore

$$x(t+pT) = \frac{1}{T}\sum_{k=-\infty}^{\infty} X_k \exp\left(j2\pi\frac{k}{T}t\right) = x(t). \tag{2.31}$$

The time function $x(t + pT)$ repeats itself with period T.

2.6 Fourier Transform

We have discussed the method of expressing a waveform with length T by the sine and cosine functions with period T. The reader may have noticed that there is no restriction on the period T. Then, what happens if the period T is made infinite?

Let's make the region of integration from $-T$ to T by keeping the waveform unchanged in Eq. (2.29), that is, by using the same time period $-T/2 \le t < T/2$ to extract the portion of the waveform, and assigning zeros to the regions $-T \le t < -T/2$ and $T/2 \le t < T$. Equation (2.29) will be rewritten using m instead of k,

$$U_m = U\left(\frac{m}{2T}\right) = \int_{-T}^{T} x(t)\exp(-j2\pi\frac{m}{2T}t)dt \tag{2.32}$$

The integration length is doubled to $2T$, and the fundamental frequency is halved to $1/2T$ but no other changes are made. The length of the extracted waveform is T but the spacing between the spectral lines is $1/2T$. Since zeros have been added to the regions $-T \le t < -T/2$ and $T/2 \le t < T$, the region of integration of Eq. (2.32) can be reduced to $-T/2 \le t < T/2$.

$$U_m = U\left(\frac{m}{2T}\right) = \int_{-T/2}^{T/2} x(t)\exp(-j2\pi\frac{m}{2T}t)dt \tag{2.33}$$

Comparing Eqs. (2.29)–(2.32), the reader will find that they are equal if $m = 2\ k$. Since m and k are both integers, the value U_m is equal to X_k when m is even.

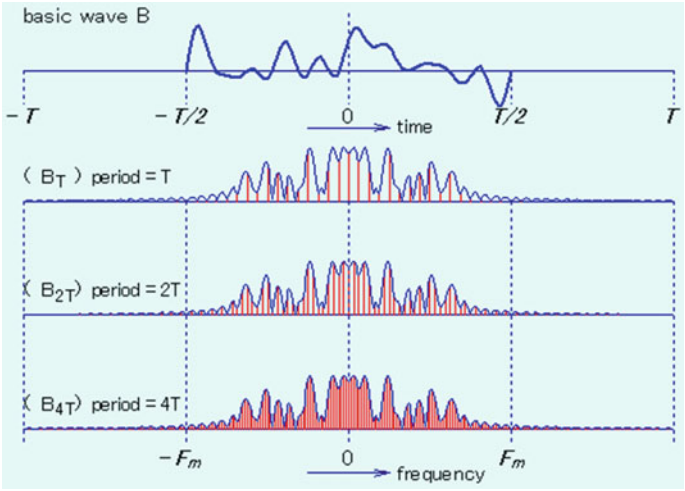

Fig. 2.11 Change in the power spectrum due to the change in the period for the computation of Fourier coefficients of waves B_T, B_{2T} and B_{4T}. Animation available in supplementary files under filename E2-11_VariP.exe

$$U_{2k} = X_k \tag{2.34}$$

What is described above is shown in Fig. 2.11. The top chart is the waveform B_T. The spectrum obtained with the integration T is shown by the vertical lines in the second chart (S_T). If zeros are added to the region $-T \leq t < -T/2$ and $T/2 \leq t < T$, and if the integration over the period $2T$ is carried out, the spectrum shown in the next chart (B_{2T}) is obtained. The shape of the spectrum distribution is not changed but the spacing between the spectral lines is halved.

In the case of the waveform that has zeros except for the region $-T/2 \leq t < T/2$, after integration over the region $-mT \leq t < mT$, the fundamental frequency becomes $1/(2mT)$. The following relation exists (m : integer).

$$U_{2mk} = X_k \tag{2.35}$$

The bottom chart in Fig. 2.11 shows the spectrum of B_{4T} for the case $m = 2$ (integration over period $-2T \leq t < 2T$). The spectral spacing is 1/2 of B_{2T} and 1/4 of B_T. The continuous thin line in each chart is the spectrum when m is made infinite, i.e., when the period of the periodic function is made infinite.

In Fig. 2.11, the same lengths of zeros are added to both sides of the extracted waveform B_T. It is also possible to add zeros to one side of the extracted waveform, but in this case, the origin of the time axis is changed and the equivalent phase shifts will be produced. However, the power spectrum is kept unchanged. This can be confirmed by running the program.

Now, let's consider the case when the extracted waveform is unchanged and the integration range is made infinite (i.e., the integration region is $-\infty \leq t < \infty$). In this case the spectral spacing becomes infinitely small and the distribution of Fourier coefficients becomes a continuous function of frequency. Then, Eq. (2.29) becomes:

$$X(f) = \lim_{m\to\infty} X\left(\frac{k}{2mT}\right) = \lim_{m\to\infty} \int_{-mT}^{mT} x(t) \exp\left(-j2\pi \frac{k}{2mT} t\right) dt \tag{2.36}$$

If we use $f = \lim_{m\to\infty} \{k/2mT\}$, the frequency f can take continuous values, and the integration region becomes $-\infty \leq t < \infty$.

$$X(f) = \int_{-\infty}^{+\infty} x(t) \exp(-j2\pi ft) dt \tag{2.37}$$

This is the equation known as the *Fourier transform* using complex exponential functions . The Fourier coefficients X_k of the periodic function are line spectra, but $X(f)$ defined by Eq. (2.37) is a continuous function of frequency. The continuous curve shown in each of the spectral charts in Fig. 2.11 is $X(f)$ obtained by letting m be infinite. As shown by Fig. 2.11, the envelope of the line spectra of a periodic waveform is the continuous spectrum of the waveform that is made from only one extracted waveform in the infinite time domain. The k-th Fourier coefficient of the periodic waveform is equal to the value of the continuous spectrum at $f = k/T$. These will be understood by considering the process starting from Eqs. (2.32) and (2.33) and reaching Eq. (2.37), which is obtained by letting the integration region be $-\infty \leq t < \infty$.

Equation (2.27) is the Fourier transform that calculates the spectrum $X(f)$ from a waveform $x(t)$ which is a function of time. It is necessary to have an inverse Fourier transform as the counterpart of the Fourier transform. This will be derived by replacing k/T in Eq. (2.28) by f and replacing the summation by the integration. Since $1/T$ in Eq. (2.28) is an inverse of time, it has the dimension of frequency, and as time T becomes infinitely large, its inverse $1/T$ should be represented as df. Then, Eq. (2.28) is rewritten as

$$x(t) = \int_{-\infty}^{+\infty} X(f) \exp(j2\pi ft) df \tag{2.38}$$

Equations (2.37) and (2.38) are the Fourier transform and inverse Fourier transform using complex exponential functions, respectively, and is known as the *Fourier transform pair*.

Let's check what happens when the waveform $x(t)$ is delayed by τ, which is represented by $x(t-\tau)$. Replacing $x(t)$ in Eq. (2.37) by $x(t-\tau)$:

$$X'(f) = \int_{-\infty}^{+\infty} x(t-\tau)\exp(-j2\pi ft)dt$$

An introduction of a new parameter $u = (t-\tau)$, since $t = u + \tau$ and $dt = du$, makes it possible to replace the parameter t by $u + \tau$.

$$\begin{aligned} X'(f) &= \int_{-\infty}^{+\infty} x(u)\exp(-j2\pi fu)\exp(-j2\pi f\tau)du \\ &= \int_{-\infty}^{+\infty} x(u)\exp(-j2\pi fu)du \cdot \exp(-j2\pi f\tau) = X(f)\exp(-j2\pi f\tau) \end{aligned} \tag{2.39}$$

The spectrum of the waveform with time delay τ is given by the product of the original Fourier spectrum $X(f)$ and$\exp(-j2\pi f\tau)$.

Conversely, the inverse Fourier transform of the product of $X(f)$ and$\exp(-j2\pi ft)$ gives the original waveform but with time delay τ. This is shown as follows. The substitution of $X(f)$ by $X(f)\exp(-j2\pi f\tau)$ gives

$$\begin{aligned} x'(t) &= \int_{-\infty}^{+\infty} X(f)\exp(-j2\pi f\tau)\exp(j2\pi ft)df \\ &= \int_{-\infty}^{+\infty} X(f)\exp\{j2\pi f(t-\tau)\}df = x(t-\tau). \end{aligned} \tag{2.40}$$

In preparation for later digital processing, let's check the Fourier transform of the unit impulse (Dirac's delta function in the time domain)$\delta(t)$. The unit impulse satisfies

$$\int_{-\infty}^{+\infty} \delta(t)dt = 1.$$

The spectrum of the unit impulse is given by

$$X(f) = \int_{-\infty}^{+\infty} \delta(t)\exp(-j2\pi ft)dt.$$

Since $\delta(t) = 0$ for $t \neq 0$ and, $\exp(-j2\pi ft) = 1$ for $t = 0$,

$$X(f) = \int_{-\infty}^{+\infty} \delta(t)\exp(-j2\pi ft)|_{t=0}dt = \int_{-\infty}^{\infty} \delta(t)dt = 1. \tag{2.41}$$

The Fourier transform of the unit impulse is equal to 1 at all frequencies.

The Fourier transform (FT) of the impulse $\delta(t-\tau)$ that exists at $t = \tau$, is obtained directly from Eq. (2.37). By letting $x(t) = \delta(t-\tau)$, we have

$$\mathrm{FT}\{\delta(t-\tau)\} = \int_{-\infty}^{+\infty} \delta(t-\tau)\exp(-j2\pi ft)dt$$

Since the integrand is nonzero at $t = \tau$, the above equation is rewritten as

$$\begin{aligned}\mathrm{FT}\{\delta(t-\tau)\} &= \int_{-\infty}^{+\infty} \delta(t-\tau)\exp(-j2\pi f\tau)dt \\ &= \exp(-j2\pi f\tau)\int_{-\infty}^{\infty} \delta(t-\tau)dt \\ &= \exp(-j2\pi f\tau)\end{aligned} \tag{2.42}$$

Equation (2.42) shows that the spectrum of an impulse that exists at $t = \tau$ is given by $\exp(-j2\pi f\tau)$. This means that the absolute value of the spectrum of an impulse is 1 for all frequencies and the phase delay at frequency f is equal to the product of the time delay and$2\pi f$. The statement above may seem superfluous since the same result has been already shown in Fig. 1.16, and is obvious from Eqs. (2.39) and (2.42). However, this result will play an important role in Chap. 4.

Let's introduce another important theorem of the Fourier transform: the energy of the time function $x(t)$, is given by the integral of the absolute Fourier transform squared over the range $-\infty \leq f < \infty$.

$$\int_{-\infty}^{+\infty} |x(t)|^2 dt = \int_{-\infty}^{+\infty} x(t)x^*(t)dt = \int_{-\infty}^{+\infty} x(t)\left[\int_{-\infty}^{+\infty} X^*(f)\exp(-j2\pi ft)df\right]dt$$

where $x^*(t)$ is the complex conjugate of $x(t)$ (the imaginary part of it would have the opposite sign of $x(t)$). By changing the order of integration,

$$\begin{aligned}\int_{-\infty}^{+\infty} |x(t)|^2 dt &= \int_{-\infty}^{+\infty} X^*(f)\left[\int_{-\infty}^{+\infty} x(t)\exp(-j2\pi ft)dt\right]df \\ &= \int_{-\infty}^{+\infty} X^*(f)X(f)df\end{aligned}$$

which gives,

$$\int_{-\infty}^{+\infty} |x(t)|^2 dt = \int_{-\infty}^{+\infty} |X(f)|^2 df \tag{2.43}$$

Equation (2.43) affirms that "the energy of the Fourier spectrum $X(f)$ obtained from the Fourier transform of $x(t)$ has the same energy as $x(t)$." This is known as *Parseval's formula*.

The same idea is applicable to the Fourier series expansion. Let's calculate the energy in one period of $x(t)$ using Eqs. (2.28) and (2.29).

$$\int_{-T/2}^{+T/2} |x(t)|^2 dt = \int_{-T/2}^{+T/2} x(t)x^*(t)dt = \int_{-T/2}^{+T/2} x(t)\left[\frac{1}{T}\sum_{k=-\infty}^{\infty} X_k^* \exp(-j2\pi\frac{k}{T}t)\right]dt$$

Reversing the order of integration,

$$\begin{aligned}\int_{-T/2}^{+T/2} |x(t)|^2 d &= \sum_{k=-\infty}^{\infty} X_k^*\left[\frac{1}{T}\int_{-T/2}^{+T/2} x(t)\exp(-j2\pi\frac{k}{T}t)dt\right] \\ &= \frac{1}{T}\sum_{k=-\infty}^{\infty} X_k^* X_k\end{aligned}.$$

Then, the following equation is obtained.

$$\int_{-T/2}^{+T/2} |x(t)|^2 dt = \frac{1}{T}\sum_{k=-\infty}^{\infty} |X_k|^2 = F\sum_{k=-\infty}^{\infty} |X_k|^2 \tag{2.44}$$

where $F = 1/T$ is the spacing of the Fourier spectrum. This is Parseval's relation in the case of a Fourier series expansion. The energy of one period of a periodic function is equal to the summation of squares of Fourier coefficients multiplied by the frequency spacing.

Appendixes 2A–C are supplements of Chap. 2. They will be useful for a better understanding of the following chapters.

2.7 Gibbs' Phenomenon

By the end of the previous section, it was shown that any periodic waveform can be expanded by a Fourier series, which requires an infinite number of harmonics. As can be seen in Fig. 2.12, the Fourier series expansions of a rectangular waveform up to the 5-th, 10-th, and 50-th harmonic gradually approach the rectangle, but overshoots are observed near the edges of the waveform. The height of the overshoot seems to approach a fixed value as the number of harmonics increases. This phenomenon was named *Gibbs Phenomenon* after the discoverer, Gibbs. Let's check how the height of the Gibbs Phenomenon is determined.

The Fourier series expansion of a periodic rectangular waveform $x(t)$ with the period T, $x(t) = -1$ for $-T/2 < t < 0$, and $x(t) = 1$ for $0 < t < T/2$, is given by

$$x(t) = \frac{4}{\pi}\sum_{k=0}^{\infty}\frac{1}{2k+1}\sin\left(2\pi\frac{2k+1}{T}t\right). \tag{2.45}$$

The partial sum up to the $(K-1)$-th harmonic is given by

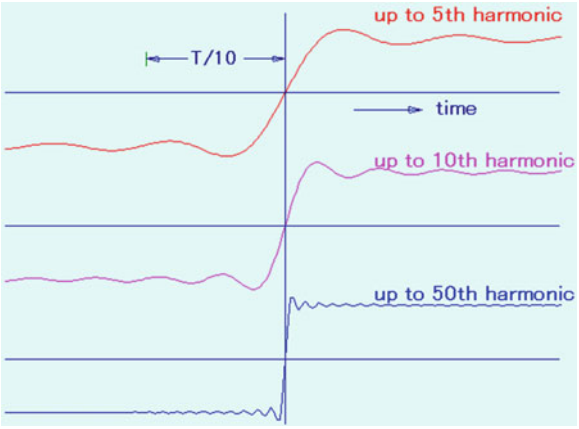

Fig. 2.12 Waveform of step wave synthesized by finite number of harmonics. Animation available in supplementary files under filename E2-12_GIBBS.exe

$$\begin{aligned} x_K(t) &= \frac{4}{\pi T}\sum_{k=0}^{K-1}\frac{T}{2k+1}\sin\left(2\pi\frac{2k+1}{T}t\right) \\ &= \frac{8}{T}\sum_{k=0}^{K-1}\int_0^t \cos\left(2\pi\frac{2k+1}{T}u\right)du. \end{aligned} \tag{2.46}$$

By exchanging the order of the sum and the integration, the following is obtained.

$$x_K(t) = \frac{8}{T}\int_0^t \sum_{k=0}^{K-1}\cos\left(2\pi\frac{2k+1}{T}u\right)du \tag{2.47}$$

Let the integrand be

$$S_K = \sum_{k=0}^{K-1}\cos\left(2\pi\frac{2k+1}{T}u\right). \tag{2.48}$$

The multiplication of S_k with $\sin(2\pi u/T)$ becomes

$$\begin{aligned} S_K\sin\left(2\pi\frac{u}{T}\right) &= \sum_{k=0}^{K-1}\left[\sin\left(2\pi\frac{u}{T}\right)\cos\left(2\pi\frac{2k+1}{T}u\right)\right] \\ &= \sin\left(2\pi\frac{u}{T}\right)\cos\left(2\pi\frac{u}{T}\right) + \sin\left(2\pi\frac{u}{T}\right)\cos\left(2\pi\frac{3u}{T}\right) + \cdots \\ &\cdots + \sin\left(2\pi\frac{u}{T}\right)\cos\left(2\pi\frac{2K-1}{T}u\right). \end{aligned}$$

Since

$$\sin\left(2\pi\frac{u}{T}\right)\cos\left(2\pi\frac{ru}{T}\right)=\frac{1}{2}\left[\sin\left(2\pi\frac{r+1}{T}u\right)-\sin\left(2\pi\frac{r-1}{T}u\right)\right]$$

it is rewritten as

$$\begin{aligned}2S_K\sin\left(2\pi\frac{u}{T}\right)&=\sin\left(2\pi\frac{2}{T}u\right)+\sin\left(2\pi\frac{4}{T}u\right)-\sin\left(2\pi\frac{u}{T}\right)+\cdots\\&\cdots+\sin\left(2\pi\frac{2K}{T}u\right)-\sin\left(2\pi\frac{2K-2}{T}u\right)\\&=\sin\left(2\pi\frac{2K}{T}u\right).\end{aligned}$$

Therefore

$$S_K=\frac{1}{2}\frac{\sin\left(2\pi\frac{2K}{T}u\right)}{\sin\left(2\pi\frac{1}{T}u\right)}. \tag{2.49}$$

Then, Eq. (2.47) becomes

$$x_K(t)=\frac{4}{T}\int_0^t\frac{\sin\left(2\pi\frac{2K}{T}u\right)}{\sin\left(2\pi\frac{1}{T}u\right)}du \tag{2.50}$$

The function $x_K(t)$. takes maxima or minima at times when its time-derivative equals 0.

$$\frac{dx_K(t)}{dt}=\frac{4}{T}\frac{\sin\left(2\pi\frac{2K}{T}t\right)}{\sin\left(2\pi\frac{1}{T}t\right)}=0 \tag{2.51}$$

Those are given by

$$t=\frac{mT}{4K}\ (m=1,2,3,\cdots,K). \tag{2.52}$$

The function $x_K(t)$ takes maxima or minima when m is odd or even, respectively. The largest of the maxima is given when m is 1.

$$x_K(\frac{T}{4K})=\frac{4}{T}\int_0^{\frac{T}{4K}}\frac{\sin\left(2\pi\frac{2K}{T}u\right)}{\sin\left(2\pi\frac{1}{T}u\right)}du$$

By the variable transformation

$$v = 2\pi \frac{2K}{T} u.$$

$x_K(t)$ is given by

$$x_K(\frac{T}{4K}) = \frac{2}{\pi} \int_0^{\pi} \frac{\sin(v)}{v} \frac{\frac{v}{2K}}{\sin\left(\frac{v}{2K}\right)} dv. \tag{2.53}$$

The limit given when K approaches infinity is

$$\lim_{K \to \infty} x_K \left(\frac{T}{2K}\right) = \frac{2}{\pi} \int_0^{\pi} \frac{\sin v}{v} dv \cong 1.17898.$$

The overshoot is approximately 18 %.

The time width of the overshoot becomes infinitely small as K approaches infinity, and therefore the power of the overshoot becomes zero. Similar phenomena are observed in functions other than rectangular, which take different values when t approaches a discontinuity from the negative and the positive directions. These are also referred to as *Gibbs' Phenomena*.

2.8 Exercises

1. What is the orthogonal property of sine and cosine functions?
2. Derive Eq. (2.8) used to obtain Fourier coefficients B_k.
3. If a function $x(t)$ defined in the region $0 \leq t < T$ is represented by a summation of an even function $x_e(t)$ and an odd function $x_o(t)$, both defined in the region $-T \leq t < T$, derive equations for $x_e(t)$ and $x_o(t)$.
4. Describe the properties of $x_e(t)$ and $x_o(t)$ defined in Problem 3.
5. When the Fourier expansion is applied to a function $x(t)$ defined in the region $0 \leq t < T$, what are the frequencies of the individual frequency components?
6. What is the complex exponential function?
7. What is the relationship between the even and odd functions in $x(t)$ and the real and imaginary parts of its complex Fourier transform $X(f)$?
8. Express a cosine wave with the phase lead of 45° using a complex exponential function.
9. Express a cosine wave with the phase lead of θ using a complex exponential function.
10. A function $x(t)$ defined in the region $-\infty < t < \infty$ as zero everywhere except in the region $0 \leq t < T$ has Fourier transform $X(f)$. When a Fourier series expansion is applied to this same function in the region $0 \leq t < T$, what would you expect to get as the Fourier series?
11. When a Fourier series expansion is applied to $x(t)$ in Problem 10 over the region $-nT \leq t < nT$, what would you expect to get as the Fourier series?

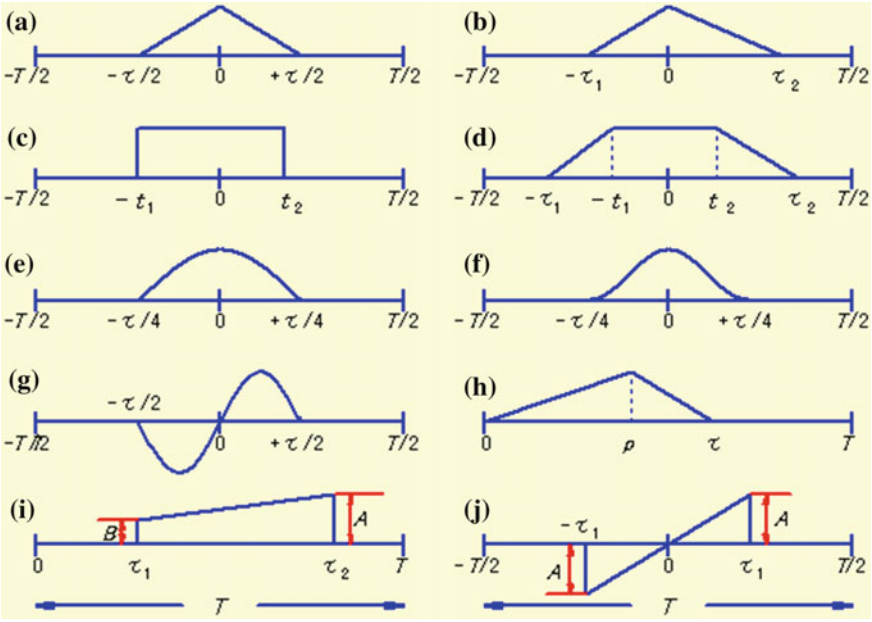

Fig. 2.13 Waveforms with period T

Give answers for $n = 1$, $n =$ arbitrary integer, and $n \cong$ an infinitely large integer.

12. Obtain Fourier coefficients of the functions (a)–(j) in Fig. 2.13. Assume the same peak value A for each waveform and the starting value in (i) be B.

Chapter 3
Numerical (Digitized) Waveforms

Old analog techniques of Fourier analyzing signals are passé due to major advances in digital technology. Modern digital processing involves sampling analog time signals that are obtained from transducers (such as microphones or accelerometers) at uniform time intervals. Taking values of a waveform at discrete times (mostly at uniform time intervals) is called *sampling* and the sampled waveform is referred to as *a numerical* (*digitized*) *waveform*. Numerical waveforms are used for:

- Storing data
- Analyzing data
- Transmitting data

When representing a waveform by a sequence of numerical values, the analyst must decide the time interval of the sampling, i.e., the *sampling time* (*or sampling period*). The first aim of this chapter is to make clear how to determine the sampling time. After that, a discussion on how to recover a continuous waveform from the sequence of sample values is given.

The number of significant digits of the digitized or sampled data is also important when sampling (i.e., *digitizing*) the analog waveforms. At the early stage of the digital age, the accuracy of the sample values was an important subject of discussion. However, due to the advancement of signal processing techniques, achieving a high degree of precision in *digitization* has become less costly. The precision of digitization should be considered depending on individual applications and, therefore, this subject is not treated in this book.

3.1 Fourier Series Expansion of Spectrum

A numerical waveform is a sequence of numbers generated from the analog waveform by the sampling process, an example of which is given in Fig. 3.1. The instantaneous value x_n at the n-th sample is called a *sample value*. If information is not lost by the sampling process, the original waveform can be reconstructed from

K. Kido, *Digital Fourier Analysis: Fundamentals*,
Undergraduate Lecture Notes in Physics, DOI: 10.1007/978-1-4614-9260-3_3,

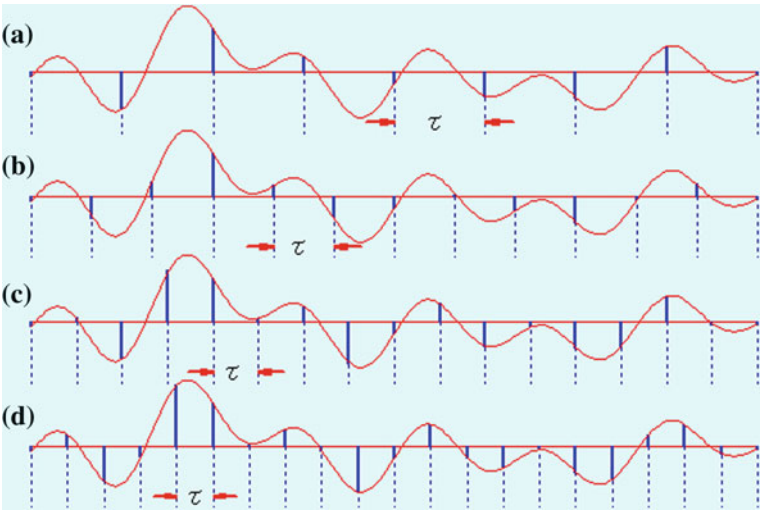

Fig. 3.1 Waveform and sequences of sample values with various sampling rates. Animation available in supplementary files under filename E3-01_SAMPLING.exe

the sample values. An obvious way to do so is to sample the waveform with a very small time interval. However, if the sample interval is too small, the data size becomes too large and sampling is not economical. On the other hand, if the sampling interval is too large, the reconstruction will be impossible.

The thick vertical lines in Fig. 3.1 represent sample values of a waveform when it is sampled at intervals that are 1/8 (a), 1/12 (b), 1/16 (c), and 1/20 (d) of the total length. The sequence shown in Fig. 3.1b is the limit of coarse sampling in the sense that it may not be possible to reconstruct the waveform when it is sampled at a wider step. However, it is difficult to determine the limit of coarse sampling visually and, therefore, a method to quantitatively determine the limit will be discussed. A hint is obtained from the spectrum and the Fourier coefficients.

It was made clear in the previous chapter that the coefficients of the Fourier series of an extracted waveform with length T from a longer continuous waveform are the amplitudes of sine and cosine waves with frequencies n/T ($n = 0, 1, 2, \ldots$). These amplitudes are equal to the amplitudes at the same frequencies on the continuous spectrum of the waveform with length T. This is shown in Fig. 3.2a. Representing a waveform by a Fourier series automatically assumes that the waveform is periodic with the period T; the assumed preceding and following waveforms are shown by the dotted lines in the Figure. Their line spectra have the spacing $1/T$; the real and imaginary parts are the coefficients of the cosine and sine waves, which are even and odd functions of frequency, respectively. This is only one example but there is a 1:1 relationship between the waveform and its spectrum. If the waveform is determined, its spectrum is also known, and vice versa.

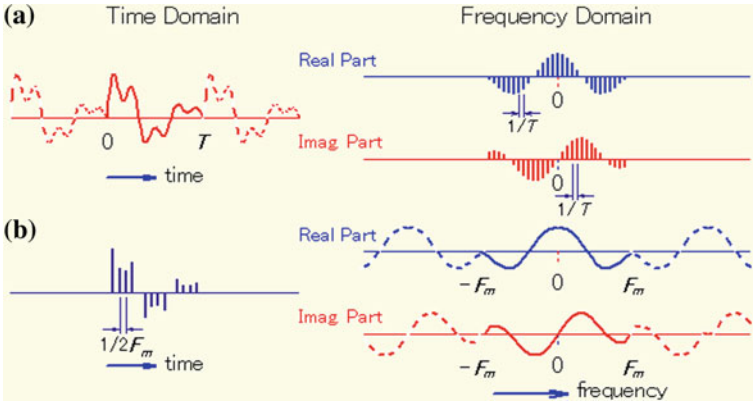

Fig. 3.2 **a** Periodic waveform with period T (**a**/*left*) and its Fourier coefficients (*line spectrum*) (**a**/*right*); **b** continuous periodic spectrum with period $2F_m$ (**b**/*right*) and its Fourier coefficients (*line pulses* with $(1/2F_m)$ spacing) (**b**/*left*)

Let's take an example of the continuous spectrum of a continuous waveform, shown by the solid line in Fig. 3.2b, where the real and imaginary parts are even and odd functions of frequency, respectively. If the spectrum outside of $\pm F_m$ is zero, the same spectrum pattern on the frequency axis with period $2F_m$ can be added without overlapping the original spectrum. Considering that the spectrum is a periodic function, the Fourier series expansion can be applied. Since the periodic spectrum has an even real part and an odd imaginary part (see Eq. (2.29) and the paragraph below it), the Fourier series (left) has only the real part, and the spectral lines are located on the "time" axis with $(1/2F_m)$ spacing.

In the previous chapter, it was shown that the Fourier coefficients (line spectra) on the frequency axis agree with the continuous spectrum (see Fig. 2.11). For the same reason, the Fourier coefficients (line spectra) of the spectrum on the time axis should agree with the continuous function (the waveform) on the time axis. That is, the coefficients are the values of the waveform at $1/2F_m$ steps. In other words, the continuous waveform is reconstructed from the sample sequence at $1/2F_m$ steps.

One thing should be mentioned. If the Fourier series of the spectrum is calculated using $\exp(-j2\pi kf/2F_m)$ for the exponential function, the Fourier series on the time domain will be reversed. This problem is solved if $\exp(j2\pi kf/2F_m)$ is used. The reader is referred to Appendix 3, which discusses this matter.

From the above discussion, the reader may have inferred that sampling with a spacing equal to or less than $1/2F_m$, is enough to represent the continuous waveform.

The discussion so far has been too qualitative. For a stricter discussion, we can refer to Eq. (2.29) in the previous chapter.

The Fourier series expansion of a spectrum is an extract of a portion of the spectrum, and it is assumed that the spectrum repeats itself on the frequency axis. Since the real and imaginary parts of the spectrum are even and odd functions,

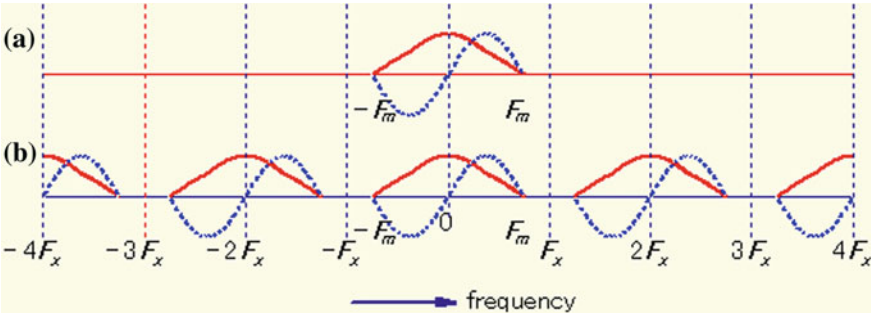

Fig. 3.3 A spectrum with the bandwidth equal to $\pm F_m$ (**a**) and a periodic spectrum with period $2F_x$ (where $F_x > F_m$) (**b**)

respectively, and they are distributed equally on the positive and negative sides of the axis, the frequency range of the extracted spectrum must have its center at the origin of the frequency axis. If the spectrum is actually distributed over a wider range than that of the extracted spectrum, the spectrum shape changes and the original waveform cannot be reconstructed. If the spectrum distribution is limited within $\pm F_m$, the range of the extracted spectrum must be within $\pm F_x$ (where $F_x \geq F_m$).

Consider the Fourier series expansion with period F_x of a spectrum shown in Fig. 3.3a. The Fourier series expansion assumes that the function is periodic as shown in Fig. 3.3b. This function has one period which is equal to the spectrum of Fig. 3.3a and it is periodic with period $2F_x$ ($\geq 2F_m$).

In order to check whether the coefficients of the Fourier series of the spectrum agree with the instantaneous values of the waveform, the waveform $x(t)$ and its spectrum $X(f)$ are required. The relationship between these two is expressed by the Fourier transform. However, since it is difficult to deal with an infinitely long waveform, it is assumed that $x(t)$ has nonzero values only within the time range $\pm T/2$. If it is necessary, the range can be made as long as desired. Then the spectrum is calculated by:

$$X(f) = \int_{-T/2}^{T/2} x(t) \exp(-j2\pi ft) dt. \tag{3.1}$$

If the spectrum $X(f)$ does not have any significant value outside the frequency range of $\pm F_m$, the range of integration of the inverse Fourier transform can be limited within $\pm F_x$ (where $F_x \geq F_m$). Therefore, the integration becomes

$$x(t) = \int_{-F_x}^{+F_x} X(f) \exp(j2\pi ft) df. \tag{3.2}$$

The Fourier series expansion is applied to the periodic spectrum shown in Fig. 3.3b, and is equal to $X(f)$ within the frequency range $\pm F_m$. The Fourier series is given by replacing t by f and $T/2$ by F_m in Eq. (2.29). Also it is necessary to change the sign of the exponential function since this is a transform from the frequency domain to the time domain (see Appendix 3). Then, the following is obtained

$$x_n = \int_{-F_x}^{+F_x} X(f) \exp(j2\pi \frac{n}{2F_x} f) df. \tag{3.3}$$

This equation is equal to Eq. (3.2) when t is replaced by $n/2F_x$. The Fourier coefficient x_n, of the periodic spectrum which is equal to $X(f)$ within the frequency range $\pm F_x$, is the sample value of $x(t)$ at $t = n/2F_x$.

$$x_n = x(n/2Fx) \tag{3.4}$$

So far, it has been shown that the sample values of $x(t)$ at $t = n/2F_x$ are obtained from the spectrum$X(f)$ of $x(t)$. If it is confirmed that the continuous waveform $x(t)$ is recovered from the sequence of sample values x_n, it implies that a method of sampling is established.

Let's review this process:

(1) $x(t)$ contains the spectrum $X(f)$ that is limited to the frequency range $\pm F_m$.
(2) Assume that the spectrum $X(f)$ of the waveform $x(t)$ is periodic with the period $2F_x$ (where $F_x \geq F_m$).
(3) Obtain the Fourier coefficients x_n from the periodic spectrum $X(f)$. The sign of the exponent of the exponential function must be positive so that the order of the coefficients agrees with the direction of the time axis.
(4) The resulting values x_n can be seen to agree with $x(t)$ at $t = n/2F_x$.
(5) The spectrum $X(f)$ is uniquely determined from the Fourier coefficients x_n (this is obvious from (3)). Since the coefficients x_n are the sample values of the waveform, it can be stated that $X(f)$ is uniquely determined from the sequence of time samples.
(6) The spectrum and the waveform have a 1:1 correspondence. Since $X(f)$ is the spectrum of a waveform $x(t)$, then, if $X(f)$ is determined, $x(t)$ is obtained by the inverse Fourier transform of $X(f)$.

The above discussion shows that the waveform $x(t)$ is determined uniquely from the sequence of sample values x_n, which are sampled with spacing $1/2F_x$. It can be stated that the method of sampling, without loss of information, has been established.

Remember that the sequence x_n, is obtained as the inverse Fourier transform of an infinitely long periodic spectrum, in which $X(f)$ is repeated infinitely with period $2F_x$. Therefore, the spectrum of the sequence x_n has an infinite distribution on the frequency axis. The reason why the spectrum has the infinite range is that each sample is an impulse that has an infinite frequency range. However, this spectrum

has the period $2F_x$, and the spectrum of the continuous waveform is limited within $\pm F_x$ and zero outside this range. Therefore, this frequency range (within $\pm F_x$) of the spectrum of x_n is called the *base frequency band*. The spacing of sequence x_n ($1/2F_x$) is called the *sampling period* and its reciprocal ($2F_x$) is called the *sampling frequency*.

3.2 Reproduction of the Continuous Waveform from the Sequence of Sample Values

It was shown in Sect. 3.1 that the original waveform can be reproduced from a sequence of sample values, which are sampled with the sampling period of $1/2F_x$, if the original waveform has a spectrum in the frequency range within $\pm F_x$. However, a concrete method of reconstructing the original waveform has not yet been derived. This is the aim of this section.

Let us summarize the previous section: the Fourier series expansion of the spectrum $X(f)$ sampled over the frequency range $-F_x$ to $+F_x$ produces a sequence of sample values x_n of a waveform $x(t)$ with sampling frequency $2F_x$. Since this sequence of sample values x_n has the sampling period $1/2F_x$, its spectrum is infinitely wide and periodic with period $2F_x$. But, since the spectrum within the band $\pm 2F_x$ is equal to the spectrum of the waveform $x(t)$ itself, then $x(t)$ can be reconstructed by the inverse Fourier transform of the spectrum within the band $\pm F_x$.

Now, an equation to calculate $X(f)$ will be derived using the fact that the sequence x_n is the coefficient of the Fourier series of that spectrum. For this purpose use Eq. (2.28) in Chap. 2, which is a formula to calculate Fourier series of a time domain waveform. To calculate the Fourier series of a spectrum, the parameters $t \to f$, $k \to n$, $T \to 2F_x$, and $X_k, \to x_n$ have to be replaced. We also need to replace j in the exponent by $-j$. Since the range of n defines the range in which the waveform exists, the number of samples is equal to $N = 2TF_x$ obtained by dividing the time length T by the sampling period $1/2F_x$. If n starts from 0, it ends at $N - 1$. Then, the Fourier series expansion of the spectrum becomes,

$$X(f) = \frac{1}{2F_x} \sum_{n=0}^{N-1} x_n \exp(-j2\pi \frac{n}{2F_x} f). \tag{3.5}$$

Because x_n is a sample sequence, the spectrum obtained by Eq. (3.5) is periodic with period $2F_x$. But, since the spectrum of the continuous waveform $x(t)$ is zero in the range outside of $\pm F_x$, the range of the inverse Fourier transform must be limited within the range $\pm F_x$. Then, $x(t)$ is calculated by

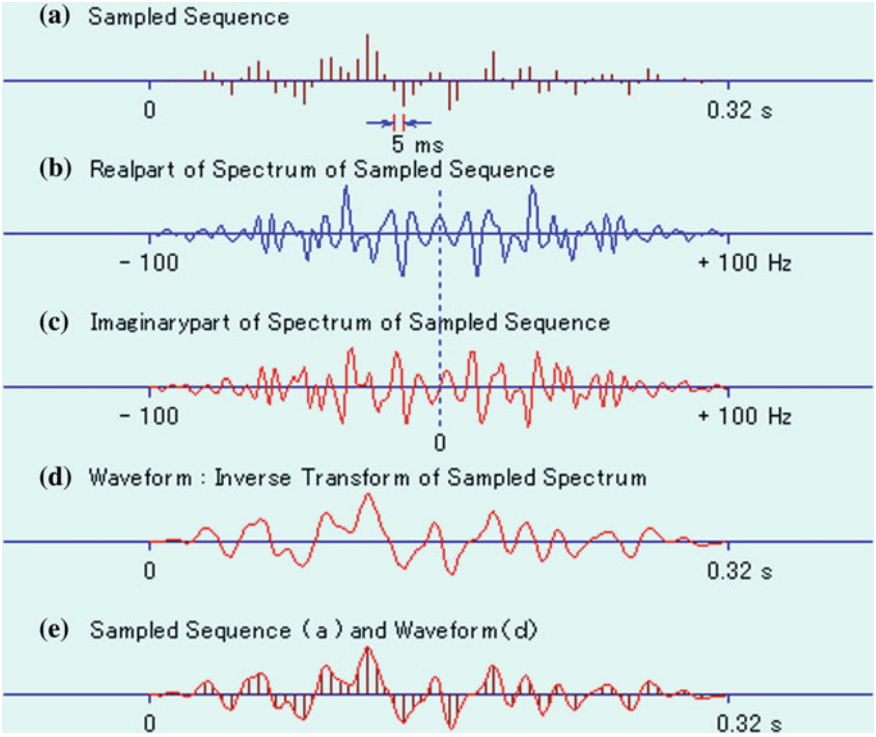

Fig. 3.4 Sequence of samples, its spectrum and time waveform. **a** Sample sequence, **b**, **c** real and imaginary parts of the spectrum of (**a**), **d** waveform obtained by the inverse Fourier transform from (**b**) and (**c**), **e** overlay of (**d**) and (**a**). Animation available in supplementary files under filename E3-04_DATrans.exe

$$x(t) = \int_{-F_x}^{+F_x} X(f) \exp(j2\pi ft) df. \tag{3.6}$$

The equations to obtain $x(t)$ from the sequence of sample values x_n sampled with the sampling period $1/2F_x$ have been formalized.

The spectrum of a sample sequence can be calculated using Eq. (3.5). A continuous waveform can then be obtained from the inverse Fourier transform of the spectrum within the range $\pm F_x$ using Eq. (3.6). Let us check this using an example.

One sequence is shown in Fig. 3.4a as an example. Figure 3.4a is a sequence of a 320 ms long waveform sampled with 5 ms sampling time, resulting in 64 samples. It is assumed that the sequence has all zero values except for these 64 samples. The spectrum obtained using Eq. (3.5) is an infinitely long periodic function with period of 200 Hz (=1/0.005 s) in the frequency domain.

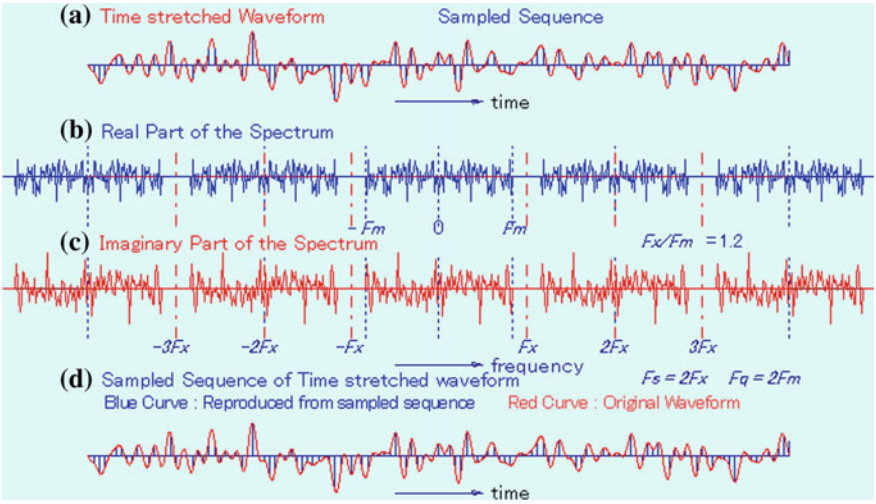

Fig. 3.5 **a** Waveform, whose spectrum is limited within $\pm F_m$, and sample values with sampling time $1/2F_x$, ($F_m \leq F_x$), **b** and **c** real and imaginary parts of the spectrum of the sample sequence, **d** sample sequence and inverse Fourier transform of the spectrum within the frequency range $2F_x$. Animation available in supplementary files under filename E3-05_SmPC.exe

The real and imaginary parts of the spectrum in the base frequency band are shown in Fig. 3.4b, c respectively. The same spectrum repeats itself outside the base band and is not shown in the figure. If the spectrum in the base band is inverse Fourier transformed, the continuous waveform shown in Fig. 3.4d is obtained. Fig. 3.4e is the overlay of Fig. 3.4a, d showing that Fig. 3.4a, d agree with each other at the sampling points.

3.3 Frequency Bandwidth and Sampling Frequency

Another example will be given as an introduction to this section. Figure 3.5a shows a waveform and its sampled values. This waveform was made so that its spectrum has nonzero values only within the frequency range $\pm F_m$. The real and imaginary parts of the spectrum $X(f)$ of the continuous waveform are shown in the base frequency bands in Fig. 3.5b, c respectively. If this waveform (Fig. 3.5a) is sampled with a sampling time $1/2F_x$, its spectrum becomes periodic with the frequency period $2F_x$. By applying Eq. (3.3) to $X(f)$, the sample values x_n (Fourier coefficients) are obtained, shown as many vertical lines with $1/2F_x$ spacing in Fig. 3.5d. Figure 3.5d also shows the original waveform. As expected, the ends of the vertical lines fall on the curve of the waveform, indicating that x_n are the sample values of the waveform. It can be seen that the waveform obtained by the inverse Fourier transform of the spectrum (Fig. 3.4b, c) within the frequency band

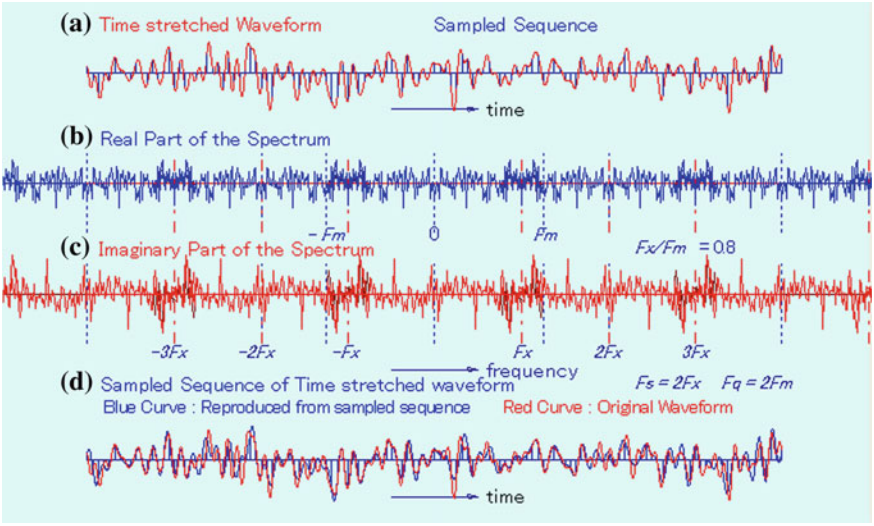

Fig. 3.6 **a** Waveform, whose spectrum is limited within $\pm F_m$, and sample values with sampling time $1/2F_x$, ($F_x \leq F_m$), **b** and **c** real and imaginary parts of the spectrum of the sample sequence, **d** sample sequence and inverse Fourier transform of the spectrum within $2F_x$ and the original waveform (*dotted line*). Animation available in supplementary files under filename E3-06_SmPC.exe

$\pm F_x = \pm 1.2F_m$ matches perfectly with the original waveform shown in Fig. 3.5a (only one curve is seen even though two curves are plotted).

It was found that, as long as the relationship $F_x \geq F_m$ is maintained as in the case of Fig. 3.5, the sample sequence is the set of the Fourier coefficients of the undistorted spectrum, and therefore a continuous waveform is recovered from the sample sequence. What happens if the condition $F_x \geq F_m$ is not satisfied? Figure 3.6 shows the case for $F_x = 0.8F_m$. Figure 3.6a shows the same waveform as in Fig. 3.5a. The sample sequence has $1/2F_x$ frequency spacing which, since $F_x = 0.8F_m$, is wider than the one shown in Fig. 3.5. The spectrum of the sample sequence is periodic with period $2F_x$. But, since the spectrum has the width $2F_m$, the spectrum overlaps with itself. As a consequence, the spectrum within the frequency range $\pm Fx$ differs from the spectrum of the continuous waveform. The properties that the real part is even, the imaginary part is odd, and their Fourier coefficients are real are still kept. If the Fourier coefficients are calculated assuming that the spectrum is periodic with period $2F_x$, the sequence of impulses shown in Fig. 3.6d is obtained. The waveform shown in Fig. 3.6a is also plotted in Fig. 3.6d. It can be seen that the ends of the vertical lines fall on the curve of both the reproduced (blue) and original (red) waveforms, indicating that x_n with period $2F_x$ are the sample values of the waveform, even though the two waveforms do not coincide.

Is it sufficient to use the sample sequence with sampling time $1/2F_x$, ($F_x \leq F_m$)? Can the original continuous waveform be reconstructed from this sequence? The answer is "no." In order to check this answer, the inverse Fourier transform is calculated using the spectrum (Fig. 3.6b, c) within the frequency range $\pm F_x$, assuming all zeros outside of the $\pm F_x$ frequency range; this is shown by the solid line in Fig. 3.6d. Unfortunately, however, it differs from the dotted line. They match only at the sampling points. The sample values shown in Fig. 3.6d are those of the samples at $1/2F_x$ steps but the original waveform of Fig. 3.6a cannot be reconstructed from this sample sequence.

Let us summarize the above results. If $F_x \geq F_m$, there is no spectral change by arranging the spectrum of the continuous waveform with period $2F_x$. Its Fourier coefficients, i.e., the sample values, are spaced on the time axis with $1/2F_x$ steps. The spectrum of this sample sequence matches that of the continuous spectrum within $\pm F_m$. Therefore, from this spectrum, the continuous waveform can be reconstructed.

On the other hand, if $F_x < F_m$, the spectrum of the sample sequence sampled with the sampling frequency $2F_x$ overlaps at both ends of the base frequency band as shown in Fig. 3.6b, c. Of course the inverse Fourier transform of the distorted spectrum differs from the original waveform, and therefore the original continuous waveform cannot be reconstructed.

In Fig. 3.5, since $F_x = 1.2F_m$, when the spectrum is repeatedly placed with period $2F_x$ on the frequency axis, the spectrum in one band does not interfere with those of neighboring bands. If $F_x > F_m$ is satisfied, the original waveform is reconstructed from the sample sequence. Therefore, two times the maximum frequency of the spectrum of the original continuous waveform is the minimum sampling frequency that enables the reconstruction of the waveform.

Let us take a different view point. If the spacing of the sample sequence is $1/F_s$, i.e., if the sampling frequency is F_s, that spacing will determine the maximum frequency of the spectrum of the waveform. The maximum frequency F_x, which is equal to $F_s/2$, is called the *Nyquist frequency*.

The reader can check what has been developed in this section by running the program with various ratios (F_x/F_m) of the Nyquist frequency F_x to the maximum frequency of the spectrum F_m.

3.4 Smoothing of Sample Sequence by Low-Pass Filtering

The explanation of the process of reconstructing the waveform from the sample sequence was that (1) the spectrum from the sample sequence is calculated using Eq. (3.5), then (2) the inverse Fourier transform is applied to the spectrum in the base band using Eq. (3.6). Although this is a roundabout way, this explanation was chosen because it clearly shows how the spectrum is treated in the reconstruction of the waveform. The reader who understands this should also realize that there is a simpler way to reconstruct the continuous waveform.

Let us examine Fig. 3.3 once again. Figure 3.3a shows that the spectrum $X(f)$ of the continuous waveform $x(t)$ is limited to the frequency range $\pm F_m$. Figure 3.3b shows the periodic spectrum with a period of two times the frequency F_x satisfying the condition $F_m \leq F_x$. Each frequency period contains the spectrum $X(f)$. The development up to Eq. (3.6) shows that the inverse Fourier transform of this infinitely long periodic spectrum becomes the sample sequence of the original waveform. Letting the spectrum become periodic is equivalent to producing a sample sequence of the waveform in the time domain. Conversely, arranging samples with $1/2F_x$ spacing forces the spectrum to be periodic with period $2F_x$.

The innermost period of the spectrum shown in Fig. 3.3b, i.e., the base band from $-F_x$ to $+F_x$, is the same spectrum as the one shown in Fig. 3.3a, and is actually the spectrum of the continuous waveform. If all spectra except for the one in the base band are removed, the remaining spectrum is that of the continuous waveform itself. In order to obtain the continuous waveform from the sample sequence, the sample sequence (actually the electrical pulse train) is fed to a low-pass filter (LPF) so that the spectra outside of the base band are removed while the spectra inside the base band are unchanged). The resulting signal is the desired continuous waveform in the time domain.

If an ideal LPF were available, all components higher than F_x (and lower than $-F_x$) would be completely removed and the low frequency components within $\pm F_x$ would be preserved without changing their amplitudes and phases. This process is exactly equivalent to the numerical process of letting the higher frequency components be zero and applying the inverse Fourier transform to the remaining data. It is a common practice that the impulse train is input to a LPF with a cutoff frequency that is higher than F_m and lower than F_x. The output of the LPF is a continuous waveform.

However, a real LPF cannot have an ideally sharp cutoff response and the phase of the waveform is also changed in the high frequency region near the cutoff frequency. This process produces changes, or distortion, in the waveform. The waveform changes due to phase distortion are usually not a big problem in cases of speech and music signals. However, if the signal is used for imaging or for studying details of transient properties of a waveform, the effect of the phase change is sometimes devastating. In order to minimize waveform change due to phase distortion, the cutoff frequency of the LPF is normally much higher than the maximum frequency of the waveform. In other words, a large F_x/F_m ratio is mostly employed.

If a sample sequence is already given, it is considered that a large F_x/F_m ratio cannot be employed. If a sample sequence with a higher sampling frequency could be generated from the given sequence, however, it becomes possible to use a large F_x/F_m ratio. There are other occasions when different sampling frequencies are required. In the following sections, some important sampling-related topics such as the *sampling theorem* are explained. Then methods of changing sampling frequencies will be discussed.

3.5 Sampling Theorem

Starting with Eq. (2.28), which expands a waveform $x(t)$ into a complex Fourier series, the waveform $x(t)$ can be recovered from the Fourier coefficients X_k, located at discrete points on the frequency axis with $1/T$ spacing. On a contrary note, the equation that is used to obtain the continuous spectrum on the frequency axis from the time sequence on the time axis will be derived. In order to mechanically modify Eq. (2.28) to an equation in a desired form, T is replaced by $2F_x$ and the spectrum X_k is replaced by the sample value x_n. Furthermore, since this is a transformation from the frequency domain to the time domain, the minus sign must be used for the exponent of the complex exponential function (see Appendix 3). Actually, what is obtained is Eq. (3.5). However, an equation that has a widened range of x_n to infinity ($n = \pm\infty$) is used.

$$\tilde{X}(f) = \frac{1}{2F_x} \sum_{n=-\infty}^{\infty} x_n \exp(-j2\pi \frac{n}{2F_x} f) \tag{3.7}$$

This spectrum is a periodic function on the frequency axis, with period $2F_x$. It is a known property of the impulse train that its spectrum is periodic on the infinitely wide frequency range.

In order to obtain the time waveform from the frequency spectrum, the inverse Fourier transform is used. However, if Eq. (3.7) is inverse Fourier transformed, the same pulse train is obtained. It is necessary to remove the spectrum outside of $\pm F_x$ in order to obtain the continuous waveform $x(t)$, which can be done by restricting the integration range from $-F_x$ to $+F_x$.

$$x(t) = \int_{-F_x}^{+F_x} \tilde{X}(f) \exp(j2\pi ft) df \tag{3.8}$$

By substituting $\tilde{X}(f)$ in Eq. (3.7) into Eq. (3.8), the following equation is obtained

$$x(t) = \frac{1}{2F_x} \int_{-F_x}^{+F_x} \sum_{n=-\infty}^{\infty} x_n \exp(-j2\pi \frac{n}{2F_x} f) \exp(j2\pi ft) df .$$

If the order of integration and summation are changed, then the following is obtained

$$\begin{aligned} x(t) &= \frac{1}{2F_x} \sum_{n=-\infty}^{\infty} x_n \int_{-F_x}^{+F_x} \exp[j2\pi f(t - \frac{n}{2F_x})] df \\ &= \frac{1}{2F_x} \sum_{n=-\infty}^{\infty} x_n \frac{\exp[j2\pi f(t - \frac{n}{2F_x})]}{j2\pi(t - \frac{n}{2F_x})} \Bigg|_{-F_x}^{+F_x} \end{aligned} . \tag{3.9}$$

By using Eq. (3.9), the equation used to calculates $x(t)$ from sample sequence x_n with sampling frequency $2F_x$ is obtained:

$$x(t) = \sum_{n=-\infty}^{\infty} x_n \frac{\sin\left[2\pi F_x\left(t - \frac{n}{2F_x}\right)\right]}{2\pi F_x\left(t - \frac{n}{2F_x}\right)}. \tag{3.10}$$

This is knows as the *Shannon–Someya'sSampling Theorem.*

As shown above, the method of obtaining the continuous waveform from the sample sequence with sampling frequency $2F_x$ has been established, where both of them perfectly agree with each other in the time domain. However, Eq. (3.10) does not contain any restriction on the sampling frequency. Once the sample sequence and its sampling time are given, a continuous waveform that perfectly fits with the sample sequence is obtained by Eq. (3.10) regardless of the original waveform. Therefore, if twice the maximum frequency of the spectrum ($2F_m$) is larger than the sampling frequency (F_x), it is clear that Eq. (3.10) cannot be used to reconstruct the original waveform. It was mentioned earlier that the frequency F_x is called the Nyquist frequency if the sampling time is equal to $1/2F_x$.

3.6 Smoothing of a Sample Sequence Using the Sampling Theorem

Even if a numerical sample sequence is converted into an electrical waveform, the waveform is still an impulse train and the original waveform is not yet reconstructed. It must be reshaped as a continuous waveform. For this purpose, Eq. (3.10) is used to interpolate between the discrete impulses. Let us investigate how Eq. (3.10), which seems very complex at first glance, produces the continuous waveform by a graphical representation. Each term of Eq. (3.10) is the product of the sample value x_n at $n/2F_x$ and the *sinc function*.

$$\mathrm{sinc}(F_x t) = \frac{\sin(2\pi F_x t)}{2\pi F_x t} \tag{3.11}$$

Figure 3.7 shows the sinc function. The sinc function takes the maximum value of 1 at $F_x t = 0$ and it gradually decreases to zero as $|F_x t|$ becomes larger and larger, while keeping its values zero when $2F_x t$ takes integer values. Each sinc function in Eq. (3.10) is a shift of Eq. (3.11) by $t = n/2F_x$ on the time axis. It takes the maximum value $t = n/2F_x$ and zeros at other sampling points ($t = m/2F_x \ \ (m \neq n)$). Therefore, the value of Eq. (3.10) takes the value x_n at each sampling point.

Now, it is known that each sinc function takes the waveform shown in Fig. 3.7 and that Eq. (3.10) is equal to the value x_n at each sampling point. Still, there is a

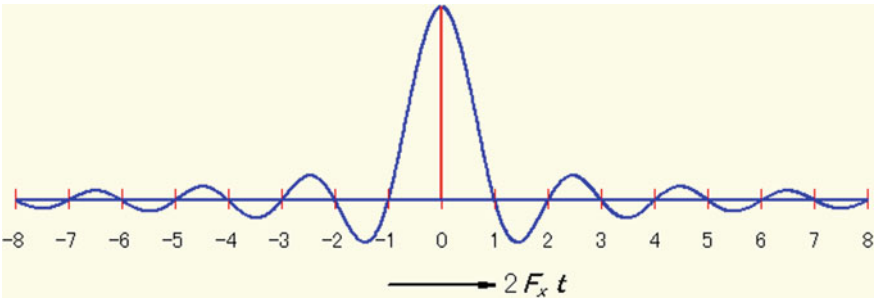

Fig. 3.7 Waveform of the sinc function $\mathrm{sinc}(F_x t) = \sin(2\pi F_x t)/(2\pi F_x t)$

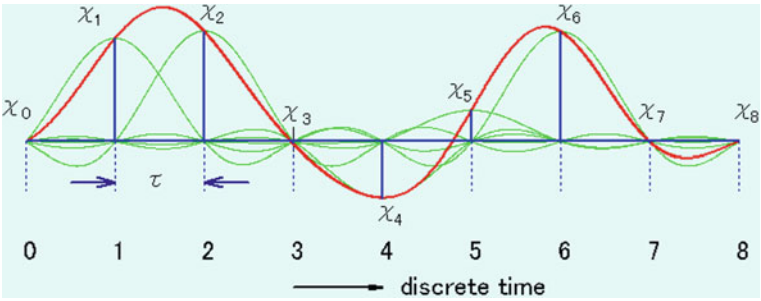

Fig. 3.8 Function $x(t)$ and individual terms calculated from the sample values $\{x_n\}$ using Eq.(3.10). Animation available in supplementary files under filename E3-08_Smpl-to-Wave.exe

remaining concern. Does Eq. (3.10) take the values of the original waveform at points other than the sampling points? It is already known from the discussions up to Sect. 3.3 that the spectrum of the original waveform is reconstructed from the Fourier coefficients that are given by the sample values, and its corresponding time function is the original continuous waveform. Therefore, there is no need to check this question theoretically but it is worthwhile to investigate it by numerical calculation.

Figure 3.8 shows the results of the $x(t)$ calculated from the sample values $\{x_n\}$with sample period of $1/2F_x$, together with the sinc functions centered at individual sampling points. As stated above, at the time $t = n/2F_x$ when the sample value x_n exists, the other sinc functions centered at times other than this are all equal to zero and, therefore, Eq. (3.10) is equal to the sample values $\{x_n\}$. At other times, Eq. (3.10) is the summation of sinc functions which are centered at the individual sampling points, which is actually the smooth original curve.

It has been shown that the original waveform $x(t)$, whose spectrum is limited within $\pm F_m$, can be reconstructed from discrete sample values if they are sampled with sampling frequency ($F_x \geq F_m$).

At this point, the reader may remind Gibbs Phenomenon. However, an expression of a waveform with the sampling frequency f_x means that frequency components above $f_x/2$ equal zero, and therefore there is no waveform discontinuity and no Gibbs Phenomenon.

3.7 Folding (Aliasing) of the Spectrum

So far, the permissible minimum value of the sampling frequency has been made clear. It has also been made clear that, if a sample sequence is obtained using a sampling frequency higher than the permissible minimum value, the original waveform is recovered. What happens if a signal is sampled using a sampling frequency lower than the minimum sampling frequency, or if the signal contains components that are higher than the Nyquist frequency? The answers to these questions are the topics of this section.

One may think that it is unnecessary to investigate this topic if the original signal is not recovered. However, it is important to know what type of result is obtained when wrong conditions are used in the measurement. When one encounters an unexpected result, this kind of knowledge is useful when guessing at the cause of the trouble.

Sine and cosine waves are convenient for the present purpose. It is known that if the signal is a sine or a cosine wave with frequency f, the sampling frequency must be higher than $2f$. When a sine wave with 32 periods is sampled, at least 64 samples are necessary to describe the signal. Or if 64 samples are used, the number of periods must be lower than 32. Let us check how the sample values and the spectrum vary by changing the frequency of the sine wave while keeping the sampling frequency constant.

Figure 3.9a shows sample values when 27–35 periods are sampled with 64 samples and Fig. 3.9b shows their power spectra. Since the numbers of the periods are integers, the spectrum components are given by infinitely narrow vertical lines and there is one line spectrum in each positive and negative frequency region of the base band.

If 32 periods of a cosine wave are sampled with 64 samples, the spacing between the two adjacent sampling points is given by $32 \times 2\pi/64 = \pi$. Therefore, if the phase φ of the first sampling point is 0, the sample values are +1, −1, +1, …. The fourth row of Fig. 3.9a, which is for the case of 32 periods, shows that the impulses of 1 and −1 repeat alternatively. Only for this case, the line spectra are at the discrete frequencies …, −94, −32, +32, +96, …. This occurs because the positive and negative components overlap with each other. Therefore, the magnitude of the line spectra in this case is twice the other cases (the difference of magnitudes is not shown in the figure).

Whether the original waveform can or cannot be reconstructed from the alternating +1 and −1 pulses is a natural question. On the condition that there are frequency components that are lower than or equal to the Nyquist frequency, the

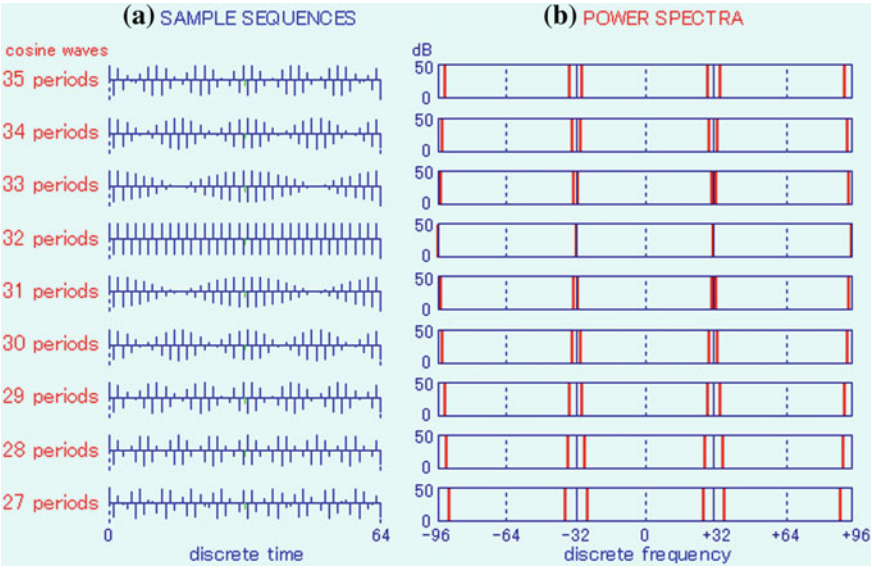

Fig. 3.9 Sample sequences (**a**) and their corresponding spectra (**b**) for the cases when there are 27–35 periods of a cosine wave in the time length of 64 sampling periods. Animation available in supplementary files under filename E3-09_Ariasing.exe

only possibility is the cosine function with the Nyquist frequency. However, if $\varphi = \pi/2$, i.e., for the case of sine function, all sample values are equal to zero and there is no way to reconstruct the waveform. The term φ has to be known at the time of sampling in order to reconstruct the waveform if 32 periods with 64 sample points are taken.

When the frequency of the waveform becomes lower (i.e., fewer periods than 32), the phase difference between the adjacent sampling points gets smaller than π, and therefore sample values take different values (see below the fourth row of Fig. 3.9a). The sample values change like a cosine wave and the maximum value is equal to the amplitude of the original cosine wave. The frequency of the line spectrum also becomes lower (see below the fourth row in Fig. 3.9b). The period of the change of the sample values included in the 64 point interval is given by $2 \times (32 - M)$, where M is the number of the period of the original waveform. In case of $M = 31$ (or 30), the number of zeros is 2 (or 4). Please remember that the number of zeros of the original waveform is given by $2\,M$, which is not easily seen from the sample values in Fig. 3.9a since the number of sampling points is not enough to show the details of the original waveform.

One may question whether the original waveform can be reconstructed from such widely varying sample values. If the spectrum of the waveform is completely zero above or equal to the Nyquist frequency, it is possible. Also, please remember that the above examples are rather special cases in the sense that each sampled waveform has an integer number of periods (from 27 to 35). If the number of the

sampling is finite and a waveform with noninteger number of periods is sampled, there is a spectrum spread and in such a case the reconstruction becomes impossible.

When the frequency of the waveform becomes higher (i.e., more periods than 32), the frequency of the line spectrum also becomes higher (i.e., the two line components move outside of the base band). However, since the spectrum must be periodic with the period of the base band (64 in this case), the line components that were outside of the base band must move into the base band in order to keep the periodicity (see above the third row in Fig. 3.9b).

Examine this from a different viewpoint. The line component moves toward the boundary of the base band as the number of period increases and reaches the boundary when the number equals 32. As the number of the periods further increases, it seems like the line component is bounced back to the base band. Or, it looks like the folding back at the boundary of a sheet of paper, on which line components that exist outside of the boundary are drawn. This is why the terminology "folding spectrum" was born. The higher frequency components greater than the Nyquist frequency $N_s/2$ and appearing in the base band are called *foldingspectra*.

The third (or second) row of Fig. 3.9a is exactly the same as the fifth (or sixth) row of Fig. 3.9a. If the sample sequences are the same, the resulting continuous waveforms are also the same. If the sample sequence is obtained by sampling the cosine waveform of 33 periods with 64 sampling points, the reconstructed continuous waveform appears to be a cosine waveform with only 31 periods.

As seen above, higher frequency components greater than the Nyquist frequency appear as lower frequency components that actually do not exist, causing a change of the waveform. The waveform distortion produced by this phenomenon is called *aliasingdistortion*.

The reader can check this by using the program attached to the figure; items to check include how the results change by changing cosine waves to sine waves and also what occurs when the waveform contains multiple components with slightly different frequencies.

What happens if there are more frequency components that are higher than the Nyquist frequency? What occurs was already shown in Fig. 3.6. Figure 3.10 shows results viewed from a different angle. Figure 3.10a shows a waveform to be analyzed and sample sequence sampled at two times the highest frequency, i.e., the minimum permissible sampling frequency. Figure 3.10b shows the waveform obtained by removing the frequency components that are higher than the Nyquist frequency, this waveform matches perfectly with the waveform of Fig. 3.10a.

Figure 3.10c shows the sample sequence sampled with 0.8 times of the sampling frequency of Fig. 3.10a. The solid line in Fig. 3.10d is the waveform obtained from (c) by removing the frequency components that are higher than the Nyquist frequency. The dotted line in Fig. 3.10d is the waveform in Fig. 3.10a. Figure 3.10e shows the difference between the two waveforms.

As Fig. 3.10 shows, if the sampling frequency is lower than the minimum permissible frequency, the waveform distortion appears almost everywhere on the

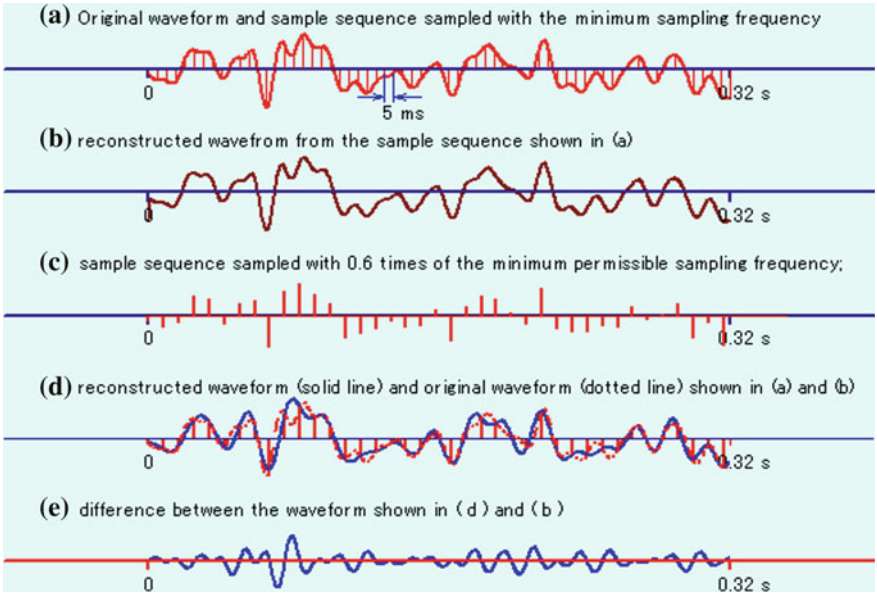

Fig. 3.10 Waveform and its sample sequences sampled with the minimum permissible sampling rate and with a sampling rate lower than that, and reconstructed waveforms. **a** Original waveform and its sample sequence sampled with the minimum permissible sampling frequency, **b** reconstructed waveform from the sample sequence shown in (**a**), **c** sample sequence sampled with 0.8 times the minimum permissible sampling frequency, **d** reconstructed waveform (*solid line*) and original waveform (*dotted line*) shown in (**a**) and (**b**), **e** difference between the two waveforms shown in (**d**) and (**b**). Animation available in supplementary files under filename E3-10_WaveReproF4 K.exe

time axis. If the sampling frequency is higher than twice the frequency of the maximum frequency components, the original waveform is reconstructed. Using the program attached to Fig. 3.10, the reader can try several cases with different sampling frequencies and waveforms.

A sample sequence numerically generated on a computer for a repetitive rectangular wave gives a series of impulses as shown in Fig. 3.11. The sample sequence appears reasonable for a rectangular wave. However, the rectangular wave has very high frequency components as seen in Fig. 1.4 and some other figures. If the sample sequence in Fig. 3.11a has a 10 ms time spacing, its spectrum is periodic with period of 100 Hz (±50 Hz) as shown in Fig. 3.11b (real part) and Fig. 3.11c (imaginary part). In order to produce a continuous waveform, all components outside of the base band must be removed. The result, with those components removed, is the wavy shape shown in Fig. 3.11d. Figure 3.11e shows the difference between the waveforms (a) and (d).

The difference between the original and reproduced waveforms shown in Fig. 3.11e is due to violation of the sampling theorem and it is not related to Gibbs Phenomenon.

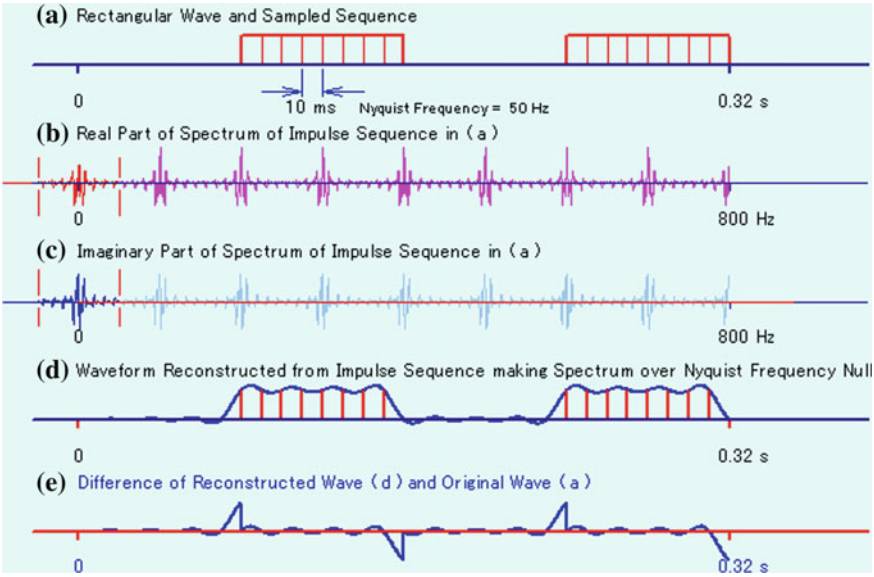

Fig. 3.11 An example of inadequate sampling rate. **a** sampling sequence made from two rectangular waves in 320 ms, **b**, **c** its real and imaginary spectrum components, respectively, **d** reconstructed waveform from the spectrum in the base band, and **e** the difference between the two continuous waveforms (**d**) and (**a**). Animation available in supplementary files under filename E3-11_ReproF4 K.exe

3.8 Sampling Frequency Conversion I (Application of the Fourier transform)

There are occasions where the sampling frequency of a sample sequence must be converted to another sampling frequency. When two signals with different sampling frequencies must be added, the sampling frequencies must be made the same.

First, consider the method of converting sampling frequencies using the Fourier transform approach. This technique is an extension of the relations among the waveform, the spectrum, and the sample sequence. Figure 3.12a shows a band limited spectrum within the frequency range $\pm F_x$, which is obtained by the Fourier transform of a continuous waveform $x(t)$ with duration T. This spectrum is continuous and is also the envelope of the Fourier coefficients X_k obtained by the Fourier series expansion of the waveform, assuming that it is periodic with period T. Let x_n be the sample sequence with sampling frequency $2F_x$ and let N be the number of sample points in the time length T. Then, since the spacing of the sample sequence is $1/2F_x$, $x_n = x\{n/(2F_x)\}$ gives the n-th sample value. Also there is a relationship $N = 2F_xT$ since $T = N \times (1/2F_x)$. The spectrum of the sample sequence x_n is periodic with period $2F_x$. as shown in Fig. 3.12b.

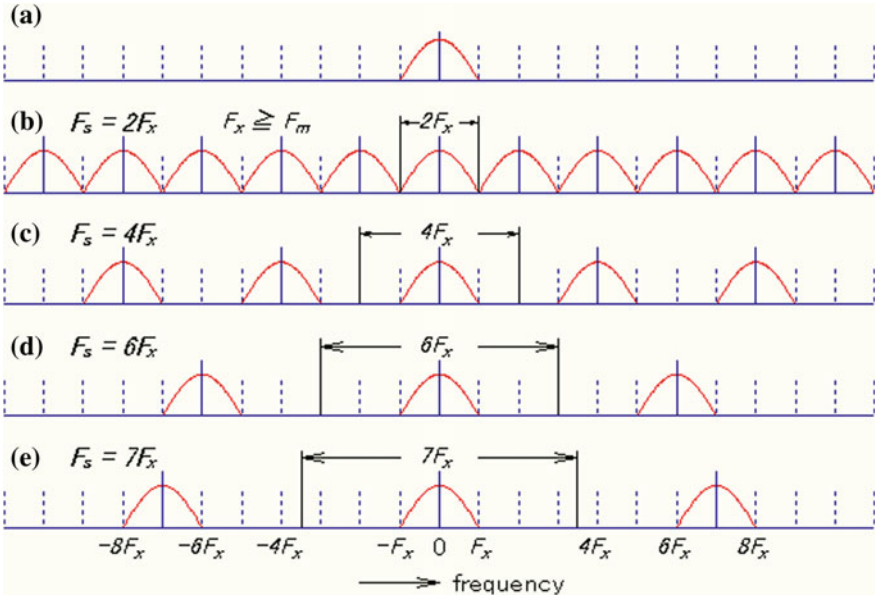

Fig. 3.12 Explanation of the method of producing sample sequence with n times the sampling frequency from a sample sequence of a continuous waveform whose frequency spectrum is limited within $\pm F_x$. **a** original spectrum, **b–e** spectra of the sample sequences of the original waveform sampled with sampling frequencies $2F_x$, $4F_x$, $6F_x$ and $7F_x$, respectively

If the same original waveform is sampled with sampling frequency $4F_x$, the spectrum of the new sample sequence is distributed on the frequency axis with period $4F_x$. Since the spectrum value outside of $\pm F_x$ is zero, the periodic spectrum becomes similar to the one shown in Fig. 3.12c. This suggests the method of getting the new sample sequence sampled with sampling frequency $4F_x$. The steps of the method are; (1) calculate the continuous spectrum from the sequence x_n, (2) obtain Fig. 3.12c by adding $N/2$ zeros on both sides of the base band (outside of the frequency range $\pm F_x$), and (3) apply the inverse Fourier transform of $2N$ data to the periodic spectrum with period $4F_x$ (Fig. 3.12c).

Let's consider the actual procedure of the method. The continuous spectrum $X(f)$ of Eq. (3.5) is given by the Fourier transform of the sample sequence x_n, which is obtained by sampling the original waveform $x(t)$ with sampling period $1/(2F_x)$. This spectrum is in the frequency band within $\pm F_x$ centered at 0 frequency (i.e., in the base band). This is a continuous spectrum and it is not suitable to convert the sampling frequency by a numerical method. However, if it is assumed that the waveform is periodic with period T, Its spectrum becomes the Fourier coefficients, and is represented by replacing f with k/T, in Eq. (3.5).

$$X_k = X\left(\frac{k}{T}\right) = \frac{1}{2F_x}\sum_{n=0}^{N-1} x_n \exp(-j2\pi \frac{n}{2F_x}\frac{k}{T}) = \frac{1}{2F_x}\sum_{n=0}^{N-1} x_n \exp(-j2\pi \frac{nk}{N}). \tag{3.12}$$

There is no need to mention that the sample values of $x(t)$ at $1/(2F_x)$ intervals are represented by the Fourier series given by X_k.

$$x_n = x(n/2F_x) = \frac{1}{T}\sum_{k=-N/2}^{N/2-1} X_k \exp(j2\pi \frac{kn}{N}). \tag{3.13}$$

In order to double the sampling frequency, zeros of $N/2$ points on both sides of the high frequency regions are added (Fig. 3.12c) and the inverse Fourier transform of $2N$ point data is calculated. Since the spectrum in the regions where $|k| > N/2$ is zero, the range of k is the same as in Eq. (3.13). With regard to the range of k, one only needs to change $2F_x$ in Eq. (3.13) to $4F_x$. The range of the sample number n is from 0 to $(2N - 1)$ instead of 0 to $(N - 1)$ since the sampling period is halved and the waveform length T is unchanged.

$$x(n/4F_x) = \frac{1}{T}\sum_{k=-N/2}^{N/2-1} X_k \exp(j2\pi \frac{kn}{4F_x T}) = \frac{1}{T}\sum_{k=-N/2}^{N/2-1} X_k \exp(j2\pi \frac{kn}{2N}) \tag{3.14}$$

Thus, it became possible to calculate the sample sequence when the sampling frequency is doubled ($2F_x$ to $4F_x$). By extending this idea, one will come up with the method of converting the sampling frequency from $2F_x$ to $6F_x$ or from $2F_x$ to $7F_x$ by referring to Fig. 3.12d, e.

At this point, the method of converting a sample sequence with sampling frequency F_s (=$2F_x$) to a sample sequence with sampling frequency pF_s has been established. This method uses the Fourier transform, which can be computed only after a full set of data is ready. This causes some amount of time delay in processing even if the computing time becomes negligibly small (because one has to wait to obtain the full data set of the Fourier transform).

In Fig. 3.12, the spectrum is shown with its center at zero frequency. However, the calculation of the spectrum given as a discrete sequence of values (numbered from 0 to N) is done by using the discrete Fourier transform (DFT). The details of calculation will be given in Appendix 4B in Chap. 4.

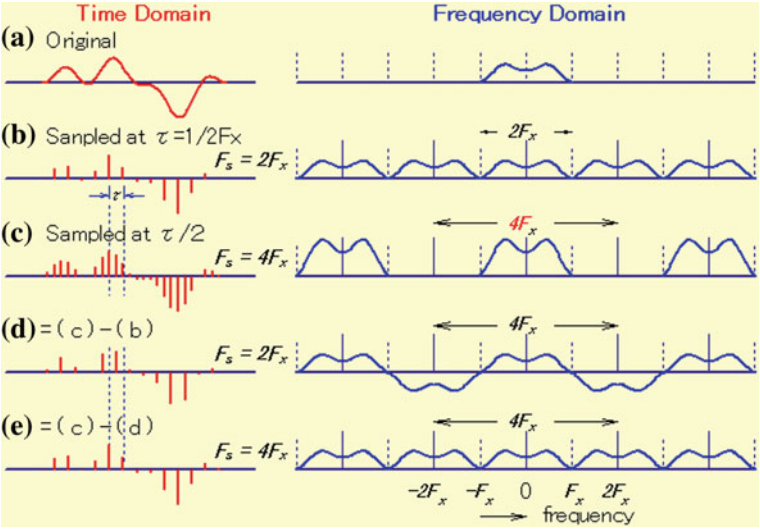

Fig. 3.13 Principle of doubling the sampling frequency by a digital LPF. **a** Original waveform (*left*) and its spectrum (*right*), **b** sample sequence with period τ (*left*) and its spectrum (*right*), **c** sample sequence with period τ/2 (*left*) and its spectrum (*right*), **d** (**c**) − (**b**), **e** (**c**) − (**d**)

3.9 Sampling Frequency Conversion II (Application of LPF)

The problem mentioned in the last section is solved by the introduction of low-pass filtering in the time domain. The principle will be explained here.

Figure 3.13a shows a continuous waveform (left) and its continuous spectrum limited within $\pm F_x$ (right). Figure 3.13b (left) shows the sample sequence obtained with sampling period τ (sampling frequency $2F_x = 1/\tau$). The impulses take the same values as the continuous waveform at the discrete times, and the spectrum of this sample sequence is an infinite periodic function with period $2F_x$ as shown in Fig. 3.13b (right).

If the same waveform (a, left) is sampled with sampling frequency $4F_x$, the sample sequence becomes like Fig. 3.13c (left). The sample values are the same as the waveform at the sample points. The spectrum of this sequence is infinitely wide and periodic with its base band period from $-2F_x$ to $+2F_x$. Since the spectrum of the original waveform is limited within $\pm F_x$, the spectrum in the region outside of $\pm F_x$ is zero. This spectrum within $\pm F_x$, has the same shape as Fig. 3.13a, b but the magnitude is two times larger than the spectra of Fig. 3.13a, b in the same region. The reason why it is doubled is that the sampling number is doubled in the same time period.

What happens when the data in Fig. 3.13b is subtracted from the data in Fig. 3.13c? Every other sample of the resulting sample sequence is zero as seen in

Fig. 3.13d (left). It appears like the sampling period is τ. Its spectrum is shown in Fig. 3.13d (right). The spectrum between F_x and $3F_x$ and $-F_x$ and $-3F_x$ are the inverse of the spectrum Fig. 3.13b since Fig. 3.13b is subtracted from Fig. 3.13c.

The sample sequence in Fig. 3.13d (left) appears like the sample sequence of the waveform Fig. 3.13a with sampling period $\tau = 1/2F_x$. In that sense, the difference from Fig. 3.13b is only that the times of the sampling are shifted by $1/4F_x$. However, there is another difference: the sample values at the time of sampling of Fig. 3.13b (left) are zero. These are the reasons why the period of Fig. 3.13d (right) is $4F_x$ and that there are regions where the signs of the spectra are reversed from those of Fig. 3.13b (right). The fact that the period of Fig. 3.13d (right) is $4F_x$ is equivalent to the fact that the sample sequence is spaced with $1/4F_x$. That is, the sample sequence in Fig. 3.13d (left) is composed of two sequences, one of them is made of sample values of the waveform Fig. 3.13a (left) with period $1/2F_x$ and the other sequence is made of all zeros spaced also with $1/2F_x$, where the zeros of the latter sequence are located amidst the data points of the former sequence.

Next, when the data in Fig. 3.13d is subtracted from the data in Fig. 3.13c, the data in Fig. 3.13e is obtained. This seems just like the sequence Fig. 3.13b (left). But it has zeros between the sample values of Fig. 3.13b (left). This sequence can be made very easily from Fig. 3.13b (left) by inserting zeros at centers of two adjacent sample points. If the region outside of $\pm F_x$ of the spectrum shown in Fig. 3.13e (right) is made zero by a digital filter with sampling rate τ/2, the output of the filter is a sample sequence with period τ/2, and its envelope agrees with the waveform Fig. 3.13a. That is, the output of the digital filter is the sample sequence with twice the original sampling frequency.

From the above discussion, a procedure for doubling the sampling frequency is given. This will be explained using Fig. 3.14.

Figure 3.14a is the sample sequence with sampling period τ (=$1/2F_x$). Figure 3.14b is the sequence obtained by inserting zeros centered between adjacent sample points. This new sequence has the period τ/2 and its spectrum is from $-2F_x$ to $-F_x$ and from $+F_x$ to $+2F_x$ and is the same as the spectrum within $\pm F_x$ (i.e., in the base band). By letting the spectra below $-F_x$ and above F_x equal zero by a digital LPF, a sample sequence with sampling period τ/2 that has spectra only within $\pm F_x$ is obtained. This is shown in Fig. 3.14c. Since the half of the spectrum has been removed and the number of samples has been doubled, the amplitude of each sample is halved. By doubling the values of the sequence Fig. 3.14c, the sequence Fig. 3.14d is obtained, which is equal to the sample sequence obtained by sampling the original continuous waveform with sampling frequency $4F_x$.

The method of inserting zeros between existing data points and letting it go through a LPF can be used not only for doubling, but also for any other integer ratios of the sampling frequency. In order to triple, two zeros can be spaced equally between adjacent sample points. However, the converting ratio must be an integer.

It is possible not only to increase the sampling frequency, but also to lower it. For example, in order to halve the sampling frequency, just use every other sample

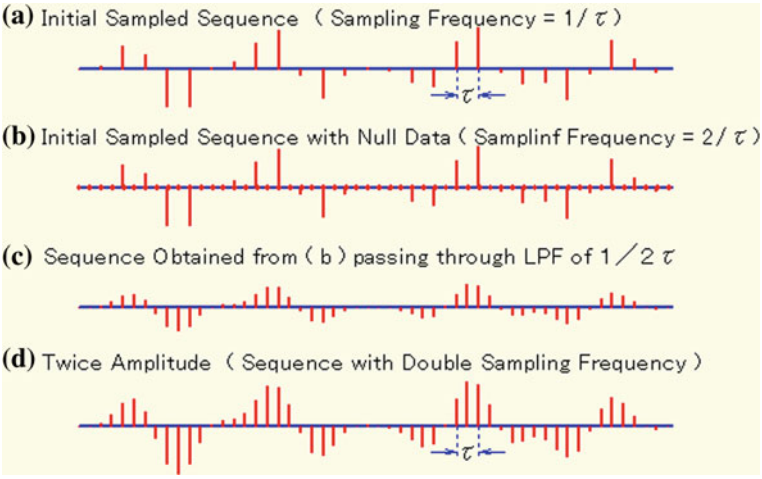

Fig. 3.14 Process of converting the sampling frequency from $2F_x$ to $4F_x$

value. If one-third of the sampling frequency is required, use one in every three samples. However, caution must be exercised. The lowered sampling frequency still must satisfy the sampling theorem. Otherwise, there will be an unrecoverable distortion.

One can also achieve 2.5 times the sampling frequency. First, increase the sampling frequency 5 times, and then halve the new sample sequence. Many other combinations are possible with some ingenuity.

3.10 Exercises

1. When sampling a continuous waveform, what are the requirements?
2. What are the necessary conditions in order for the inverse Fourier transform to be real?
3. What is the necessary condition in order to represent a waveform, whose spectrum is limited within $\pm F_m$, by a sample sequence.
4. Explain why one cannot reconstruct a waveform whose spectrum is limited within $\pm F_m$ when it is sampled with the sampling period of $1/2F_m$.
5. What happens to the reconstructed continuous waveform when one samples a waveform with a sampling frequency lower than the Nyquist frequency?
6. Given a sample sequence which is obtained by sampling a waveform, whose spectrum is limited within $\pm F_m$, with the sampling frequency $2F_x$ ($\geq F_m$). If one could input this sequence to an ideal digital LPF with cutoff frequency F_c, what kind of differences between the input and output sequences should one expect?
7. A waveform is reconstructed from a sample sequence obtained by sampling an original waveform, whose spectrum is limited within $\pm F_m$, with sampling

frequency F_s which is lower than, but close to, $2F_m$. What kind of difference does one expect between the spectra of the original and the reconstructed waveform?

8. Explain the method of making a sample sequence with sampling frequency pF_s from a sample sequence obtained with sampling frequency F_s from a waveform whose spectrum is limited within $\pm F_m$. Discuss cases for various p.

Chapter 4
Discrete Fourier Transform

The Fourier transform is an integral of the product of a signal (waveform) to be analyzed and a complex exponential function with an arbitrary frequency (see Eq. (2.37)). In theoretical discussions, it is possible to deal with continuous functions. However, since a continuous function requires an infinite number of points to describe, it is not suitable for a numerical analysis using a digital computer. That is why the waveform is converted to a finite length sample sequence and numerical analysis is applied to it, as explained in Chap. 3. Instead of directly applying the Fourier transform, theoretical formulae that are applicable to a finite number of sample values should be defined. The pair of formulae developed for this purpose is the Discrete Fourier Transform (DFT) pair, which will be explained in this chapter.

The transform pair can be represented by sine and cosine functions, but it can also be represented by cosine functions only. This is called the Discrete Cosine Transform (DCT), which is often used for data reductions and discussed at the end of this chapter and in Chap. 6 of volume II of this book.

4.1 Fourier Transform of Discrete Sequence of Numbers

First, let us consider a sample sequence, sampled with constant time spacing from a continuous waveform, and see how its Fourier transform is represented. At the top of Fig. 4.1, a sequence of impulses as well as its original waveform $x(t)$ are shown.

If the sampling period is τ, the time length of the waveform is T, and the number of samples is N, then the relation $T = N\tau$ holds. We define the start of the waveform as the origin of the time axis ($t = 0$). Then, the first sample has 0 time delay and amplitude $x(0)$, the second sample has time delay τ and amplitude $x(\tau)$, the nth sample has time delay $n\tau$ and amplitude $x(n\tau)$, and so on. Then, the sample sequence can be represented as a weighted series of impulses:

K. Kido, *Digital Fourier Analysis: Fundamentals*,
Undergraduate Lecture Notes in Physics, DOI: 10.1007/978-1-4614-9260-3_4,

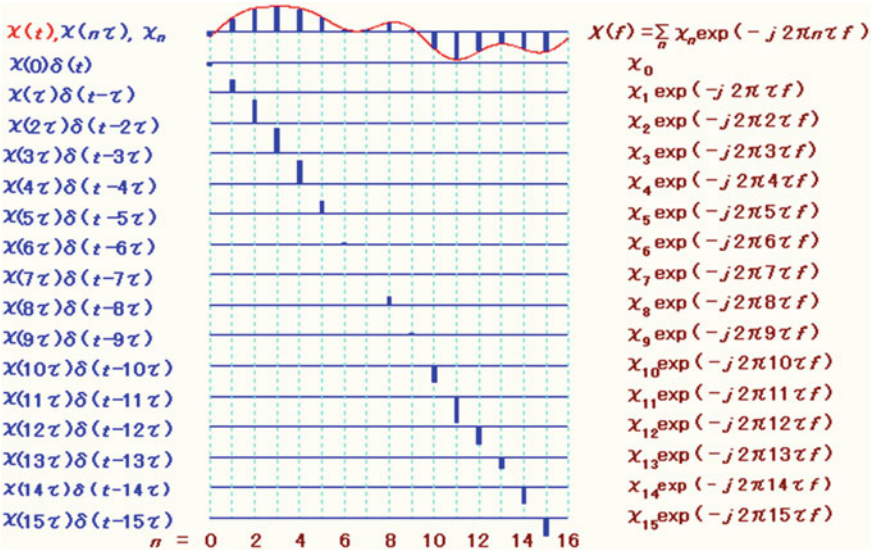

Fig. 4.1 Derivation of the formula for the DFT by representing the waveform as a sequence of impulses with magnitudes of sample values at discrete sampling times and by making the summation of spectra of the impulses

$$x(0)\delta(t) + x(\tau)\delta(t-\tau) + x(2\tau)\delta(t-2\tau) + \cdots + x(n\tau)\delta(t-n\tau) + \cdots$$

Each term of the above equation is taken one by one from the sample values of the top row of Fig. 4.1. Beginning with the second row, one impulse is shown in each row with its equation on the left side of each row. By adding all these impulses, the sample sequence shown in the top row is obtained. If we represent the sample sequence by $x_s(t)$, it is given by

$$x_S(t) = \sum_{n=0}^{N-1} x(n\tau)\delta(t-n\tau) \tag{4.1}$$

The Fourier transform of the sample sequence $x_s(t)$, is the sum of the Fourier transforms of the individual impulses, each of which has a separate time delay $n\tau$. The Fourier transform of an impulse that has time delay τ has been already given by Eq. (2.42). It follows that the Fourier transform $X_n(f)$ of the nth impulse $x(n\tau)\delta(t-n\tau)$ is given by

$$X_n(f) = x(n\tau)\exp(-j2\pi n\tau f) \tag{4.2}$$

Then, the Fourier transform of Eq. (4.1) is given by

$$\mathrm{FT}\{x_S(t)\} = \sum_{n=0}^{N-1} x(n\tau)\exp(-j2\pi n\tau f) \tag{4.3}$$

This equation indicates that the Fourier transform of the N point sample sequence $x_s(t)$ of $x(t)$ with spacing τ is given by the summation of N complex exponential functions. In Eq. (4.3), there are parameters for the continuous (analog) waveform such as τ and f. However, these parameters will take on discrete values for the reasons explained below.

Since the spectrum is limited within $\pm F_x$, and there are N points in the time period from 0 to T, which is sampled with period $\tau = 1/2F_x$, the following relationship exists between τ and N:

$$\tau = 1/2F_x = T/N \tag{4.4}$$

Since the frequency spectrum is the set of Fourier coefficients of the waveform with period T, it follows that the frequencies of the components are integer multiples of $1/T$. That is, $\mathrm{FT}\{x_s(t)\}$, which is the Fourier transform of $x_s(t)$ given by Eq. (4.1), takes the discrete frequencies given by

$$f = k/T \quad k = 0, 1, 2, \ldots \tag{4.5}$$

Substituting Eqs. (4.4) and (4.5) into Eq. (4.3), the following equation is obtained for the Fourier transform:

$$\mathrm{FT}\{x_S(t)\} = \sum_{n=0}^{N-1} x(n\tau)\exp\left(-j2\pi\frac{nk}{N}\right) \tag{4.6}$$

Representing the sample value $x_s(n\tau)$ of $x_s(t)$ at every τ by x_n, and the Fourier coefficients at each frequency $f = k/T$ by X_k, Eq. (4.6) is rewritten as

$$X_k = \sum_{n=0}^{N-1} x_n \exp\left(-j2\pi\frac{nk}{N}\right) \tag{4.7}$$

This is the formula of the Fourier transform of a sample sequence with N samples, called the *discrete Fourier transform* (DFT) of $x(t)$ in the sense that it is the Fourier transform of a discrete sequence. The variables k and n are called the *discrete frequency* and the *discrete time*, respectively. When it is necessary to show that it is a transform of N point data, it is called the *N pointDFT*. Sometimes, the DFT is called the *finite Fourier transform* since the number of data on the time axis is finite.

The equation of definition of the discrete Fourier transform has now been derived. Still, the region of the variable k needs to be defined. From the discussions up to Chap. 3, we know that the negative frequency spectrum is also necessary. If

the length of the waveform, whose spectrum is within $\pm F_x$, is T, the number of the Fourier coefficients with f_0 (= $1/T$) steps should be

$$2F_x/f_0 = 2F_xT$$

From Eq. (4.4), this must be equal to N. Therefore, the absolute value of k is from 0 to $N/2$. That is, the frequency range is from $-F_x$ to $+F_x$ and the discrete frequency range is nominally from $-N/2$ to $+N/2$. If N is even, the discrete frequency range should be $-N/2$ to $+N/2-1$. The numbers of the positive and negative frequency components are different, but this is not a serious problem. If N is odd, the number of integers in the range from $-(N-1)/2$ to $+(N-1)/2$ is N. Therefore, this is the proper range for odd N.

Since it has been shown that the real part of the spectrum corresponds to an even function and the imaginary part corresponds to an odd function, the spectrum in the negative frequency range is easily established from the spectrum in the positive frequency range. For this reason, only the positive frequency components from $k = 0$ to $N/2-1$ or $(N-1)/2$ are required to describe the spectrum.

If Eq. (4.7) is used only for calculating the spectrum, the above conclusion is enough. However, when the inverse equation is required, the one that calculates the waveform from the spectrum, the range of k from 0 to $N/2$ is not sufficient and the full range from $-N/2$ to $+N/2-1$ must be used. The inversion equation will be derived in Sect. 4.2, and the range of k will be discussed again.

4.2 Inverse Discrete Fourier Transform (IDFT)

Equation (4.7) is equivalent to Eq. (2.37), which is the Fourier transform of a continuous waveform. We need another equation which is equivalent to Eq. (2.38), the inverse Fourier transform. Although it is possible to derive the inverse discrete Fourier transform by inverting each component of the line spectrum, we will take a different approach here.

In the Fourier transform pair given by Eqs. (2.37) and (2.38), there are minus and plus signs in the argument of the exponential functions, and the integrations are with respect to t and f, respectively.

For the inversion, let us try the same process described above, i.e.: multiplying both sides of Eq. (4.7) by $\exp(+j2\pi nk/N)$ and summing with respect to the discrete frequency$k$. The parameter n in the right-hand side of Eq. (4.7) must be changed. The range of the parameter should be $k = -N/2 \sim N/2 - 1$ for even k, and $k = -(N - 1)/2 \sim (N - 1)/2$ for odd k. However, since X_k is periodic with period N, we can also let the range of k be from 0 to N as in Eq. (4.7). Since this is permissible, k can be handled the same way without regard to being even or odd. The result becomes as follows:

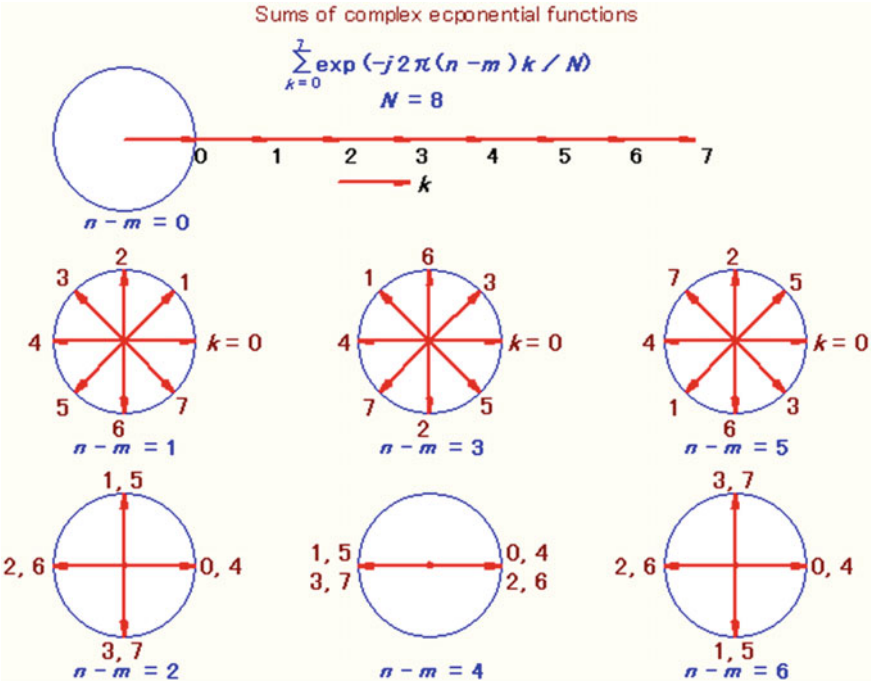

Fig. 4.2 Vectors that represent $\exp\{j2\pi(n-m)k/N\}$ and their summation for the case with $N = 8$

$$\sum_{k=0}^{N-1} X_k \exp(j2\pi nk/N) = \sum_{k=0}^{N-1} \exp(j2\pi nk/N) \sum_{m=0}^{N-1} x_m \exp(-j2\pi mk/N).$$

Reversing the order of summation, we get the following equation:

$$\begin{aligned}\sum_{k=0}^{N-1} X_k \exp(j2\pi nk/N\} &= \sum_{m=0}^{N-1}\sum_{k=0}^{N-1} x_m \exp\{j2\pi(n-m)k/N\} \\ &= \sum_{m=0}^{N-1} x_m \sum_{k=0}^{N-1} \exp\{j2\pi(n-m)k/N\}.\end{aligned}$$

The sum of the exponential functions can be obtained easily using the following reasoning:

In case of $m = n$, since $\exp\{j2\pi(n-m)k/N\} = 1$, the sum with respect to k is N. Therefore, the right-hand side of the above equation is equal to Nx_n when $m = n$. In case of $m \neq n$, the exponential functions are the vectors that are shown by the arrows in Fig. 4.2 ($N = 8$ is assumed). In these cases, the summation is always zero. Now, since

$$x_n \sum_{k=0}^{N-1} \exp\left(j2\pi \frac{(n-m)k}{N}\right) = \begin{cases} Nx_n & n = m \\ 0 & n \neq m \end{cases}$$

the equation above this one can be rearranged as follows:

$$x_n = \frac{1}{N} \sum_{k=0}^{N-1} X_k \exp\left(j2\pi \frac{nk}{N}\right). \tag{4.8}$$

Equation (4.8) is called the *inverse discrete Fourier transform* (*IDFT*) of X_k. You can confirm that you will get X_k when you substitute x_n obtained from this equation into the equation of the discrete Fourier transform, Eq. (4.7).

Equations (4.7) and (4.8) together are called *the discrete Fourier transformpair*. These equations are almost the same and they have a good symmetry except that: (a) the sign of the argument of the complex exponential function in the forward and inverse transforms is negative and positive, respectively; and (b) in the forward transform, the summation stands alone and in the inverse transform it is divided by N. Sometimes, in order to make the pair more symmetric, the following pair of equations is used.

$$X_k = \frac{1}{\sqrt{N}} \sum_{n=0}^{N-1} x_n \exp\left(-j2\pi \frac{nk}{N}\right) \tag{4.9}$$

$$x_n = \frac{1}{\sqrt{N}} \sum_{k=0}^{N-1} X_k \exp\left(j2\pi \frac{nk}{N}\right) \tag{4.10}$$

One more problem should be made clear. The range of k was taken from 0 to $N-1$ instead of from $-N/2$ to $N/2-1$. The only reason for doing this was that X_k is periodic with period N. The question is "Is this sufficient?"

Let us use a new variable p that satisfies $k = N-p$ in the range $k \geq N/2$. Then, $X_k \exp(j2\pi nk/N)$ can be rewritten as

$$\begin{aligned} X_k \exp(j2\pi nk/N) &= X_{N-p} \exp\{j2\pi n(N-p)/N\} \\ &= X_{N-p} \exp\{j2\pi n(-p)/N\} \exp(j2\pi n) \\ &= X_{N-p} \exp\{j2\pi n(-p)/N\} \end{aligned}$$

From this equation, it is known that the data number and the discrete frequency have the correspondence shown in Fig. 4.3. The circles in Fig. 4.3 have the data number and the discrete frequency outside and inside the circles, respectively, for the cases $N = 8$ (even, left) and $N = 9$ (odd, right). Whatever k is, the upper half of the data numbers corresponds to the negative frequency $k-N$.

If not otherwise mentioned, the term "frequency" will be used in place of "discrete frequency".

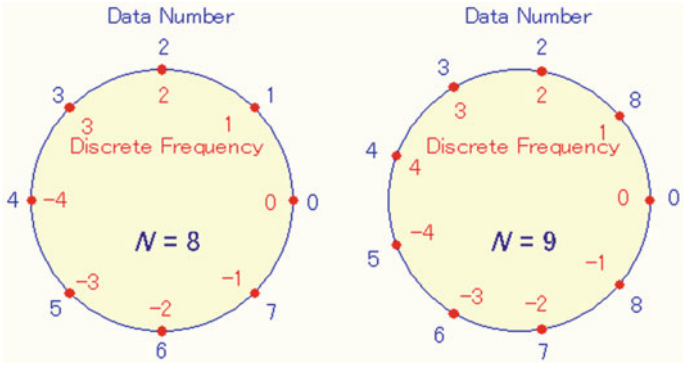

Fig. 4.3 Relation between the data number and the discrete frequency on the frequency axis

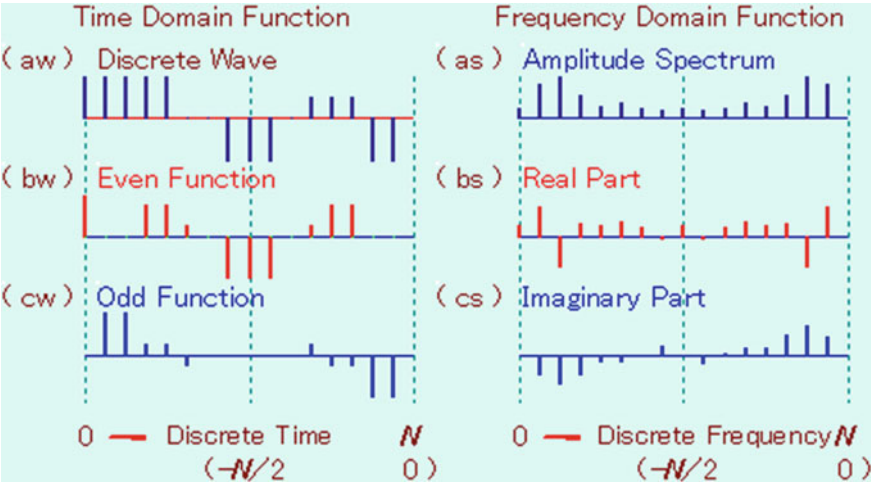

Fig. 4.4 Discrete sample sequence and its even and odd parts and their IDFTs. (aw): 16-point sample sequence, (as): amplitude spectrum of (as), (bs): real part of DFT of (aw), (cs): imaginary part of DFT of (aw), (bw): IDFT of (bs), (cw): IDFT of (cs). Animation available in supplementary files under filename E4-04_DFT_Ana.exe

Let us check the relationship between the real and imaginary parts and the time function. If we represent the DFT of the 16-point sample sequence shown in Fig. 4.4(aw) by $R_k + \mathrm{j}I_k$, then the real and imaginary parts:

$$R_k = \mathrm{Re}\{X_k\} = \sum_{n=0}^{N-1} x_n \cos\left(2\pi \frac{nk}{N}\right) \tag{4.11}$$

$$I_k = \mathrm{Im}\{X_k\} = -\sum_{n=0}^{N-1} x_n \sin\left(2\pi\frac{nk}{N}\right) \tag{4.12}$$

become as shown in Fig. 4.4(bs), (cs), respectively. Since the amplitude spectrum is given by the square root of the sum of the squares of real and imaginary parts, the amplitude spectrum is as shown in Fig. 4.4(as). The positive frequency range is given by k from 0 to $N/2-1$ (=7) and the negative frequency range is given by k from $N/2$ (=8) to $N-1$ (=15). The negative frequency corresponding to this range is from $-N/2$ (-8) to -1. Figure 4.3 will help you understand this relationship between the data number and the real frequency. The real part of the spectrum is an even function because the cosine function is even, and the imaginary part is an odd function because the sine function is odd.

The IDFTs of Fig. 4.4(bs), (cs) are given by Fig. 4.4(bw), (cw), respectively. Fig. 4.4(bw) is an even function and Fig. 4.4(cw) is an odd function. The sum of the even and odd functions is given by Fig. 4.4(aw). It is possible, therefore, to separate Fig. 4.4(aw) into the even function Fig. 4.4(bw) and the odd function Fig. 4.4(cw) without using a complex operation such as the DFT.

4.3 The DFT and the Fourier Transform

Formulae for the DFT and IDFT have been derived in the previous sections. Let us consider a little more about the relationships between the discrete and continuous Fourier transforms.

It is already known that line spectra with spacing $(1/T)$ are obtained as a set of Fourier coefficients through the Fourier expansion of a waveform with period T, and that the spectrum of a sequence with spacing τ $(=1/2F_x)$ is obtained as a set of Fourier coefficients through the Fourier expansion of a spectrum whose components are limited to the frequency range $\pm F_x$.

Since the sample sequence is a sequence of impulses with individual amplitudes, the Fourier transform of the n-th impulse is a complex number $(x_n \exp(-j2\pi fn/2F_x))$ with amplitude x_n and with phase $-j2\pi fn/2F_x$ which is proportional to frequency f, where n is the sample number, $(1/2F_x)$ is the sampling period, and $n/2F_x$ is the (discrete) sample time. By adding all these terms, the equation of the DFT is obtained. The equation of the IDFT is obtained from the DFT with the idea that it is one of the two members of the transform pair. One can also confirm that it is valid as the equation of the inverse transform. With these thoughts in mind, let us summarize the relationships between the continuous/periodic/discrete waveforms and their corresponding continuous/discrete/periodic spectra.

Figure 4.5a shows the continuous waveform (left) and its continuous spectrum (right). The waveform is limited to the range from 0 to T, and its spectrum is limited within $\pm F_x$. If the waveform is real, the spectrum is complex, and the real and imaginary parts are even and odd functions of the frequency, respectively.

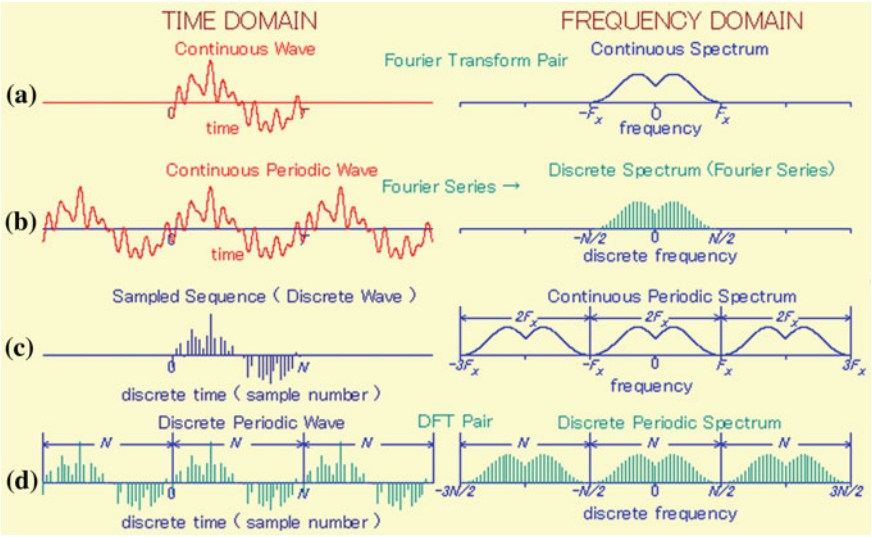

Fig. 4.5 Relations between waveforms and their spectra. **a** Finite continuous waveform and its finite continuous spectrum (assuming no significant components outside $-F_x$ and F_x), **b** continuous periodic waveform and its discrete spectrum, **c** finite sample sequence and its continuous periodic spectrum, **d** periodic sample sequence and its discrete periodic spectrum

For simplicity, however, the spectrum is drawn as an even function. The time and frequency domain functions in Fig. 4.5a are continuous and limited within their own ranges and are null (*or at least no significant components*) outside of those regions. The relationship between these two functions is established by the Fourier transform pair given by Eqs. (2.37) and (2.38).

$$X(f) = \int_{-\infty}^{+\infty} x(t) \exp(-j2\pi ft)dt \quad (2.37) \tag{4.13}$$

$$x(t) = \int_{-\infty}^{+\infty} X(f) \exp(j2\pi ft)df \quad (2.38) \tag{4.14}$$

When it is assumed that the waveform repeats itself infinitely with period T, its spectrum is given by the line spectrum with spacing $1/T$. It is known from discussions in Chap. 2 that the envelope of this line spectrum is given by Fig. 4.5a, right. There is a 1:1 correspondence between the periodic waveform and the line spectrum, indicating that when one of them is determined the other is also determined. These relations have already been given by Eqs. (2.28) and (2.29).

$$x(t) = \frac{1}{T} \sum_{k=-\infty}^{\infty} X_k \exp\left(j2\pi \frac{k}{T} t\right) \quad \text{also (2.28)} \tag{4.15}$$

$$X_k = \int_{-T/2}^{T/2} x(t) \exp\left(-j2\pi \frac{k}{T} t\right) dt \quad \text{also (2.29)} \tag{4.16}$$

This pair relation is shown in Fig. 4.5c. The spectrum in Fig. 4.5c is the one obtained by assuming that the spectrum in Fig. 4.5a (right) repeats itself infinitely with period $2F_x$. If the Fourier expansion is applied to this periodic function, the sample values (Fourier coefficients) are located only at integer multiples of $1/2F_x$ on the time axis. The envelope of the Fourier coefficients is equal to the waveform in Fig. 4.5a (left). The sample values x_n, which are Fourier coefficients, are given by Eq. (3.3), and the continuous periodic spectrum is obtained from the sample values x_n, by Eq. (3.5).

$$x_n = \int_{-F_x}^{+F_x} X(f) \exp\left(j2\pi \frac{n}{2F_x} f\right) df \quad (3.3) \tag{4.17}$$

$$X(f) = \frac{1}{2F_x} \sum_{n=0}^{N} x_n \exp\left(-j2\pi \frac{n}{2F_x} f\right) \quad (3.5) \tag{4.18}$$

If it is assumed that a continuous waveform with finite length is periodic, its corresponding frequency spectrum function becomes an impulse sequence. If we assume that a continuous spectrum with finite length is periodic, its corresponding time function becomes an impulse sequence. Figure 4.5d shows the case when both the time and frequency functions are finite length sample sequences. It should be remembered that a periodic function, even if it is an impulse sequence, can be expanded as a Fourier series, and therefore, both the waveform and the spectrum become impulse sequences. The relations between the two sequences with length N is given as the DFT pair, which is shown here again.

$$X_k = \sum_{n=0}^{N-1} x_n \exp\left(-j2\pi \frac{nk}{N}\right) \quad (4.7) \tag{4.19}$$

$$x_n = \frac{1}{N} \sum_{k=0}^{N-1} X_k \exp\left(j2\pi \frac{nk}{N}\right) \quad (4.8) \tag{4.20}$$

It should be kept in mind that both x_n and X_k are infinite functions with period N.

In the past, it was very difficult to carry out the forward and backward (inverse) Fourier transforms by use of analog computers, but with the advent of digital computers, it is now easy to numerically calculate Eqs. (4.19) and (4.20). Of course, these are discrete Fourier transforms and one must remember that the relationship between the waveform and the spectrum is like the one shown in Fig. 4.5.

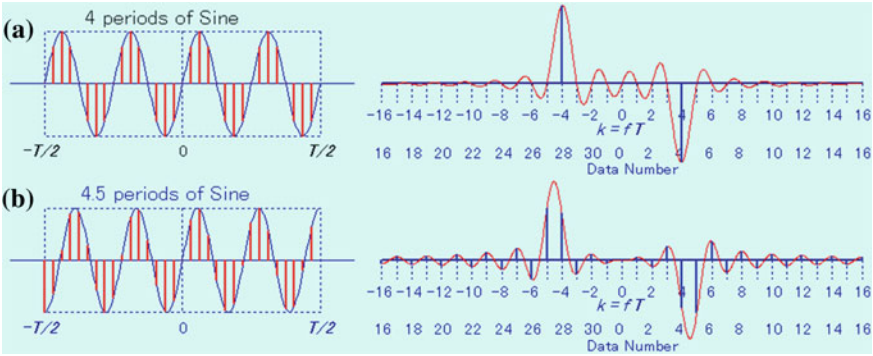

Fig. 4.6 Sample sequences of sine waveforms (*left*) and their spectra (*right*). **a** 4 periods in the sequence, **b** 4.5 periods in the sequence. Animation available in supplementary files under filename E4-06_Sine.exe

4.4 Waveform and Its DFT

Thus far, the basic idea of the DFT has been discussed. In order to better apply the DFT to real problems, it is useful to have familiarity with DFTs of a variety of signals with known properties. Let us look at several examples.

DFTs with $N = 32$ or 64 data points will be used because a smaller number makes it easier to understand the relationship between the discrete sample sequence and the discrete spectrum. Since the number of examples that can be listed in this book is limited, other examples are included in the related program.

4.4.1 Sine and Cosine Waves

The spectra of the sine $\sin(2\pi ft)$ and cosine $\cos(2\pi ft)$ waves have frequency components only at $\pm f$. However, depending on the way these waveforms are extracted, the calculated spectrum may take different shapes. This is because the extracted waveform is treated as one period of an infinitely long periodic waveform.

Figure 4.6 (left) shows a sample sequence of a sine wave, and Fig. 4.6 (right) shows its spectrum. Figure 4.7 shows the same for a cosine wave. Figures 4.6a and 4.7a have exactly 4 periods in the window (that is, the frequency is 4) and in these cases, the periodic waveforms become exactly the original sine and cosine waves, respectively. Therefore, their spectra have positive and negative frequency components at $k = 4$ and $k = -4$, respectively, as shown by the thick blue vertical lines. The thin red line envelopes are the continuous spectrum distributions obtained by the Fourier transform assuming that the waveforms outside the region $\pm T/2$ are zero. In these cases, the continuous spectra give exactly the same values

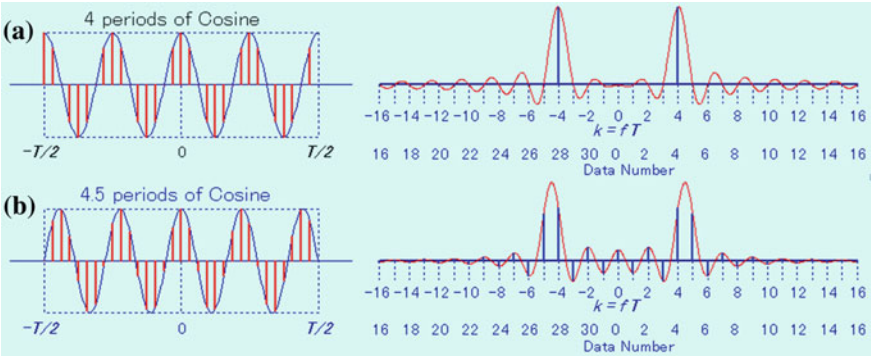

Fig. 4.7 Sample sequences of cosine waveforms (*left*) and their spectra (*right*). **a** 4 periods in the sequence, **b** 4.5 periods in the sequence. Animation available in supplementary files under filename E4-07_Cos.exe

at $k = 4$ and $k = -4$. At the other discrete frequencies, the continuous spectrum distributions are always zero.

On the other hand, if the number of wave periods is a noninteger value like Fig. 4.5 (see Figs. 4.6b and 4.7b), the peak frequency and the frequencies at which the continuous spectra are zero are not integers. Since the values obtained by the DFT occur only at integer frequencies, many nonzero frequency components are observed.

The general definition of "frequency" is the number of periods per second. Here, it is defined as the number of periods in the window length (=T): the frequencies in (a) and (b) are 4 and 4.5, respectively.

The waveform in Fig. 4.6 is a sine function and its spectrum is purely imaginary; the waveform in Fig. 4.7 is a cosine function and its spectrum is purely real. The reason is that the former is antisymmetric and the latter is symmetric when the time origin is taken at the center of the waveforms. If this origin is shifted, there will be a proportional phase shift, and the spectrum will contain both real and imaginary parts. In general, the spectral distribution is not as simple as these two cases.

4.4.2 Phase and Spectrum

Figure 4.8 shows the case with the sine wave shifted to the left on the time axis. There are 64 sample points in each sample sequence and there are 6 waves in each sequence. That is, the frequency is 6 (using the above definition). Therefore, the line spectra are located at ± 6. Since the time shifts are 1/8 and 1/3, respectively, of one fundamental period, the phases are 45° (Fig. 4.8a) and 120° (Fig. 4.8b), respectively. Since $\cos 45° = \sin 45°$, the magnitudes of the real and imaginary

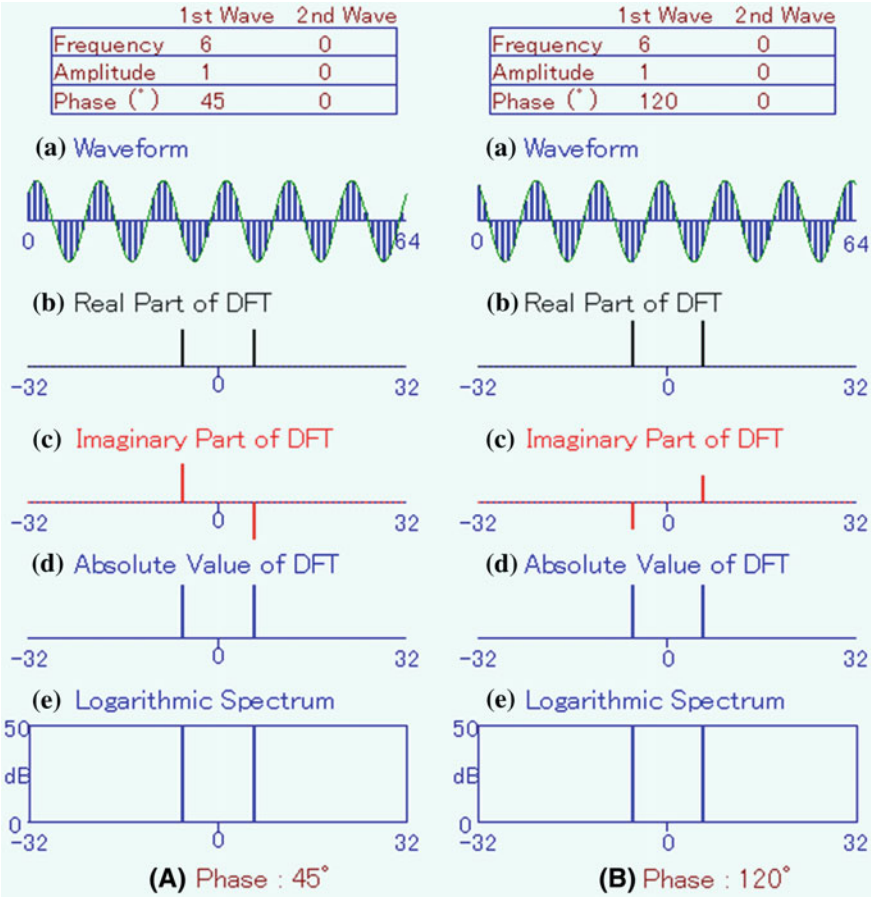

Fig. 4.8 Waveforms and their spectra. **a** Sample sequence of 6 period sine waves with 45° (A) and 120° (B) phase shifts: **b** real part of the spectrum, **c** imaginary part of the spectrum, **d** absolute value of the spectrum, **e** power spectrum in dB. Animation available in supplementary files under filename E4-08_SC.exe

parts of the spectrum (a) are the same. The real and imaginary parts of the spectrum of (b) are $\cos 120°$ and $\sin 120°$, respectively. The magnitude of the spectrum is independent of the phase.

4.4.3 Harmonics

If a 2nd harmonic, with amplitude 0.5 and zero time shift, and a 3rd harmonic, with amplitude 0.5 and 1/4 period shift to the left, are added to the left and right waveforms shown in Fig. 4.8, respectively, the waveforms and spectra take the

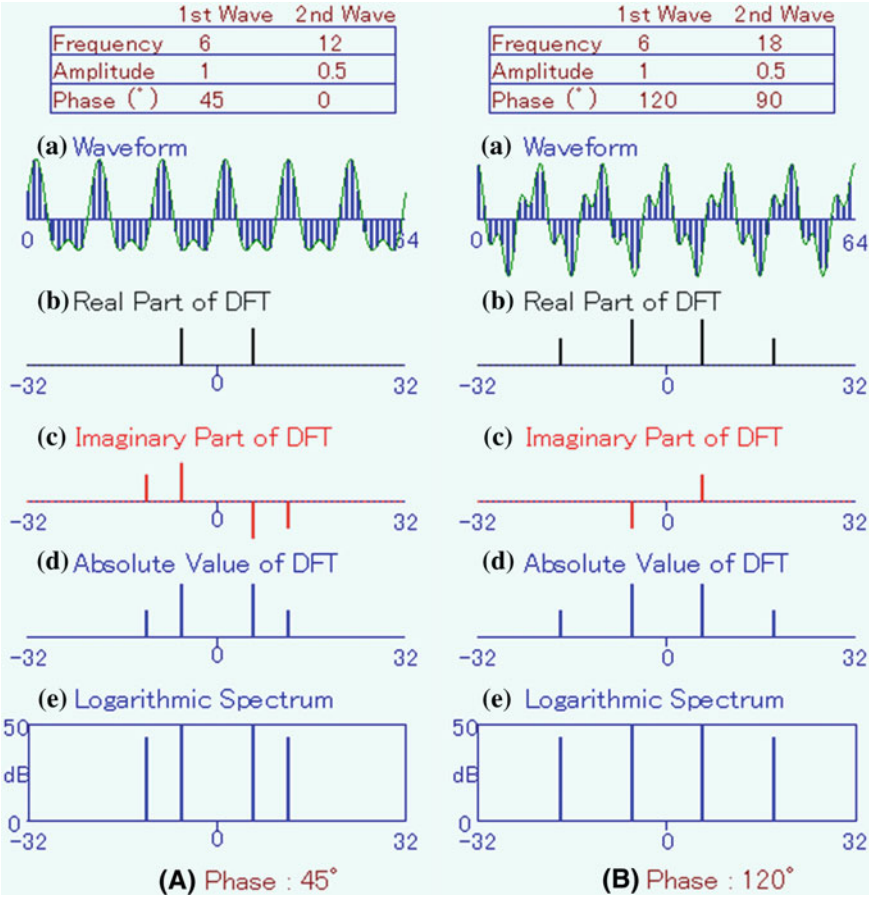

Fig. 4.9 Waveform and spectral changes when a second harmonic and a shifted third harmonic are added to the waveform in Fig. 4.8 (fundamental). The amplitudes of the 2nd and the 3rd harmonics are 0.5 and their phase shifts are 0° and 90°, respectively. Animation available in supplementary files under filename E4-09_SC.exe

form shown in Fig. 4.9. Since the DFT is a linear transformation, even when the harmonics are added, the fundamental components of the spectrum do not change. Since the initial phase of the 2nd harmonic is 0°, the spectrum of the harmonic appears only in the imaginary part (see (A)). And, since the initial phase of the third harmonic is 90° (i.e., it is a cosine wave), the spectrum of the harmonic appears only in the real part.

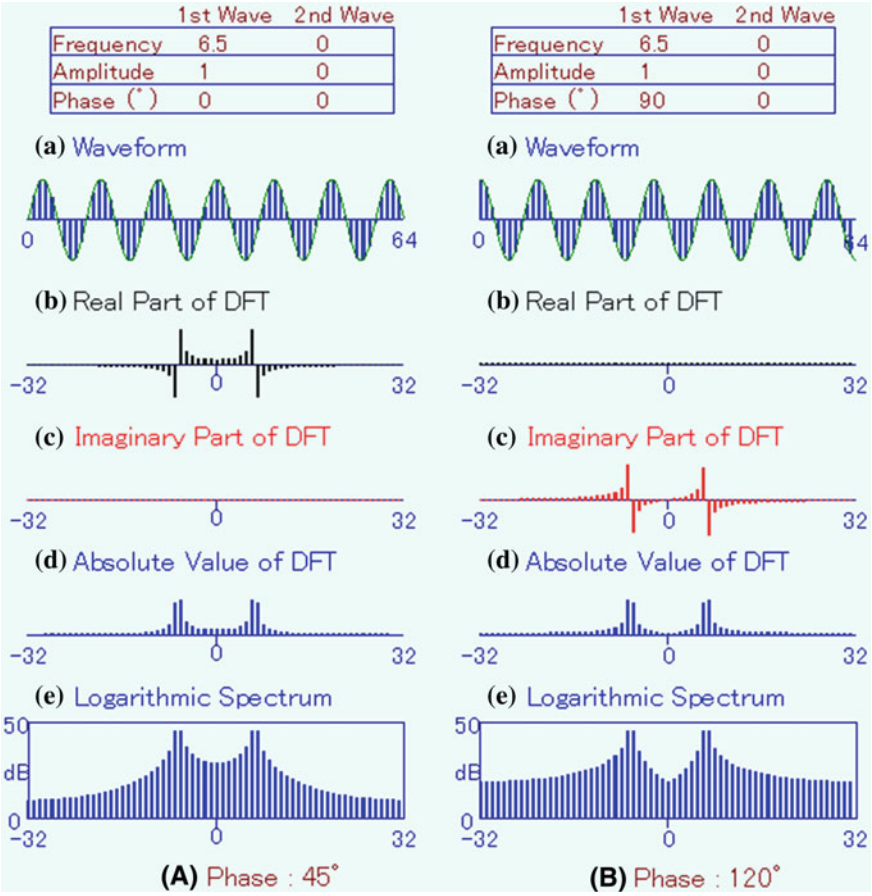

Fig. 4.10 64-point sample sequences and their DFTs. Animation available in supplementary files under filename E4-10_SC.exe

4.4.4 Symmetric and Antisymmetric Waveforms

The above example was for the case when the frequency is an integer. Let us check the case with noninteger frequency. Figure 4.10 shows the case when the frequency is 6.5. The top row shows two sample sequences with 64 point data. Figure 4.10A (top) is a sine wave starting with $n = 0$. Since the frequency is 6.5, the sample at $N - n$ is equal to the sample at n, i.e., the waveform is symmetric. Therefore, the spectrum has only the real components, which are distributed at many frequencies.

Figure 4.10B (top) shows the case with the cosine waveform (or sine with 90° phase shift). In this case, the magnitude of the value at $N-n$ is equal to that of the value at n with the opposite sign, i.e., the sample sequence is antisymmetric (odd

function). In this case, the real part might be expected to be zero. But it is not completely zero because the value at N, which corresponds to the value at $n = 0$, is not included in the sequence. If the value at $n = 0$ were removed from the sequence, the sequence would become purely antisymmetric. Therefore, the spectrum is actually the sum of the purely imaginary components, corresponding to the antisymmetric part of the sequence, and the spectrum corresponding to the impulse at $n = 0$. Each line of the latter spectrum is constant, with magnitude $1/N$. However, since the asymmetry is very small, the real components of the spectrum are hard to discern in the figure.

The above-mentioned constant components are specific with DFT analysis. If the waveform is infinitely long, N becomes infinitely large and their effect becomes negligible. But, for finite sequences, these components sometimes become noticeable.

Since the sequence with the first component removed is purely antisymmetric, its spectrum is purely imaginary. But, the components are distributed at many discrete frequencies because the number of the period is not an integer.

4.4.5 Sine Waveforms with Noninteger Frequencies

Figure 4.11A shows a waveform with four sine waves (left) and its spectrum (right). The number of periods of the sine waves in the 64-point sample sequence is 4, 9.5, 14, and 21, respectively. The phases of the third and fourth waves are 90° and 180°, respectively. These four waves are not harmonically related. Since the first, third, and fourth waves have integer frequencies, each of them has a line spectrum at the expected positive and negative integer frequencies. But the frequency of the second wave is not an integer, and its spectrum is distributed at various frequencies.

From Fig. 4.11A, one can see that the spectrum of the combined four waves is the summation of the individual spectra of the four waves. This is an important property of linear transformation.

4.4.6 Too Wide Sample Spacing

What type of spectrum would be expected from the DFT of a sample sequence obtained by sampling a waveform, which contains a frequency spectrum within $\pm f_{\mathrm{m}}$, using a sampling frequency less than $2f_m$? This has already been discussed in Figs. 3.6, 3.9, and 3.10 from the standpoint of recovering the waveform. Let us consider this problem again from the standpoint of spectrum changes.

One example is shown in Fig. 4.11B. The waveform contains sine waves with frequencies of 8, 16, and 35. The sample sequence has 64 sample data points and, therefore, the sampling frequency is considered to be 64. In this case, the

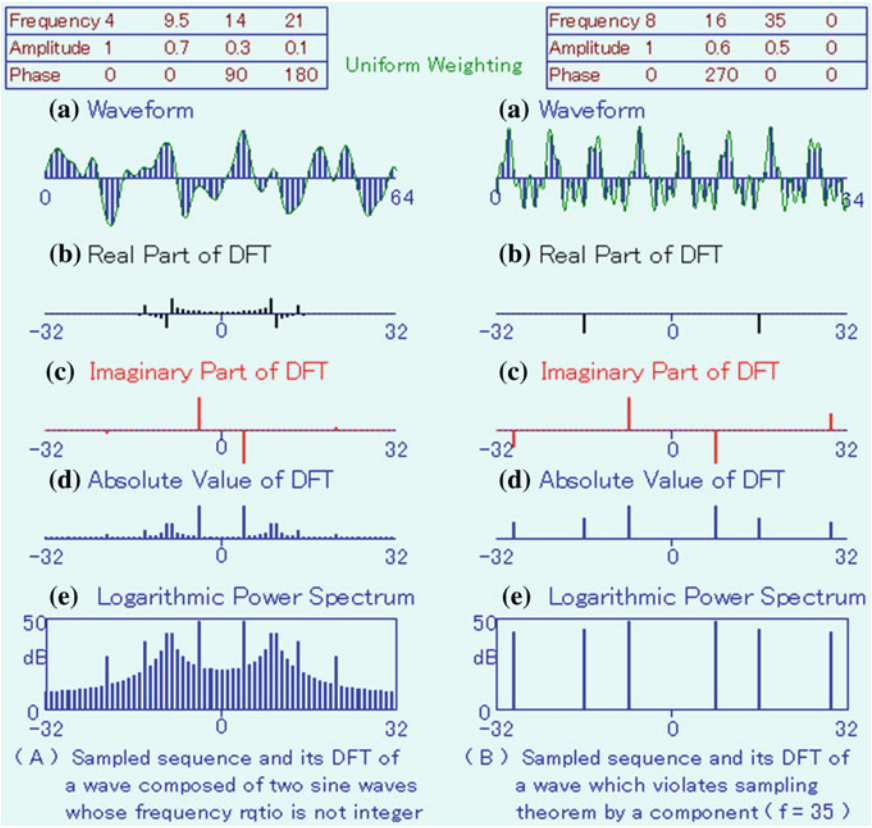

Fig. 4.11 *A* Waveform that contains four integer and noninteger frequency waves, and its spectrum. *B* Waveform that contains a wave that has 35 periods in the 64-point sample sequence, and its spectrum. Frequencies, amplitudes, and phases of each wave are shown in the charts at the *top*. Animation available in supplementary files under filename E4-11_SPC.exe

frequency component that is higher than 32 is not properly evaluated. In the figure, the spectra of the waves with frequencies 8 and 16 are observed at the expected locations. However, those of the wave with frequency 35 (=32 + 3) are observed at 29 (=32 − 3), and at −29 (=−32 + 3).

As had already been explained in Fig. 4.9, line spectra should appear at ±35, but in the 64-point DFT, the frequency spectrum is periodic, with the base band from −32 to +32 and the next period (right-side band) centered at +64 ranging from +32 to +96. The line spectrum expected at 35 lines to the left of center +64 appears at 29 (=64 − 35) in the base band. Also the line spectrum expected at 35 lines to the right of center −64 of the left-side band appears at −29 (=−64 + 35) in the base band. These are examples of the *folding spectrum* mentioned in Chap. 3. It is clear that the original waveform cannot be reconstructed from a spectrum with *aliasing*

distortion, since the "aliased" spectral lines at ±29 will be misinterpreted as corresponding to a frequency of 29.

Even when these distortions exist, low frequency spectral components that are not affected by these distortions (i.e.: the actual and aliased frequencies do not overlap) may be correctly represented. However, the possibility of aliasing will always exist if the sample frequency is not selected with the highest-frequency component taken into account.

4.4.7 Rectangular Wave

Consider a 64-point sample sequence, which contains two periods. Each period is made of 3 positive pulses, 11 zeros, 5 negative pulses, 11 zeros, and 2 positive pulses. Figure 4.12A shows the sample sequence and its spectra. The first pulse is at the origin of the time axis. If it is considered that the region from $n = N/2$ to $N - 1$ represents the negative time region, the sample sequence is symmetric. Therefore, the spectrum contains only the real part. The spectrum at zero frequency (dc component) is zero since the average of the sample sequence is zero.

The-64 point sample sequence shown in Fig. 4.12B also contains two periods. Each period is made of 16 equal pulses and remaining 16 zeros. This sample sequence could be divided into two sub-sequences: one a constant pulse train with 0.5 amplitudes; the other made of 16 positive, 16 negative, 16 positive, and 16 negative pulse trains with 0.5 absolute amplitudes. The first sequence is symmetric, minus one data point, the second is antisymmetric. The large real DC component corresponds to the first sequence; the many equally-spaced short lines along the frequency axis occur for the same reason given in Fig. 4.10B. There is also a antisymmetric imaginary part, which corresponds to the second, antisymmetric sequence.

Many waveforms can be made graphically. These are useful when learning the properties of the DFT. The reader is encouraged to try other examples using the program attached to Fig. 4.12.

4.5 Discrete Cosine Transform (DCT)

It was made clear that one must use complex numbers in order to calculate the DFT, even though the waveforms one analyzes are real. The discrete cosine transforms introduced in this section make it possible to calculate the DFT using only real numbers. There are four types of these DFTs, and one of them is used with photo, movie, and acoustic signals to reduce the data size.

The seed has already been planted in Chap. 1. In Fig. 1.9, it was shown that a rectangular wave that was offset from the center could be divided into two parts, one of which is an even function (symmetric) and the other is an odd function

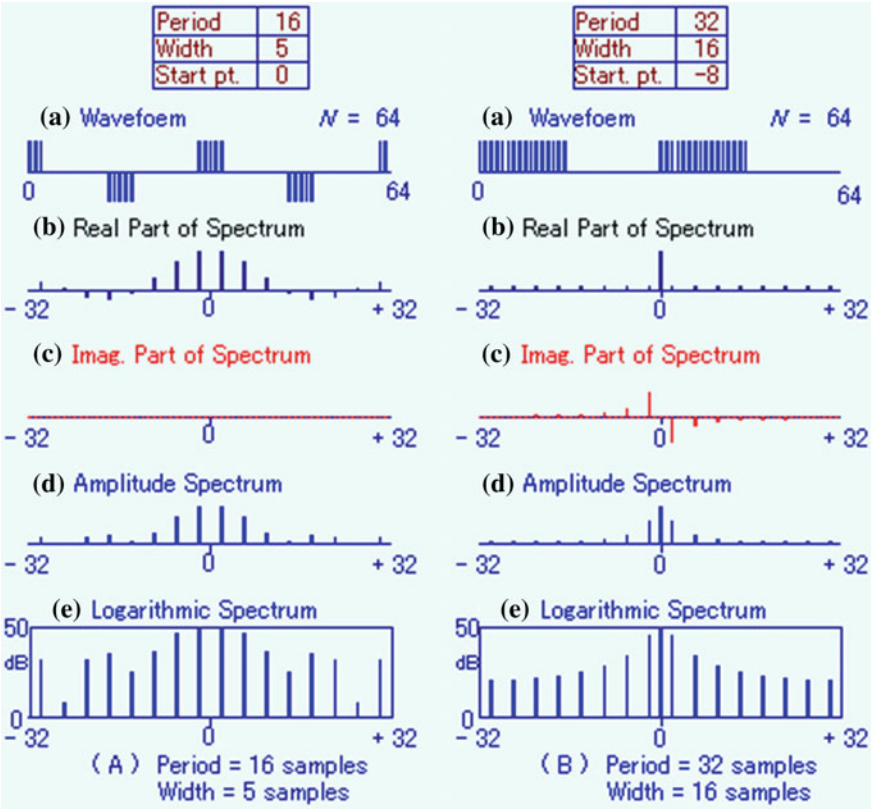

Fig. 4.12 Examples of sample sequences of periodic rectangular waveforms and their spectra. Animation available in supplementary files under filename E4-12_GeoWaveDFT.exe

(antisymmetric). The former can be represented only by cosine functions and the latter only by sine functions. In Sect. 2.3, it was shown that if a reversed function is added in the region from $-T$ to 0 to a waveform defined in the region from 0 to T, the resulting waveform becomes an even function in the region from $-T$ to T, and it can be represented using only cosine functions. The coefficients are given by Eqs. (2.19) and (2.20). Since the resulting waveform is even, the numerical calculation can be done with real numbers, and the results are also real. The DCT is derived by extending this idea.

Both real and imaginary parts are needed to obtain the original waveform from the DFT of the sample sequence (see Fig. 4.4 if one wants to make sure). One cannot reconstruct the original waveform using only the real part of the spectrum. As indicated before, the usefulness of the DCT lies in making the function even (symmetric).

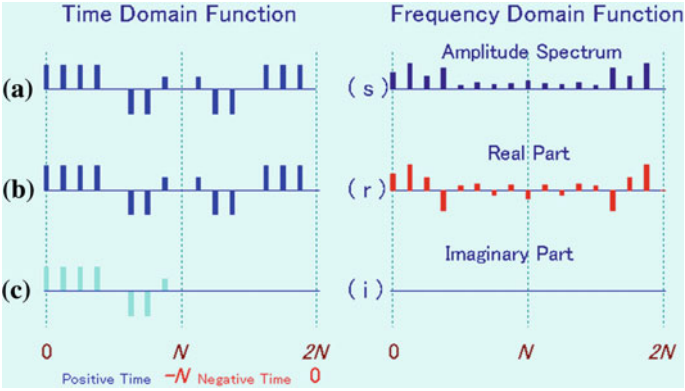

Fig. 4.13 2*N*-point DFT of *N*-point sequence augmented by a symmetric *N*-point sequence, so that only cosine functions are needed. **a** original *N*-point numerical sequence from $n = 0$ to $n = N - 1$; **b** 2*N*-point symmetric sequence built from (**a**); (r) and (i) real and imaginary parts of the DFT of the 2*N*-point sequence (**b**); **c** IDFT of (*r*) and (*i*). Animation available in supplementary files under filename E4-13_DCT.exe

It is not necessary that the input of the DCT (the sequence to be transformed by the DCT) be a time function. But, in this section, the inputs will be treated as time functions and the outputs as frequency functions.

Let us apply the DCT to the sample sequence shown in Fig. 4.13a. This is a sequence given in the region from 0 to $N - 1$. There are no samples in the region from N to $2N$. Before performing the $2N$ point DFT, the samples in the region N to $2N$ are arranged symmetrically with those in the region from 0 to $N - 1$. The symmetric sample sequence is shown in Fig. 4.13b.

The DFT of the 2*N*-point sample sequence, which is an even function, gives only the real spectrum, as shown in Fig. 4.13r, i. In the process of obtaining the DFT, the imaginary part that involves products and sums of the sine functions is identically zero, and there is no need to do the related calculations. The necessary operations can be performed using only real numbers. Since the spectrum of this sequence is periodic and symmetric, the operation that obtains the time sequence from this spectrum (IDFT) can also be performed using only real numbers. The result is shown in Fig. 4.13c, which is identical with (b), as expected. The first half of the sequence (c) is exactly the same as sequence (a). If the second half of sequence (c) is then abandoned, the resulting sequence is the original sequence.

It can be said that modifying the original sequence and executing the forward and inverse transforms using only the cosine functions is too roundabout, in the sense that it requires us to add the same length sequence to the original sequence and then, after the inverse conversion, the latter half of the sequence has to be thrown away.

What would happen if the DFT with cosine functions only is applied to a sequence that has zeros in the region from N to $(2N - 1)$ as shown in Fig. 4.14a,

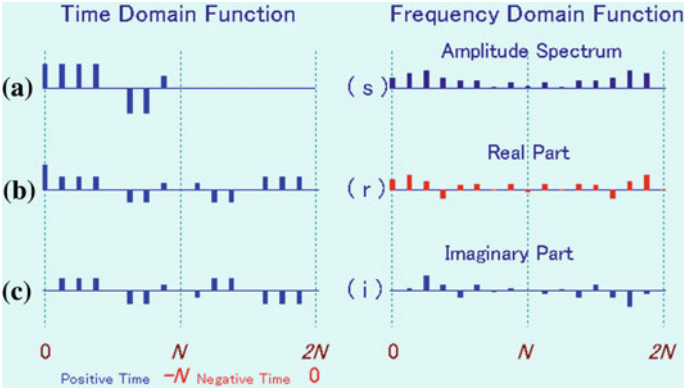

Fig. 4.14 2*N*-point DFT of *N*-point numerical sequence with successive *N*-point zeros. **a** original *N*-point numerical sequence from $n = 0$ to $n = N - 1$, zeros from *N* to 2*N*−1, (r) real part of 2 *N*-point DFT of (**a**), (i) imaginary part of 2*N*-point DFT of (**a**), **b** 2*N*-point IDFT of (*r*). **c** 2*N*-point IDFT of (*i*). Animation available in supplementary files under filename E4-14_DCT.exe

instead of the even sequence given by Fig. 4.13b? The real part of the DFT is given by,

$$X_c(k) = \sum_{n=0}^{2N-1} x(n) \cos\left(2\pi \frac{nk}{2N}\right) \tag{4.21}$$

The imaginary part of the DFT is given by,

$$X_S(k) = -\sum_{n=0}^{2N-1} x(n) \sin\left(2\pi \frac{nk}{2N}\right) \tag{4.22}$$

The two parts are shown in Fig. 4.14r, i, respectively. The amplitude spectrum is shown in Fig. 4.14s. Note that this amplitude spectrum is different from Fig. 4.13s, obviously because waveforms Figs. 4.13b and 4.14a are different.

Since one likes to use only the real part, let us find out what one will get when the IDFT is applied to the real part of the spectrum, Fig. 4.14r. Since the real part is symmetrical, the IDFT equation is given by,

$$x_c(k) = \frac{1}{N} \sum_{k=0}^{2N-1} X_c(k) \cos\left(2\pi \frac{nk}{N}\right) \tag{4.23}$$

This is the same as Eq. (4.21) except for the division by *N*. The result is shown in Fig. 4.14b.

The length of this sequence is 2*N* and the time range $N \leq n < 2N$ also has nonzero values. But, let us pay attention only to the left-hand time range $0 \leq n < N$.

The sequence Fig. 4.14b is equal to the sequence Fig. 4.14a at $n = 0$, and is half of the latter for $1 \leq n < N$. If our purpose is only to recover the original sequence, it can be done by using only the first half $(0 \leq n < N)$ of Eq. (2.23), keeping the value at $n = 0$ as it is, and doubling the values for $1 \leq n < N$. But this is a stopgap measure.

In the forward and inverse transforms, using only cosine functions, if the augmented sequence is symmetric with values in the negative time range, the original sequence is recovered. If the sequence has zeros in the range $N \leq n < 2N$, the recovered sequence becomes half the original except at $n = 0$. This is because the time function is the summation of the IDFTs of the real and imaginary parts and at $n = 0$, only the real part contributes to the inverse transform.

Let us reconsider Fig. 4.14a, b. The time sequence (a) has zeros in the range $N \leq n < 2N$. Its spectrum sequence (r) obtained by using only the cosine functions is a symmetric $2N$ point sequence. If the inverse transform is applied to this sequence again using only cosine functions, one gets the symmetric time sequence (b). As mentioned earlier, one then recovers the original sequence by doubling this sequence except at $n = 0$.

In this example, the spectrum sequence has $2N$ length, which is a transform of an N point sequence using only the cosine functions. It is natural to consider whether there might exist an N-point spectrum that gives a similar time sequence when it is inverse transformed. If so, then an N-point cosine transform pair becomes possible. This way of thinking suggests that the following transform pair may exist:

$$X(k) = AC_k \sum_{n=0}^{N} D_n x(n) \cos\left(\pi \frac{kn}{N}\right) \tag{4.24}$$

$$x(n) = BD_n \sum_{k=0}^{N} C_k X(k) \cos\left(\pi \frac{kn}{N}\right) \tag{4.25}$$

where A and B are constants and C_k and D_n are coefficients dependent on k and n, respectively. If one can determine these constants, the goal is achieved. The upper limit of n is extended to N, so that terms for $n = N$ can be used.

In order for the above two equations to be a transform pair, the result of substituting $X(k)$ of Eqs. (4.24) into (4.25) must be equal to $x(n)$ and vice versa.

The substitution becomes:

$$x'(n) = BD_n \sum_{k=0}^{N} C_k A C_k \sum_{m=0}^{N} D_m x(m) \cos\left(\pi \frac{km}{N}\right) \cos\left(\pi \frac{kn}{N}\right).$$

Changing the order of summation, this can be rewritten as:

$$x'(n) = \frac{AB}{2} D_n \sum_{m=0}^{N} D_m x(m) \sum_{k=0}^{N} C_k^2 \left[\cos\left\{ \pi \frac{k(m+n)}{N} \right\} + \cos\left\{ \pi \frac{k(m-n)}{N} \right\} \right]. \tag{4.26}$$

First, consider the Σ with respect to k in Eq. (4.26), for the case $m \neq n$. A similar summation was experienced in Sect. 4.2 (see Fig. 4.2). The differences are: (i) the summation of the real part of $\exp(j\pi k(m \pm n)/N\}$ instead of $\exp\{j2\pi k(m \pm n)/N\}$, and ii) the maximum of k is N instead of $N - 1$. The angle of the vector $\pi k(m \pm n)/N$ starts from zero ($k = 0$) and ends at $\pi(m \pm n)$ ($k = N$). If $(m \pm n)$ is odd, the (real parts of the) first and the last vectors cancel each other (assuming that $C_0 = C_N$) and the summation of the remaining vectors is also zero (assuming that $C_1 = C_2 = \cdots = C_{N-1}$). If $(m \pm n)$ is even, the vector for $k = N/2$ and the vectors for $k = 0$ and $k = N$ will cancel each other if C_k is defined by:

$$\{C_k^2\} = \{\frac{1}{2}, 1, 1, \ldots 1, \frac{1}{2}\}.$$

The summation of the remaining vectors is also zero. Therefore, it is necessary to consider only the case when $m = n$.

For the case of $m = n$, the summation of the first term in [ ] is zero for the same reason stated above. The sum of the second terms in [ ] for $0 < k < N$ is equal to $N - 1$, and the sum of the second terms for $k = 0$ and N is 1 because $C_0^2 = C_N^2 = 1/2$. Then, the total summation is equal to N. Therefore, except for the special cases of $n = 0$ and $n = N$, Eq. (4.26) becomes,

$$x'(n) = \frac{AB}{2} D_n^2 N x(n). \tag{4.27}$$

If $n = m = 0$ or $n = m = N$, the summation with respect to k is equal to $2N$, and, therefore, Eq. (4.26) becomes,

$$x'(n) = \frac{AB}{2} D_n^2 2N x(n) \tag{4.28}$$

If D_n is defined the same way as C_k by,

$$\{D_n^2\} = \{\frac{1}{2},\ 1,\ 1,\ \ldots 1,\ \frac{1}{2}\}$$

Equation (4.28) is equal to Eq. (4.27).

In order for $x'(n)$ to be equal to $x(n)$, the following condition is necessary.

$$ABN/2 = 1$$

If one defines A and B to satisfy above equation by

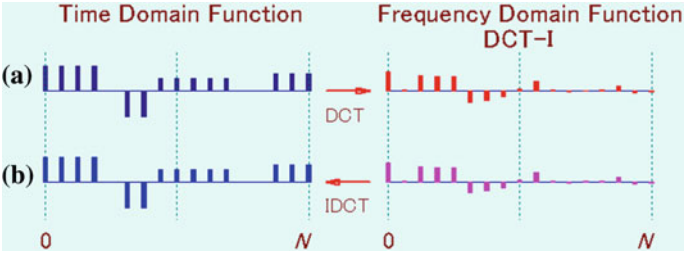

Fig. 4.15 Example of transforms by DCT-I and IDCT-I. **a***left* time sequence, *right* its DCT-I, **b***right* same spectrum as (**a**, *right*), **b***left* IDCT-I of (**b**, *right*). Animation available in supplementary files under filename E4-15_DCT-1.exe

$$A = B = \sqrt{\frac{N}{2}}$$

a symmetric transform pair is obtained using only the cosine functions:

$$X(k) = \sqrt{\frac{2}{N}} C_k \sum_{n=0}^{N} C_n x(n) \cos\left(\pi \frac{kn}{N}\right) \tag{4.29}$$

$$x(n) = \sqrt{\frac{2}{N}} C_n \sum_{k=0}^{N} C_k X(k) \cos\left(\pi \frac{kn}{N}\right) \tag{4.30}$$

where

$$\{C_k^2\} = \{\frac{1}{\sqrt{2}},\ 1,\ 1,\ \ldots 1,\ \frac{1}{\sqrt{2}}\}. \tag{4.31}$$

This is one of several possible *cosine transform pairs* and is called the *DCT-I*.

Figure 4.15 shows an example of a numerical calculation for the case of $N = 16$. Figure 4.15a (left) is the time sequence and its DCT is Fig. 4.15a (right). Figure 4.15b (right) is Fig. 4.15a (right) repeated and its IDCT is given by Fig. 4.15b (left). Of course, Fig. 4.15a (left), b (left) are identical.

4.6 Extension of the Discrete Cosine Transform

In the DCT-I, one can interpret that the sequence is arranged symmetrically on the positive and negative sides of n, and half of the data from $n = 0$ to $n = N$ is transformed. Consequently, the data at $n = 0$ to $n = N$ are overlapped and the values are doubled. The coefficient C_n is used to adjust this problem.

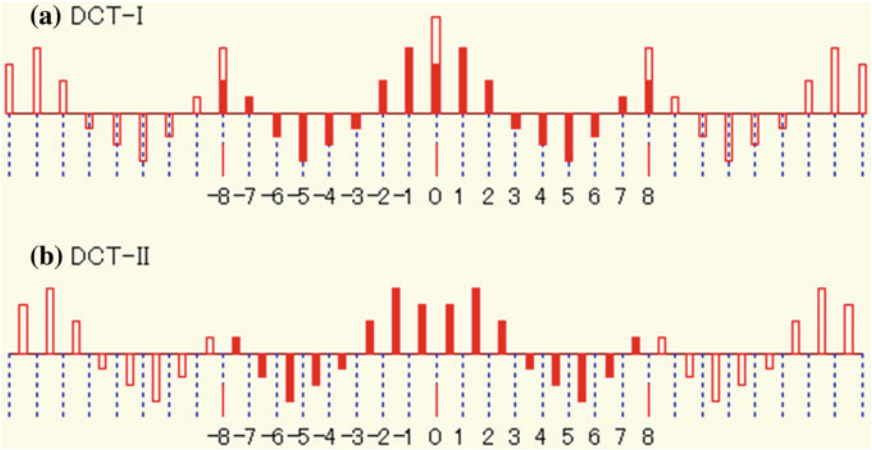

Fig. 4.16 Two ways of making a sequence even. **a** With $n = 0$ at the center; **b** by shifting each data sequence by 1/2 outward from $n = 0$. The void columns are shown to illustrate that the frequency spectrum is periodic

There is a different point of view. Equations (4.29) and (4.30) both use $\cos(\pi kn/N)$, which takes the same value when $n = 0$ and $n = N$. This makes it necessary to adjust C_n in order to make the transform pair valid. Even if the symmetry property is preserved, it is not natural to have $(N + 1)$ data points when the semicircumference is divided by N.

As a method of solving this problem while preserving complete symmetry, the arrangement of data shown in Fig. 4.16b is a candidate. The numbering of data is from 0 to $N - 1$, and the positions of all data are shifted by 1/2 of the discrete time interval. There are N data in both the positive and negative ranges of n and the total number is $2N$, which seems to be congenial with the $2N$ point DFT.

Since the sequence $x(n)$ is shifted by 0.5 on the time axis and since there is no overlap of the data, as shown in Fig. 4.16b, there is no need to use the coefficient D_n. Then, Eq. (4.24) can be rewritten as

$$X(k) = AC_k \sum_{n=0}^{N-1} x(n) \cos\left(\pi \frac{k(n+0.5)}{N}\right). \tag{4.32}$$

By comparison with Eqs. (4.24) and (4.25), the inverse transform of this equation must be

$$x(n) = B \sum_{k=0}^{N-1} C_k X(k) \cos\left(\pi \frac{k(n+0.5)}{N}\right). \tag{4.33}$$

In order for these two equations to be a transform pair, one must determine the coefficients A, B, and C_k.

The substitution of Eq. (4.32) into Eq. (4.33) gives

$$x'(n) = AB\sum_{k=0}^{N-1} C_k^2 \sum_{m=0}^{N-1} x(m)\cos\left\{\pi\frac{k(m+0.5)}{N}\right\}\cos\left\{\pi\frac{k(n+0.5)}{N}\right\}$$
$$= \frac{AB}{2}\sum_{m=0}^{N-1} x(m)\sum_{k=0}^{N-1} C_k^2\left[\cos\left\{\pi\frac{k(m+n+1)}{N}\right\} + \cos\left\{\pi\frac{k(m-n)}{N}\right\}\right].$$

The second cosine terms in the last Σ are equal to 1 for $m = n$, and if $k = 0$, both cosine terms are equal to 1 for all m and n. Therefore, if $C_0^2 = 1/2$ and $C_k^2 = 1$ $(k > 0)$, the Σ with respect to k is N for $m = n$. Except for the case $m = n$, the summation with respect to k is zero. Therefore, the result is

$$\frac{ABN}{2} = 1.$$

That is, if

$$A = B = \sqrt{\frac{2}{N}}.$$

Equations (4.32) and (4.33) can also be members of a discrete cosine transform pair. These formulae are rewritten as

$$X(k) = \sqrt{\frac{2}{N}}C_k\sum_{n=0}^{N-1} x(n)\cos\left(\pi\frac{k(n+0.5)}{N}\right) \tag{4.34}$$

$$x(n) = \sqrt{\frac{2}{N}}\sum_{k=0}^{N-1} C_k X(k)\cos\left(\pi\frac{k(n+0.5)}{N}\right) \tag{4.35}$$

where

$$C_0 = \sqrt{1/2}, C_k = 1{:}k > 0.$$

The discrete cosine transform pair given by Eqs. (4.34) and (4.35) is called the *DCT-II*.

In the DCT-II, the discrete time axis has been shifted by 0.5. As you can easily guess, the transform pair is still valid even if k and n are exchanged, in which case the discrete frequency is shifted by 0.5. This transform pair is given by

$$X(k) = \sqrt{\frac{2}{N}}\sum_{n=0}^{N-1} C_n x(n)\cos\left(\pi\frac{(k+0.5)n}{N}\right) \tag{4.36}$$

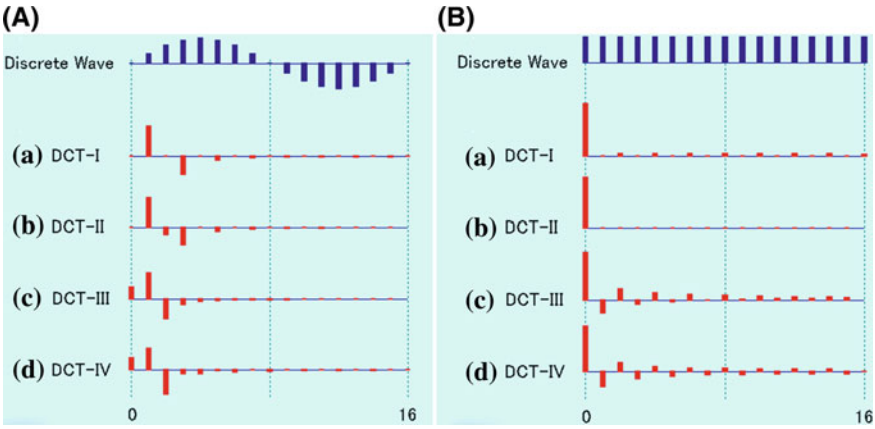

Fig. 4.17 Two waveforms and their DCT spectra obtained by DCT-1, DCT-II, DCT-III, and DCT-IV. Animation available in supplementary files under filename E4-17_DCT_A.exe

$$x(n) = \sqrt{\frac{2}{N}} C_n \sum_{k=0}^{N-1} X(k) \cos\left(\pi \frac{(k+0.5)n}{N}\right) \tag{4.37}$$

where

$$C_0 = \sqrt{1/2}, C_n = 1 : n > 0.$$

This is the discrete cosine transform called the *DCT-III*.

Moreover, by shifting both axes by 0.5, another transform is available. This is the transform which is called the *DCT-IV*.

$$X(k) = \sqrt{\frac{2}{N}} \sum_{n=0}^{N-1} x(n) \cos\left\{\pi \frac{(k+0.5)(n+0.5)}{N}\right\} \tag{4.38}$$

$$x(n) = \sqrt{\frac{2}{N}} \sum_{k=0}^{N-1} X(k) \cos\left\{\pi \frac{(k+0.5)(n+0.5)}{N}\right\} \tag{4.39}$$

In this transform, there is no need to specify constants.

So far, there have been derived four pairs of forward and inverse cosine transforms. Details of the derivation of DCT-III and DCT-IV are not shown, but both can be easily accomplished if one refers to the derivations of the DCT-I and DCT-II. These derivations are left as exercises.

Figure 4.17 shows two example time sequences and their spectra obtained by the four types of DCTs. Fig. 4.17A shows a one period sine wave and the four spectra; and (B) shows a DC signal and the four spectra. The time sequence of (B) has a nonzero value at $n = N$, but this is necessary only for DCT-I. There is no

further need to show that the inverse transforms (Eqs. 4.30, 4.35, 4.37, and 4.39) each give exactly the same original time waveform.

Notice that the different DCTs produce different spectra. The constant time sequence (B) should produce only the DC component, but it does not. The DCTs of the single-period sine sequence are quite different from the spectrum obtained by the DFT. In fact, the DCTs of the single-period sine sequence have many high-frequency components. DCTs produce much more complicated spectral shapes than the DFT.

The spectrum obtained by the DFT is understood to describe the frequency components of the original waveform. But, the DCTs shown above cannot be interpreted this way. Nevertheless, the DCT components of the one-period sine wave are limited to the low-frequency region, indicating that the DCT has some capability of frequency analysis. Because of this property as well as the property that only real numbers are handled in the DCTs, they are widely used for data reduction of images and sounds.

In the program of Fig. 4.17, the reader can choose any one of eight examples of 16-point waveforms and apply a DCT to it and then apply the IDCT to the spectrum using only a selected number of lowest order harmonics. The program shows the differences between the original and recovered waveforms in percent, which indicates that higher order harmonics can be neglected if small differences are tolerated. In many cases, the DCT-II seems more advantageous than others, but a more advanced discussion will be given in Chap. 13.

4.7 Exercises

1. What is the number of data points of the spectrum obtained by the N point DFT?
2. When the DFT of an N-point real sequence x_n is given by $X_n = R_n + jI_n$, what is the DFT of the imaginary sequence jx_n?
3. What are the differences between the N-point DFTs of purely real and purely imaginary sequences?
4. If the real and imaginary parts of an N-point DFT are neither even nor odd, what properties does the original N-point sequence have?
5. Can one obtain the DFT of the real part of a complex sequence from the DFT of the complete complex sequence? If yes, explain how it is obtained.
6. Must the time sequence satisfy the sampling theorem in order for the DFT pair to be valid?
7. The N-point DFT of a real sequence x_n is X_k. Can one obtain the original sequence x_n using only the values of X_k in the range from $k = 0$ to $k = N/2 - 1$? If yes, describe the method.
8. In the problem above, what is the answer if the sequence x_n is complex?
9. When sampling a waveform which has frequency components up to $1.2F_x$ [Hz], with sampling frequency $2F_x$ [Hz], is it possible to obtain the

correct spectrum of the original waveform from the DFT of the sampled sequence?

10. With regard to the spectrum of the above problem, what is the upper frequency limit of the correct spectrum?
11. Describe the reason why the high-frequency components of (A) are smaller than those of (B) in Fig. 4.10.
12. Derive Parseval's formula for a discrete sequence using Eqs. (4.9) and (4.10).
13. Derive the transform pair DCT-III.
14. Derive the transform pair DCT-IV.
15. In Fig. 4.17, the spectra of a constant time sequence are given. The DCT-III and DCT-IV spectra have larger high-frequency components than the DCT-II spectrum, which gives only the DC component. Explain why.

Chapter 5
Fast Fourier Transform

The digital Fourier transform (DFT) pair introduced in Chap. 4 is a very useful formula for numerical operations of the Fourier transform. However, if one tries to perform the calculation, it requires a large number of computations. In order to calculate an N-point DFT or IDFT, it requires N^2 times of summation and multiplication. Therefore, the computation of the DFT of several tens of points is not really practical. Even in the year of 1965, when fast computers were being developed, the DFT of more than 1,000 points was not easy to perform. In that year, an epoch-making algorithm of the fast Fourier transform (FFT) was invented by Cooley and Tukey [1–2]. It reduced the computation time to several hundredths of that required for N^2 computations, and engineering applications of the Fourier transform explosively expanded.

The algorithm of the fast Fourier transform is the one which reduces the number of summation and multiplication by successively conducting the calculation for smaller groups of data when N is a product of several integer numbers. First, in this chapter, *the decimation in time of the FFT algorithm*, which decomposes the DFT computation into successively smaller DFT computations, is introduced. Next, *the decimation in frequency of the FFT algorithm*, which divides the output sequence into smaller subsequences, is introduced. Then, several examples of computations following these principles are described.

5.1 Decimation in Time Algorithm

In this section, an N-point sequence will be dealt with, where N is given by a product of other integers, i.e., $N = LM$. At first, the original sequence is divided into L-point subsequences by choosing data at M intervals. The N-point DFT is obtained from the results gained by applying an L-point DFT to M subsequences. It will be shown that the number of summations and multiplications is reduced this way rather than directly applying an N-point DFT to the original sequence. This method is referred to as the *decimation in time algorithm* in the sense that the sequence is divided into M subsequences by taking the samples in M steps.

K. Kido, *Digital Fourier Analysis: Fundamentals*,
Undergraduate Lecture Notes in Physics, DOI: 10.1007/978-1-4614-9260-3_5,

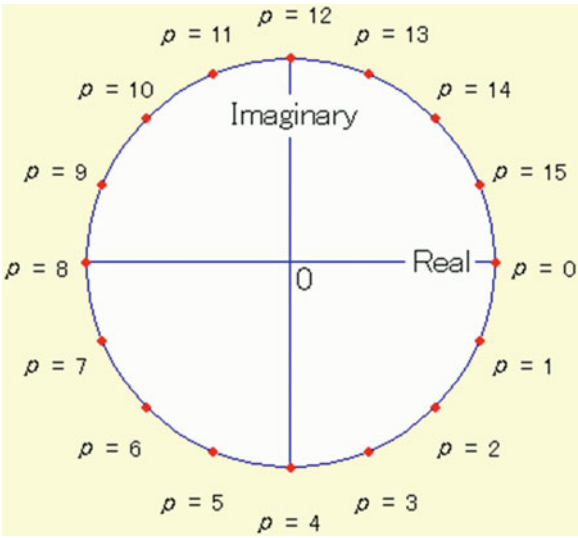

Fig. 5.1 Rotational factor W_N^p for $N = 16$

Before going into the details of FFT, a complex exponential function is defined as:

$$W_N = \exp(-j2\pi \frac{1}{N}) \tag{5.1}$$

W_N is the first point on the unit circle among N points which are given by dividing the circumference by N. The points are counted clockwise starting from the point on the positive real axis as shown in Fig. 5.1. Then W_N^p represents the p-th point on the unit circle. W_N^0 is on the crossing of the real positive axis and the circle. As p increases, the point moves clockwise on the unit circle. For this reason, W_N^p is called a *rotational factor*. W_N^{-1} is sometimes called a *primitive N-th root of unity* or a *weighting kernel*.

Equations (4.19) and (4.20) are rewritten using W_N^p as follows:

$$X(k) = \sum_{n=0}^{N-1} x(n) \exp(-j2\pi \frac{nk}{N}) = \sum_{n=0}^{N-1} x(n) W_N^{nk} \tag{5.2}$$

$$x(n) = \frac{1}{N} \sum_{k=0}^{N-1} X(k) \exp(j2\pi \frac{nk}{N}) = \frac{1}{N} \sum_{k=0}^{N-1} X(k) W_N^{-nk} \tag{5.3}$$

In order to obtain $X(k)$ from Eq. (5.2), N multiplications of $x(n)$ and W_N^{nk} and (N − 1) summations are necessary. Since k takes N values, the total number of multiplication and summation is given approximately by N^2. If N is given by a product of some integers, there is a method of reducing the number of the

computation. One should notice that the multiplications and summations are carried out using complex numbers.

If N is a product of L and M,

$$N = LM \tag{5.4}$$

The DFT of Eq. (5.2) is rewritten as

$$\begin{aligned} X(k) &= \sum_{r=0}^{L-1} x(rM) W_N^{rMk} + \sum_{r=0}^{L-1} x(rM+1) W_N^{(rM+1)k} + \cdots + \sum_{r=0}^{L-1} x(rM+M-1) W_N^{(rM+M-1)k} \\ &= \sum_{r=0}^{L-1} x(rM) W_L^{rk} + \sum_{r=0}^{L-1} x(rM+1) W_L^{rk} W_N^{k} + \cdots + \sum_{r=0}^{L-1} x(rM+M-1) W_L^{rk} W_N^{(M-1)k} \end{aligned}$$

Each term $\sum_{r=0}^{L-1} x(rM+\mu) W_L^{rk}$ $(\mu = 0,\ 1,\ \ldots,\ M-1)$ in the above equation has L multiplications and summations. However, since W_N^{rk} is a periodic function of rk with period L, it takes on only L values, and therefore, $\sum_{r=0}^{L-1} x(rM+\mu) W_L^{rk}$ is an L-point DFT. Then, the above equation can be written as

$$\begin{aligned} X(k) = {} & \mathrm{DFT}_L\{x(rM)\} + \mathrm{DFT}_L\{x(rM+1)\} W_N^{k} + \cdots \\ & + \mathrm{DFT}_L\{x(rM+M-1)\} W_N^{(M-1)k} \end{aligned} \tag{5.5}$$

where $\mathrm{DFT}_L\{x(n)\}$ represents an L-point DFT of $x(n)$.

By this decomposition, N-point DFT becomes the sum of M products of L-point DFT and $W_N^{\mu k}$ $(\mu = 0,\ 1,\ \ldots,\ M-1)$. Figure 5.2 shows the flow of this calculation process. The small arrows in the figure indicate multiplications by $W_N^{\mu k}$. The value of μ is given in the box where the line with the arrow starts and the value of k is given by $X(k)$ at the end of the same line.

In Fig. 5.2, the time domain function $x(n)$ is divided into M groups by selecting the values in M steps. On the other hand, $X(k)$ in the frequency domain is aligned in the increasing order of k. In the original paper [4], this method is called *the decimation in time FFT algorithm*.

Now, one can count the number of multiplications. By dividing N into L times M (Eq. (5.5)), there are M multiplications of L-point FFT times $W_N^{\mu k}$. The range of k is from 0 to $N-1$, and therefore, the total number of multiplication in this step is MN. The L-point FFT requires multiplication of L^2 times, and the number of L-point FFT is M. Then, the total number of multiplications for the L-point FFT is $L^2 M$. After all, the total number of multiplications required is $MN + L^2 M = (M+L)N$, since $N = LM$.

If $N = LM$, except for the cases where either L or M is 1 or L and M are both 2, the relation $(M+L) < N$ holds. Therefore, the total number of multiplication is reduced to $(M+L)N$ from N^2.

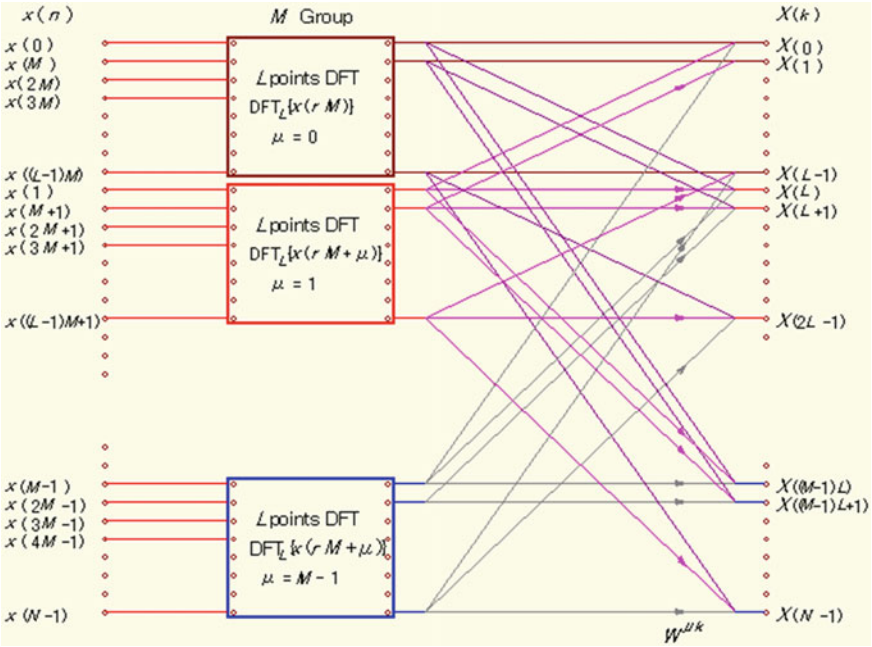

Fig. 5.2 Signal flow for the case of decomposition of an N-point DFT into L-point DFTs of number M

If L or M is a product of two other integers, the reduction of the number of multiplications is possible by the same decomposition. For example, if $L = PQ$, the number of multiplications necessary for an L-point FFT is reduced to $(P + Q)L$. Then, the total number of multiplications is reduced from $(M + L)N$ to $(M + P + \mathrm{Q})N$. By the same way, if

$$N = P_1 \cdot P_2 \cdot \ldots \cdot P_J \tag{5.6}$$

the number of multiplication is reduced from N^2 to

$$N(P_1 + P_2 + \ldots + P_J) \tag{5.7}$$

In a special case, if N is given by

$$N = r^m \tag{5.8}$$

the number of multiplications becomes

$$mrN = rN \log_r N \tag{5.9}$$

In this relationship, the practically unnecessary multiplication by $W_N^0 = 1$ is included. The reduction of numbers is also applicable to the numbers of summations.

As will be stated in Section 5.3, if $r = 2$, the number given by Eq. (5.9) is further reduced to 1/4. Now check the reduction of computation for a practical example. If $r = 2$ and $m = 10$, N is equal to 1,024 and the number of multiplications in direct computation is approximately 1,050,000 ($\approx N^2$). The number given by Eq. (5.9) is equal to 20,480 ($=mrN$), which is approximately 1/50 of N^2. As N increases, the reduction ratio increases. This much of reduction of the computation time due only to the algorithm is very rare.

It is clear from Eqs. (5.2) and (5.3) that, if $W_N^{\mu k}$ is replaced by $W_N^{-\mu k}$, exactly the same process can be used to calculate the IDFT, where an additional operation of division by N is necessary. Hereafter, calculation of the IDFT by the FFT algorithm will be called the IFFT.

5.2 Decimation in Frequency Algorithm

If $N = LM$, the frequency domain function $X(k)$ can be divided into L groups by selecting the values in L steps. Applying an M-point FFT to each group, the number of computation can be reduced. This method is called *decimation in frequency FFT algorithm.*

The first step in this case also starts by dividing Eq. (5.2). The spectrum $X(k)$ is divided into L groups $\{X(0), X(L), X(2L), \ldots, X((M-1)L)\}$, $\{X(1), X(L+1), X(2L+1), \ldots, X((M-1)L+1)\}, \ldots,$ and $\{X(L-1), X(2L-1), X(3L-1), \ldots, X((N-1)\}$. Figure 5.3 shows $X(k)$ arranged in these L groups. The parameter k in the L groups can be represented as

$$k = rL, rL+1, rL+2, \ldots, rL+L-1,$$

where $r = 0, 1, \ldots, M-1$. Then, Eq. (5.2) is divided into L groups:

$$\begin{aligned} X(rL) &= \sum_{n=0}^{N-1} x(n) W_N^{rLn} \\ X(rL+1) &= \sum_{n=0}^{N-1} x(n) W_N^{(rL+1)n} \\ &\vdots \\ &\vdots \\ X(rL+L-1) &= \sum_{n=0}^{N-1} x(n) W_N^{(rL+L-1)n} \end{aligned} \tag{5.10}$$

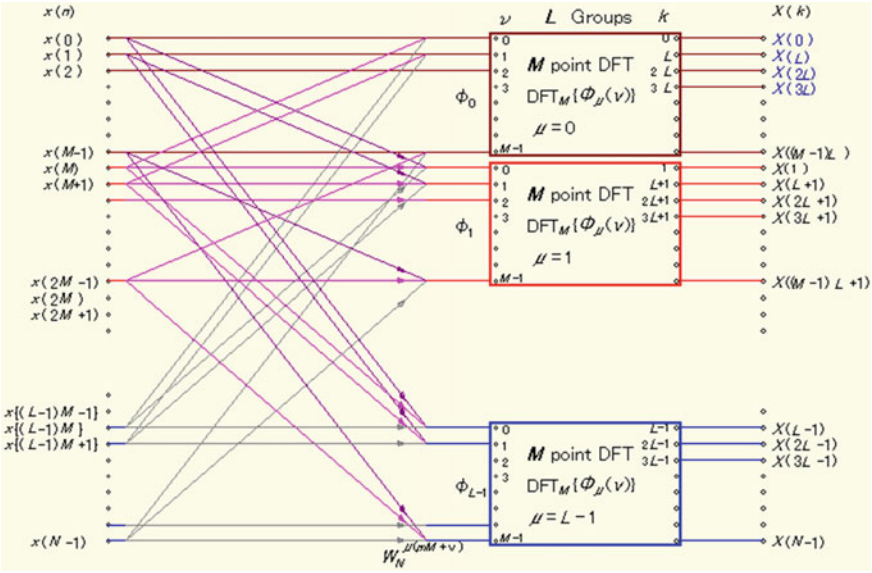

Fig. 5.3 Signal flow of N-point DFT by the decimation in frequency algorithm

The multiplication and summation of the right-hand side of the first equation can be divided into L groups by grouping them in the descending order.

$$\begin{aligned} X(rL) &= \sum_{n=0}^{M-1} x(n) W_N^{rLn} + \sum_{n=M}^{2M-1} x(n) W_N^{rLn} + \cdots + \sum_{n=(L-1)M}^{LM-1} x(n) W_N^{rLn} \\ &= \sum_{v=0}^{M-1} x(v) W_N^{rLv} + W_N^{rLM} \sum_{v=0}^{M-1} x(M+v) W_N^{rLv} + \cdots \\ &\quad + W_N^{rL(L-1)M} \sum_{v=0}^{M-1} x\{(L-1)M+v\} W_N^{rLv} \end{aligned}$$

where $N = LM$, $W_N^{rLM} = W_N^{rN} = 1$, $W_N^{rLv} = W_M^{rv}$. Furthermore, since r is an integer,

$$\begin{aligned} X(rL) &= \sum_{v=0}^{M-1} x(v) W_M^{rv} + \sum_{v=0}^{M-1} x(M+v) W_M^{rv} + \cdots + \sum_{v=0}^{M-1} x\{(L-1)M+v\} W_M^{rv} \\ &= \sum_{v=0}^{M-1} \left[x(v) + x(M+v) + \cdots + x\{(L-1)M+v\} \right] W_M^{rv} \end{aligned} \tag{5.11}$$

This is the M-point DFT of the sum of L terms taken in M steps. The second and higher order equations in Eq. (5.10) can be handled similarly. In these cases, each term taken in M steps is multiplied by the rotation factor as shown in Eq. (5.12).

$$\begin{aligned}
X(rL+\mu) &= \sum_{n=0}^{M-1} x(n) W_N^{(rL+\mu)n} + \sum_{n=M}^{2M-1} x(n) W_N^{(rL+\mu)n} + \cdots + \sum_{n=(L-1)M}^{LM-1} x(n) W_N^{(rL+\mu)n} \\
&= \sum_{v=0}^{M-1} x(v) W_N^{(rL+\mu)v} + W_N^{(rL+\mu)M} \sum_{v=0}^{M-1} x(M+v) W_N^{(rL+\mu)v} + \cdots \\
&\quad + W_N^{(rL+\mu)(L-1)M} \sum_{v=0}^{M-1} x\{(L-1)M+v\} W_N^{(rL+\mu)v} \\
&= \sum_{v=0}^{M-1} x(v) W_N^{(rL+\mu)v} + W_N^{\mu M} \sum_{v=0}^{M-1} x(M+v) W_N^{(rL+\mu)v} + \cdots \\
&\quad + W_N^{\mu(L-1)M} \sum_{v=0}^{M-1} x\{(L-1)M+v\} W_N^{(rL+\mu)v} \\
&= \sum_{v=0}^{M-1} \left[x(v) W_N^{\mu v} + x(M+v) W_N^{\mu(M+v)} + \cdots + x\{(L-1)M+v\} W_N^{\mu\{(L-1)M+v\}} \right] W_M^{rv}
\end{aligned} \tag{5.12}$$

The bracketed term of the above equation is expressed as $\phi_\mu(v)$:

$$\begin{aligned}
\phi_\mu(v) &= \left[x(v) W_N^{\mu v} + x(M+v) W_N^{\mu(M+v)} + \cdots + x\{(L-1)M+v\} W_L^{\mu\{(L-1)+v\}} \right] \\
&= \sum_{m=0}^{L-1} x(mM+v) W_N^{\mu(mM+v)}
\end{aligned} \tag{5.13}$$

The number of $\phi_\mu(v)$ is L ($\mu = 0,\ 1,\ \ldots, L-1$). By looking back at Eqs. (5.11) and (5.12), it is found that Eq. (5.11) is the M-point DFT of $\phi_0(v)$ and Eq. (5.12) is the M-point DFTs of $\phi_\mu(v)$ for $\mu \geq 1$. These can be expressed by the single equation:

$$X(rL+\mu) = \sum_{v=0}^{M-1} \phi_\mu(v) W_M^{rv} \tag{5.14}$$

The operations in the L boxes in Fig. 5.3 are the operations of Eq. (5.14), starting from $\mu = 0$ (top box) and ending with $\mu = L-1$ (bottom box). Since r takes values from 0 to $M-1$, all spectrum components ($LM = N$) are calculated.

Now count the number of operations. From Eq. (5.14) it is known that the M-point DFT is necessary in order to calculate one of $X(rL+\mu)$ terms. Since r takes M values, the (sub) total number of calculations (multiplication and summation) is

M^2. The parameter μ also takes L values, and therefore the total number of calculation is equal to LM^2 (=NM). Before the calculation of Eq. (5.14), $\phi_\mu(v)$ given by Eq. (5.13) must be calculated L times since $\mu = 0, 1, \ldots, L-1$. From Eq. (5.13) it is known that L calculations are necessary for one v, and v varies from 0 to $M-1$, then the number of calculations becomes LM. By multiplying by L, the number becomes L^2M (=LN).

In overall, $\phi_\mu(v)$ (Eq. (5.13)) requires LN calculations, and from $\phi_\mu(v)$, $X(k)$ (Eq. (5.14)) is obtained by MN calculations, resulting in the total number of $N(L+M)$ calculations (multiplications and summations). This number is equal to that of the decimation in time FFT algorithm.

It may not be necessary to describe the reduction of the number of operation in the case where M is a product of two integers.

Figure 5.3 shows the process of selecting values of $X(k)$ in L steps, and dividing into L groups, and then applying M-point DFTs to the L groups. The order of data number of each M-point DFT is different from the original order. This is due to the division in the frequency domain. This algorithm is called *decimation in frequency FFT algorithm* in the original paper [4].

5.3 2^m-Point FFT by Decimation in Time Algorithm

In the preceding sections, reasons for the reduction of number of operations have been given, but they are not necessarily enough to write programs. So, in this and following sections, explanations that lead to programming of FFT algorithms will be given for the case $N = 2^m$.

It was shown in Sect. 5.2 that if $N = r^m$, the number of operations is reduced from N^2 to $mrN = rN\log_r N$. The integer r can take any value, but the case $r = 2$ is the easiest and simplest to program. There are other cases than $r = 2$ that give a smaller number of operations [5], but there are not enough differences in the ratio of reduction to employ those cases. Therefore, one will start with

$$N = 2^m \tag{5.15}$$

In the case of Eq. (5.15), the decomposition given by Eq. (5.5) using $L = N/2$ and $M = 2$ becomes

$$\begin{aligned} X(k) &= \mathrm{DFT}_{N/2}\{x(2r)\} + \mathrm{DFT}_{N/2}\{x(2r+1)\}W_N^k \\ &= \sum_{r=0}^{N/2-1} x(2r)W_{N/2}^{2rk} + W_N^k \sum_{r=0}^{N/2-1} x(2r+1)W_{N/2}^{(2r+1)k} \\ &= B_p + C_p W_N^k \qquad p = k \mod (N/2) \end{aligned} \tag{5.16}$$

where

$$B_p = \sum_{r=0}^{N/2-1} x(2r) W_{N/2}^{2rp}$$
$$C_p = \sum_{r=0}^{N/2-1} x(2r+1) W_{N/2}^{(2r+1)p}$$

The case $m = 3$ (i.e. $N = 8$) provides an example that is easy to understand. For induction of equations for this case, a property given by

$$W_N^k = -W_N^{(k-N/2)} \tag{5.17}$$

should be pointed out. The relation given in Eq. (5.17) can be easily understood by the vector representation given by Fig. 5.4.

In general, both B_p and C_p are complex, therefore, there are 4 multiplications and summations of real numbers in Eq. (5.16).

For the case of $N = 8$, B_p and C_p in Eq.(5.16) will be expressed in more detail.

$$\begin{aligned}
B_0 &= x(0)W_4^0 + x(2)W_4^0 + x(4)W_4^0 + x(6)W_4^0 \\
B_1 &= x(0)W_4^0 + x(2)W_4^2 + x(4)W_4^4 + x(6)W_4^6 \\
B_2 &= x(0)W_4^0 + x(2)W_4^4 + x(4)W_4^0 + x(6)W_4^4 \\
B_3 &= x(0)W_4^0 + x(2)W_4^6 + x(4)W_4^4 + x(6)W_4^2 \\
C_0 &= x(1)W_4^0 + x(3)W_4^0 + x(5)W_4^0 + x(7)W_4^0 \\
C_1 &= x(1)W_4^1 + x(3)W_4^3 + x(5)W_4^5 + x(7)W_4^7 \\
C_2 &= x(1)W_4^2 + x(3)W_4^6 + x(5)W_4^2 + x(7)W_4^6 \\
C_3 &= x(1)W_4^3 + x(3)W_4^1 + x(5)W_4^7 + x(7)W_4^5
\end{aligned}$$

Using these B_p and C_p, Eq. (5.16) is rewritten as

$$\begin{aligned}
X(0) &= B_0 + C_0 W_8^0 \\
X(1) &= B_1 + C_1 W_8^1 \\
X(2) &= B_2 + C_2 W_8^2 \\
X(3) &= B_3 + C_3 W_8^3 \\
X(4) &= B_0 + C_0 W_8^4 = B_0 - C_0 W_8^0 \\
X(5) &= B_1 + C_1 W_8^5 = B_1 - C_1 W_8^1 \\
X(6) &= B_2 + C_2 W_8^6 = B_2 - C_2 W_8^2 \\
X(7) &= B_3 + C_3 W_8^7 = B_3 - C_3 W_8^3
\end{aligned} \tag{5.18}$$

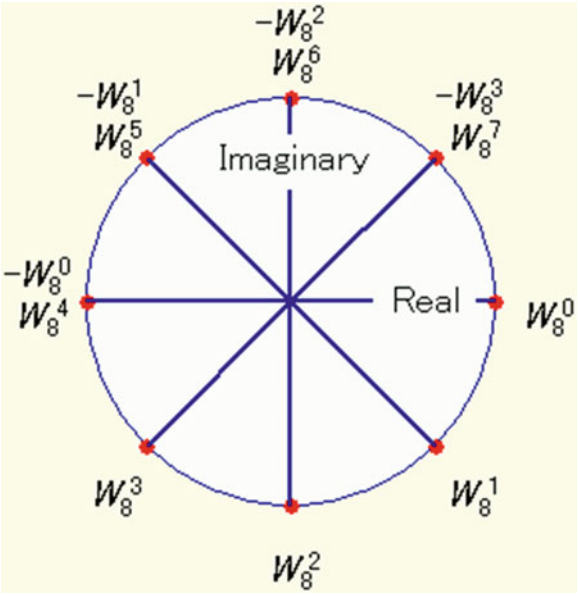

Fig. 5.4 Explanation of Eq. (5.17) for the case $N = 8$

$W_8^4 \sim W_8^7$ are replaced by $-W_8^0 \sim -W_8^3$ by the relation Eq. (5.17), which are shown in the latter four lines in Eq. (5.18). Therefore, the number of multiplications is reduced to 1/2.

Equation (5.18) shows that summations of DFT(B_k) of even terms of $x(n)$ and DFT (C_k) of odd terms of $x(n)$ multiplied by the rotation factors give from $X(0)$ to $X(3) = X(N/2 - 1)$, and the subtractions give from $X(4) = X(N/2)$to $X(7) = X(N - 1)$. The operation of the process is shown in Fig. 5.5. The arrows in the figure indicate multiplications by coefficients and if "-1" is shown near the arrow, it means the reversal of the sign. Therefore, the multiplications are necessary for W_8^k ($k = 0,\ 1,\ 2,\ 3$) except for $k = 0$ ($W_8^0 = 1$).

Furthermore, the operations to calculate B_m and C_m (m = 0, 1, 2, 3, 4) are also shortened by being divided into two N/4-point DFTs. In the calculation of B_m, the first DFT gives D_0 and D_1 by using even terms $X(0)$ and $X(4)$ as its input and the second DFT gives E_0 and E_1 by using odd terms $X(2)$ and $X(6)$ as its input. In the same way, the calculation of C_m (m = 0, 1, 2, 3, 4) is replaced by two N/4-point DFTs, giving F_0, F_1, G_0, and G_1. These are shown by the set of equations below.

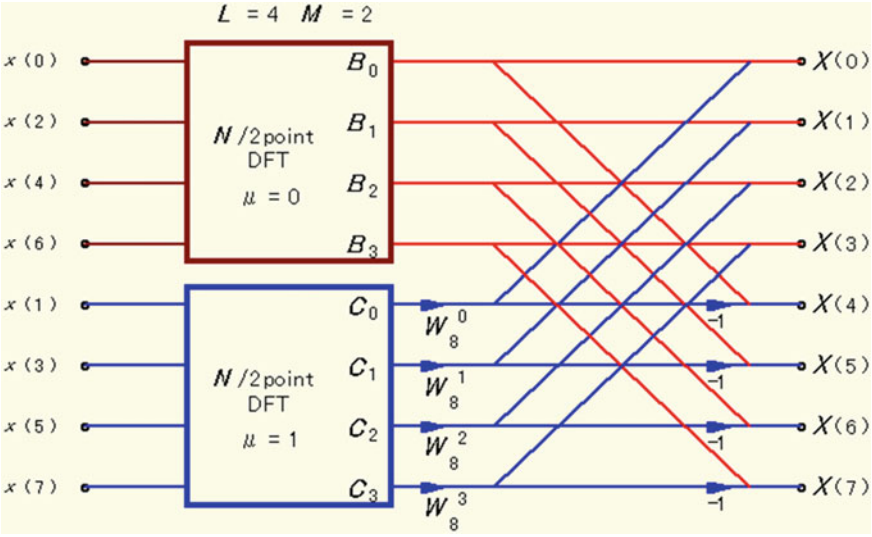

Fig. 5.5 Signal flow of 8-point DFT of $x(n)$ by the decimation in time algorithm. The 8-point DFT is decomposed into two 4-point DFTs of even and odd order terms expressed by Eq. (5.18)

$$
\begin{aligned}
B_0 &= D_0 + E_0 W_8^0 \\
B_1 &= D_1 + E_1 W_8^2 \\
B_2 &= D_0 + E_0 W_8^4 = D_0 - E_0 W_8^0 \\
B_3 &= D_1 + E_1 W_8^6 = D_1 - E_1 W_8^2 \\
C_0 &= F_0 + G_0 W_8^0 \\
C_1 &= F_1 + G_1 W_8^2 \\
C_2 &= F_0 + G_0 W_8^4 = F_0 - G_0 W_8^0 \\
C_3 &= F_1 + G_1 W_8^6 = F_1 - G_1 W_8^2
\end{aligned}
\tag{5.19}
$$

In Eq. (5.19), by the use of Eq. (5.17), the numbers of multiplications necessary to calculate the third and fourth lines and the sixth and seventh lines are halved by using results of the first and second lines and the fourth and fifth lines, respectively. Using these results, $N/2$-point DFTs to calculate B_m and C_m in the signal flow of Fig. 5.5 are replaced by $N/4$-point DFTs in Fig. 5.6.

The number of calculations of B_m and C_m, which are $N/2$-point DFTs, is reduced by replacing by D_k, E_k, F_k, and G_k, which are $N/4$-point DFTs. By the same way, the number of calculations of D_k, E_k, F_k, and G_k, can be reduced by using $N/8$-point DFTs. Since $N = 8$, the $N/8$-point DFTs are the values themselves of the time sequence, and D_k, E_k,, F_k, and G_k, are the 2-point DFTs with two values of the sequence as inputs.

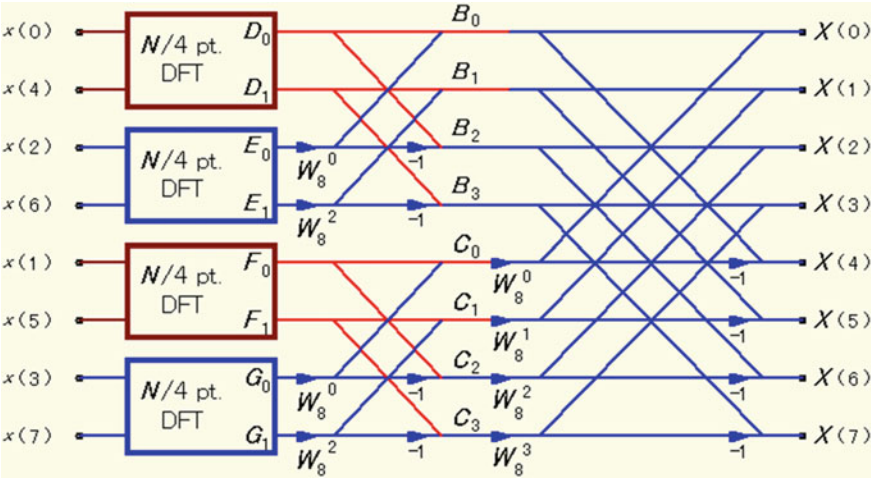

Fig. 5.6 Signal flow of 8-point DFT of $x(n)$ by use of Eq. (5.19), where B_k and C_k are obtained replacing $N/2$-point DFTs by $N/4$-point DFTs

The rotation factors used in 2-point DFTs are W_8^0 and W_8^4. However, since $W_8^0 = 1$ and $W_8^4 = -1$, the necessary operation is only to change the sign when multiplying by W_8^4. Then D_k, E_k, F_k, and G_k, $(k = 0, 1)$ are given only by additions and subtractions:

$$\begin{aligned}
D_0 &= x(0) + x(4)W_8^0 = x(0) + x(4) \\
D_1 &= x(0) + x(4)W_8^4 = x(0) - x(4) \\
E_0 &= x(2) + x(6)W_8^0 = x(2) + x(6) \\
E_1 &= x(2) + x(6)W_8^4 = x(2) - x(6) \\
F_0 &= x(1) + x(5)W_8^0 = x(1) + x(5) \\
F_1 &= x(1) + x(5)W_8^4 = x(1) - x(5) \\
G_0 &= x(3) + x(7)W_8^0 = x(3) + x(7) \\
G_1 &= x(3) + x(7)W_8^4 = x(3) - x(7)
\end{aligned} \tag{5.20}$$

By changing the first DFTs in Fig. 5.6 to the additions and subtractions of sample values using Eq. (5.20), the signal flow shown in Fig. 5.7 is obtained.

As shown above, the basic operation of FFT is given by

$$\left.\begin{aligned} y_h &= u_h + v_h W_N^{ph} \\ y_{h+s} &= u_h - v_h W_N^{ph} \end{aligned}\right\} \tag{5.21}$$

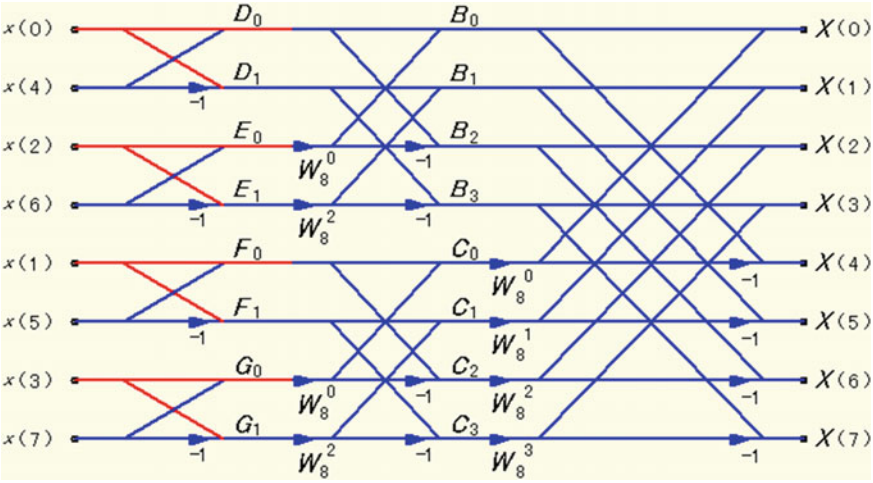

Fig. 5.7 Signal flow of 8-point DFT of $x(n)$. The first operation is $N/4$-point DFTs to obtain D_k, E_k, F_k, and G_k. Each $x(n)$ corresponds to an $N/8$-point DFT

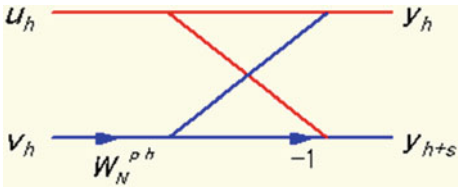

Fig. 5.8 Butterfly computation in the decimation in time algorithm

where

$$
\begin{aligned}
&N = 2^M \\
&s = 2^r \qquad (r = 0,\ 1,\ 2,\ \cdots,\ M-1) \\
&h = 0,\ 1,\ 2,\ \cdots,\ s-1 \\
&p = N/2^{r+1}
\end{aligned}
$$

The signal flow in this operation is shown in Fig. 5.8. Since the shape looks like the unfolded wings of a butterfly, it is referred to as a *butterfly computation*. The FFT calculation proceeds while changing the sample values and coefficients one after another. In writing FFT programs, the choice of inputs at each stage has to be made clear.

In the explanation so far, $N = 2^3 = 8$ has been assumed and, in this case, three stages of butterfly computation is necessary as shown in Fig. 5.7. The parameter m can be an arbitrary positive integer for 2^m-point FFT and its signal flow graph can be drawn. Once the signal flow is drawn, the choice for the input to the butterfly computation is made clear and the programming becomes possible.

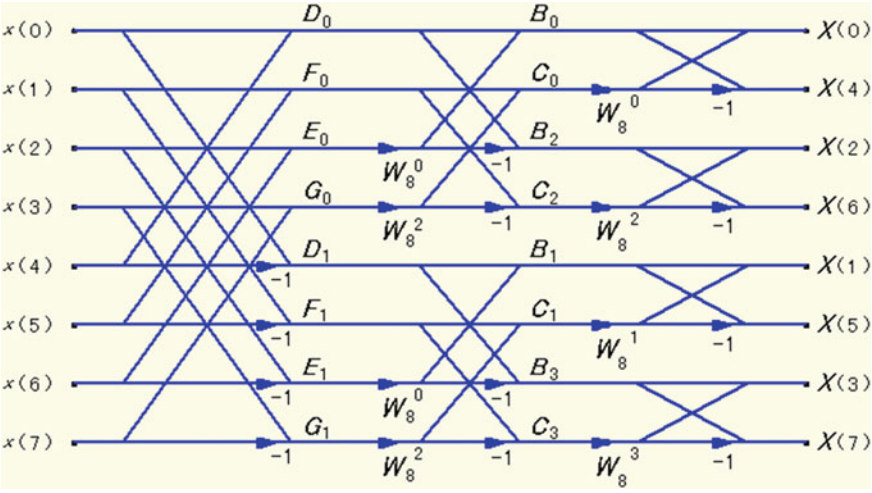

Fig. 5.9 Signal flow when the order in the vertical direction of the signal flow in Fig. 5.7 is changed without changing the order of the data in the time domain

If one tries to write a program following the chart in Fig. 5.7, one must first rearrange the order of sample values. Since the data is chosen every other step, the order of data becomes 0, 4, 2, 6, 1, 5, 3, 7.

However, the rearranging of the data is not a must. A method that does not require the rearrangement of data can be made possible by keeping the flow of data as they are, and changing the process of calculation in the vertical order. For that purpose, every straight line is moved to the position following the order of the input data without changing the connection to other straight lines. For example, the straight line $x(1) \rightarrow F_0 \rightarrow \mathrm{C}_0 \rightarrow X(4)$ is moved to the second from the top right below the straight line of $x(0) \rightarrow D_0 \rightarrow B_0 \rightarrow X(0)$. Next, the straight line $x(2) \rightarrow E_0 \rightarrow B_2 \rightarrow X(2)$ is moved below the line of $x(1)$. Conducting this process one by one, the order of the input data of the left-hand side can be made in the ascending order, which is shown in Fig. 5.9.

No change of operation has been made from Figs. 5.7, 5.8 and 5.9, but the order of the final data has been changed because of the change in the order of the straight lines.

It has been shown that the order of the input data need not be changed, and the FFT can be carried out correctly if the order of the final data is rearranged.

5.4 2^m-Point FFT by Decimation in Frequency Algorithm

In this section, a slightly different approach from Sect. 5.3 will be taken. Let's start with $N = 2^m$, as in Sect. 5.3. The list of equations to obtain $X(k) = X_k$ in the ascending order of k is shown below.

$$\begin{aligned}
X_0 &= x_0W_8^0 + x_1W_8^0 + x_2W_8^0 + x_3W_8^0 + x_4W_8^0 + x_5W_8^0 + x_6W_8^0 + x_7W_8^0\\
X_1 &= x_0W_8^0 + x_1W_8^1 + x_2W_8^2 + x_3W_8^3 + x_4W_8^4 + x_5W_8^5 + x_6W_8^6 + x_7W_8^7\\
X_2 &= x_0W_8^0 + x_1W_8^2 + x_2W_8^4 + x_3W_8^6 + x_4W_8^8 + x_5W_8^{10} + x_6W_8^{12} + x_7W_8^{14}\\
X_3 &= x_0W_8^0 + x_1W_8^3 + x_2W_8^6 + x_3W_8^9 + x_4W_8^{12} + x_5W_8^{15} + x_6W_8^{18} + x_7W_8^{21}\\
X_4 &= x_0W_8^0 + x_1W_8^4 + x_2W_8^8 + x_3W_8^{12} + x_4W_8^{16} + x_5W_8^{20} + x_6W_8^{24} + x_7W_8^{28}\\
X_5 &= x_0W_8^0 + x_1W_8^5 + x_2W_8^{10} + x_3W_8^{15} + x_4W_8^{20} + x_5W_8^{25} + x_6W_8^{30} + x_7W_8^{35}\\
X_6 &= x_0W_8^0 + x_1W_8^6 + x_2W_8^{12} + x_3W_8^{18} + x_4W_8^{24} + x_5W_8^{30} + x_6W_8^{36} + x_7W_8^{42}\\
X_7 &= x_0W_8^0 + x_1W_8^7 + x_2W_8^{14} + x_3W_8^{21} + x_4W_8^{28} + x_5W_8^{35} + x_6W_8^{42} + x_7W_8^{49}
\end{aligned} \tag{5.22}$$

By choosing the equations with even k (0, 2, 4, 6) and using the property that the rotation factor is periodic with period 8, the four equations shown below are obtained.

$$\begin{aligned}
X_0 &= x_0W_8^0 + x_1W_8^0 + x_2W_8^0 + x_3W_8^0 + x_4W_8^0 + x_5W_8^0 + x_6W_8^0 + x_7W_8^0\\
X_2 &= x_0W_8^0 + x_1W_8^2 + x_2W_8^4 + x_3W_8^6 + x_4W_8^0 + x_5W_8^2 + x_6W_8^4 + x_7W_8^6\\
X_4 &= x_0W_8^0 + x_1W_8^4 + x_2W_8^0 + x_3W_8^4 + x_4W_8^0 + x_5W_8^4 + x_6W_8^0 + x_7W_8^4\\
X_6 &= x_0W_8^0 + x_1W_8^6 + x_2W_8^4 + x_3W_8^2 + x_4W_8^0 + x_5W_8^6 + x_6W_8^4 + x_7W_8^2
\end{aligned} \tag{5.23}$$

Since the sets of the first four and the second four rotation factors in these equations are the same, these equations can be rewritten by changing the order of the rotation factors:

$$\begin{aligned}
X_0 &= (x_0 + x_4)W_4^0 + (x_1 + x_5)W_4^0 + (x_2 + x_6)W_4^0 + (x_3 + x_7)W_4^0\\
X_2 &= (x_0 + x_4)W_4^0 + (x_1 + x_5)W_4^1 + (x_2 + x_6)W_4^2 + (x_3 + x_7)W_4^3\\
X_4 &= (x_0 + x_4)W_4^0 + (x_1 + x_5)W_4^2 + (x_2 + x_6)W_4^0 + (x_3 + x_7)W_4^2\\
X_6 &= (x_0 + x_4)W_4^0 + (x_1 + x_5)W_4^3 + (x_2 + x_6)W_4^2 + (x_3 + x_7)W_4^1
\end{aligned} \tag{5.24}$$

If one define

$$b_i = x_i + x_{i+4} \tag{5.25}$$

Equation (5.24) becomes

$$\begin{aligned} X_0 &= b_0 W_4^0 + b_1 W_4^0 + b_2 W_4^0 + b_3 W_4^0 \\ X_2 &= b_0 W_4^0 + b_1 W_4^1 + b_2 W_4^2 + b_3 W_4^3 \\ X_4 &= b_0 W_4^0 + b_1 W_4^2 + b_2 W_4^0 + b_3 W_4^2 \\ X_6 &= b_0 W_4^0 + b_1 W_4^3 + b_2 W_4^2 + b_3 W_4^1 \end{aligned} \tag{5.26}$$

These four equations can be expressed in one equation:

$$X_k = \sum_{p=0}^{N/2-1} (x_p + x_{p+N/2}) W_{\frac{N}{2}}^{\frac{pk}{2}} = \sum_{p=0}^{N/2-1} b_p W_{\frac{N}{2}}^{\frac{pk}{2}} \tag{5.27}$$

where $k = 0, 2, 4, \ldots, N-2$. This is exactly the $N/2$-point DFT. Using the same approach, the list of equations with odd $k(1, 3, 5, 7)$ are given by

$$\begin{aligned} X_1 &= x_0 W_8^0 + x_1 W_8^1 + x_2 W_8^2 + x_3 W_8^3 + x_4 W_8^4 + x_5 W_8^5 + x_6 W_8^6 + x_7 W_8^7 \\ X_3 &= x_0 W_8^0 + x_1 W_8^3 + x_2 W_8^6 + x_3 W_8^1 + x_4 W_8^4 + x_5 W_8^7 + x_6 W_8^2 + x_7 W_8^5 \\ X_5 &= x_0 W_8^0 + x_1 W_8^5 + x_2 W_8^2 + x_3 W_8^7 + x_4 W_8^4 + x_5 W_8^1 + x_6 W_8^6 + x_7 W_8^3 \\ X_7 &= x_0 W_8^0 + x_1 W_8^7 + x_2 W_8^6 + x_3 W_8^5 + x_4 W_8^4 + x_5 W_8^3 + x_6 W_8^2 + x_7 W_8^1 \end{aligned} \tag{5.28}$$

These equations can be rewritten following the procedure after Eq. (5.23) as

$$\begin{aligned} X_1 &= (x_0 + x_4 W_8^4) W_8^0 + (x_1 + x_5 W_8^4) W_8^1 + (x_2 + x_6 W_8^4) W_8^2 + (x_3 + x_7 W_8^4) W_8^3 \\ X_3 &= (x_0 + x_4 W_8^4) W_8^0 + (x_1 + x_5 W_8^4) W_8^3 + (x_2 + x_6 W_8^4) W_8^6 + (x_3 + x_7 W_8^4) W_8^1 \\ X_5 &= (x_0 + x_4 W_8^4) W_8^0 + (x_1 + x_5 W_8^4) W_8^5 + (x_2 + x_6 W_8^4) W_8^2 + (x_3 + x_7 W_8^4) W_8^7 \\ X_7 &= (x_0 + x_4 W_8^4) W_8^0 + (x_1 + x_5 W_8^4) W_8^7 + (x_2 + x_6 W_8^4) W_8^6 + (x_3 + x_7 W_8^4) W_8^5 \end{aligned}$$

Using the relation $W_8^4 = -1$ and W_8^p is a periodic function with period 8, the above four equations can be rewritten as

$$\begin{aligned} X_1 &= (x_0 - x_4) W_4^0 + (x_1 - x_5) W_8^1 W_4^0 + (x_2 - x_6) W_8^2 W_4^0 + (x_3 - x_7) W_8^3 W_4^0 \\ X_3 &= (x_0 - x_4) W_4^0 + (x_1 - x_5) W_8^1 W_4^1 + (x_2 - x_6) W_8^2 W_4^2 + (x_3 - x_7) W_8^3 W_4^3 \\ X_5 &= (x_0 - x_4) W_4^0 + (x_1 - x_5) W_8^1 W_4^2 + (x_2 - x_6) W_8^2 W_4^0 + (x_3 - x_7) W_8^3 W_4^2 \\ X_7 &= (x_0 - x_4) W_4^0 + (x_1 - x_5) W_8^1 W_4^3 + (x_2 - x_6) W_8^2 W_4^2 + (x_3 - x_7) W_8^3 W_4^1 \end{aligned} \tag{5.29}$$

By defining

$$c_i = (x_i - x_{i+4}) W_4^i \tag{5.30}$$

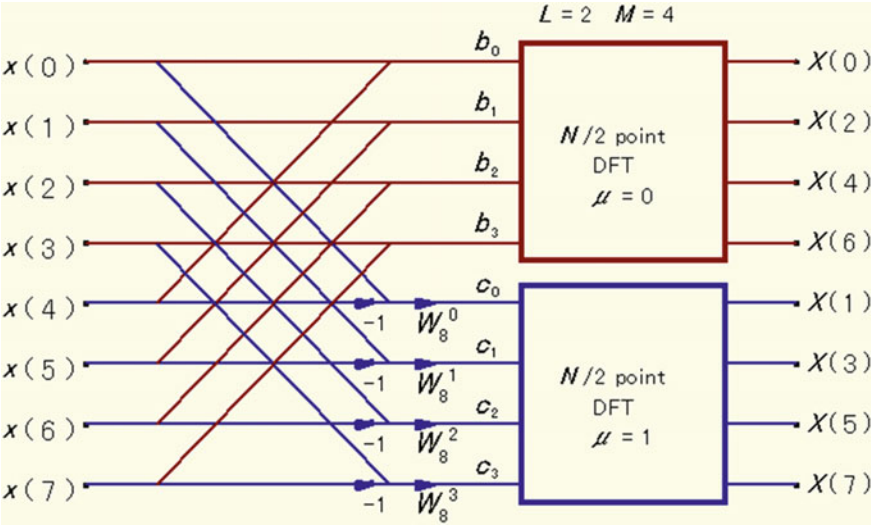

Fig. 5.10 Decomposition of 8-point DFT following Eqs. (5.24) and (5.29) (principle of the decimation in frequency algorithm)

Equation (5.29) become

$$\begin{aligned} X_1 &= c_0 W_4^0 + c_1 W_4^0 + c_2 W_4^0 + c_3 W_4^0 \\ X_3 &= c_0 W_4^0 + c_1 W_4^1 + c_2 W_4^2 + c_3 W_4^3 \\ X_5 &= c_0 W_4^0 + c_1 W_4^2 + c_2 W_4^0 + c_3 W_4^2 \\ X_7 &= c_0 W_4^0 + c_1 W_4^3 + c_2 W_4^2 + c_3 W_4^1 \end{aligned} \tag{5.31}$$

The above four equations can be expressed in one equation:

$$X_k = \sum_{p=0}^{N/2-1} (x_p - x_{p+N/2}) W_N^p W_{N/2}^{p(k-1)/2} = \sum_{p=0}^{N/2-1} c_p W_{N/2}^{p(k-1)/2} \tag{5.32}$$

where $k = 1, 3, 5, \ldots, N-1$.

Since Eqs. (5.24) and (5.29) are $N/2$ (=4)-point DFTs for even and odd k, respectively, the signal flow can be expressed by Fig. 5.10.

Each of four DFTs in Fig. 5.11 can be replaced by two DFTs with two inputs. In this case, since $N = 8$, it is necessary not to multiply the rotation factor but to just perform additions and subtractions. Figure 5.12 is the signal flow including this step.

The common operation in these Figures is that the additions of two inputs are kept as they are, and subtractions of the two inputs are multiplied by the rotational factor. This operation is almost the same as the butterfly operation in the

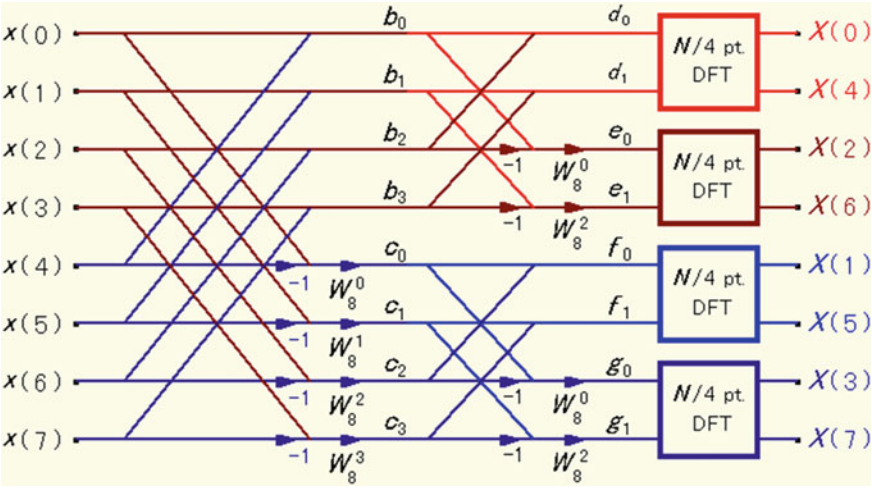

Fig. 5.11 Signal flow of 8-point DFT by the decimation in frequency algorithm, where two $N/2$ (=4)-point DFTs are decomposed into four $N/4$ (=2)-point DFTs of even and odd order terms

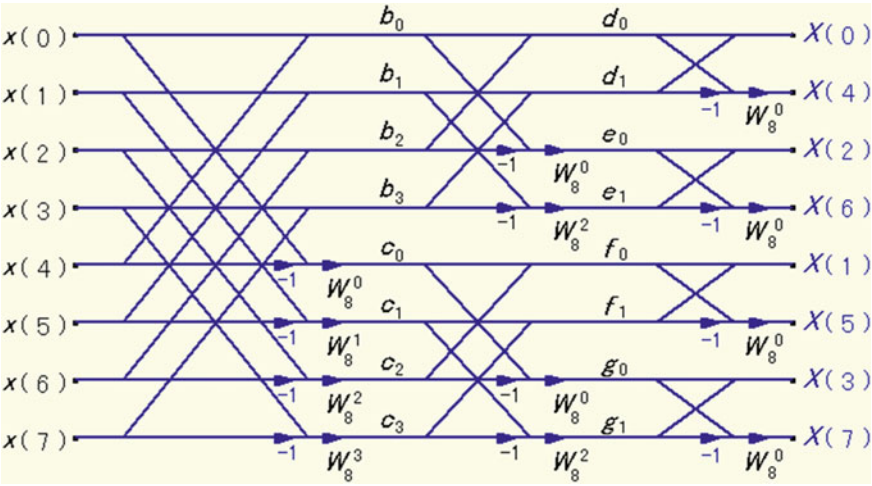

Fig. 5.12 Signal flow of 8-point FFT by the decimation in frequency algorithm

decimation in time FFT except for the place of multiplication of the rotational factor as shown in Fig. 5.13.

Expressing two inputs by u_h and v_h, and output by y_h, this operation can be expressed by

$$\left.\begin{aligned} y_h &= u_h + v_h \\ y_{h+s} &= (u_h - v_h)W_N^{sh} \end{aligned}\right\} \tag{5.33}$$

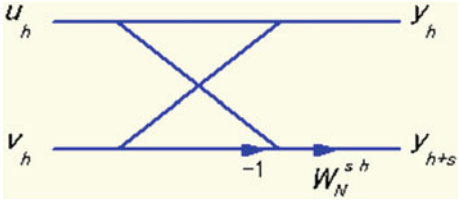

Fig. 5.13 Butterfly computation in the decimation in frequency algorithm

where

$$N = 2^M$$
$$s = 2^r \qquad (r = 0,\ 1,\ 2, \cdots,\ M-1)$$
$$h = 0,\ 1,\ 2,\ \cdots,\ s-1$$

The process of the decimation in frequency FFT is to divide into $N/2$-point DFTs that give every other data of the spectrum and again divide into $N/4$-point DFTs that give every other data of the spectrum, and therefore, the order of the spectrum changes in every step as shown in Fig. 5.13.

For this reason, the spectrum at the end must be rearranged in the *bit-reversed order* (this will be mentioned later). This order rearrangement is also possible at the input stage and in this case the rearrangement at the spectrum stage is not necessary.

By rearranging the order of the straight lines without changing the operations on them or connections to other lines, Fig. 5.12 can be redrawn as Fig. 5.14, where the order rearrangement is conducted at the input stage.

5.5 Rearrangement of the Bit-Reversed Order

Figures of signal flows of FFT show that, if one of the orders of the time domain data $x(n)$ or the spectrum data $X(k)$ is in the ascending order, the other is in a "random" order. The order may look "random" but it is a result of a systematic operation, therefore the order is also systematic. The order [0, 4, 2, 6, 1. 5. 3. 7] in the case of 8-point FFT is referred to as *bit-reversed order*. If one understands the reason for its regularity, one will also understand why it is called bit-reversed order. So, let's check why the order [0, 4, 2, 6, 1. 5. 3. 7] is obtained.

At the beginning of Sect. 5.4, the data were selected in every other step. In order to see what it means, the data numbers in the ascending order are expressed using the binary system, which is shown in Table 5.1. If one selects data in every other step, that is, if one selects even numbers first and then odd numbers, one is selecting numbers whose rightmost bits are zeros first, and then the numbers whose rightmost bits are ones. The results of the numbers after the first rearrangement are shown in Table 5.2.

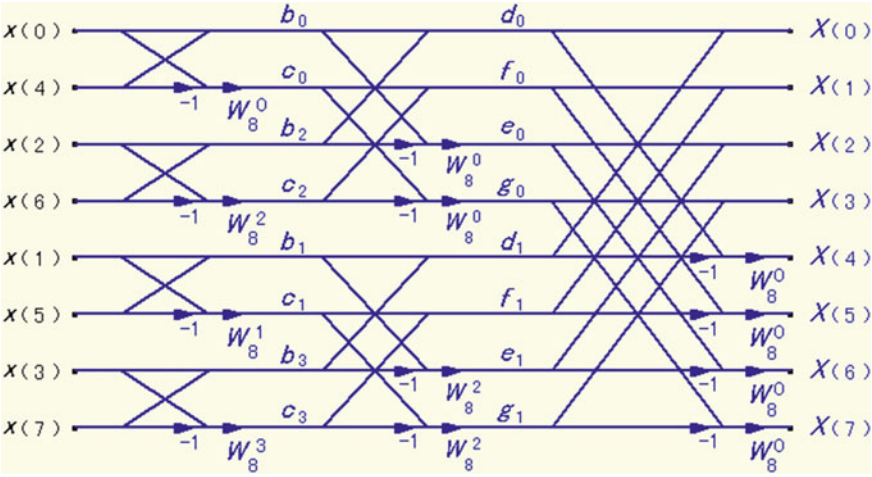

Fig. 5.14 Signal flow by the decimation in frequency FFT, where the bit reversal is performed at the first step of the process

Table 5.1 Time-sequence

Order			
0	0	0	0
1	0	0	1
2	0	1	0
3	0	1	1
4	1	0	0
5	1	0	1
6	1	1	0
7	1	1	1

Table 5.2 After the first

Rearrangement			
0	0	0	0
2	0	1	0
4	1	0	0
6	1	1	0
1	0	0	1
3	0	1	1
5	1	0	1
7	1	1	1

The second rearrangement is to select data in every other step from the first group whose rightmost bits are zeros and then from the second group whose rightmost bits are ones. This means to select data whose second bits are zero first, and then data whose second bits are ones for each group. This second rearrangement gives Table 5.3. There is no need to do so anymore because the

Table 5.3 After the second

(Last) Rearrangement			
0	0	0	0
4	1	0	0
2	0	1	0
6	1	1	0
1	0	0	1
5	1	0	1
3	0	1	1
7	1	1	1

leftmost bits in each group made of two numbers are already in that order (zero first and one next).

If one compares the orders of bits between Tables 5.1 and 5.3, one will find that the bits are reversed. For even larger numbers such as $N = 16, 32,\ldots$, this relation always holds. This is why the term "*bit-reversed order*" is used.

So far, a special case with $N = 8$ has been considered. Next, consider the general case with $N = 2^m$. If one expresses decimal numbers from $n = 0$ to $n = N - 1$ using binary numbers, they can be expressed as

$$\phi(N) = b_{m-1}b_{m-2}b_{m-3}\cdots b_2b_1b_0 \tag{5.34}$$

where b_k represents 0 or 1. These binary numbers are aligned in ascending order from the smallest 0 0 0 $\cdots$ 0 (m bits) to the largest 1 1 1 $\cdots$ 1 (m bits). The total number is equal to N (=2^m) and the first and the second half of the leftmost bits (most significant bit) of the numbers from 0 to N are 0 and 1, respectively. The first and the second half of the second bits of the first half numbers from 0 to $N/2 - 1$ are 0 and 1, respectively. This is the same for the second half numbers from $N/2$ to N. The first and the second half of the third bits of the numbers of the first quarter from 0 to $N/4 - 1$ are 0 and 1, respectively. This is the same for the numbers of the remaining three quarters. The same thing is valid to the last bits from the left (the least significant bit). The first and the second (half) of the least significant bits of the first pair of the numbers, which are 0 and 1 (=$N/2^m$), are 0 and 1, respectively. The same thing is valid from the second pair, 2 and 3, to the last pair, $N - 2$ and $N - 1$, of the numbers.

In the first step of the operation, the numbers whose last bits (rightmost bits) are 0s are selected. Then, the last bits of the remaining numbers become all 1s. In the second step, the same selection is made for each of the first and second half of the numbers. That is, the numbers, whose second from the right bits are 0s, are selected, making those of the remaining numbers all 1s. In the third step, the same selections are made for the third bits from the right.

If one expresses the numbers after the rearrangement by

$$\psi(N) = c_{m-1}c_{m-2}c_{m-3}\cdots c_2c_1c_0 \tag{5.35}$$

c_0 becomes equal to b_{m-1} by the first step, c_1 becomes equal to b_{m-2} by the second step, and so on. Finally, the all bits are reversed.

5.6 Speed-Up Technique by Parallel Computation

One method of speeding up the computation will be introduced here, not only for the reduction of computing time but also for the understanding of the basic properties of the DFT.

This method can be applied only when one intends to obtain FFTs of two real signals, $x(n)$ and $y(n)$. Let's see what one gets if one performs a DFT of a signal with its real part $x(n)$ and imaginary part $y(n)$. Define the complex signal $z(n)$ by

$$z(n) = x(n) + j \cdot y(n) \tag{5.36}$$

The DFT of Eq. (5.36) is computed by

$$\begin{aligned} Z(k) &= \mathrm{DFT}[z(n)] = \sum_{n=0}^{N-1} \{x(n) + j \cdot y(n)\} \exp\left(-j2\pi \frac{nk}{N}\right) \\ &= \sum_{n=0}^{N-1} x(n) \exp\left(-j2\pi \frac{nk}{N}\right) + j \cdot \sum_{n=0}^{N-1} y(n) \exp\left(-j2\pi \frac{nk}{N}\right) \\ &= X(k) + j \cdot Y(k) \end{aligned} \tag{5.37}$$

If one defines real and imaginary parts of $Z(k)$, $X(k)$, and $Y(k)$ by $Z_{\mathrm{R}}(k)$, $X_{\mathrm{R}}(k)$, and $Z_{\mathrm{I}}(k)$, $X_{\mathrm{I}}(k)$ and $Y_{\mathrm{I}}(k)$, Eq.(5.37) becomes

$$Z_R(k) + j \cdot Z_I(k) = X_R(k) - Y_I(k) + j\{X_I(k) + Y_R(k)\} \tag{5.38}$$

Since real and imaginary parts of $X(k)$ and $Y(k)$ are even and odd, respectively, one obtains the following relations from the real part of $Z(k)$:

$$Z_R(-k) + Z_R(k) = X_R(-k) - Y_I(-k) + X_R(k) - Y_I(k) = 2X_R(k)$$

and

$$Z_R(-k) - Z_R(k) = X_R(-k) - Y_I(-k) - X_R(k) + Y_I(k) = 2Y_I(k)$$

and, from the imaginary part of $Z(k)$:

$$Z_I(-k) + Z_I(k) = X_I(-k) + Y_R(-k) + X_I(k) + Y_R(k) = 2Y_R(k)$$

and

$$Z_I(-k) - Z_I(k) = X_I(-k) + Y_R(-k) - X_I(k) - Y_R(k) = -2X_I(k)$$

$X_{\mathrm{R}}(k)$, $X_{\mathrm{I}}(k)$, and $Y_{\mathrm{R}}(k)$, $Y_{\mathrm{I}}(k)$ are obtained from the above equations. Since k has periodicity with period N, $-k$ can be replaced by $N - k$. Then, the real and imaginary parts of DFTs of $X(k)$ and $Y(k)$ are calculated by

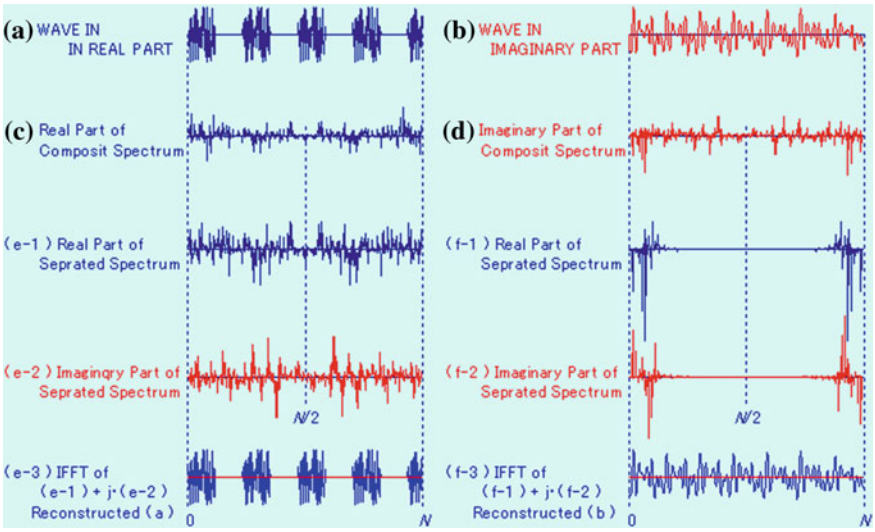

Fig. 5.15 Example of accomplishing two FFTs of two real sequences by one FFT of one complex sequence, whose real and imaginary parts are given by the two real sequences. Animation available in supplementary files under filename E5-15_PLLFFT.exe. **a** Wave in real part, **b** wave in imaginary part, **c** real part of composite spectrum, **d** imaginary part of composite spectrum, e-1 real part of separated spectrum, e-2 imaginary part of separated spectrum, e-3 IFFT of (e-1) + j·(e-2) reconstructed (**a**), f-1 real part of separated spectrum, f-2 imaginary part of separated spectrum, f-3 IFFT of (f-1) + j·(f-2) reconstructed (**b**)

$$\left.\begin{aligned} X_R(k) &= [Z_R(k) + Z_R(N-k)]/2 \\ X_I(k) &= [Z_I(k) - Z_I(N-k)]/2 \\ Y_R(k) &= [Z_I(k) + Z_I(N-k)]/2 \\ Y_I(k) &= [-Z_R(k) + Z_R(N-k)]/2 \end{aligned}\right\} \tag{5.39}$$

The range of k is from 0 to $N-1$. The spectrum from $k = N/2$ to $k = N-1$ can be obtained using Eq. (5.39) or using the properties that the real parts are even functions and the imaginary parts are odd functions.

By employing this method, the DFTs of two real sequences can be calculated in one FFT, making it possible to reduce the computation time to almost one-half when many DFTs of real numbered sequences are calculated.

Examples of calculation by this method are shown in Fig. 5.15. Figure 5.15c, d are the real and imaginary parts of the FFT of a complex signal, whose real and imaginary parts are given by Fig. 5.15a, b, respectively. Both the time and frequency axes cover the range from 0 to N (=512 in the present case). The spectra in the range from $k = 0$ to $k = N/2 - 1$ and from $k = N/2$ to $k = N - 1$ are for positive and negative frequencies, respectively.

The differences of Fig. 5.15c, d from the previous cases are that the real part (c) is not symmetric and the imaginary part (d) is not antisymmetric. This is because

(c) and (d) are the real and imaginary parts of FFT of a complex signal. All previous examples were real-time signals and therefore, the real parts of the FFT were symmetric and the imaginary parts were antisymmetric. The real and imaginary parts of the time signal in the present case are given by Fig. 5.15a, b, respectively. The real parts (Fig. 5.15e-1, f-1) and imaginary parts (Fig. 5.15e-2, f-2) of the two time signals Fig. 5.15a, b, are calculated by the use of Eq. (5.39). The real and the imaginary parts of the spectra of the two signals are even and odd, respectively, because the two signals are real.

5.7 Exercises

1. What is b when W_N^{kL} is expressed in the form W_M^b, where $N = LM$ and L, M, k, and b are all integers ?
2. In the above problem, what are the ranges of b and k?
3. Discuss efficient methods of computation of 360-point DFT.

Chapter 6
DFT and Spectrum

One of the important purposes of Fourier analysis is to obtain spectra of waveforms. For that purpose, DFTs are performed on numerical sequences made from waveforms using a computer or a similar fast operational device. In Chap. 5, the FFT, the fast computational algorithm of the DFT has been introduced. However, application of the DFT is sometimes troublesome because, as explained in Chap. 4, a finite-length waveform extracted from a very long sine or cosine waveform sometimes contains spurious frequency components that do not exist in the original waveform.

Assume that a waveform is observed during some finite period of time, with no knowledge of the signal outside the observed period. Nevertheless, the DFT of the observed data gives the spectrum of a periodic waveform that infinitely repeats the observed finite-length waveform.

The spurious frequency components appear because there is a discontinuity between the two ends of the extracted waveform. This will be made clear during discussions in this chapter. Various methods of eliminating or reducing the discontinuity will be investigated and it will be shown that gradually reducing the amplitudes near the two ends is a very effective means of minimizing the discontinuity.

6.1 Periodogram

So far, it has been shown that, if the DFT is applied to N points of data extracted from a sample sequence of a waveform, N-point complex spectral data are obtained. However, there are spectral differences depending on the location of the N-point data in the sample sequence. This effect is checked using a long periodic waveform.

First, a case of an extracted 64-point data set which contains an integer number of cycles is considered. The original waveform is calculated using the equation below.

K. Kido, *Digital Fourier Analysis: Fundamentals*,
Undergraduate Lecture Notes in Physics, DOI: 10.1007/978-1-4614-9260-3_6,

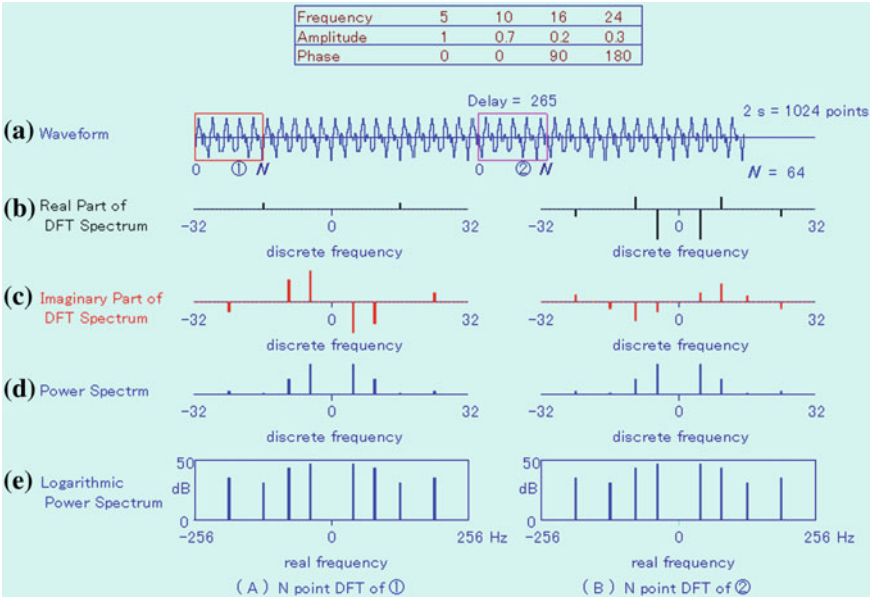

Fig. 6.1 Waveform comprised of four sine components given by Eq. (6.1), with DFTs of 64-point sample sequences extracted from two different locations. **a** Waveform, **b** spectrum (real), **c** spectrum (imaginary), **d** power spectrum, and **e** power spectrum in dB. Animation available in supplementary files under filename E6-01_PeriG.exe

$$x(n) = \sin\left(2\pi\frac{5n}{64}\right) + 0.7\sin\left(2\pi\frac{10n}{64}\right) + 0.2\cos\left(2\pi\frac{16n}{64}\right) - 0.3\sin\left(2\pi\frac{24n}{64}\right) \tag{6.1}$$

The calculated waveform from $n = 0$ to $n = 512$ is shown in Fig. 6.1a and 64-point DFTs are shown in Fig. 6.1b–d. If it is assumed that the length of the 512-point data set is one second (unit time length), the sampling frequency is 512 Hz, and the maximum analysis (Nyquist) frequency is 256 Hz. The left- and the right-hand side columns of Fig. 6.1b–d show the results of 64-point DFTs of the extracted data, indicated by ① and ②, respectively, in Fig. 6.1a.

From previous analysis, it is known that the spectral components are linear. However, the real part (b) and imaginary part (c) of the spectrum are different depending on the position of the extracted waveform. This is due to the phase change caused by the difference of the position on the time axis. Since the magnitudes of the components do not change regardless of the phase change, the power spectrum, Fig. 6.1d, stays unchanged. Figure 6.1e shows the power spectrum using a decibel scale (refer to Appendix 6A for "decibel"). The power spectrum is symmetric with respect to k (frequency).

In order to show the wide range of amplitudes of the power spectrum, the decibel scale is used. The 3rd and 4th components in Fig. 6.1d are slightly visible, but in Fig. 6.1e, they become clearly visible. For this reason, the logarithmic power spectrum will be frequently used.

The horizontal scales in Fig. 6.1b–d shows the sample numbers, while that in Fig. 6.1e shows the real frequency. The maximum frequency is one-half the sampling frequency (=256 Hz, Nyquist frequency).

If the data analyzed from $n = 0$ (the start of the waveform), the phases of Eq. (6.1) could be obtained from the real and imaginary parts. However, in most cases of real signal analysis, the $n = 0$ position is arbitrary. The phases obtained will be different from those defined by Eq. (6.1), and dividing the spectrum into real and imaginary parts becomes meaningless. The power spectrum, on the other hand, is independent of the origin of the extraction and is a good indication of the spectral property of the waveform.

However, if the number of cycles in the N-point data set is not an integer, the situation is not so simple. To check this, DFTs of waveforms of sine waves calculated from Eq. (6.2) are investigated.

$$x(n) = \sin\left(2\pi\frac{5.2}{64}n\right) + 0.7\sin\left(2\pi\frac{10.3n}{64}\right) + 0.2\cos\left(2\pi\frac{16.2n}{64}\right) - 0.3\sin\left(2\pi\frac{24.4n}{64}\right) \tag{6.2}$$

The 512-point waveform and two different DFTs are shown in Fig. 6.2. The real and imaginary parts of the two DFTs are different for the same reason as shown in Fig. 6.1. The power spectra, obtained by the squared sum of the real and imaginary parts, are also different depending on the location of the extraction as can be seen by the decibel representation (Fig. 6.2e). If the two spectral distributions are examined, it is difficult to imagine that they are obtained from the same original waveform Eq. (6.2).

In Fig. 6.1, each sine component is represented by a pair of line spectra. In Fig. 6.2, however, the spectrum displays a spreading. The difference comes from the fact that, in Figs. 6.1 and 6.2, there are integer and non-integer number of periods (cycles) in the 64-point data, respectively. It has already been shown that the spectrum displays spreading if the number of periods in the sample sequence is not an integer.

In the first case, Fig. 6.1, the power spectrum is independent of location of the sample sequence, and therefore, it is correct to say that the obtained power spectrum is that of the original waveform. However, in the second case, Fig. 6.2, the power spectrum changes as the location of extraction changes. The power spectrum in each case is that of the extracted waveform and not of the original waveform. The spectrum obtained by the DFT is that of the infinitely long periodic series of the extracted waveforms, which is mostly different from the original waveform. To clarify this difference, the spectrum obtained by the DFT is referred

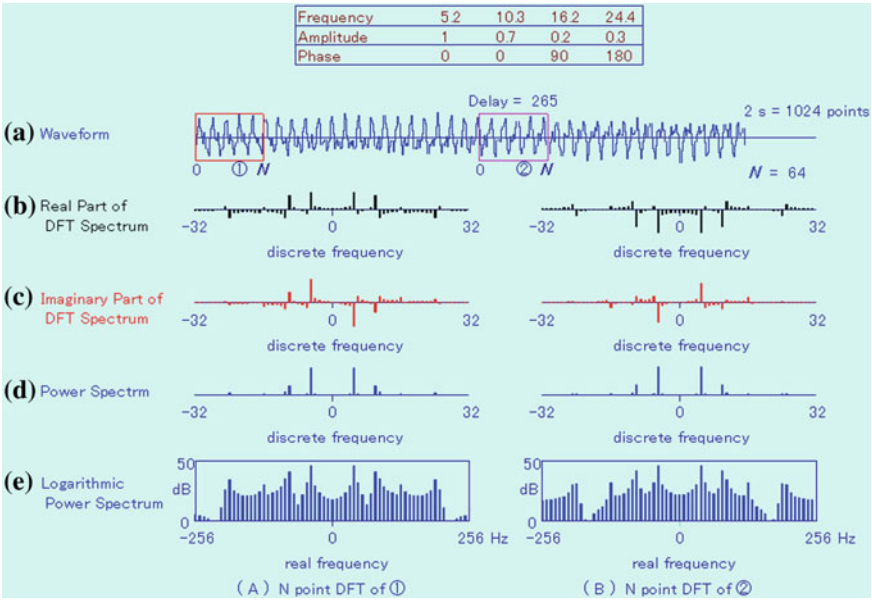

Fig. 6.2 Waveform comprised of four sine components described in the box at the *top* and two DFTs of 64-point sample sequences extracted from two different locations. **a** Waveform, **b** spectrum (real), **c** spectrum (imaginary), **d** power spectrum, and **e** power spectrum in dB. Animation available in supplementary files under filename E6-02_PeriG.exe

to as the *DFT spectrum* . The absolute squared value of the complex DFT spectrum is called the *periodogram*, which is the power spectrum obtained by the DFT.

The periodogram is a function of the discrete frequency k of the N-point DFT. This is defined by

$$P_{xx}(k) = |X(k)|^2 = X^*(k)X(k) \tag{6.3}$$

or

$$P_{xx}(k) = \frac{1}{N}|X(k)|^2 = \frac{1}{N}X^*(k)X(k) \tag{6.4}$$

The periodogram is a presentation of the absolute squared values of each spectrum line, and its dimension is power. If Eq. (6.3) is used, the magnitude is proportional to the sample number N. To avoid this problem, the definition given by Eq. (6.4) is also used. Eq. (6.4) gives the power spectral density, which is independent of the sample number N.

The periodogram given by Eq. (6.4) is equal to the power spectrum of the original waveform when an integer number of periods is included in the sample sequence. Even when this is not so, the result given by Eq. (6.4) is the power spectrum of the waveform in the analysis band, and therefore, it is not wrong to

call this the power spectrum. However, to avoid ambiguity, the term *periodogram* will be used whenever necessary.

It is natural to consider that the average of the periodogram obtained by shifting the beginning of the sample sequence may give an estimate of the power spectra of the original (overall) waveform. However, it has been proven that this does not give an exact estimate but a biased estimate [7]. Instead of presenting the proof here, a different approach will be given.

Since the waveform is defined by Eq. (6.2), the power spectrum should be given by four lines in the positive frequency range. Since there are many spectral lines in Fig. 6.2c, d, and since each component is given by the sum of squares of the real and imaginary parts, they can never be negative and their averaging never approaches zero. This is the simple explanation of the reason why the averaging of the periodogram never becomes the power spectrum.

As shown above, it is impossible to estimate the correct power spectrum from the DFTs. Why, then, is the DFT used? The DFT does not give an exact estimate of the power spectrum, but it still gives a result that is not completely meaningless. The result is the power spectrum of the periodic waveform. Before giving up, a method that gives a better estimate of the power spectrum of the original waveform will be searched.

Some additional explanations in Fig. 6.2 will be given because several similar figures are shown in the following sections. Figure 6.2b, c are the real and imaginary parts of the N-point DFT. They take positive and negative values, which are indicated by the lines above and below the horizontal axis, respectively. The frequency is not shown by the order of DFT, but the negative frequency components are shown on the left-hand side of the horizontal axis.

In some cases, the amplitude spectrum, the square root of the power spectrum (periodogram), will be shown. This is because small power spectral components, which are almost invisible, may become visible when the amplitude spectrum is used. For example, a power spectrum of 0.01 is difficult to identify on the graph with a full scale of one, but the corresponding amplitude spectrum of 0.1 may be easily identified. This can be confirmed by running the attached program.

Figure 6.2e is the decibel representation of the power spectrum. From the definition of the decibel, the power and the amplitude spectra give identical results. The decibel scale can display a very wide range of magnitudes (see Appendix 6A).

6.2 Uncertainty Principle

In this section, the discussion is concentrated on the relationship between the frequency resolution and the length of the sample sequence. The main purpose of the frequency analysis is to obtain exact values of frequencies and levels of sine and cosine components that are comprised in the waveform. It was shown that the analysis of a sample sequence with length T gives frequency components that are integer multiples of $1/T$, i.e., k/T, $k = 0, 1, \ldots, N-1$.

As it has been made clear in Chaps. 3 and 4, the frequency spacing of the line spectra of the DFT of a finite-length waveform with length T, i.e., the spacing between the adjacent samples in the frequency domain, is $1/T$. If a two-period-long waveform of a 100-Hz sine wave is analyzed, the time length is 0.02 s and its reciprocal is 50 Hz. This means that the frequency spacing of the DFT of the two-period-long waveform of the 100-Hz sine wave is 50 Hz. The frequency, 100 Hz, is the integer multiple of 50 Hz, and the waveform of 100 Hz or its harmonics can be analyzed without error. However, what happens when a 260 Hz wave is included, or if the 100-Hz signal is changed to 90 Hz? If an answer does not exist, then the frequency analysis has no meaning.

It is clear that this can be solved by lengthening the window length (analysis time), based on Chap. 3. If a spectrum spacing that is narrower than 5 Hz is required, the time window length should be longer than 1/5 (s). In this window length, there are 20 periods of the 100-Hz wave. If the maximum frequency of the highest components is 1,000 Hz, the sampling frequency should be more than 2,000 Hz. Therefore, the sampling number in the window should be 400 or more. Since the number 400 is not equal to an integer power of two, it is not convenient to apply the FFT algorithm. If the sampling number 512 is chosen without changing the sampling frequency, the window length becomes equal to 0.256 s, and the frequency spacing is equal to 3.9 Hz. If the sampling number 1,024 is chosen, a spectrum with 1.95 Hz spacing is obtained.

Differences between results obtained using different time window lengths will be made clearer by analyzing a real signal with various window lengths, rather than by studying the numbers mentioned above. One example of analysis is shown in Fig. 6.3. In this figure, results of a 32-point DFT and a 512-point DFT, both from $n = 0$, are shown by (A) and (B), respectively. In case (A), the frequency resolution is too coarse, and it is difficult to get an idea of what kind of frequency structure the waveform has. In case (B), it can be clearly seen that the waveform consists of four frequency components, and it can be guessed the relative amplitudes of the four components.

The logarithmic power spectrum of Fig. 6.3B(d) shows many small components other than the four large frequency components. This is due to the fact that the numbers of cycles in the extracted waveform are not integers.

From the above discussion, it is clear that frequency resolution improves with increasing analysis length. Using T and Δf to represent the analysis time length and frequency resolution between adjacent spectral lines, respectively, the following relation holds:

$$\Delta f \cdot T = 1 \tag{6.5}$$

This relation is derived from the discussions in Chap. 2 and Eqs. (4.4) and (4.5) in Chap. 4. If the analysis time T is lengthened in order to get a fine frequency structure within a small period around a specific time, the result is an increase in frequency resolution from Eq. (6.5). Equation (6.5) shows that both parameters cannot be made small at the same time.

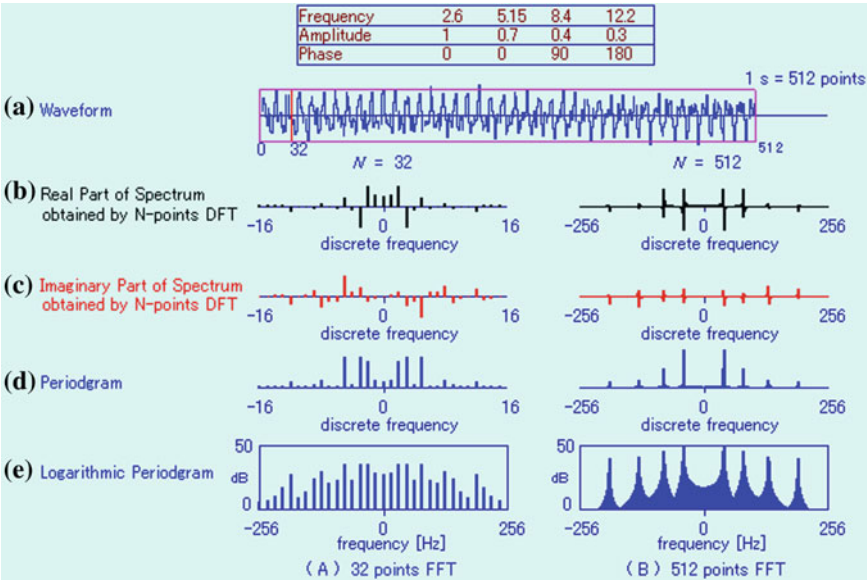

Fig. 6.3 Comparison of 32-point DFT and 1,024-point DFT with waveform composed of four frequency components. **a** Wave form, **b** spectrum (real), **c** spectrum (imaginary), **d** power spectrum, and **e** power spectrum in dB. Animation available in supplementary files under filename E6-03_PeriG.exe

The above relation is analogous to the uncertainty principle in quantum mechanics: *the product of the measurement errors of the position of an electron and its momentum cannot be made smaller than some finite number*. For this reason, Eq. (6.5) is referred to as *the uncertainty principle* in frequency analysis.

From Eq. (6.5), the analysis time length required to obtain frequency resolution less than Δf is given by Eq. (6.6)

$$T \geq 1/\Delta f \tag{6.6}$$

In practice, it is common that the number of FFT points has higher priority than the time length itself. Therefore, we will derive a relation that takes this into account.

The sampling frequency must be higher than two times the maximum frequency (f_m) of the signal, and the analysis time length must be determined by the required frequency resolution of the spectrum. The sampling interval τ is given by

$$\tau < 1/(2f_m) \tag{6.7}$$

From Eqs. (6.6) and (6.7), the number of DFTs, N, is chosen so that it satisfies the equation:

$$N(= T/\tau) > 2f_m/\Delta f_m \tag{6.8}$$

The number N given by Eq. (6.8) can be used as a point number of the DFT. If the widely used FFT algorithm is employed, a number N' that satisfies Eq. (6.8) should be used ($N' = 2^M \geq N, \quad M$: integer).

6.3 Spreading of the Spectrum

In Sect. 6.2, the relationship between the frequency resolution and the analysis time length was made clear. But some other things must also be made clear. As shown in Figs. 6.2 and 6.3, there is a spreading of spectrum if the number of cycles in the analysis time window is not an integer. If this happens, small components with different frequencies may be buried in the spread spectrum.

It has already been shown that the spread of the spectrum becomes less as the analysis time length gets longer. But lengthening of the analysis time is not a very efficient means of reducing the spreading of the spectrum. The relationship between these two should be made clear. Sometimes, there are cases when the analysis time cannot be made longer.

Some more examples of spectrum changes due to the analysis time change are examined. Two examples of 512-point sample sequences of original signals made of four frequency components are considered. All of the components of sequence (A) have integer frequencies (number of cycles in the 512 points) as shown in the table at the top. However, if a sub-sequence made of 128 consecutive points is employed, the analysis time is 0.25 s. The sequence contains an integer number of cycles of the first and the fourth components and their spectra become lines without spreading. But, this is not the case for the second and third components. This can be seen marginally in Fig. 6.4b, c. The spreading of the power spectrum is very difficult to identify in Fig. 6.4d. But, if the decibel scale is used for the vertical axis, the wide range of spectra becomes visible without regard to the amplitude or the power spectrum representations.

If the frequencies of the four components are increased by 3 %, all of the numbers of the four components in the 128-point sequence are non-integers, all components have spreading as shown in Fig. 6.4B. This spreading is sometimes called the leakage of spectrum and it can be narrowed if the analysis time is made longer but it never disappears.

Figure 6.5 shows the periodogram of DFTs with different data numbers. The waveform is the same as shown in Fig. 6.4. In this figure, the data number is changed progressively from 64 (a) to 1,024 (e), being doubled in each step. Since the sampling frequency is 512 Hz, the length of the 64-point sequence is 0.125 s. The first component (64 Hz) has the period of 0.015625 s (=1/64). Therefore, there are eight cycles in the sequence. In this case, the DFT of this component appears as the eighth line spectrum from the zero frequency. The spectra of the other waves are spread since the numbers of periods in the 64-point sequence are not integers. Figure 6.5b shows the 128-point sequence. In the analysis time length of 0.25 s,

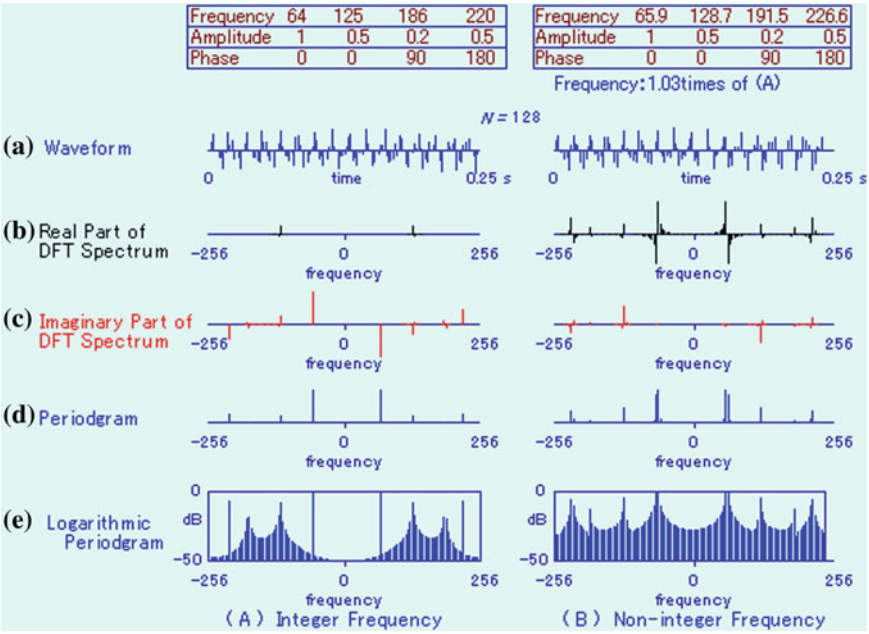

Fig. 6.4 Two waveforms comprised of four sine components shown in the boxes at the *top* and two DFTs. **a** Waveform, **b** spectrum (real), **c** spectrum (imaginary), **d** periodogram, and **e** periodogram in dB. Animation available in supplementary files under filename E6-04_PeSP.exe

there are 55 periods of the 220 Hz fourth wave component, and a line spectrum occurs at the 55th line in (b). In Fig. 6.5c, the 3rd wave component appears as the line spectrum at the 93rd line. In Fig. 6.5d, the 2nd wave component appears as the line spectrum at the 125th line as well as the other three components. The results do not change any more even if the analysis time length is doubled to 1,024.

In the case of Fig. 6.5B, since the frequencies are 1.03 times of those in Fig. 6.5A, none of the numbers of periods of the four waves in the analysis time length become an integer, and therefore, no pure line spectrum is observed. However, as the analysis time length increases, the spread of the spectrum is reduced, resulting in better frequency separation.

6.4 Analysis of Short Waves

It has been made clear that frequency resolution gets finer with increasing analysis time length. This is possible only when the original signal is long enough. If the signal itself is short or if the signal changes its property drastically, the analysis time length cannot be made long enough for a required frequency resolution. Even in these cases, it is expected that the frequency resolution will be made finer if the

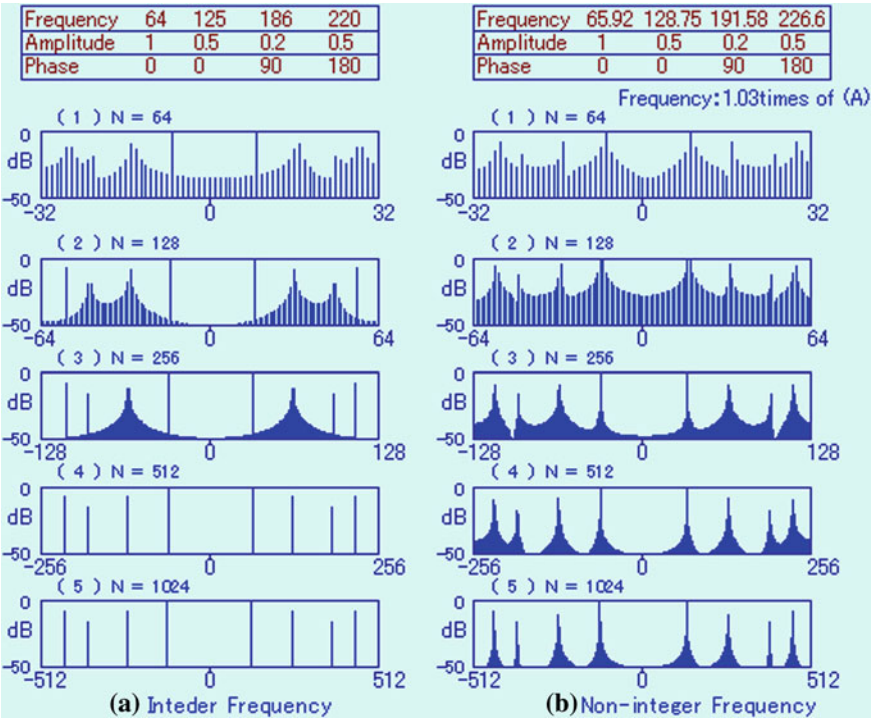

Fig. 6.5 Periodogram with various point numbers of DFT of the two waveforms shown in Fig. 6.4. Animation available in supplementary files under filename E6-05_PrSP.exe

analysis time length is increased by adding zero data after (or before) the original signal and increasing the data number of the DFTs. If this works, it would be beneficial to investigate the fine structures of the spectra of waves with short wave lengths. Since the spectrum of the null signal is zero, an essential change of the spectrum of the zero-padded signal may not happen.

This concept will be examined using similar waves. After a 32-point sequence, a 224-point zero sequence is added and the 256-point DFT is calculated. Results are shown in Fig. 6.6. In this figure, the spectral shape is shown by the envelope obtained by connecting the individual spectral peaks. In general, if the frequency resolution is high, this type of representation of the spectrum is a better way to indicate the spectral fluctuation.

In Fig. 6.6A, since the frequency of the fundamental component is 16 Hz in the 256-point data length, the sample length of one period of the fundamental is 16. Therefore, there are exactly two periods in the 32-point length sequence. The other three components are the harmonics of the fundamental component, and therefore, there are integer numbers of periods in the 32-point sequence. In this case, a 32-point DFT gives the perfect result as shown in Fig. 6.6e. However, in the case of (B), the fundamental frequency is 16.5 Hz, resulting in a non-integer number of

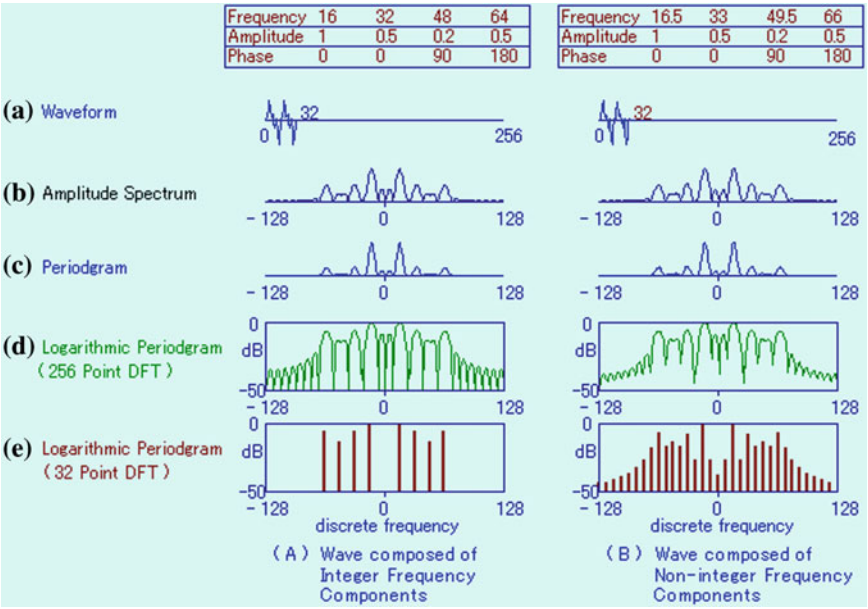

Fig. 6.6 256-point sample sequences and DFTs of the two waveforms comprised of the four sine components shown in the boxes at the *top*. The first 32-point sample sequences are those of the waveforms and 224-point zero samples are added in series. **a** Waveform, **b** amplitude spectrum, **c** periodogram, **d** periodogram in dB, and **e** periodogram in dB of the 32-point DFT. Animation available in supplementary files under filename E6-06_FrWSP.exe

periods in the 32-point sequence. The periodogram obtained by the 32-point DFT, which is shown by Fig. 6.6B(e), does not give the impression that the original wave consists of four frequency components.

By adding 224-point zeros to the 32-point sample sequences, and by calculating DFTs for the sequences (A) and (B), the results shown by Fig. 6.6b, c, d were obtained. The spectra shown in Fig. 6.6b, c, d are the amplitude spectrum, the power spectrum, and the power spectrum in dB, respectively. There are 256 spectral lines, but since the peaks of the lines are connected, the spectrum distributions appear continuous. The spectra of the 1st, 2nd, and 4th components, with large amplitudes, appear as the wide lobes shown in Fig. 6.6b, c, d. However, the spectrum of the relatively small 3rd component appears to have a lobe with a dent at its center. Also, there are other peaks over the entire frequency range.

It is interesting to note that the 32-point DFTs of (A) and (B) are very different, but the zero-added 256-point DFTs are very similar, as shown in Fig. 6.6b, c, d.

It seems that there is something valuable in adding zeros and increasing the data length. The question of how the spectral distribution changes as the number of added zeros increases will now be considered.

Figure 6.7 shows waveforms and their 64-, 128-, 256-, and 512-point DFT results when zeros are added to the 32-point data of Fig. 6.6B. If no zeros are

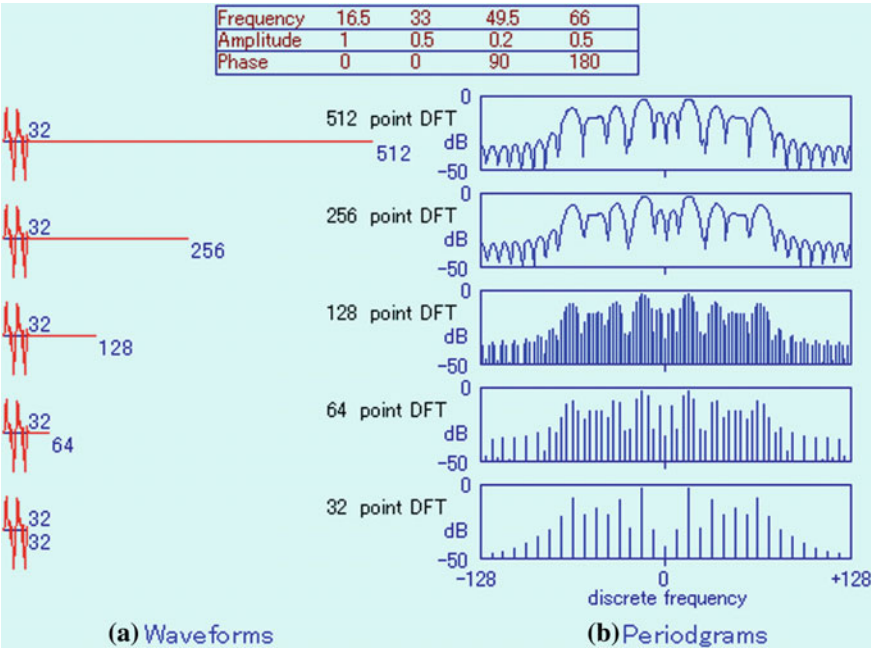

Fig. 6.7 DFTs (periodogram in dB) with various point numbers. The waveform consists of the four sine components shown in the box at the *top*. The first 32-point sample sequence is from the waveform shown in the box at the *top*, and various numbers of zero samples are added in series. Animation available in supplementary files under filename E6-07_WLength.exe

added, the result is the same as (e) of Fig. 6.6B. As the number of zeros increases, the logarithmic periodic power spectrum becomes similar to that of Fig. 6.6A. From this spectrum, one could guess that there are components near the peak frequencies of the large lobes (because this fact is already known!). However, it is impossible to tell that the original waveform consists of four harmonic components, and the frequencies and amplitudes of each component cannot be precisely determined. The 256- or 512-point DFT is better than the 32- or 64-point DFT, but still far from a complete description because only two periods of the fundamental component are included in the 32-point (non-zero) data.

It is reasonable to think that zero-added DFTs of short waveforms may improve the frequency resolution, but the results are not very impressive. A further increase in the data number of the DFT (more than 512 in Fig. 6.7) may not improve the situation.

Next, consider the spectrum change when the length of the non-zero data is varied. Figure 6.8 shows the 256-point DFT for the cases when 128 zeros are added to the 128 sample data of the signals in Fig. 6.6. Since the non-zero data lengths are longer this time, the spectrum clearly shows the existence of the four

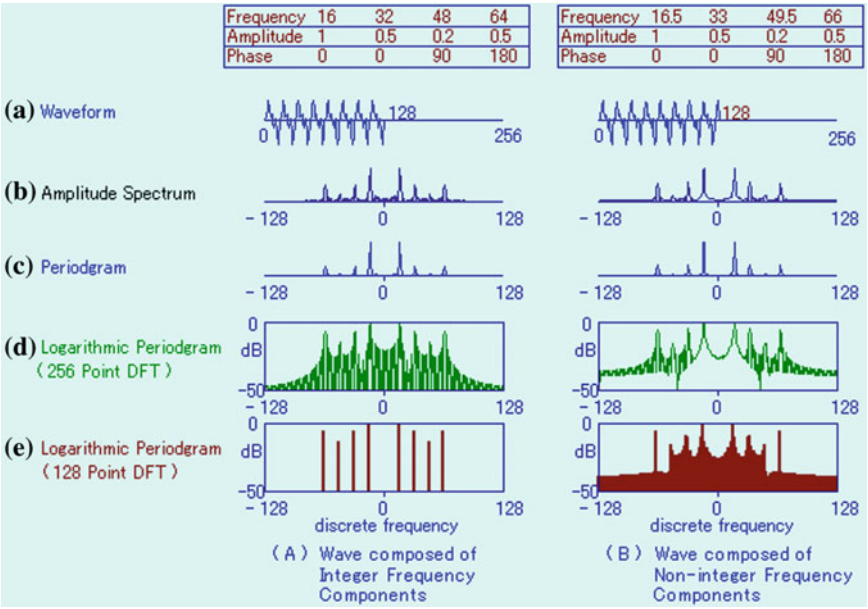

Fig. 6.8 256-point sample sequences and DFTs of the two waveforms comprised of the four sine components shown in the boxes at the *top*. The first 128-point sample sequences are those of the waveforms and 128-point zero samples are added in series. **a** Waveform, **b** amplitude spectrum, **c** periodogram, **d** periodogram in dB, and **e** periodogram in dB of the 128-point DFT. Animation available in supplementary files under filename E6-08_FrWSP.exe

components. Other phantom components are still observed but the frequency structure is better presented compared to the results of the previous figure.

The frequency structure becomes finer as the analysis signal length is increased. Then, spectrum changes will be examined as the analysis signal length is varied while the total number of DFT points is kept constant.

Figure 6.9 shows the results for the cases when the number of non-zero data points is increased from 0 to 240 while keeping the total length at 256. Frequencies of the components are increased by 1 % from those used in Fig. 6.6A in this example.

The upper chart in Fig. 6.9 is the case when all 256 points from the original data are used. However, all four components exhibit spreading of the spectrum since they are discontinuous between the beginning and the ending of the signal. The next chart shows the case with 128 non-zero data points. The spreading is even more pronounced than in the previous case. This trend increases as the number of non-zero data points is further reduced. Smaller components, even if they exist, may not be detected since they are covered by the spectrum spreading of the larger components.

The spreading of the spectrum should be reduced for a better analysis of the frequency structure of a signal in general. In the following sections and in Chap. 7, this will be the main topic of discussion.

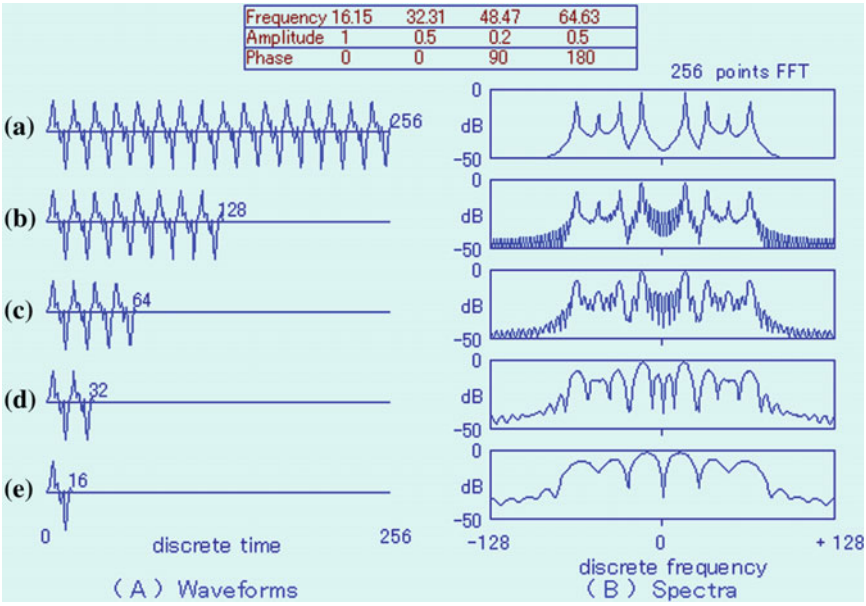

Fig. 6.9 256-point sample sequences and periodograms (in dB) of the waveform shown in Fig. 6.6a. The first 16-, 32-, 64-, 128-, and 256-point sample sequences are those of the waveform and the remaining sequences are filled with zeros. Animation available in supplementary files under filename E6-09_WLength.exe

6.5 DFT of Sine Waves

In seeking to answer the question raised at the end of Sect. 6.4, the first example shown in Fig. 6.10 will be considered.

In Fig. 6.10A, the 32-point sample sequence of a five-period sine waveform is shown by (a); the real and imaginary parts of its spectrum (32 point DFT) by (b) and (c), respectively; the amplitude spectrum by (d); and the periodogram in dB by (e). Figure 6.10B shows those of a sample sequence of a 5.6-period sine waveform in the sample time.

From what was learned in Chap. 5, the following can be mentioned. In the case of Fig. 6.10A, there are exactly five periods (cycles) in the sample sequence and, therefore, the spectrum should appear at discrete frequencies ± 5 as line components. Since the waveform is a sine function, the spectrum should be purely imaginary. In the case of Fig. 6.10B, however, the spectrum spreads and both real and imaginary components exist. From the periodogram, Fig. 6.10B(e), it is difficult to imagine that the analyzed waveform is a single sinusoidal function. It would be more reasonable to conclude that there are many sine components around frequency 5 or 6.

The reason why spectrum spreading occurs is that the DFT coefficients of a sample sequence are actually those of the infinitely long periodic function with period T, which is given by the product of point number of the DFT and the sample

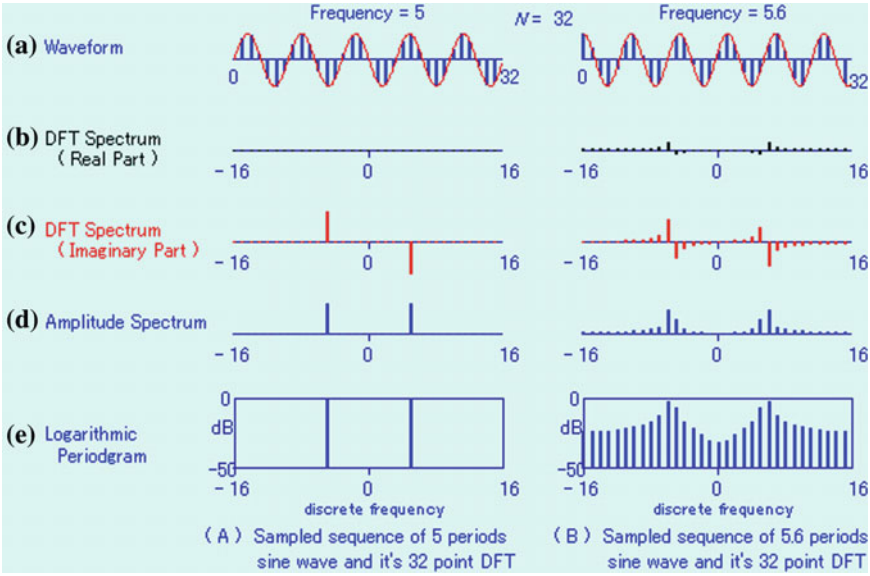

Fig. 6.10 **A** Sample sequence with five cycles in it and its 32-point DFT and **B** sample sequence with 5.6 cycles in it and its 32-point DFT. Animation available in supplementary files under filename E6-10_SinSP.exe

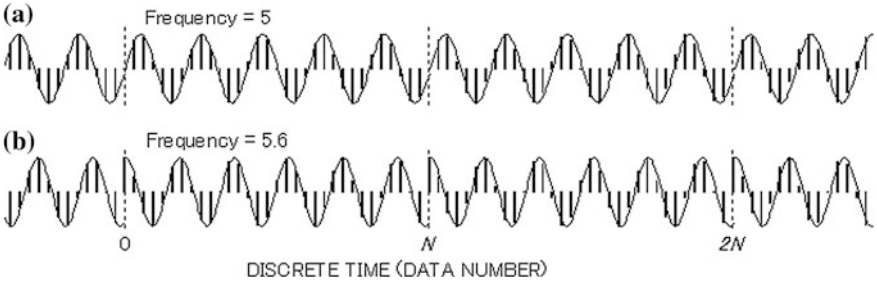

Fig. 6.11 **a** Periodic waveform of a sample sequence with five cycles in it and **b** periodic waveform of a sample sequence with 5.6 cycles in it

period (spacing between adjacent samples). Figure 6.11a, b shows the analyzed waveforms with the duration of $5T$ and $5.6T$ s, respectively. If there are an integer number of cycles in the sample sequence, the cascaded waveform becomes continuous, as shown in Fig. 6.11a. If there are a non-integer number of cycles in the sample sequence, the cascaded waveform becomes discontinuous, as shown in Fig. 6.11b. Many frequency components, described by complex numbers, are necessary to synthesize discontinuous waveforms of the type shown in Fig. 6.10b.

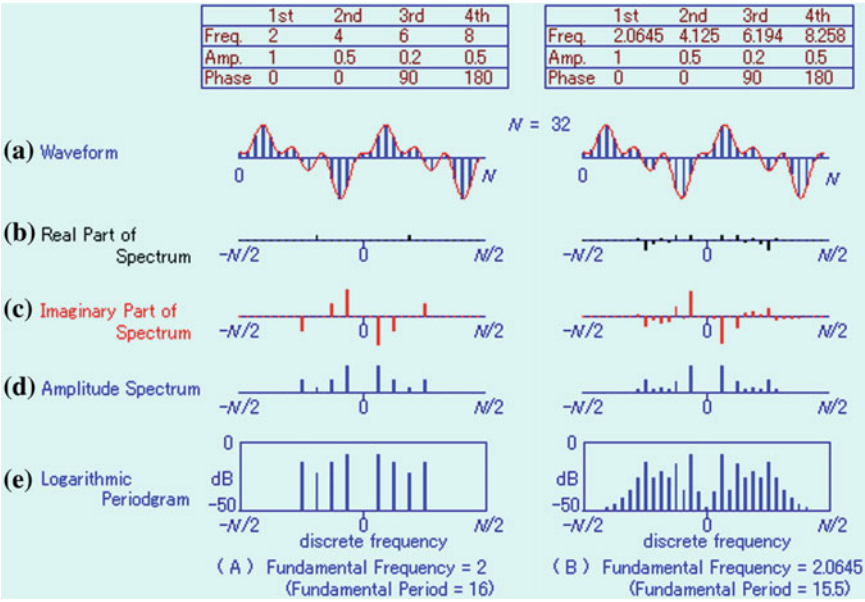

Fig. 6.12 Waveforms made of fundamental and lowest three harmonics, and their 32-point DFTs. **A** The frequency of the fundamental component is two (fundamental period is 16), and **B** the frequency of the fundamental component is 2.0645 (fundamental period is 15.5). Animation available in supplementary files under filename E6-12_SinSPS.exe

6.6 Removal of Discontinuity by the Adjustment of the Sampling Frequency

As the previous sections have shown, if the number of cycles in the sample sequence is an integer, the spectrum becomes linear. Then it may be possible to adjust the sampling period so that the number of cycles in the sample sequence becomes an integer. This is possible if there is only one component. If there are two or more, this is possible only when those components are all in harmonic relationship. Otherwise this idea is not practical.

Most musical instruments produce harmonic components. The appropriate sampling frequency may not be determined after the first trial but after several trials. With this concept in mind, some examples will be examined.

Figure 6.12 is an example of 32-point DFT of a waveform comprised of four sine components. In Fig. 6.12a, the fundamental component has two periods in the 32-point sample sequence. The other three components are at 2, 3, and 4 times higher frequencies of the fundamental. Therefore, all components have integer numbers of periods in the sample sequence, and the sample values at n and $n + 16$ are identical (16 is the period of the present waveform of analysis). In this case the harmonic components are obtained with no error by the 32-point DFT as shown in Fig. 6.12a.

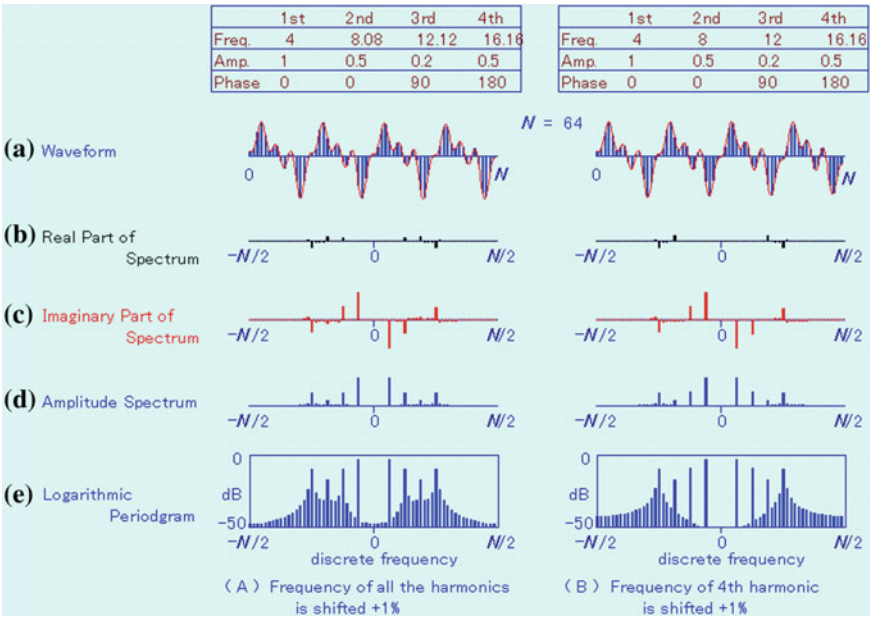

Fig. 6.13 64-point DFTs of two waveforms made of fundamental and lowest three harmonics. **A** Three harmonics have 1 % higher frequencies than the integer multiples of the fundamental frequency. **B** The fourth harmonic has 1 % higher frequency than the integer multiple of the fundamental frequency. Animation available in supplementary files under filename E6-13_SinSP.exe

In Fig. 6.12b, all four components have the same frequency ratios as in (A). However, in this case, the sample period is given by dividing the time length of two periods of the fundamental component by 31 (instead of 32 in (A)). Then, the period of the waveform becomes 15.5 (instead of 16 as in (A)). In other words, the fundamental frequency becomes 2.0645… (=32/15.5), which is not an integer.

The small change in the sampling frequency or the sampling period causes a large spectrum difference as shown in Fig. 6.12. The difference of the sampling period is only 3.2 % (=1/31), but the spectrum distributions are significantly different. Even if one is very careful in determining the sampling frequency in order to obtain the correct harmonic components, a small misadjustment of the sampling frequency may lead to meaningless results.

A case will now be examined where the frequencies of the "harmonics" are slightly off from the integer multiples of the frequency of the fundamental component. This has a practical meaning since some musical instruments such as pianos have the characteristic called "inharmonicity." The question is: what kind of results does one obtain when the sampling frequency is adjusted to the frequency of the fundamental component.

One example is shown in Fig. 6.13. The waveform shown here is almost the same as the previous one. The length of the sample sequence is 64 (twice the

previous case), and therefore, the spectral density is also twice the previous case. Since the sampling frequency is adjusted so that there are four cycles of the fundamental component in the sample sequence, its discrete frequency is four. In Fig. 6.13a, the second and higher "harmonics" have 1 % higher frequencies than the integer multiples of the fundamental frequency, resulting in the spreading of their spectra. In Fig. 6.13b, only the fourth "harmonic" is given 1 % higher frequency than four times the fundamental frequency (its amplitude is one-half of the fundamental component). Figure 6.13b shows that a wide spreading of the spectrum is caused when even a single component has non-integer frequency. This indicates that low amplitude harmonics may be buried under the spread spectra of higher amplitude harmonics.

The above discussion shows that the idea of adjusting the sampling frequency so that an integer number of cycles of the fundamental component is included in the sample sequence does not work if the "harmonics" are actually slightly different from integer multiples of the frequency of the fundamental component.

6.7 Removal of Discontinuity by the Weighting of Sample Sequences

The N-point DFT of a waveform is a Fourier transform of a periodic function that repeats the N-point sample sequence infinitely. As has been explained in many cases, if there is a discontinuity at the junctions between two adjacent periods, the abrupt changes of the waveform cause spreading of the spectrum. Generally, the spreading of the spectrum is proportional to the magnitude of the discontinuity (leakage of spectrum). Even when zeros are added to the sample sequence, there are still discontinuities at the junction: those jumping up to some value from zero and those falling from some value to zero, causing the spreading of the spectrum (see Sect. 6.4).

The above discussion indicates that if the tail of the sample sequence is smoothly connected to the head of the sample sequence, the spreading of the spectrum may be reduced. The same thing can be said when zero data are added to a sample sequence. The sample sequence should be smoothly reduced to zero at both ends in order to reduce the abrupt change in the modified sample sequence used for the analysis. The removal of the abrupt change of the waveform can be achieved by tapering (or weighting) the beginning and the end of the sample sequence gradually to zero. If the amplitude of one sequence gradually approaches zero and the beginning of the next sequence (which is the identical sequence) also gradually increases from zero, there should be no abrupt change in the waveform. However, a question may be raised, "Is it safe to modify the waveform in this way?" To answer this question, consider the effect of this modification of the waveform on the spectrum, using a periodogram of a sine wave.

Consider the case of a 64-point sample sequence which has 5.5 cycles (periods) of a sine wave. Figure 6.14a shows the sample sequence and its periodogram. The

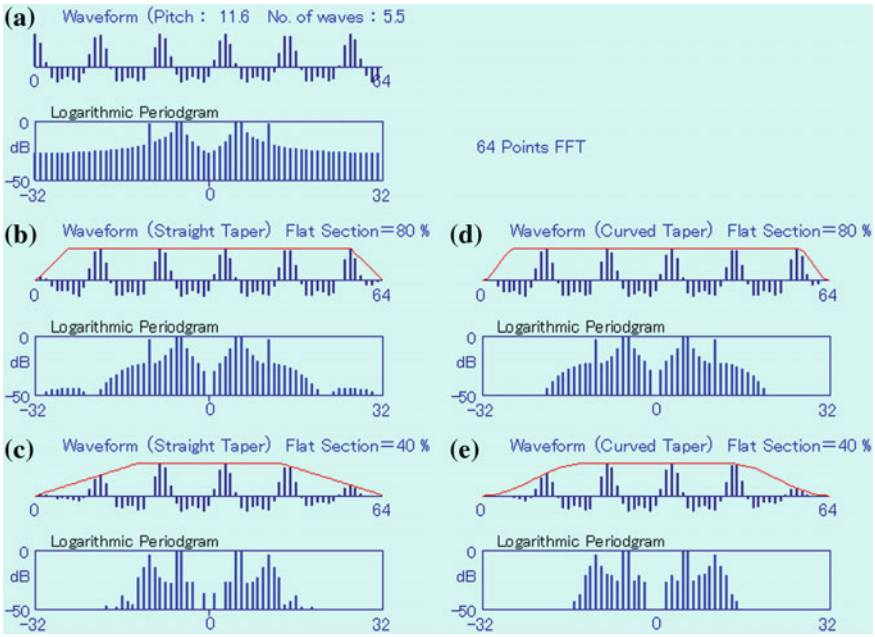

Fig. 6.14 The effect of tapering on the periodogram (64-point DFT) of a sine wave with frequency 5.5. **a** Without tapering, **b** linear tapering with 80 % flat area, **c** linear tapering with 40 % flat area, **d** sine-squared tapering with 80 % flat area, and **e** sine-squared tapering with 40 % flat area. Animation available in supplementary files under filename E6-14_TaperSP.exe

periodogram exhibits a wide spreading. Next, taper (fade in and fade out) this sequence. The amplitudes of the beginning and ending (20 % of the total sequence length) are linearly tapered. The remaining 80 % in the middle is not modified. The sample sequence and its periodic power spectrum are shown in Fig. 6.14b. Although the spectrum is far from a single line spectrum, the spreading is much narrower than in Fig. 6.14a. The peak of the spectrum exists between frequencies 5 and 6, and since the levels at 5 and 6 are the same, it is reasonable to guess that the peak frequency is 5.5. This is what would be expected, because the number of sine cycles in the sample sequence is 5.5.

In order to reduce the slope of the tapering, the portion of the unmodified region is reduced from 80 to 40 %. The result is shown in Fig. 6.14c, where it seems that the spreading is reduced over the case of (b).

The slopes used in Fig. 6.14b, c are linear. It may be more effective to use a curved (e.g., sine-squared) tapering. For this purpose the functions

$$\frac{1}{2}\left[1 - \cos\left(\frac{n\pi}{\tau}\right)\right] = \sin^2\left(\frac{\pi}{2}\frac{n}{\tau}\right) \quad n = 0, 1, \ldots, \tau$$

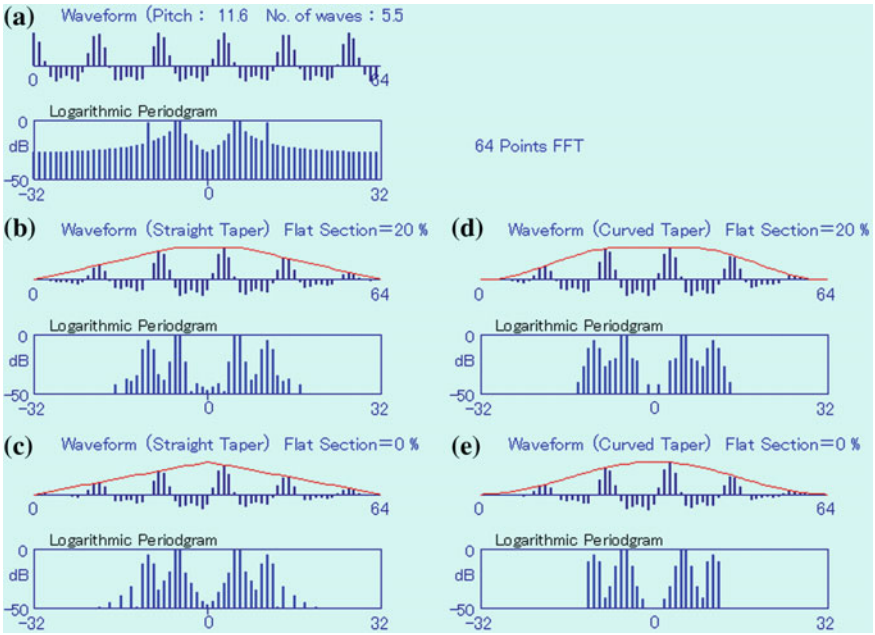

Fig. 6.15 The effect of tapering on the periodogram (64-point DFT) of two sine waves with frequency 5.5 and 11 (the amplitude of the latter is half of the former). **a** Without tapering, **b** linear tapering with 20 % flat area, **c** linear tapering with 0 % flat area, **d** sine-squared tapering with 20 % flat area, and **e** sine-squared tapering with 0 % flat area. Animation available in supplementary files under filename E6-15_TaperSP.exe

and

$$\frac{1}{2}[1 - \cos(\frac{\pi}{2}\frac{N-n}{\tau})] = \sin^2(\frac{\pi}{2}\frac{N-n}{\tau}) \quad n = N-\tau, N-\tau+1, \ldots, N$$

are applied to the beginning and ending of the sample sequence, respectively. The former and latter functions gradually start from 0 (1) and gradually end at 1(0), respectively. The modified sample sequences using the above functions for the cases with $\tau = 0.1N$ and $\tau = 0.3N$, and their power spectra, are shown in Fig. 6.14d, e, respectively. There is not much improvement of these results compared to those of (b) and (c).

The previous case is for a single sine wave. A higher frequency resolution is required when there are two or more components. Next consider a case with two frequency components with a 1:2 frequency ratio. The second harmonic has an amplitude of 0.5 compared to one for the fundamental component. The flat area is further reduced to 20 and 0 % (previous cases were 80 and 40 %).

Results are shown in Fig. 6.15. Even without tapering, the second harmonic is clearly seen in (a). Since the number of cycles of the second harmonic is 11 (integer), its line spectrum stands out from the spread spectra of the first component.

If there are other components with smaller amplitudes or slightly different frequencies, they may not be detected.

As shown in Fig. 6.15b–e, tapering works to reduce the possibility of such masking. The cases (c) and (e) with the 0 % flat area seems to work better than the cases (b) and (d) with the 20 % flat area. It is very attractive that the spreading of the second harmonic in (e) is very narrow. However, is it safe to modify the sample sequence to such a degree that there is no flat area? It is necessary to investigate the effect of the modification.

The above results show that the idea of tapering both ends of the waveform to reduce the abrupt change at the junction is promising. At this stage, tapering with 0 % flat area seems to work better than the other cases. However, not much more is known than what has been seen in some numerical examples about the effect of tapering (weighting). In the next chapter, the theoretical meaning of various kinds of weighting will be considered.

6.8 Exercise

1. The N-point DFT of a sample sequence has 1 at $n = m$ and $N - m$ and zeros at all other points. What is the original waveform?
2. The N-point DFT of a sample sequence is j at $n = m$ and $-j$ at $N - m$ and zeros at all other points. What is the original waveform?
3. The N-point DFT of a sample sequence has -1 at $n = m$, 0.5 at $n = k$, -1 at $N-m$, -0.5 at $N-k$, and zeros at all other points. What is the original waveform?
4. The N-point DFT of a sample sequence has several distinct line spectra and other many smaller components around them. What kind of property does the original waveform have?
5. In the case where the period of a sine wave is not an integer multiple of the inverse of the period of an N-point sample sequence, what kind of DFT do you expect? Why?
6. What is the definition of periodic power spectrum?
7. In what cases does the periodic power spectrum become identical with the power spectrum of the total waveform?
8. Can you get any information about the frequency of a signal if you have data measured only at a single instant time?
9. What is the frequency resolution of a waveform with duration T?
10. What is the uncertainty principle in frequency analysis?
11. There are 11 cycles of one sine wave and 13.5 cycles of another sine wave in an N-point sample sequence. Can you tell what components compose the wave from the N-point DFT?
12. There are cases when the periodic power spectrum has a discrete line spectrum, and when it has a distributed spectrum. State examples for each such case.
13. In what cases does the imaginary part of an N-point DFT become zero?
14. In what cases are both the real and imaginary parts of an N-point DFT non-zero?

Chapter 7
Time Window

It was shown that tapering both ends of the sample sequence improves the amplitude and frequency resolutions even if the number of waves in the sample sequence is not an integer. However, the discussion stopped short of developing the relationship between tapering concepts and their resulting improvements. The aim of this chapter is to make clear the consequences of tapering and to develop guidelines for the selection of types of tapering.

Weighting functions that taper (or cut off) both ends of sample sequences are called *time windows*. The properties of various windows, which are called with different names, were enthusiastically investigated right after the invention of the FFT algorithm.

7.1 Fourier Transform of a Product of Two Time Functions

The tapering of both ends of a time sequence is actually the multiplication of that time function by a time window function. Therefore, the resulting spectrum is known if the spectrum of the product of two functions is known.

Let $x(t)$ and $w(t)$ be the time function to be analyzed and the time window function (or simply, time window), respectively, and $X(f)$ and $W(f)$ be their corresponding continuous Fourier transforms. The transform pairs are given by Eqs. (7.1) to (7.4).

$$X(f) = \int_{-\infty}^{+\infty} x(t) \exp(-j2\pi ft)dt \tag{7.1}$$

$$x(t) = \int_{-\infty}^{+\infty} X(f) \exp(j2\pi ft)df \tag{7.2}$$

$$W(f) = \int_{-\infty}^{+\infty} w(t) \exp(-j2\pi ft)dt \tag{7.3}$$

K. Kido, *Digital Fourier Analysis: Fundamentals*,
Undergraduate Lecture Notes in Physics, DOI: 10.1007/978-1-4614-9260-3_7,

$$w(t) = \int_{-\infty}^{+\infty} W(f)\exp(j2\pi ft)df \tag{7.4}$$

Our concern is with the Fourier transform of the product of $x(t)$ and $w(t)$. The aim of this chapter is to investigate how the spectrum of the time function changes when multiplied by a window function. In general, any time function is expressed by the summation of several sine waves. Therefore, it is necessary to understand how the spectrum of a sine wave changes when multiplied by a window function. This multiplication process is equivalent to amplitude modulation in communication systems, as used in AM radio broadcasting technology.

Let $x(t)$ be a sine wave with frequency f_0. One needs to calculate the product of $x(t)$ and $w(t)$. If it is assumed that $w(t)$ exists only in the region $-T/2 \le t \le T/2$ and has zero amplitude outside of this region, then the Fourier Transform integration is expressed by:

$$\text{FT}\ [x(t)w(t)] = \int_{-T/2}^{+T/2} \sin(2\pi f_0 t)w(t)\exp(-j2\pi ft)dt \tag{7.5}$$

Expressing the sine function as a pair of complex functions by use of Euler's formula, the above equation is rewritten as:

$$\begin{aligned}\text{FT}\ [x(t)w(t)] &= \int_{-T/2}^{+T/2} \frac{\exp(j2\pi f_0 t) - \exp(-j2\pi f_0 t)}{j2} w(t)\exp(-j2\pi ft)dt \\ &= \frac{1}{j2}\int_{-T/2}^{+T/2} w(t)\exp\{-j2\pi(f - f_0)t\}dt \\ &\quad - \frac{1}{j2}\int_{-T/2}^{+T/2} w(t)\exp\{-j2\pi(f + f_0)t\}dt.\end{aligned} \tag{7.6}$$

Since the window function $w(t)$ is zero outside of $-T/2 \le t \le T/2$, its Fourier transform given by Eq. (7.3) is expressed by the following equation.

$$W(f) = \int_{-\infty}^{+\infty} w(t)\exp(-j2\pi ft)dt = \int_{-T/2}^{+T/2} w(t)\exp(-j2\pi ft)dt \tag{7.7}$$

The only difference between Eq. (7.7) and (7.6) is that f is replaced by $(f - f_0)$ or $(f + f_0)$. Therefore, Eq. (7.6) can be rewritten as

$$\text{FT}\ [w(t)\sin(2\pi f_0 t)] = \frac{1}{j2}[W(f - f_0) - W(f + f_0)] \tag{7.8}$$

When a cosine wave is used instead of the sine wave, the following equation is obtained by the same methodology.

$$\text{FT}\ [w(t)\cos(2\pi f_0 t)] = \frac{1}{2}[W(f - f_0) + W(f + f_0)] \tag{7.9}$$

If the time function is composed of L number of sine and cosine functions,

$$x(t) = \sum_{i=0}^{L-1} A_i \cos(2\pi f_i t) + \sum_{i=0}^{L-1} B_i \sin(2\pi f_i t) \tag{7.10}$$

the Fourier transform of the product of this time function and the time window is given by the summation of Eqs. (7.8) and (7.9) each multiplied by the Fourier coefficients A_i and B_i.

$$\begin{aligned}\text{FT}\ [w(t)x(t)] = &\frac{1}{2}\sum_{i=0}^{L-1} A_i[W(f - f_i) + W(f + f_i)] \\ &+ \frac{1}{j2}\sum_{i=0}^{L-1} B_i[W(f - f_i) - W(f + f_i)]\end{aligned} \tag{7.11}$$

.

This equation reveals that the spectrum $W(f)$ of the window function $w(t)$ is shifted on the frequency axis to $W(f - f_i)$ and $W(f + f_i)$ by the frequencies $\pm f_i$ of the sine and cosine functions. Therefore, in order to investigate the effect of the window function, one only needs to investigate the spectrum of the window function instead of the spectrum of the product of the time function and the window function.

On the basis of this understanding, the spectra of various window functions will be examined.

7.2 Spectra of Tapered Functions

Let's consider the results shown in Figs. 6.14 and 6.15 from a different point of view, that is, as frequency shifted spectra of time window functions.

Spectra of various time window functions are shown in Fig. 7.1. The $W(t)$ shown in Fig. 7.1a is without tapering, the $W(t)$ shown in (b) and (c) are linearly tapered, the $W(t)$ shown in (d), (e), and (f) are tapered by sine squared functions. In each of the charts, the top graph is the time window function and the bottom is its corresponding spectrum. The length of the window, T, is the same for all charts. The percentages of the window functions with flat area are: 100 % for (a), 80 % for (b) and (e), 40 % for (c) and (f), and 0 % for (d). The spectra are shown in the range $\pm 32/T$. The vertical axis is shown in dB so that amplitudes as small as 3/1000 of full scale may be visible.

The spectrum (Fig. 7.1a) of the rectangular window, which jumps up and down stepwise at t = 0 and T, has a very wide frequency domain spreading. The shapes

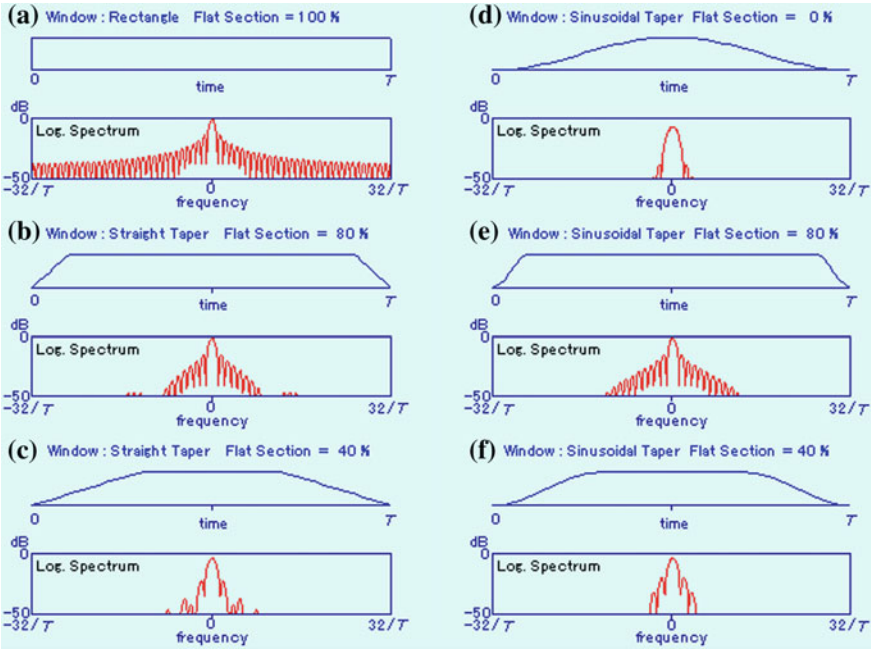

Fig. 7.1 Comparison of spectra of the weighting functions (windows) used in Chap. 6 (see Figs. 6.14 and 6.15). Animation available in supplementary files under filename E7-01_TaperingSP.exe

of the spectra shown in Figs. 6.14a and 6.15a are the results of shifting the spectrum of the rectangular window by $\pm f_0$, where f_0 is the frequency of the sine wave. The superimposed spectrum takes a relatively large value even at frequency 0, since the spectrum in Fig. 7.1a takes a finite value at $\pm f_0$ (the frequency is ± 5.5 Hz in Fig. 6.14a). The spectrum shown in Fig. 6.15a is an addition of a second harmonic which has two line spectra at ± 11Hz.

The spectrum shown in Fig. 6.14b is the superposition of the two spectra which are obtained by shifting the spectrum of Fig. 7.1b. The time window shown in Fig. 7.1b is linearly tapered in the 10 % ranges from both ends, and its spectral spreading is smaller than the rectangular window without tapering. If the tapering is increased to 30 % as in Figs. 6.14c and 7.1c, the spreading is further reduced and the spectral distributions centered at $\pm f_0$ are separated in a larger degree.

The window functions shown in Fig. 7.1a–c are linearly tapered time windows, while the ones shown in Fig. 7.1d–f are curvilinearly tapered windows. The function of the curvilinear taper in the range from $t = 0$ to $t = \tau - T$ is given by

$$w(t) = 0.5 - 0.5\cos(2\pi t/\tau) \tag{7.12}$$

and in the range from $t = T - \tau$ to $t = T$ is given by

$$w(t) = 0.5 - 0.5\cos\{2\pi(T - t)/\tau\}. \tag{7.13}$$

A distinctive feature of these functions is that the gradients at both ends are zero, and therefore, the windows in Fig. 7.1d–f smoothly change from 0 to 1 and 1 to 0. The time τ is the duration of the curvilinear portion and if the flat area is 0, 40, or 80 %, then τ is equal to 0.5, 0.3, or 0.1 T, respectively. One can see the effect of smooth tapering in the spectra of Fig. 7.1d–f, d and e of Figs. 6.14 and 6.15.

It was stated at the end of Chap. 6 that the effect of sine functions given by Eqs. (7.12) and (7.13) was not significant. Let us consider the reason using Fig. 7.1. The comparison of Fig. 7.1b and e shows that the spreading of (b) is smaller than that of (e) if levels below −40 dB are neglected, indicating that the straight line type window is better. Further, it seems that the windows with smaller flat areas have spectral distributions more concentrated at the center. However, if Fig. 7.1c and f are compared, (f) is better. And among all, the spectrum of Fig. 7.1d with zero flat area has the best performance in every respect.

The above discussion showed that the sine function type tapering with zero flat area is the better time window. The function defined by Eqs. (7.12) and (7.13) with $\tau = 0.5\ T$ is called Hanning weighting, and the time window with this weighting is called the *Hanning window*. It is one of the most common windows in use in frequency analysis applications. The properties of this window will be discussed together with other windows in Sect. 7.4.

If there is an integer number of periods of a sinusoidal signal in the rectangular window, there is one discrete line spectrum in each of the positive and negative frequency region. This is only possible when the window is rectangular. However, the spectrum of the rectangular window has the spreading as shown in Fig. 7.1a. These two facts seem contradictory with each other.

The spectrum obtained by the DFT has values only at frequencies, which are integer multiples of the inverse of the window time length (n/T). On the other hand, the spectrum of the rectangular window is zero at these frequencies except for $n = 0$. This has been shown in Figs. 4.6 and 4.7 in Chap. 4. More explanations may be necessary to explain this matter.

The spectrum of the rectangular window, that is equal to 1 in the range $-T/2 < t < T/2$ and equal to 0 outside, is given by Eq. (2.37) in Chap. 2, which becomes as follows:

$$\begin{aligned} W(f) &= \int_{-T/2}^{+T/2} \exp(-j2\pi ft)dt \\ &= j\frac{1}{2\pi f}\exp(-j2\pi ft)\Big|_{-T/2}^{+T/2} = j\frac{\exp(-j\pi fT) - \exp(j)}{2\pi f} \\ &= T\frac{\sin(\pi fT)}{\pi fT}. \end{aligned} \tag{7.14}$$

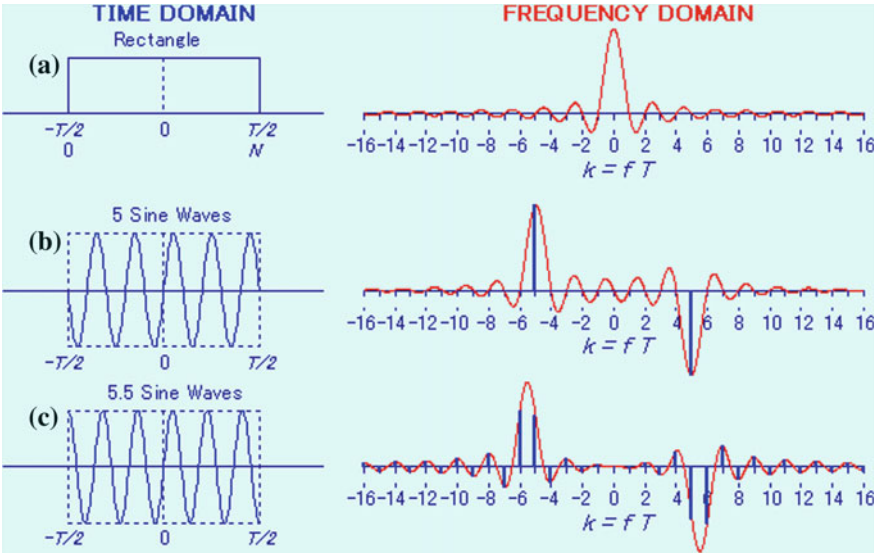

Fig. 7.2 Rectangular window and sine waves extracted by the rectangular window and their spectra. **a** Rectangular window, **b** sine wave with 5 periods in the window, and **c** sine wave with 5.5 periods in the window. Animation available in supplementary files under filename E7-02_RectWindSP.exe

This is called the "sinc function", which was studied in Sect. 3.6 (see Eq. (3.11) and Fig. 3.7). The sinc function takes the maximum value 1 at $x = \pi fT = 0$ and decreases to zero amplitude as $|x|$ gets larger and larger. The sinc function is equal to zero (crosses the x-axis) when fT takes integer values (i.e., $f = k/T \quad k \neq 0$). The rectangular window (left) and its spectrum (right) are shown in Fig. 7.2a.

The spectrum of a sine and cosine wave extracted by the rectangular window are given by Eqs. (7.8) and (7.9), respectively. Figure 7.2b, c show results for the sine waves.

Shown in Fig. 7.2b is the case when there are exactly 5 periods in the window $-T/2 \leq t \leq T/2$. The spectrum is the sum of the two spectra of (a) that are centered at frequencies $fT = +5$ (sign reversed) and (b) -5. Since the spectrum of DFT exists only at frequencies when fT takes integer values, all values except for the frequencies at $fT = +5$ (sign reversed) and -5 are equal to zero.

On the other hand, if there are 5.5 periods in the window as shown in Fig. 7.2c, the spectrum is the sum of the two spectra of the rectangular wave that are centered at frequencies $fT = +5.5$ (sign reversed) and -5.5. The frequencies at which the spectrum becomes zero are not integers. In this case, the spectrum of the windowed wave is not zero at integer values of fT, as shown by the thick line in Fig. 7.2c, and the line spectrum exhibits a wide distribution.

The spectrum shown in Fig. 6.14a in Chap. 6 is the same case (there are 5.5 periods in T) as this one. Since the spectrum is shown using a decibel scale, the small values appear larger but actually they are of the same amplitude.

7.3 DFT of Short Waveforms

In the previous section, waveforms that exist in the whole range of the time window was dealt with. In this section, waveforms with short duration or cases when short portions of quickly changing waveforms must be analyzed will be considered. This analysis has already been discussed in Chap. 6 (see Figs. 6.6, 6.7, 6.8 and 6.9), where zero amplitude data were added to increase the number of DFT points. In these figures, the problem was the spreading of the spectrum. The analysis in Sects. 7.1 and 7.2 suggests that tapering both ends of short waveforms may reduce the spreading of the spectrum.

For this analysis use the weighting function (d) in Fig. 7.1, which looks the best compared to other windows in the figure. This window is referred to as the Hanning window, but naming and other details will be described in the next section. The results are shown in Figs. 7.3 and 7.4.

From the discussion of Fig. 6.7 and considering that the effective length of the window becomes approximately 1/2 of the rectangular window, a 64-point window is used. Figure 7.3a shows the windowed waveforms, (b) their power spectra using a linear scale, and (c) the power spectra using a decibel scale (see footnote).

The spectrum in Fig. 7.3A illustrates the case when all four components have integer frequencies (i.e., integer numbers of periods in the total DFT length (=256)), while (B) illustrates the case where the 1st and the 3rd components have non-integer frequencies. The difference between (A) and (B) is very small. Both of them show similar spectra, with four main peaks, without regard to the number of periods in the window length (or the frequencies of the components).

Since zero data are appended to the waveforms as shown in (a), the power spectra shown in (b) and (c) are not exactly the "periodgrams" of the Hanning windowed waveform.

The data given in Fig. 7.4 shows the effects when the Hanning window length is varied from 32 to 96 points in 16 steps ((A): waveform, (B): power spectrum, (C): power spectrum in dB). The Hanning window is applied to the extracted (short) waveform.

In Fig. 7.4, when the window length is 32, only two rounded peaks are observed. However, if the length is increased to 48, all four components of the waveform become visible. As the length is further increased, the separation between the components is also increased. Figure 7.3 suggests that similar results may be obtained even if the frequencies are not integers. They are not shown here but one can check by running the program attached to Fig. 7.4.

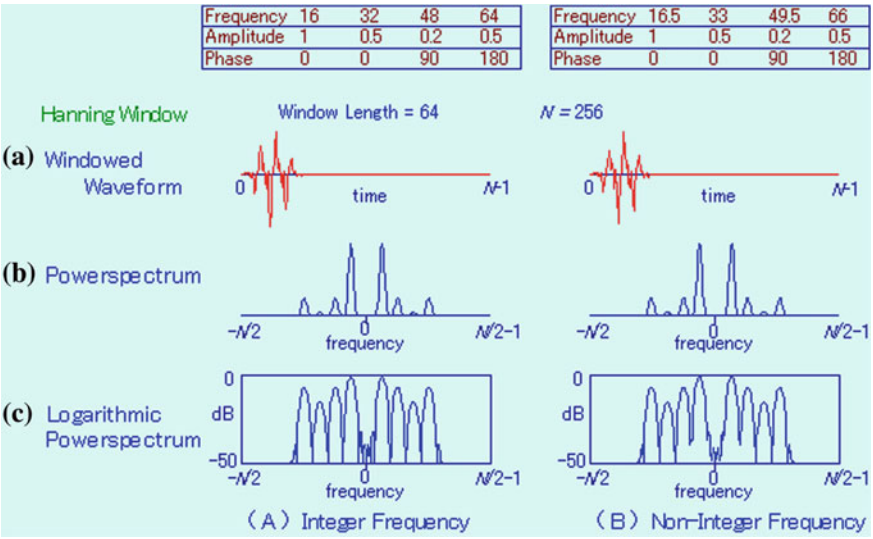

Fig. 7.3 Results of 256 point DFTs of the waveforms shown in the tables at the top (same as those used in Fig. 6.8). The 64 point Hanning window is applied to the waveforms and zeros are added to the 192 remaining points. Animation available in supplementary files under filename E7-03_L0SP.exe

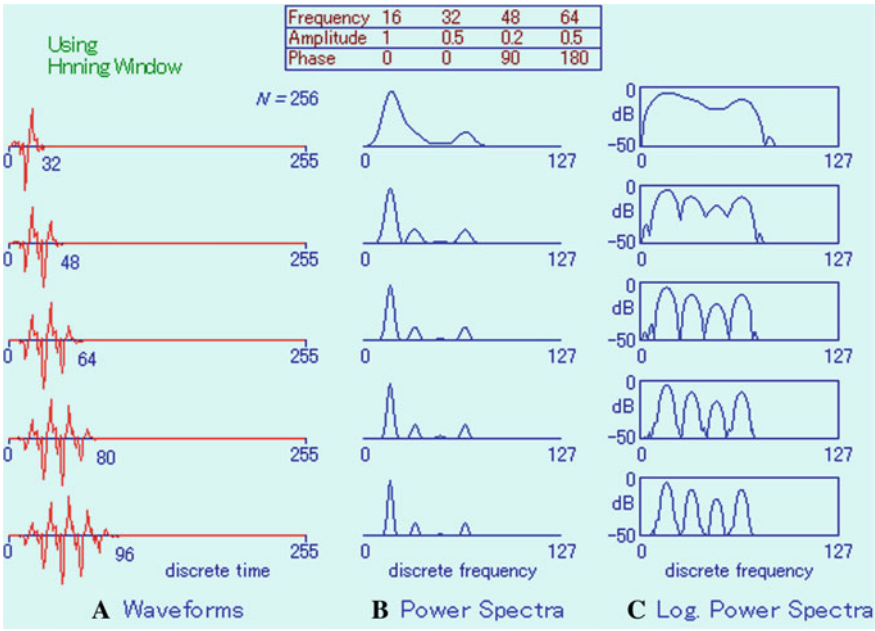

Fig. 7.4 Results of 256 point DFTs of the waveforms shown in the table at the top (same as in Fig. 6.9). The Hanning window length is varied from 32 to 96 in 16 steps. Animation available in supplementary files under filename E7-04_L0SP.exe

By comparing the above results with those from Figs. 6.6, 6.7, 6.8 and 6.9, one can conclude that tapering is also effective when the DFT is applied to short extracted waveforms with additions of zero data.

One may note that a longer window length will produce a better frequency separation. The improvement of the spectrum can be checked by choosing different window lengths in the programs attached to Figs. 7.3 and 7.4.

It has been shown that the use of weighting functions such as the Hanning window is recommended even when the DFT is applied to short extracted waveforms: the windowed waveforms are then zero padded to improve the frequency resolution. We should remember that the effective window length is shortened by the windowing, therefore, the number of the periods in the window should not be too small.

7.4 Various Time Windows

The terminology *time window* is in general used to describe the extraction of a smaller portion from a longer waveform or sample sequence. However, at the same time, some kind of weighting is being performed on the extracted waveform. Depending on the weighting functions, various names are given to individual time window functions.

The purpose of the time window function in DFT analysis is to obtain the precise spectral information of the waveform while suppressing generation of extraneous spectral components that do not exist in the original waveform. However, what is actually obtained is the periodogram, which is not exactly the same as the power spectrum of the original waveform (even after many averages have been taken) as previously described in Chap. 6.1.

Usage of time windows affects the power of the waveform as well as its spectrum. With these observations in mind, several well-known windows will be examined.

7.4.1 Rectangular Window

Extracting a portion of a waveform with the uniform weighting is referred to as "sampling without weighting" or "applying a rectangular window." As was demonstrated in Chap. 6, if the number of periods of a harmonic in the window is an integer, the spectrum of the waveform is obtained with no error. If not, the spectrum demonstrates some spreading. However, since the rectangular window does not distort waveforms, it is the most basic and important window.

The spectra of the rectangular window and a portion of a sine waveform extracted with the rectangular window were shown in Fig. 7.2. It is possible to quantitatively explain these spectra by substituting the spectrum of the rectangular

window into $W(f)$ in Eq. (7.8) for a sine wave, Eq. (7.9) for a cosine wave, and Eq. (7.11) for a general waveform. In order to do this, the spectrum of the rectangular window must be formulated.

The rectangular window with length T is expressed by Eq. (7.15) for the continuous system. Its spectrum is expressed by Eq. (7.16).

$$w_r(t) = \begin{cases} 1 & (-T/2 \le t < T/2) \\ 0 & (\text{otherwise}) \end{cases} \tag{7.15}$$

$$W_r(f) = T\frac{\sin(\pi fT)}{\pi fT} \tag{7.16}$$

For the discrete system, the rectangular window with N sample length is defined by:

$$w_r(n) = 1 \quad (0 \le n \le N-1) \tag{7.17}$$

Its N-point DFT is given by

$$W_r(k) = \begin{cases} N & (k=0) \\ 0 & k \ne 0 \end{cases} \tag{7.18}$$

However, Eq. (7.18) is the spectrum of an infinitely long waveform that repeats Eq. (7.17) infinite times. This waveform is continuous and equal to 1 everywhere, representing a direct current. This is not the spectrum of the waveform $w(t)$ given by Eq. (7.15), which is 0 for $-\infty < t < -T/2$, 1 for $-T/2 \le t \le T/2$ and 0 for $T/2 < t < \infty$.

In order to calculate the spectrum of an extracted waveform in an N-point time window, the spectrum of the time window which is continuous both in the time and the frequency domains is necessary. Equation (7.18), which is obtained as the discrete spectrum of the time window which is periodic with the period of the window length as the consequence of N-point DFT, has nothing to do with what is needed. Therefore, the equations of discrete spectra of time windows will not be shown.

Figure 7.5 shows the rectangular window and its continuous spectrum. This spectrum has its maximum at a frequency 0 Hz, and smaller peaks at other frequencies than zero Hz. This is a common trait for all time windows, i.e., the main peak at the center (0 Hz) and smaller peaks around it (at frequencies other than 0 Hz).

The spectrum in Fig. 7.5 becomes zero ($-\infty$ in dB) at the frequencies when fT is a positive or negative integer. Since this is valid from $fT = \pm 1$, the rectangular window has the narrowest main lobe compared to other types of windows. On the other hand, the fact that the side lobes do not decrease much compared to the main lobe is the disadvantage of this window in frequency analysis.

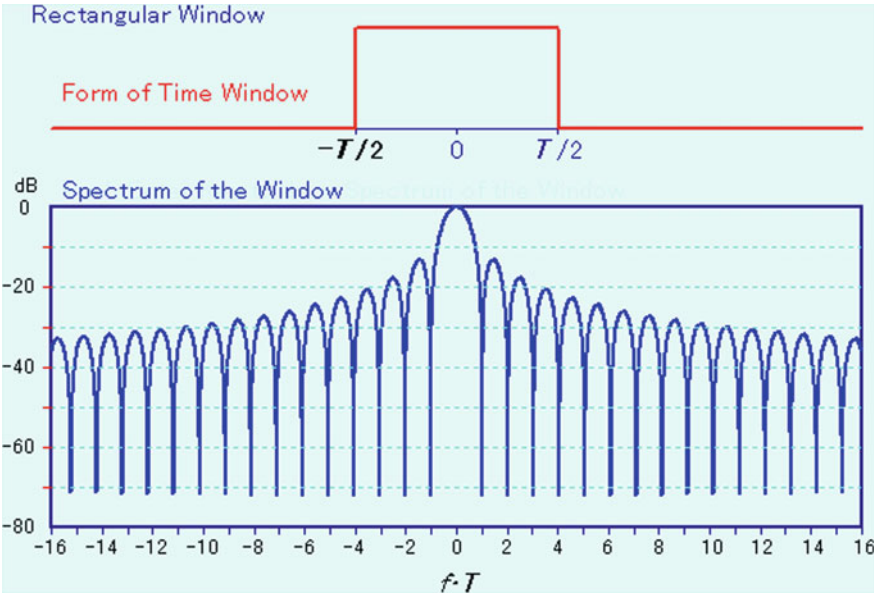

Fig. 7.5 Rectangular time window and its spectrum. Animation available in supplementary files under filename E7-05_Rect_Wind_Spec.exe

On the other hand, if the number of periods in the time window is equal to an integer, the correct spectrum is obtained in the discrete display, which is an advantage of this window.

7.4.2 Hanning Window (Von Hann Window)

The Hanning window function was proposed by Julius Von Hann, but following the naming of the Hamming window, it is called the "Hanning window." The spectrum of Hanning window in the continuous time and frequency domains, and the Hanning window function in the discrete time domain, are shown (see Figs. 6.15e and 7.1d).

$$w_n(t) = w_r(t)\left\{0.5 + 0.5\cos\left(2\pi\frac{t}{T}\right)\right\} = w_r(t)\cos^2\left(\frac{\pi t}{T}\right) \tag{7.19}$$

$$W_n(f) = 0.5T\frac{\sin\pi fT}{\pi fT} + 0.25T\left\{\frac{\sin\pi(fT-1)}{\pi(fT-1)} + \frac{\sin\pi(fT+1)}{\pi(fT+1)}\right\} \tag{7.20}$$

$$w_n(n) = 0.5 - 0.5\cos\left(\frac{2\pi n}{N}\right) = \sin^2\left(\frac{\pi n}{N}\right) \quad (0 \le \mathrm{n} \le N-1) \tag{7.21}$$

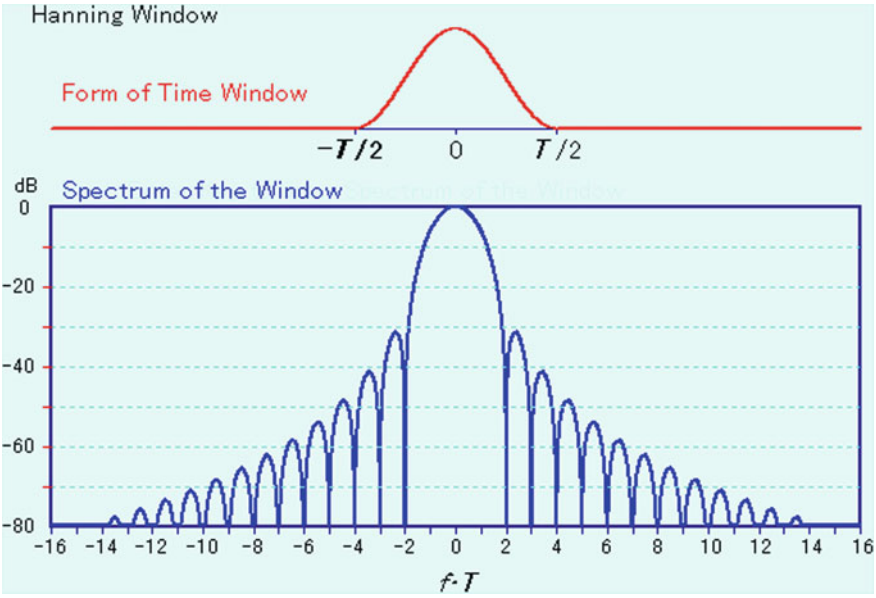

Fig. 7.6 Hanning window with length T and its spectrum. Animation available in supplementary files under filename E7-06_Hann_Wind_Spec.exe

$$\text{power reduction} = 4.26\,\text{dB} \tag{7.22}$$

The Hanning window and its spectrum are shown in Fig. 7.6. Compared to Fig. 7.5, the side lobes decrease more rapidly as their distance from the lobe center increases. The width of the main lobe, which influences the frequency resolution, is twice that of the rectangular window. The frequencies at which the spectrum becomes zero are given by $fT = \pm m$ (integer, $m \geq 2$). This spectrum has the least spreading compared to the other tapered windows shown thus far.

Time waveforms and spectra of sine waves extracted by use of the Hanning window are shown in Fig. 7.7b, c, while Fig. 7.7a shows that of the Hanning window itself. The spectra of (b) and (c) are superpositions of the spectra, that are obtained by frequency shifting the spectrum of (a) by $\pm k$ ($k = fT$) and also by the sign reverse of the spectrum for $+k$. If k is an integer (b), the spectrum has its maximum at the frequency, and has two components of magnitude 0.5 at its both sides($\pm$ ($k \pm 1$)). At the worst case, $k = 5.5$, (c), there are two components with almost the same magnitude at the two adjacent positive integer frequencies $[k]$ and $[k] + 1$, and at negative frequencies $-[k]$ and $-([k] + 1)$, where $[k]$ is an integer that does not exceed $|k|$. The spreading of the spectrum outside of these two components is smaller compared to that of the rectangular window (see Fig. 7.2c). This is an advantage in frequency analysis when the number of periods in the window is not an integer (which is very common in practical applications).

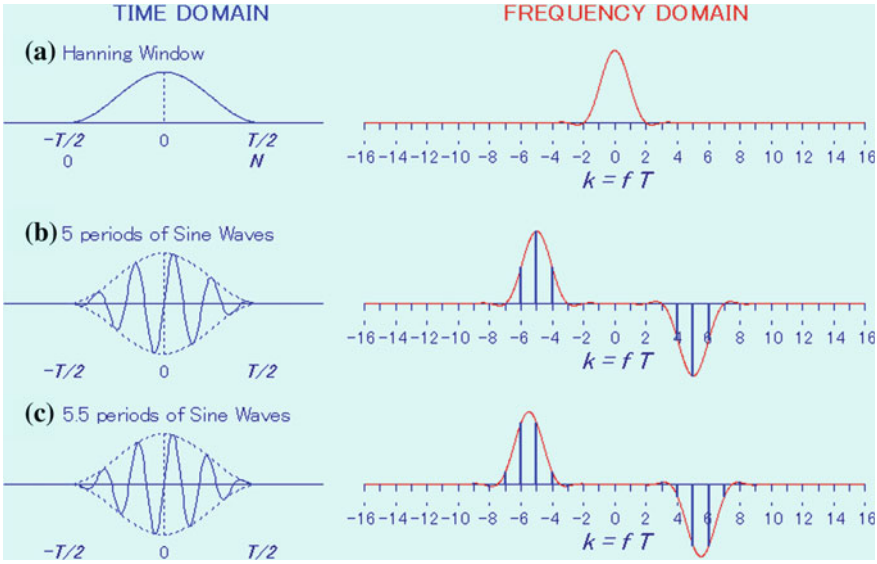

Fig. 7.7 Waveforms and spectra of the Hanning window and those of extracted sine waveforms by the Hanning window. Animation available in supplementary files under filename E7-07_HanWindSP.exe

The Hanning window function in the continuous time domain (Eq. 7.19) has its center at $t = 0$ so that it is convenient to see the properties of the window. If $t = 0$ is used as the starting point for the continuous window function, a phase shift due to the time shift is introduced and the spectrum becomes more complex. The discrete time domain has its starting point at $n = 0$ so that the formula of DFT can be directly applied. If the range $-N/2 \leq n < N/2$ is used for the discrete window function, it does not match with the common range of the DFT, $0 \leq n < N - 1$. This is the reason why different ranges are used for the continuous and discrete systems even though there is a slight difference between the two formulae.

Waveforms of sine and cosine waves extracted by the Hanning window and their spectra obtained by 64-point DFT are shown in Fig. 7.8. Figure 7.8A and B are for the case with 8 and 8.5 periods in the window, respectively. Figure 7.8A and B have purely imaginary and purely real spectra, respectively, because the former is an odd function and the latter is an even function. Since the data point N-n corresponds to -n, the oddness or evenness can be judged by the anti-symmetry or symmetry of the wave with regard to the vertical dotted line at $N/2$.

In Fig. 7.8A with 8 periods in the window, there are spectral lines at frequencies ± 8, and smaller spectra on both sides of them. In Fig. 7.8B with 8.5 periods in the window, there are positive and negative spectral lines with the same magnitudes at ± 8 and ± 9 and there are smaller spectral lines around them. The difference of the signs of the components between Figs. 7.7 and 7.8 is due to the

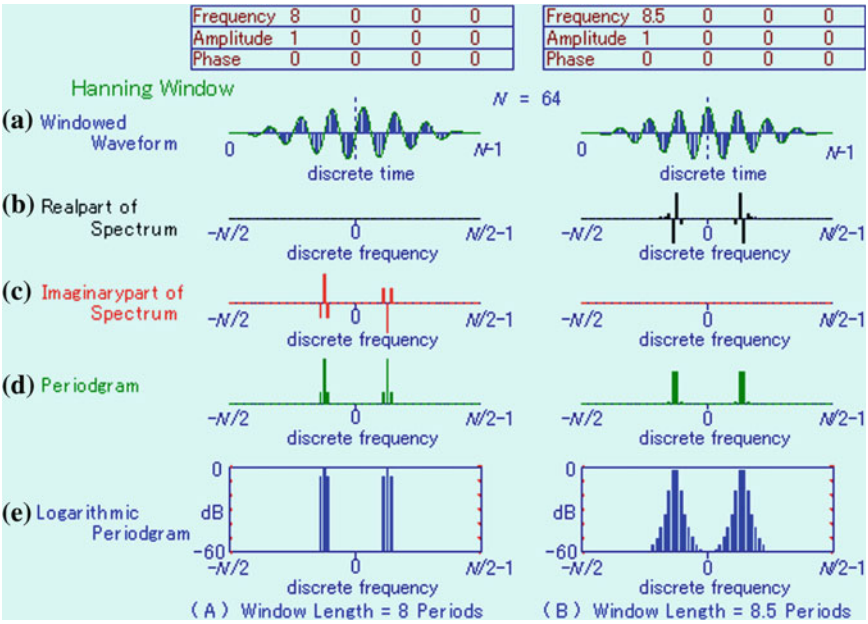

Fig. 7.8 Waveforms and spectra of sine waves obtained by the 64-point Hanning window. (A): 8 periods in the window, (B): 8.5 periods in the window. Animation available in supplementary files under filename E7-08_Haning.exe

phase shift introduced by the difference in the starting time. Other than that, the results of the two figures are basically the same.

A tapered window such as the Hanning window loses the total power in the window because of the reduction of the amplitude. The power ratio, expressed as P_{RN}, between the waves extracted by the Hanning and the rectangular windows is given by:

$$P_{RN} = \frac{1}{T}\int_{-T/2}^{T/2}\left[0.5 + 0.5\cos\left(2\pi\frac{t}{T}\right)\right]^2 dt = 0.375 \tag{7.23}$$

Expressing in dB, this is equal to -4.26 dB (= 10 log(0.375), see Eq. (7.22)). In the introduction of following windows, the power reductions obtained by the same calculation will be shown after the time windows and their spectra.

When applying the Hanning window, there will be 3 frequency components around each signal component, even under the best sampling conditions. It can be said that the precise power spectrum cannot be obtained by the DFT as described in Chap. 6.1.

7.4.3 Hamming Window

The Hanning window has several good features but one disadvantage is that the side lobes nearest to the main lobe are relatively large. If there are two components close to each other and one of them is less than -30 dB compared to the other, the smaller component may be buried under the side lobes of the larger component. Is there any possibility to further reduce the nearest side lobe?

If the spectra of the rectangular and Hanning windows are compared with this in mind, it is observed that the signs of the side lobes for $|fT| = 2$ and 3 are negative, whereas, those of the rectangular window are positive. Therefore, if the magnitudes of two windows are adjusted and combined so that those side lobes will cancel each other, the combined window will have lower side lobes.

The window shape and the spectrum of the Hamming window constructed from this concept are shown in Fig. 7.9. Since the rectangular window is added to the Hanning window, the side lobes in the region $4 \leq |fT|$ do not decrease much below 1/100 of the main lobe (−40 dB).

The window function $w_m(t)$, its spectrum $W_m(f)$, the window function in the discrete system $w_m(n)$ and the corresponding power reduction are shown below.

$$w_m(t) = w_r(t)\left\{R + (1-R)\cos\left(2\pi\frac{t}{T}\right)\right\} \tag{7.24}$$

$$W_m(f) = RT\frac{\sin\pi fT}{\pi fT} + \frac{1-R}{2}T\left\{\frac{\sin\pi(fT-1)}{\pi(fT-1)} + \frac{\sin\pi(fT+1)}{\pi(fT+1)}\right\} \tag{7.25}$$

$$w_m(n) = R - (1-R)\cos\left(\frac{2\pi n}{N}\right) = 2R - 1 + 2(1-R)\sin^2\left(\frac{\pi n}{N}\right) \quad (R = 0.5435, \quad 0 \leq n \leq N-1) \tag{7.26}$$

$$\text{power reduction} = -4.0\,\text{dB} \tag{7.27}$$

As shown in Fig. 7.9, the main lobe has almost the same width as that of the Hanning window, but the nearest side lobes are lower than −40 dB. However, a large portion of the side lobes stays above −50 dB. Therefore, the analysis of components down to −40 dB is possible but not below −50 dB. The Hamming window is often used in cases where the components below −40 dB can be neglected and when the separation of components is important. Since it is rare that analog equipment in speech transmission would have a dynamic range of more than 40 dB, this window is commonly used in the processing of speech.

The spreading of the spectrum becomes greatest when the number of periods of the waveform in the window is equal to an integer $n + 0.5$, and if not, it becomes smaller than expected from Fig. 7.9. Figure 7.10A shows the largest spectrum spreading with the number of the periods equal to 8.5 (amplitude of the wave is 1). Figure 7.10B demonstrates the case when three more components are added. The

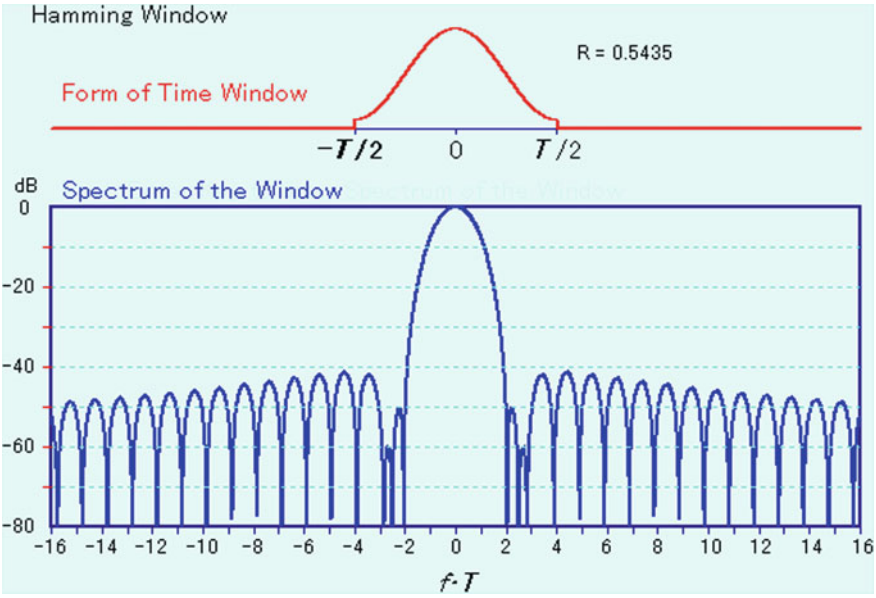

Fig. 7.9 Hamming window with length T and its spectrum. Animation available in supplementary files under filename E7-09_Hamm_Wind_Spec.exe

amplitudes and number of periods are 0.5, 0.1, and 0.01, and 4, 13.5 and 18.8, respectively. In this case even the fourth component with amplitude 1/100 (−40 dB) is detected. Below this level, it becomes difficult or impossible to detect using the Hamming window.

The programs attached to the figures enable the reader to check the spectrum changes of the sine waves extracted by different types of windows.

7.4.4 Blackman-Harris Window

For detection of even smaller components than the Hamming window can do, it may be possible by lowering the slope of the window on the time axis. At the same time, action must be taken to lower the side lobes near the main lobe. The "Blackman-Harris window" was invented with this intention; this window is shown in Fig. 7.11.

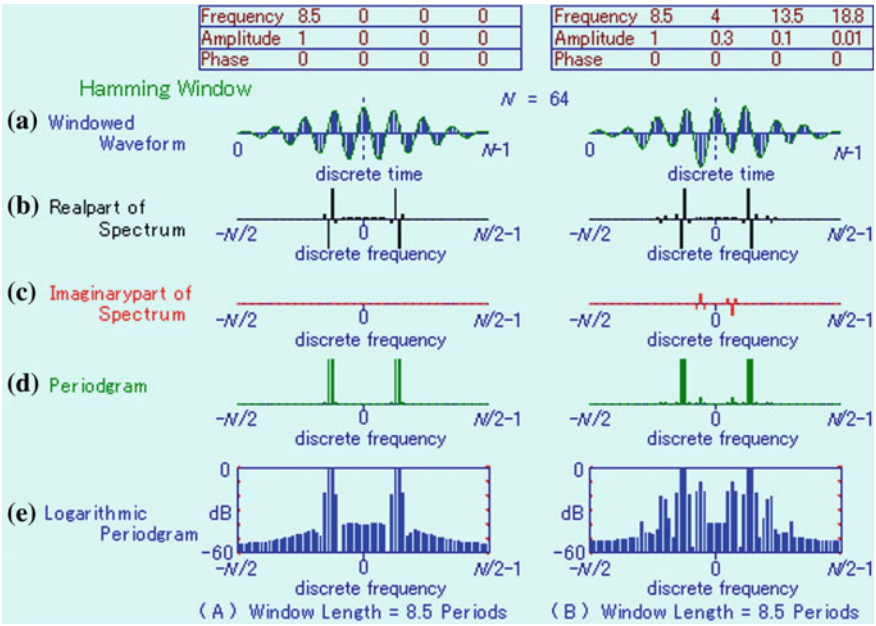

Fig. 7.10 Examples of frequency analysis by the Hamming window. Animation available in supplementary files under filename E7-10_Hamming.exe

The window function $w_B(t)$, its spectrum$W_B(f)$, the window function in the discrete system$w_B(n)$ and the power reduction are shown below.

$$w_B(t) = w_r(t)\left\{B_1 + B_2\cos\left(2\pi\frac{t}{T}\right) + B_3\cos\left(4\pi\frac{t}{T}\right)\right\} \tag{7.28}$$

$$\begin{aligned} W_B(f) = {} & B_1 T\frac{\sin\pi fT}{\pi fT} + \frac{B_2}{2}T\left\{\frac{\sin\pi(fT-1)}{\pi(fT-1)} + \frac{\sin\pi(fT+1)}{\pi(fT+1)}\right\} \\ & + \frac{B_3}{2}T\left\{\frac{\sin\pi(fT-2)}{\pi(fT-2)} + \frac{\sin\pi(fT+2)}{\pi(fT+2)}\right\} \end{aligned} \tag{7.29}$$

$$w_B(n) = B_1 - B_2\cos\left(\frac{2\pi n}{N}\right) + B_3\cos\left(\frac{4\pi n}{N}\right) \qquad (0 \le n \le N-1) \tag{7.30}$$

$$B_1 = 0.4232,\ B_2 = 0.4975,\ B_3 = 0.0792$$

$$\text{power reduction} = 5.14\,\text{dB} \tag{7.31}$$

Other windows, with different coefficients than those of the Blackman-Harris window, can further reduce the level of the side lobes. These may be preferable in some applications of frequency analysis. However, the difficulties described in the next paragraph must be considered.

The levels of the side lobes are much lower than those of the previously introduced windows, but the width of the main lobe is three times that of the

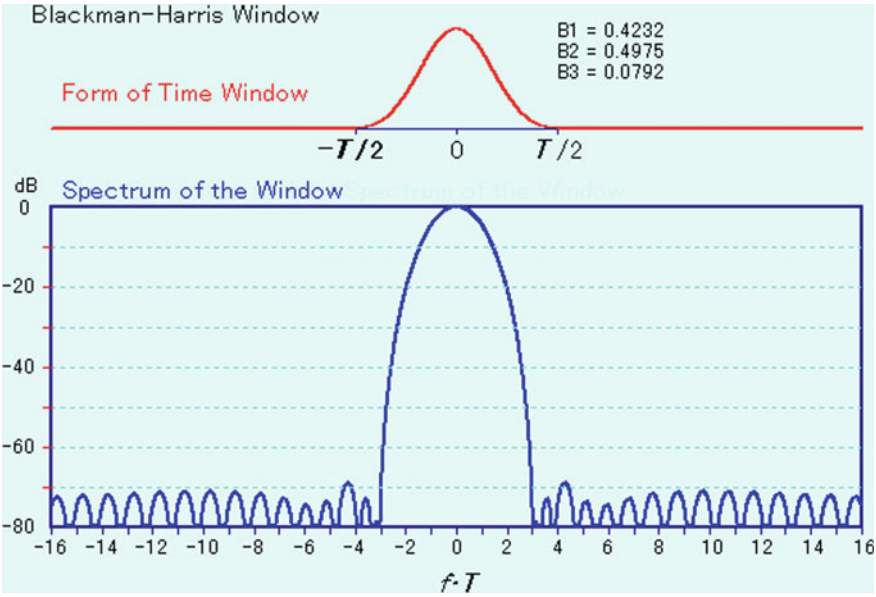

Fig. 7.11 Window shape and spectra of the Blackman-Harris window. Animation available in supplementary files under filename E7-11_BlkHarris_Wind_Spec.exe

rectangular window. It can be generally said that lowering the levels of the side lobes results in increased width of the main lobe. Widening the main lobe and reducing the levels of side lobes are caused by smoothing the rise and fall of the start and end of the window, and narrowing the center part that has a larger weight. The power reduction also becomes larger. Of course, this type of window may not be appropriate when fine frequency resolution is required.

7.4.5 Half-Sine Window and Riesz Window

Each of the previous three types of windows has a relatively narrow effective window length because the center part of the window is narrowed in order to smoothly connect to zero at both ends of the window. This means that a narrower portion of the window is observed even if the sampling is made for a longer duration.

The half-sine window is used with the opposite idea: to use the wider range of the window. The feature of this window is that the width of the main lobe is relatively narrow (approximately 3/4 of the Hanning window, or 1.5 of the rectangular window) and the levels of the side lobes are not so high. They quickly reduce as the distance from the main lobe increases (Fig. 7.12).

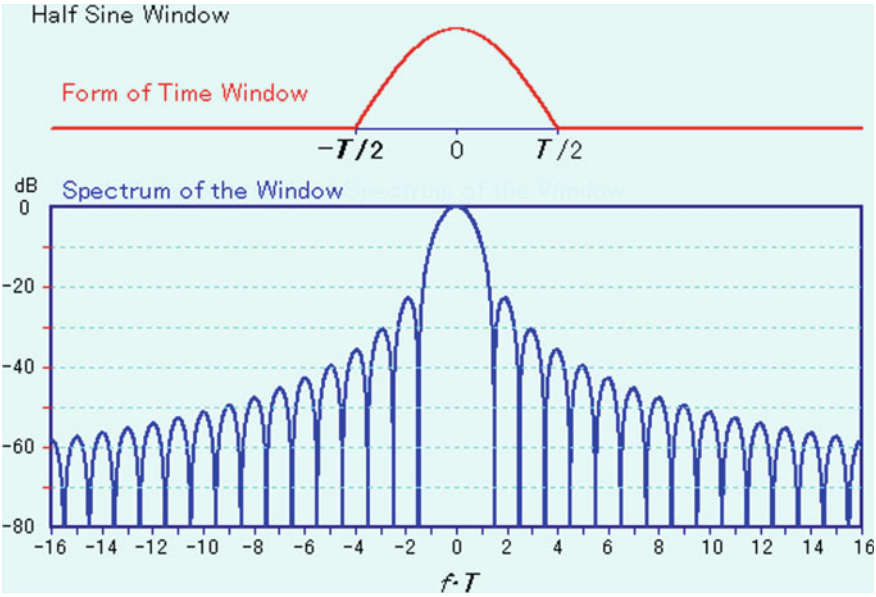

Fig. 7.12 Half-sine window function with length T and its spectrum. Animation available in supplementary files under filename E7-12_HalfSine_Wind_Spec.exe

The half-sine window function $w_s(t)$, its spectrum $W_s(f)$, the window function in the discrete system $w_s(n)$ and the power reduction are shown below.

$$w_S(t) = w_r(t)\cos\left(2\pi\frac{t}{T}\right) \tag{7.32}$$

$$W_S(f) = 0.5T\left\{\frac{\sin\pi(0.5-fT)}{\pi(0.5-fT)} + \frac{\sin\pi(0.5+fT)}{\pi(0.5+fT)}\right\} \tag{7.33}$$

$$w_S(n) = \cos\pi\left(\frac{n}{N}-\frac{1}{2}\right) = \sin\frac{\pi n}{N} \qquad (0 \le n \le N-1) \tag{7.34}$$

$$\text{power reduction} = 3\,\text{dB} \tag{7.35}$$

The spectrum of the half-sine window also has zeros at $1/T$ intervals. A major difference is that the frequencies of the zeros are at ± 1.5, ± 2.5, $\pm 3.5\ldots$ instead of the integer frequencies of the rectangular and Hanning windows. The spectrum of the half-sine window takes maxima at integer frequencies. For this reason, the spectrum of an integer frequency component is widely spread. If the frequency is given by $f = n + 0.5$ (n: integer), only two line spectra appear at $f = n \pm 0.5$ (four if the negative frequency components are counted). This result is the reverse of those achieved with the Hanning and Hamming windows.

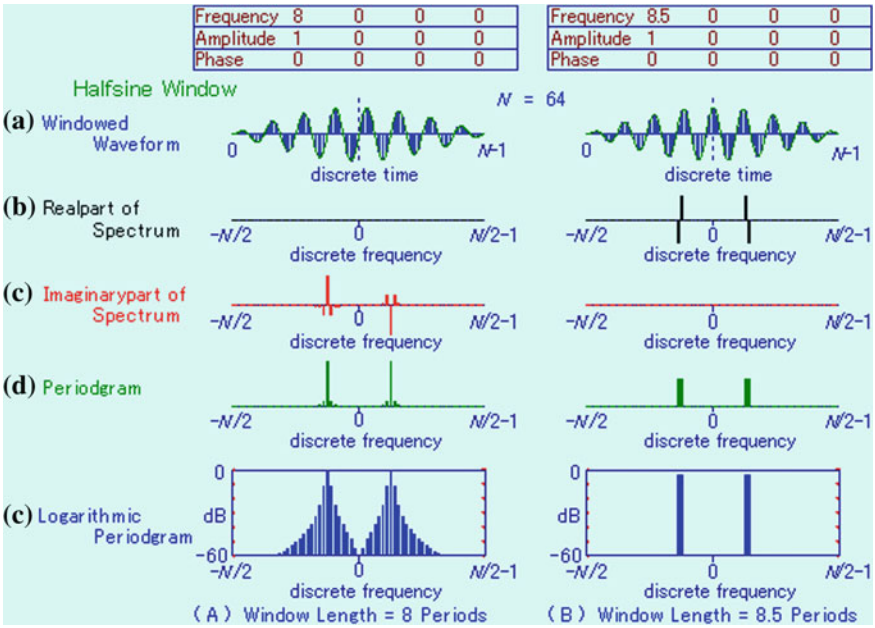

Fig. 7.13 Waveforms and their spectra extracted by the half-sine window. Animation available in supplementary files under filename E7-13_HalfSine.exe

Figure 7.13 shows the extracted waveforms and their spectra for the cases with 8 and 8.5 periods in the window. As Fig. 7.13A shows, if the frequency is 8, the spectrum is widely spread. On the other hand, if the frequency is given by $f = 8 + 0.5$ (n : integer) as shown in Fig. 7.13B, the center of the main lobe coincides with the discrete frequency, and there are two line spectra in each of the positive and negative frequency regions.

It is interesting to see that the outcomes (A) and (B) of Fig. 7.8 are reversed in Fig. 7.13. It is possible to envision this without looking at the spectrum of the window but by considering that a beat is produced when two components with the same amplitudes and with slightly different frequencies are superimposed. The one period of the beat is equal to the length of the time window T.

Most of the windows now in use are expressed by sine functions. But, almost the same window as the half-sine window is expressed without using the sine function, and is given by:

$$w_z(t) = w_r(t)\left\{1 - \left(\frac{2t}{T}\right)^2\right\} \tag{7.36}$$

This window, shown in Fig. 7.14, is called Riesz window. The shape of this function is similar to that of the half-sine window and, of course, their spectra are also similar even though the equations look different. A difference is that the

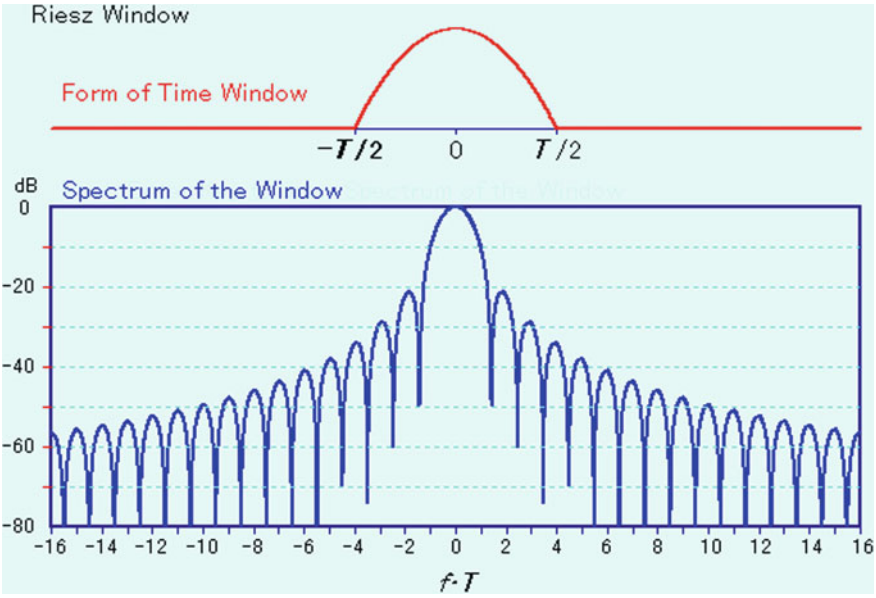

Fig. 7.14 Riesz window function with length T and its spectrum Animation available in supplementary files under filename E7-14_Riesz_Wind_Spec.exe

power reduction is approximately 0.27 dB less. Also since the frequencies of zero spectrum are not equal to $n + 0.5$ (n: integer), the spectrum for a waveform with $(n + 0.5)$ periods in the window exhibits more spreading than the two line spectra of the half-sine window (see Fig. 7.13).

The spectrum of the Riesz window defined by Eq. (7.36) in the continuous domain, its window function in the discrete domain, and power reduction are shown below.

$$W_z(f) = 2T\frac{\sin \pi fT - \pi fT \cos \pi fT}{\pi^3 f^3 T^3} \tag{7.37}$$

$$w_z(n) = 1 - \frac{2}{N}\left(n - \frac{N}{2}\right)^2 \tag{7.38}$$

$$\text{power reduction} = -2.73\,\text{dB} \tag{7.39}$$

7.4.6 Flat-Top Window

None of windows have a flat region at the top of the main lobe of the spectrum. Therefore, the magnitudes of components analyzed by these windows are

dependent on the number of periods included in the window length. One window, called the *flat-top window*, was invented with the idea to avoid this problem where the window shape is folded at both ends. To accomplish such a shape, the sinc function (the spectrum of rectangular wave) is multiplied by a Hamming or Hanning window.

The flat-top window is designed in the following manner:

(1) In order to produce a rectangular spectrum with height $1/f_b$, and width $\pm f_b/2$, its time window should be its inverse Fourier transform $\sin(\pi f_b t)/(\pi f_b t)$.
(2) Since $\sin(\pi f_b t)/(\pi f_b t)$ has unlimited time length, it will be limited within $\pm 2/f_b$.(the total window length is $4/f_b$). This window will be positive within the region $-1/f_b \le t \le 1/f_b$and negative in the region $-2/f_b \le t \le -1/f_b$ and $1/f_b \le t \le 2/f_b$.
(3) The Hamming window is then applied to gradually reduce the time window to zero at $t = \pm 2/f_b$in order to avoid the spreading of the spectrum.

The window function $w_F(t)$ and its spectrum $W_F(f)$in the continuous domain and the window function $w_F(n)$ in the discrete domain and the power reduction are given below.

$$w_F(t) = w_r(t)\left\{0.54 + 0.46\cos\left(2\pi\frac{t}{T}\right)\right\}\frac{\sin(4\pi t/T)}{4\pi t/T} \tag{7.40}$$

$$W_F(f) = W_m(f) * W_{2/T}(f) = \int_{-\infty}^{\infty} W_m(g)W_{2/T}(f-g)dg \tag{7.41}$$

where

$$\begin{aligned} W_{2/T}(f) &= \begin{cases} 1 & -2/T \le f \le 2/T \\ 0 & f < -2/T,\ 2/T < f \end{cases} \\ w_F(n) &= \left\{0.54 - 0.45\cos\left(\frac{2\pi n}{N}\right)\right\}\frac{\sin 2\pi(1-2n/N)}{2\pi(1-2n/N)} \end{aligned} \tag{7.42}$$

$$\text{power reduction} = -7.0\,\text{dB} \tag{7.43}$$

This window takes negative values at the 1/4 lengths close to the ends as seen in Fig. 7.15. The effective length is the shortest among the windows that have been introduced, i.e., the power reduction of this window is the largest. In order to completely separate two line spectra, the window length must be at least 5 times the inverse of the frequency difference. Even with this disadvantage, this window is useful when obtaining accurate magnitudes of line spectra.

The dependence of magnitude of a sine wave on the number of periods in the time window, using the rectangular, Hamming, and flat-top windows, is illustrated in Fig. 7.16. The number of periods is between 5 and 6. The left-hand graph shows the ratios of the magnitude obtained by the three windows, relative to the true

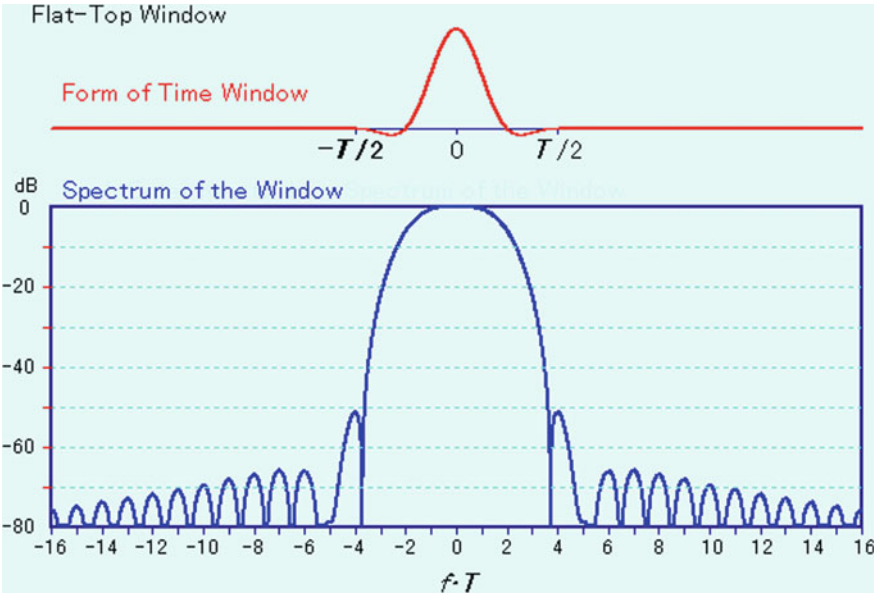

Fig. 7.15 Flat-top window with length T and its spectrum. Animation available in supplementary files under filename E7-15_Flat-Top_Wind_Spec.exe

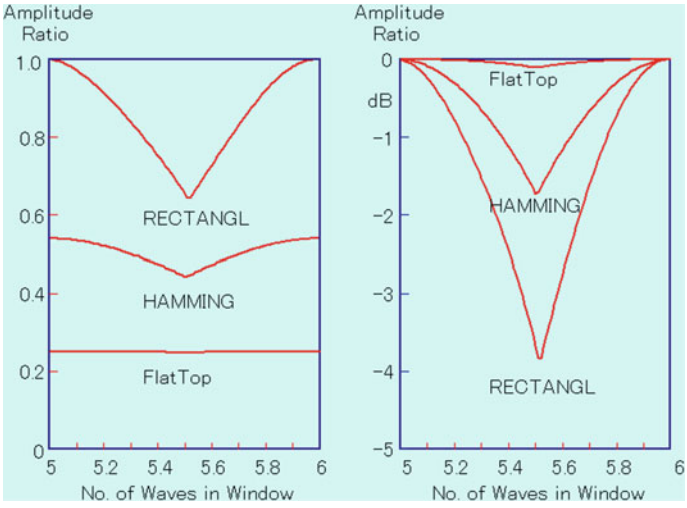

Fig. 7.16 Dependence of magnitudes of sine waves obtained by the FFT on the number of periods in the rectangular, Hamming, and flat-top windows. Animation available in supplementary files under filename E7-16_FTW.exe

magnitude, and the right-hand graph shows them in decibel scale (0 dB is the maximum magnitude obtained by each window). For all three windows, the results are almost constant even when the number of periods in the window is between 10 and 11.

The left-hand graph shows the variation of the estimated magnitude. The magnitude of the original waveform is four times the magnitude obtained using the flat-top window. The reduction of power is significant but the dependence on the number of periods in the window is very small. The maximum reductions for the rectangular, Hamming, and flat-top windows are −3.9, −1.4, and −0.1 dB, respectively.

7.4.7 Bartlett Window

A linearly tapered window that has no flat region was introduced in Chap. 6. This window is called the "Bartlett window" or "triangular window." From the results given in Fig. 6.15c this window is seen to have a better characteristic than expected from its simple shape. The spectrum of this window is shown in Fig. 7.1c, but since it is convenient to compare the Bartlett window with other windows, equations, and figures for this window will be shown next.

The Bartlett window function, which has the shape of an isosceles triangle, linearly increases from 0 to 1 in the region $-T/2 \le t \le 0$ and linearly decreases from 1 to 0 in the region $0 \le t \le T/2$. The window function $w_\Delta(t)$, its spectrum $W_\Delta(f)$in the continuous domain, window function $w_\Delta(n)$ in the discrete domain, and the power reduction are given as follows.

$$w_\Delta(t) = \begin{cases} 0 & |t| > T/2 \\ 1 + 2t/T & -T/2 \le t \le 0 \\ 1 - 2t/T & 0 \le t \le T/2 \end{cases} \tag{7.44}$$

$$W_\Delta(f) = \frac{T}{4} \frac{\sin^2(\pi f T/2)}{(\pi f T/2)^2} \tag{7.45}$$

$$w_\Delta(n) = \begin{cases} 2n/N & 0 \le n < N/2 \\ 2(1 - n/N) & N/2 \le n < N \end{cases} \tag{7.46}$$

$$\text{power reduction} = -4.77\,\text{dB} \tag{7.47}$$

The shape of this window and its spectrum are shown in Fig. 7.17. One apparent difference is that the width of the side lobes is twice the width of the side lobes of the other windows. The width of the main lobe is about the same with those of the half-sine and Hanning windows. Compared with the half-sine window, the first side lobe is slightly smaller but the reduction of the levels of the side lobes is significantly slower. This window is used in frequency analysis on very few

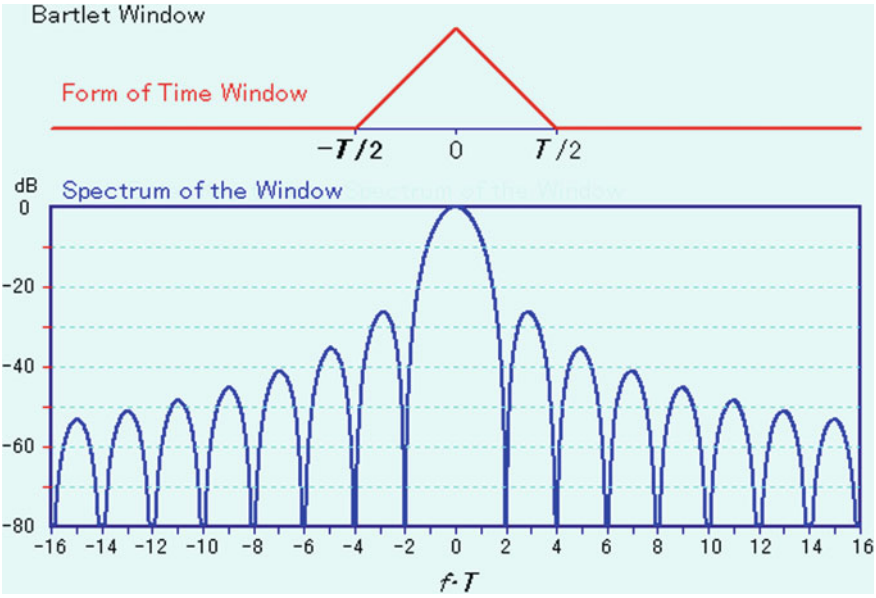

Fig. 7.17 Bartlett window with length T and its spectrum. Animation available in supplementary files under filename E7-17_Bartlett_Wind_Spec.exe

occasions, but its weighting is automatically introduced when an auto-correlation function of a finite sequence is calculated.

7.4.8 Gaussian Window

The Gaussian function (normal probability density function) has a special feature that its Fourier transform is also a Gaussian function. This property is explained in Appendix 7B. In this section this function is introduced as a window function.

The normal probability density function is given by:

$$p(t) = \frac{1}{\sqrt{2\pi}\sigma} \exp\left(-\frac{t^2}{2\sigma^2}\right) \tag{7.48}$$

where σ is the standard deviation. Its Fourier transform is given by:

$$P(j\omega) = \exp\left(-\frac{\sigma^2}{2}\omega^2\right) \tag{7.49}$$

If this function is used as a time window, the functions in the time and the frequency domains have the same forms and they have a convenient duality. However, the Fourier transform pair shown above is valid only in the infinite time

Fig. 7.18 Dependence of the power reduction on the parameter m of the Gaussian window and relation to power reductions of other windows

and frequency domains. Since the time window for the DFT must be finite, Eq. (7.48) must be modified in order to be used as a window.

The Gaussian window function is determined by letting $T/2$ (T : window length) be equal to integer m times σ. Then, the window function and the spectrum are given as follows.

$$w_G(t) = w_r(t)\frac{2m}{\sqrt{2\pi}T}\exp\left(-\frac{2m^2}{T^2}t^2\right) \tag{7.50}$$

$$W_G(2\pi f) = \exp\left(-\frac{\pi^2 T^2}{2m^2}f^2\right) \tag{7.51}$$

$$w_G(n) = \exp\left\{-\frac{2m^2}{N^2}\left(n-\frac{N}{2}\right)^2\right\} \quad (0 \le n \le N-1) \tag{7.52}$$

The power reduction of the Gaussian window is a function of m, as shown by Fig. 7.18. The range of the horizontal axis, m (= T/σ), is from 1 to 3 and the vertical axis is the power reduction in dB.

The minimum and maximum power reductions of the previously introduced windows are 2.7 dB (Riesz window) and 7 dB (flat-top window), respectively. These are within the range of m from 1 to 3. The power reductions of the other windows are shown in the graph for comparison. For example, the power reduction of the Hanning window corresponds to $m = 1.95$ for the Gaussian window.

The spectrum of the Gaussian window is of course affected by m. The window function and its spectrum shown in Fig. 7.19 is for $m = 1.95$. This spectrum has a narrower main lobe than that of the Hanning window, which is a good feature for

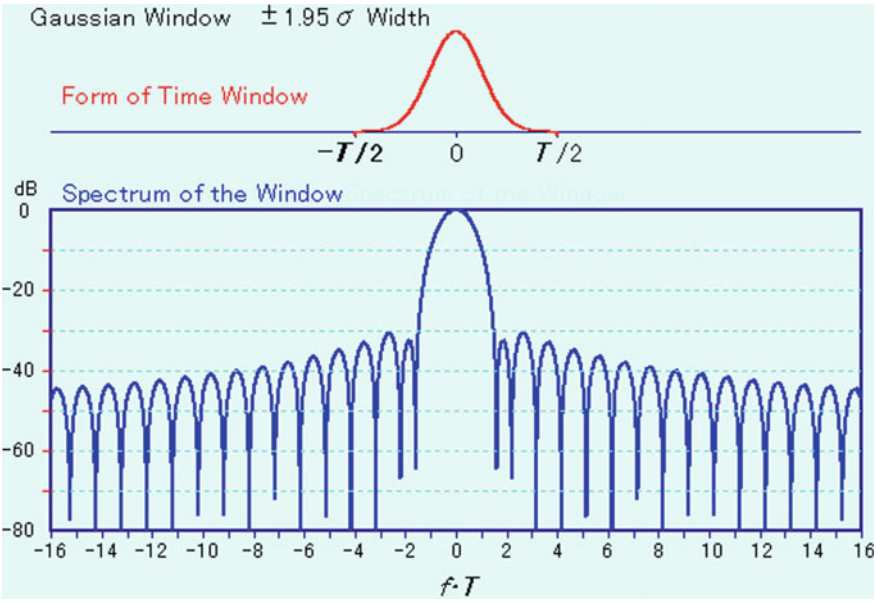

Fig. 7.19 Gaussian window with length T and its spectrum. Animation available in supplementary files under filename E7-19_Gaussian_Wind_Spec.exe

frequency analysis. By running the program attached to this figure, one can check for other values of m.

It can be seen that the spectrum is also Gaussian by overlapping the linear spectrum on the window function. The window shape and the spectrum shape nicely overlap with each other, especially if $m = 2.5$ is chosen.

7.5 Comparison of Windows by the Results of Frequency Analysis

Properties of various windows have been described in the previous sections. Each window has advantages and disadvantages. It may not be easy to choose one of them among so many windows. As one guide for the selection of windows, the results of frequency analysis of a synthesized waveform with many sine components will be shown.

To simulate a noisy signal with many line spectra, a signal with 30 sine components of various magnitudes are synthesized and analyzed using the rectangular, Hanning, Hamming, Blackman-Harris, half-sine, Riesz, flat-top, and Bartlett windows. Results of the analysis are shown in Fig. 7.20. The dots in the figure identify computed frequencies and magnitudes of the 30 components. The

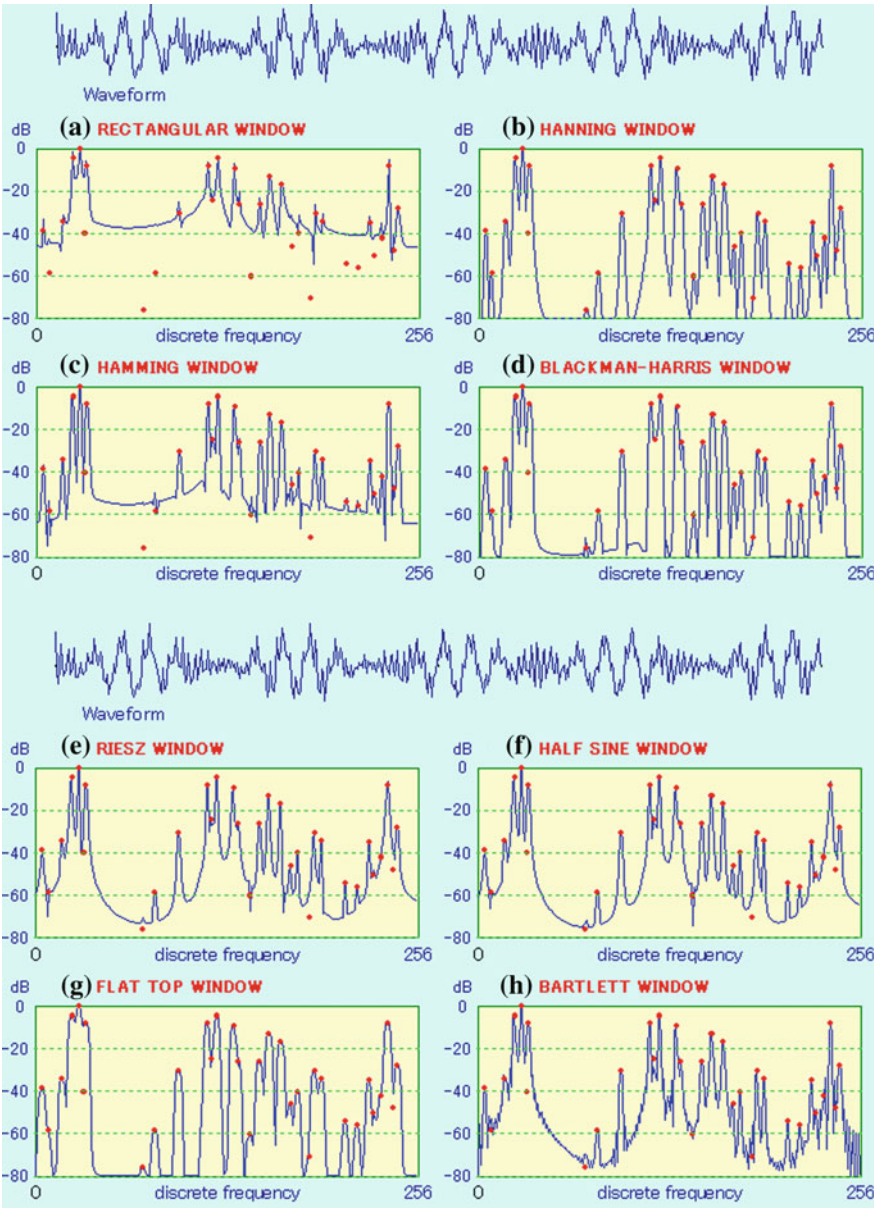

Fig. 7.20 Comparison of results of frequency analysis of a multi-component waveform by the use of eight windows. The dots show the frequencies and magnitudes of all components. Animation available in supplementary files under filename E7-20_AnaCompo.exe

purpose of the frequency analysis is to determine exact positions (frequencies and magnitudes) of these dots in each chart.

Figure 7.20a shows that if the FFT is directly applied to the sample sequence, that is if the rectangular window is used, the chance of missing components more than 20 dB (1/10) lower than the maximum component is very large.

In general, there are few occasions when a component which is smaller than 1/100 (−40 dB) of the maximum component must be detected. All windows except for the rectangular (a) and the flat-top (g) windows pass this criterion. If low levels in the regions without frequency components and detections of small components adjacent to large components are important, the Hamming window (c) should be a good choice. Compared with the Hanning window (b), the former seems to perform slightly better than the latter if levels above −40 dB are considered.

If the lowest level for the detection of components is lowered to −50 dB, the Hamming window (c) starts to have difficulty. If further lowered to −60 dB, the Hanning window (b) does better. In this case, the Blackman-Harris window (d) may be a better choice. As Fig. 7.11 shows, the Blackman-Harris window has very low side lobes (below −70 dB). But it is difficult to find an advantage of the Blackman-Harris window (d) over the Hanning window (b) when the two charts are compared.

Furthermore, in practical applications, due to linearity and noise problems, it is very difficult to detect components lower than −60 dB from the maximum level. In such a case, a different approach should be taken.

From the above discussions, it is considered that the Hanning window is a good choice for most practical applications. However, since the Hanning window sometimes gives incorrect results in frequency response function estimation, the Hanning window is not always the better choice.

7.6 Exercise

1. Derive Eq. (7.8) in the text.
2. Explain why a window such as the Hanning window should be used in DFT analysis even when zero data are added to a short waveform.
3. In the analysis of a short waveform, there should be at least three periods of a wave in the time window. Explain why.
4. If there is an integer number of periods of a wave in the window, there is one line spectrum each in the positive and negative frequency regions, but if there are non-integer periods of the wave, the spectrum has a spreading. Explain why.
5. If there is an integer number of periods of a wave in the Hanning or Hamming windows, there are three line spectra each in the positive and negative frequency regions. Explain why.
6. If there is an integer number of periods of a wave in the Blackman-Harris window, how many line spectra are in the positive and negative frequency regions?

Appendix

Appendix 2A Fourier Transform of the Step Function

The unit step function equals one-half of the summation of the dc component with magnitude 1 and the sign function.

$$u(t) = \frac{1}{2}[1 + \mathrm{sgn}(t)] \tag{2A.1}$$

The Fourier transform of the sign function is given as the extreme case of the integral of the exponential functions $\exp(\sigma t)\ \ (t<0)$ and $\exp(-\sigma t)\ \ (t>0)$ with $\sigma \to 0$

$$\begin{aligned}
&\int_{-\infty}^{+\infty} \mathrm{sgn}(t)\exp(-j2\pi ft)dt \\
&\quad = \int_{-\infty}^{0} \exp(\sigma t)\exp(-j2\pi ft)dt + \int_{0}^{+\infty} \exp(-\sigma t)\exp(-j2\pi ft)dt \\
&\quad = \frac{1}{(\sigma - j2\pi f)}\exp\{(\sigma - j2\pi f)t\}\Big|_{-\infty}^{0} + \frac{1}{(-\sigma - j2\pi f)}\exp\{(-\sigma - j2\pi f)t\}\Big|_{0}^{+\infty} \\
&\quad = \frac{1}{(\sigma - j2\pi f)} - \frac{1}{(\sigma + j2\pi f)} = \frac{\sigma - j2\pi f - \sigma - j2\pi f}{\{\sigma^2 + (2\pi f)^2\}} = \frac{-j4\pi f}{\sigma^2 + (2\pi f)^2}.
\end{aligned} \tag{2A.2}$$

By letting $\sigma \to 0$, Eq. (2A.2) becomes

$$\int_{-\infty}^{+\infty} \mathrm{sgn}(t)\exp(-j2\pi ft)dt = \frac{1}{j\pi f}. \tag{2A.3}$$

The Fourier transform of 1 is give by the delta function,

$$\int_{-\infty}^{+\infty} 1 \cdot \exp(-j2\pi ft)dt = \delta(f). \tag{2A.4}$$

Therefore, the Fourier transform of the unit step function Eq. (2A.1) is given by

$$U(f) = \frac{1}{2}\delta(f) + \frac{1}{j2\pi f}. \tag{2A.5}$$

K. Kido, *Digital Fourier Analysis: Fundamentals*,
Undergraduate Lecture Notes in Physics, DOI: 10.1007/978-1-4614-9260-3,

Appendix 2B Fourier Transforms of Sine Functions

The Fourier transform of the sine function $\sin(2\pi f_0 t)$, which is periodic from $-\infty$ to $+\infty$, is considered nonexistent. However, it can be calculated by a similar approach as in 2A. A Fourier transform of a sine function with a finite duration from $t = -T/2$ to t $= T/2$ is calculated first and then T is made infinite.

$$\begin{aligned} F\{\sin(2\pi f_0 t)\} &= \int_{-T/2}^{T/2} \sin(2\pi f_0 t)\exp(-j2\pi f t)dt \\ &= \frac{1}{j2}\int_{-T/2}^{T/2} \{\exp(j2\pi f_0 t) - \exp(-j2\pi f_0 t)\}\exp(-j2\pi f t)dt \\ &= \frac{1}{j2}\int_{-T/2}^{T/2} \exp\{j2\pi(f_0 - f)t\}dt - \frac{1}{j2}\int_{-T/2}^{T/2} \exp\{-j2\pi(f_0 + f)t\}dt \\ &= \frac{1}{j2}\frac{\exp\{j2\pi(f_0 - f)t\}|_{-T/2}^{T/2}}{j2\pi(f_0 - f)} - \frac{1}{j2}\frac{\exp\{-j2\pi(f_0 + f)t\}|_{-T/2}^{T/2}}{-j2\pi(f_0 + f)} \\ &= \frac{\sin\{2\pi(f_0 - f)T/2\}}{j2\pi(f_0 - f)} - \frac{\sin\{2\pi(f_0 + f)T/2\}}{j2\pi(f_0 + f)} \\ &= j\frac{T}{2}\left[\frac{\sin\{2\pi(f_0 + f)T/2\}}{2\pi(f_0 + f)T/2} - \frac{\sin\{2\pi(f_0 - f)T/2\}}{2\pi(f_0 - f)T/2}\right]. \end{aligned} \tag{2B.1}$$

This spectrum is concentrated at two locations around $f = +f_0$ and $-f_0$ and equal to 0 at $f = f_0 \pm n/T$ and $-f_0 \pm n/T$. The amplitudes gradually reduce to zero as the frequency moves away from $+f_0$ or $-f_0$. The peak value is approximately equal to $jT/2$ at $f = -f_0$ and $-jT/2$ at $f = +f_0$. The reason why "approximately" is used is that the term which has a maximum at $f = -f_0$ (the first term in Eq. 2B.1) does not necessarily equal to zero at $f = f_0$. This is true also for the second term. If the number of the periods in T is an integer, the values are exactly equal to $jT/2$ at $f = -f_0$ and $-jT/2$ at $f = +f_0$.

These results are for the case with finite duration. If T is made infinite, the spectrum exists only at $f = \pm f_0$ and the magnitude $T/2$ becomes infinite. It can be understood that the energy of the wave becomes infinite as $T \to \infty$, but the width of the peak $2/T$ becomes infinitely small, and thus the product of the height and the width does not change and is equal to 1.

Then, we can derive the Fourier transforms of the infinitely long sine and cosine waves as follows (Fig. 2B).

$$F\{\sin(2\pi f_0 t)\} = j\frac{1}{2}[\delta(f + f_0) - \delta(f - f_0)]. \tag{2B.2}$$

$$F\{\cos(2\pi f_0 t)\} = \frac{1}{2}[\delta(f + f_0) + \delta(f - f_0)]. \tag{2B.3}$$

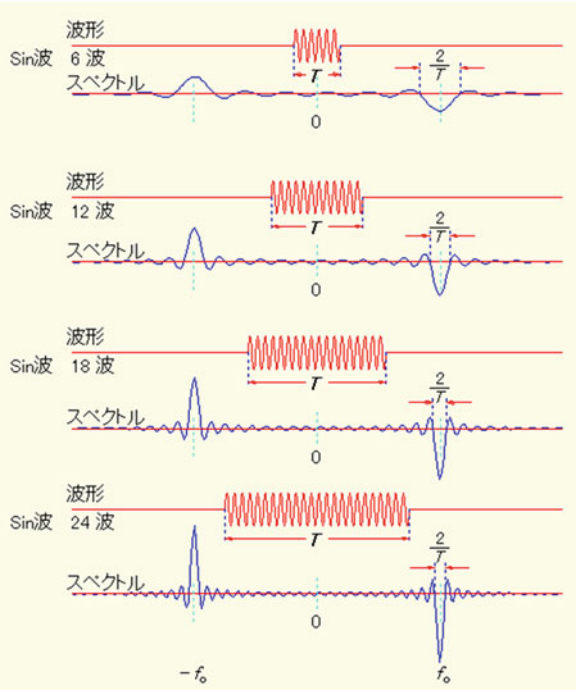

Fig. 2B Relation between the length of the sine function and its spectrum

Appendix 2C Fourier and Inverse Fourier Transforms

The Fourier and inverse Fourier transforms are defined by Eqs. (2.37) and (2.38), respectively, that are almost identical with each other. Let us calculate the Fourier (not "inverse") transform $x'(t)$ of the function $X(f)$ which is given by

$$x'(t) = \int_{-\infty}^{+\infty} X(f) \exp(-j2\pi tf) df \tag{2C.1}$$

where the minus sign in the exponential function is used. By replacing t by $-t'$, it is rewritten as

$$\begin{aligned} x'(-t') &= \int_{-\infty}^{+\infty} X(f) \exp(j2\pi t'f) df \\ &= x(t'). \end{aligned} \tag{2C.2}$$

Since $x(t')$ is the same with $x(t)$, then

$$\begin{aligned} x'(-t') &= x(t) \\ &\text{or} \\ x'(t) &= x(-t) \end{aligned} \tag{2C.3}$$

is obtained.

Eq. (2C.3) shows that, if the Fourier transform of $x(t)$ is known as $X(f)$ the Fourier transform of $X(f)$ is $x(-t)$.

Appendix 3A Calculation of Fourier Transform of a Spectrum

The spectrum $X(f)$ of a function $x(t)$ that is zero outside of the region $-T/2 \leq t \leq T/2$ is give by

$$X(f) = \int_{-T/2}^{+T/2} x(t) \exp(-j2\pi ft) dt. \tag{3A.1}$$

Let us obtain the Fourier transform of $X(f)$ for the case when it is zero outside of the region $-F_x \leq t \leq F_x$.

$$\tilde{x}(t) = \int_{-F_m}^{+F_m} X(f) \exp(-j2\pi ft) df. \tag{3A.2}$$

Replacing $X(f)$ in Eq. (3A.2) by Eq. (3A.2), we have

$$\begin{aligned} \tilde{x}(t) &= \int_{-F_m}^{+F_m} \int_{-T/2}^{+T/2} x(\tau) \exp(-j2\pi f\tau) d\tau \exp(-j2\pi ft) df \\ &= \int_{-T/2}^{+T/2} x(\tau) [\int_{-F_m}^{+F_m} \exp\{-j2\pi f(\tau + t)\} df] d\tau \end{aligned}$$

where the order of integrals has been changed in the last equation. Since the integral with respect to f in the last equation is equal to $2F_x$ if $\tau + t = 0$ and equal to zero otherwise, the last equation can be rewritten as

$$\tilde{x}(t) = 2F_x \int_{-T/2}^{+T/2} x(-t) d\tau = 2F_x T \cdot x(-t) \tag{3A.3}$$

The inverse Fourier transform gives a time reversed signal instead of the original signal. If $\exp(j2\pi ft)$ is used in Eq. (3A.2), this time reversal can be avoided. As far as the Fourier transform pair is defined by Eqs. (2.36) and (2.37), $\exp(-j2\pi ft)$ and $\exp(j2\pi ft)$ must be used in the forward and inverse Fourier transforms, respectively.

Appendix 4A Parseval's Formula

The conservation of energy between the time domain signal and the frequency domain spectrum is kept as shown by the Parseval's formula (see Eq. 2.43). This is also valid in the DFT. The energies in the time domain and the frequency domain

are calculated using the definition equations of DFT given by Eqs. (4.7) and (4.8). The energy in the time domain is given by Eq. (4.7):

$$\sum_{n=0}^{N-1}|x_n|^2=\sum_{n=0}^{N-1}x_n x_n^*=\sum_{n=0}^{N-1}x_n\frac{1}{N}\sum_{k=0}^{N-1}X_k^*\exp(-j2\pi kn).$$

By changing the order of the multiplication and summations, the above equation becomes

$$\sum_{n=0}^{N-1}|x_n|^2=\frac{1}{N}\sum_{k=0}^{N-1}X_k^*\sum_{n=0}^{N-1}x_n\exp(-j2\pi kn)=\frac{1}{N}\sum_{k=0}^{N-1}X_k^*X_k=\frac{1}{N}\sum_{k=0}^{N-1}|X_k|^2.$$

Therefore,

$$\sum_{n=0}^{N-1}|x_n|^2=\frac{1}{N}\sum_{k=0}^{N-1}|X_k|^2. \qquad (4A.1))$$

This is not equivalent to the Parseval's formula given by Eq (2.43). There is the term $1/N$ in the right side of Eq. (2.43). This indicates that the energy in the frequency domain is N times of the energy in the time domain. Obviously, this is not correct. This was introduced because we used the transform pair Eqs. (4.7) and (4.8) which does not have the symmetry. If the transform pair Eqs. (4.9) and (4.10) is used, this problem is removed. The derivation is left as your exercise (Problem 4.12).

Appendix 4B Increasing the Sampling Frequency of DFT by Integer Multiples

In the N-point DFT, the first and the last $N/2$ point data in the frequency domain are for the positive and negative frequencies. If another N -point zero data are added in the middle, and if $2N$-point IDFT is conducted, a time sequence with twice of the original sampling frequency is obtained as can be seen in Fig. 4B. Figure 4Ba is the original time sequence. Figure 4Bb shows the N-point data in the frequency domain. Figure 4Bc shows spectrum data with after the addition of zero data. The original data in the two regions in $0 \le k \le N/2$ and in $N/2 \le k < N$ are moved to the two regions $0 \le k' \le N/2$, and $3N/2 \le k' < 2N$, respectively, where k' is the frequency in the $2N$-point DFT. The remaining region from $N/4$ to $3N/4$ are filled with zero data. The IDFT of Fig. 4Bc gives the $2N$-point time domain sample sequence, Fig. 4Bd.

The procedure explained above is the case when the sampling frequency is doubled. You can think of other cases to increase the sampling frequency by adding even number of zeros in the middle.

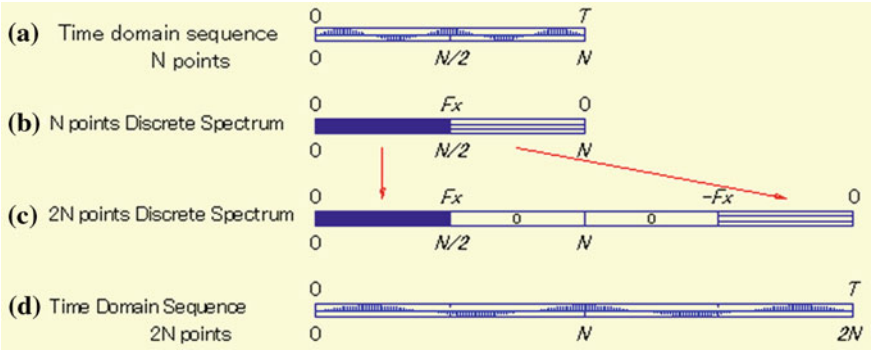

Fig. 4B Procedure to obtain a 2*N*-point time sequence from the *N*-point time sequence by doubling the sampling frequency

Appendix 6A Decibel

The symbol "dB" is an abbreviation for "decibel" or "deci-Bell," which is used as a unit of representing a ratio of two powers (or energies). The decibel Y of a power ratio E/E_0 is calculated by:

$$Y = 10\log_{10}(E/E_0). \tag{6A.1}$$

Since the power is proportional to squares of magnitudes of physical quantities such as voltage, current, force, velocity, sound power, etc., Eq. (6A.1) is rewritten as

$$Y = 10\log\left(x^2/x_0^2\right) = 20\log(x/x_0) \tag{6A.2}$$

where x and x_0 represent arbitrary and reference magnitudes of voltage, current, force, velocity, sound power, etc., respectively.

If a voltage is 10 times of a reference voltage, the ratio in dB is 20. If the power ratio is 10, then it is 10 in dB. The relation of the power ratio and dB is shown in Fig. 6A.

"Bell" is after Abraham Bell, which is defined by $Y\ (\text{in Bell}) = \log_{10}(E/E_0)$. If the voltage ratio is 2, it is 0.6 Bell and if the ratio is 10, it is 2 Bell. Since these values are too small, "deci-bell" is used to enlarge the scale by 10.

Appendix 7A Fourier Transform of a Product of Two Functions

Let us obtain the formula for a Fourier transform $Y(f)$ of a product of two functions, $x(t)$ and $w(t)$.

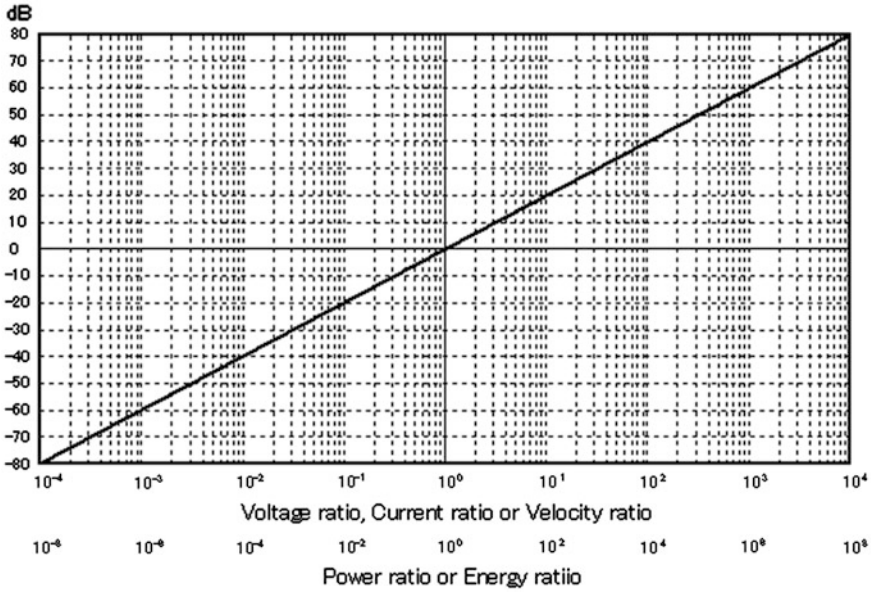

Fig. 6A Relation between power ratios and decibels. Since the power and energies are proportional to voltage, current, force, velocity, sound pressure, etc., the horizontal axis is shown with two scales

$$Y(f) = \int_{-\infty}^{+\infty} x(t)w(t)\exp(-j2\pi ft)dt. \tag{7A.1}$$

By substituting $x(t)$ by Eq. (7.2) (f is replaced by ϕ), we have

$$\begin{aligned} Y(f) &= \int_{-\infty}^{+\infty}\int_{-\infty}^{+\infty} X(\phi)\exp(j2\pi\phi t)d\phi \cdot w(t)\exp(-j2\pi ft)dt \\ &= \int_{-\infty}^{+\infty} X(\phi)\int_{-\infty}^{+\infty} w(t)\exp\{-j2\pi(f-\phi)t\}dt{\cdot}d\phi \\ &= \int_{-\infty}^{+\infty} X(\phi)W(f-\phi)d\phi. \end{aligned} \tag{7A.2}$$

By substituting $w(t)$ by Eq. (7.4) (f is replaced by φ), we have

$$\begin{aligned} Y(f) &= \int_{-\infty}^{+\infty}\int_{-\infty}^{+\infty} W(\phi)\exp(j2\pi\phi t)d\phi \cdot x(t)\exp(-j2\pi ft)dt \\ &= \int_{-\infty}^{+\infty} W(\phi)\int_{-\infty}^{+\infty} x(t)\exp\{-j2\pi(f-\phi)t\}dt \cdot d\phi \\ &= \int_{-\infty}^{+\infty} W(\phi)X(f-\phi)d\phi. \end{aligned} \tag{7A.3}$$

Equations (7A.2) and (7A.3) show that the Fourier transform of a product of two functions is given by the convolution of the two functions in the frequency domain (explained in Chap. 1 in Volume II of this book).

Appendix 7B Fourier Transform of the Normal (Gaussian) Probability Density Function

The normal (Gaussian) probability density function is given by Eq. (4.48), which is shown here again.

$$p(t) = \frac{1}{\sqrt{2\pi}\sigma}\exp\left(-\frac{t^2}{2\sigma^2}\right) \tag{7B.1}$$

where σ is the standard deviation. It is known that the integral of this equation with respect to t from $-\infty$ to $+\infty$ is equal to 1.

$$\int_{-\infty}^{+\infty} p(t)dt = \frac{1}{\sqrt{\pi}}\Gamma\left(\frac{1}{2}\right) = 1 \tag{7B.2}$$

where $\Gamma(x)$ is the Gamma function. The Fourier transform of this equation is calculated as follows:

$$\begin{aligned} P(j\omega) &= \frac{1}{\sqrt{2\pi}\sigma}\int_{-\infty}^{+\infty}\exp\left(-\frac{t^2}{2\sigma^2}\right)\exp(-j\omega t)dt \\ &= \frac{1}{\sqrt{2\pi}\sigma}\exp\left(-\frac{\sigma^2\omega^2}{2}\right)\int_{-\infty}^{+\infty}\exp\left\{-\left(\frac{t}{\sqrt{2}\sigma}+j\frac{\sigma\omega}{\sqrt{2}}\right)^2\right\}dt. \end{aligned} \tag{7B.3}$$

By replacing t by $z = t + j\sigma^2\omega$ (complex variable), the integral with respect to t from $-\infty$ to $+\infty$ becomes a line integral on the z-plane from $-\infty + j\sigma^2\omega$ to $+\infty + j\sigma^2\omega$, a straight line parallel to the real axis. However, the integrand $\exp\{-(1/2\sigma^2)z^2\}$ is regular between the real axis and the line of integral, the integral does not change even if the line of integral is shifted to the real axis. Therefore, Eq. (7B.3) becomes

$$P(j\omega) = \frac{1}{\sqrt{2\pi}\sigma}\exp\left(-\frac{\sigma^2\omega^2}{2}\right)\int_{-\infty}^{+\infty}\exp\left(-\frac{z^2}{2\sigma^2}\right)dz. \tag{7B.4}$$

Since the integrand is an even function of z, the range of integration can be changed from 0 to ∞. Furthermore, replacing z by ξ ($\xi = z^2$, $dz = d\xi/2z = d\xi/2\sqrt{\xi}$), the integral becomes

$$2\int_0^{\infty}\exp\left(-\frac{z^2}{2\sigma^2}\right)dz = \int_0^{\infty}\frac{1}{\sqrt{\xi}}\exp\left(-\frac{\xi}{2\sigma^2}\right)d\xi. \tag{7B.5}$$

This has the same form as the Laplace transform of $1/\sqrt{t}$, which is shown below.

$$\int_0^\infty \frac{1}{\sqrt{\xi}} \exp\left(-\frac{\xi}{2\sigma^2}\right) d\xi = \sqrt{2\pi}\sigma. \tag{7B.6}$$

Then, Eq. (7.49) is obtained.

$$P(j\omega) = \exp\left(-\frac{o^2}{2}\omega^2\right) \quad (7.49). \tag{7B.7}$$

References

1. J. Makhoul, A fast cosine transform in one and two dimensions. IEEE Trans. Acoust. Speech Sig. Proc. **28**(1), 27–34 (1980) (Chap. 4.5)
2. J.W. Cooley, J.W. Tukey, An algorithm for the machine calculation of complex fourier series. Math. Comput. **19**, 297–301 (1965). (Chap. 5.0)
3. J.W. Cooley, P.A.W. Lewis, P.D. Welch, Historical notes on the fast fourier transform. IEEE Trans. Audio and Electroacoust. **AU-15**(2), 76–79 (1967) (Chaps. 5.0, 5.1)
4. Y. Suzuki, T. Sone, K. Kido, A new FFT algorithm of radix 3, 6, and 12. IEEE Trans. ASSP **ASSP-34**(2), 380–383 (1986) (Chap. 5.3)
5. G. Zelniker, F.J. Taylor, in *Advanced Digital Signal processing*. (Markel Dekker Inc, New York, 1994), pp.592–597 (Chap. 6.1)

Following are References for General Reading

6. A.V. Oppenheim, R.W. Shafer, in *Digital Signal Processing*. (Prentice-Hall Inc, Upper Saddle River, 1975)
7. Papoulis, in *Signal Analysis*. (McGraw-Hill Book Co, New York, 1977)
8. J.O. Smith, in *Mathematics of the Discrete Fourier Transform* (*DFT*), 2nd edn. (BookSurge Publishing, online book, 2008)

K. Kido, *Digital Fourier Analysis: Fundamentals*,
Undergraduate Lecture Notes in Physics, DOI: 10.1007/978-1-4614-9260-3,

Answers

Chapter 1

1. Cosine wave with the same frequency.
2. Negative (sign-reversed) cosine wave with the same frequency.
3. Negative (sign-reversed) sine wave with the same frequency.
4. Sine wave with the same frequency.
5. Sine wave with amplitude $\sqrt{2}$, the same frequency, and a phase leading by $\pi/4$ (45°).
6. Add a cosine wave with the same frequency and with amplitude $1/\sqrt{3}$.
7. Symmetric waveform with respect the origin t = 0.
8. Anti-symmetric waveform with respect the origin t = 0.
9. See Fig. 1.17.
10. Delayed in time without changing the waveform.
11. (b), (c), (g), (i)
12. (a), (d), (e), (j), (k), (m), (n)
13. (f), (h), (l), (o), (p)
14. If only the sine terms are used, the obtained waveform is 1/2 of the waveform (i). If only the cosine terms are used, the obtained waveform is symmetric waveform. whose left half is 1/2 of the original waveform.
15. Relpace (i) with (c) in Answer (14).

Chapter 2

1. See 2.1.
2. Multiply $\sin(2\pi kt/T)$ instead of $\cos(2\pi kt/T)$ which is multiplied to each term of Eq. (2.1) to obtain Eq. (2.3).
3. For $t > 0$, $x_e(t) = x_o(t) = x(t)/2$.
   For $t < 0$, $x_e(-t) = x_e(t) = x(t)/2$ and $x_o(-t) = -x_o(t) = -x(t)/2$.
   At $t = 0$, it should be considered that

$$x_e(0) + x_o(0) = [x_e(t)_{t\to -0} + x_e(t)_{t\to 0} + x_o(t)_{t\to -0} + x_o(t)_{t\to 0}]/2 = x(0)/2$$

4. The spectrum of $x_e(t)$ is an even function (purely real). The spectrum of $x_o(t)$ is an odd function (purely imaginary).

K. Kido, *Digital Fourier Analysis: Fundamentals*,
Undergraduate Lecture Notes in Physics, DOI: 10.1007/978-1-4614-9260-3,

5. k/T (k : 0, ±1, ±2, …)
6. See Sect. 1.7 (it is assumed that the exponent is purely imaginary).
7. The real part is an even function and the imaginary part is an odd function.
8. $\exp(j2\pi ft + j\pi/4)$ or $\frac{1(1+j)}{\sqrt{2}}\exp(j2\pi ft)$. The real part is the cosine function.
9. $\exp(j2\pi ft + j\theta)$ or $(\cos\theta + j\sin\theta)\exp(j2\pi ft)$. The real part is the cosine function.
10. The Fourier coefficient of the kth order term is given by $X(k/T)$.
11. For $n = 1$, the Fourier coefficient of the kth order term is given by $X(k/2T)$. For integers $n > 1$, the Fourier coefficient of the kth order term is given by $X(k/2nT)$. For $n \to \infty$, the Fourier coefficient of the kth order term is given by $X(f)$.
12. The Fourier coefficients of (a), (b), and (h) are given by the sum of the Fourier coefficients of the ascending and descending triangular waves.

The Fourier coefficients of the ascending triangular waves starting at $t = \tau_1$ and ending at $t = \tau_2$ are given by

$$A_0 = \frac{\tau_2 - \tau_1}{2T} \text{ (same for the descending triangular wave)}$$

$$A_k = \frac{2T}{\tau_2 - \tau_1}\frac{1}{4k^2\pi^2}\left\{\cos\left(2k\pi\frac{\tau_2}{T}\right) - \cos\left(2k\pi\frac{\tau_1}{T}\right)\right\} + \frac{2}{2k\pi}\sin\left(2k\pi\frac{\tau_2}{T}\right)$$

$$B_k = \frac{2T}{\tau_2 - \tau_1}\frac{1}{4k^2\pi^2}\left\{\sin\left(2k\pi\frac{\tau_2}{T}\right) - \sin\left(2k\pi\frac{\tau_1}{T}\right)\right\} - \frac{2}{2k\pi}\cos\left(2k\pi\frac{\tau_2}{T}\right)$$

$$B_k = \frac{2T}{\tau_2 - \tau_1}\frac{1}{4k^2\pi^2}\left\{\sin\left(2k\pi\frac{\tau_2}{T}\right) - \sin\left(2k\pi\frac{\tau_1}{T}\right)\right\} - \frac{2}{2k\pi}\cos\left(2k\pi\frac{\tau_2}{T}\right)$$

The Fourier coefficients of the descending triangular waves starting at $t = \tau_1$ and ending at $t = \tau_2$ are given by

$$A_k = \frac{2T}{\tau_2 - \tau_1}\frac{1}{4k^2\pi^2}\left[\cos\left(2k\pi\frac{\tau_2}{T}\right) - \cos\left(2k\pi\frac{\tau_1}{T}\right)\right] - \frac{2}{2k\pi}\sin\left(2k\pi\frac{\tau_1}{T}\right)$$

$$B_k = \frac{2T}{\tau_2 - \tau_1}\frac{1}{4k^2\pi^2}\left[\sin\left(2k\pi\frac{\tau_2}{T}\right) - \sin\left(2k\pi\frac{\tau_1}{T}\right)\right] + \frac{2}{2k\pi}\cos\left(2k\pi\frac{\tau_1}{T}\right)$$

The answers for (a), (b), and (h) will be obtained by assigning proper values to τ_1 and τ_2 in the above equations.

The answers to (i) and (j) are given by the combination of answers of (c) and (d).

(a) $A_0 = \frac{\tau}{2T}$

$$A_k = \frac{4}{T\tau}\left(\frac{T}{2\pi k}\right)^2\left\{1 - \cos\left(2\pi\frac{k}{T}\tau\right)\right\}$$

$$B_k = 0$$

(b) $A_0 = \frac{\tau_1+\tau_2}{2T}$

$$A_k = \frac{2}{T}\left(\frac{T}{2\pi k}\right)^2\left(\frac{1}{\tau_1}+\frac{1}{\tau_2}\right) - \frac{2}{T}\left(\frac{T}{2\pi k}\right)^2\left\{\frac{1}{\tau_1}\cos\left(2\pi\frac{k}{T}\tau_1\right)+\frac{1}{\tau_2}\cos\left(2\pi\frac{k}{T}\tau_2\right)\right\}$$
$$B_k = -\frac{2}{T\tau_1}\left(\frac{T}{2\pi k}\right)^2\sin\left(2\pi\frac{k}{T}\tau_1\right) - \frac{2}{T\tau_2}\left(\frac{T}{2\pi k}\right)^2\sin\left(2\pi\frac{k}{T}\tau_2\right)$$

(c) $A_0 = \frac{t_1+t_2}{T}$

$$A_k = \frac{1}{\pi k}\left\{\sin\left(2\pi\frac{k}{T}t_2\right)+\sin\left(2\pi\frac{k}{T}t_1\right)\right\}$$
$$B_k = \frac{1}{\pi k}\left\{\cos\left(2\pi\frac{k}{T}t_1\right)-\sin\left(2\pi\frac{k}{T}t_2\right)\right\}$$

(d) $A_0 = \frac{\tau_1-t_1}{2T}+\frac{t_1+t_2}{T}+\frac{\tau_2-t_2}{2T}$

$$\begin{aligned}A_k = {} & \frac{2}{T}\frac{1}{\tau_1-t_1}\left(\frac{T}{2\pi k}\right)^2\left\{\cos\left(2\pi\frac{k}{T}t_1\right)-\cos\left(2\pi\frac{k}{T}\tau_1\right)\right\}-\frac{1}{\pi k}\sin\left(2\pi\frac{k}{T}t_1\right)\\ & +\frac{1}{\pi k}\left\{\sin\left(2\pi\frac{k}{T}t_2\right)+\sin\left(2\pi\frac{k}{T}t_1\right)\right\}\\ & +\frac{2}{T}\frac{1}{\tau_2-t_2}\left(\frac{T}{2\pi k}\right)^2\left\{\cos\left(2\pi\frac{k}{T}t_2\right)-\cos\left(2\pi\frac{k}{T}\tau_2\right)\right\}-\frac{1}{\pi k}\sin\left(2\pi\frac{k}{T}t_2\right)\end{aligned}$$

$$\begin{aligned}B_k = {} & \frac{2}{T}\frac{1}{\tau_1-t_1}\left(\frac{T}{2\pi k}\right)^2\left\{\sin\left(2\pi\frac{k}{T}\tau_1\right)-\sin\left(2\pi\frac{k}{T}t_1\right)\right\}-\frac{1}{\pi k}\cos\left(2\pi\frac{k}{T}t_1\right)\\ & +\frac{1}{\pi k}\left\{\cos\left(2\pi\frac{k}{T}t_1\right)-\sin\left(2\pi\frac{k}{T}t_2\right)\right\}\\ & +\frac{2}{T}\frac{1}{\tau_2-t_2}\left(\frac{T}{2\pi k}\right)^2\left\{\sin\left(2\pi\frac{k}{T}t_2\right)-\sin\left(2\pi\frac{k}{T}\tau_2\right)\right\}+\frac{1}{\pi k}\cos\left(2\pi\frac{k}{T}t_2\right)\end{aligned}$$

(e) $A_0 = \frac{1}{\pi}\frac{\tau}{T}\,A_k = \frac{\tau}{\pi(T+k\tau)}\sin\{\frac{\pi}{2}(1+\frac{k\tau}{T})\} + \frac{\tau}{\pi(T-k\tau)}\sin\{\frac{\pi}{2}(1-\frac{k\tau}{T})\}$

(f) $A_0 = \frac{\tau}{2T}$, $A_k = \frac{\tau}{T}\frac{1}{\pi k\tau/T}\sin\left(\pi\frac{k\tau}{T}\right) + \frac{\tau/T}{2}\left\{\frac{\sin\{\pi(1+\frac{k\tau}{T})\}\pi(1+k\tau/T).}{+\frac{\sin\{\pi(1-\frac{k\tau}{T})\}}{\pi(1-k\tau/T)}}\right\}$

(g) $B_k = \tau\frac{\sin\left(\pi-\pi\frac{\tau}{T}k\right)}{\pi(T-k\tau)} - \tau\frac{\sin\left(\pi+\pi\frac{\tau}{T}k\right)}{\pi(T+k\tau)} = \frac{2T\tau}{\pi\left\{T^2-(k\tau)^2\right\}}\sin\left(\pi\frac{k\tau}{T}\right)$

(h) $A_0 = \frac{1}{T}\int_0^{+\tau} f(t)dt = \frac{\tau}{2T}$

$$A_k = \frac{2}{T}\int_{-\tau/2}^{+\tau/2}\cos(2\pi\frac{t}{\tau})\cos(2\pi\frac{k}{T}t)dt$$

Chapter 3

1. To reproduce the original waveform with the minimum sampling number.
2. The real part of the spectrum is even and the imaginary part of the spectrum is odd.
3. The sampling time should be less than $1/2F_m$.
4. The components above F_x are changed from those of the original waveform if the sampling frequency is $2F_x$ ($F_x < F_m$) (see Fig. 3.6).
5. Smoother waveform than the original.
6. If $F_c < F_m$, the spectrum above F_c of the original waveform is lost, and the waveform becomes smoother. If $2F_x - F_m > F_c > F_m$, the original spectrum is reserved and the original waveform is reconstructed. If $F_c > 2F_x - F_m$, unnecessary spectrum is left, and the original waveform is not reconstructed.
7. There is not much difference in the low frequency region but there will be a difference due to the aliasing in the region near F_m (see Fig. 3.6).
8. (1) See Sect. 3.8. You can obtain the sample values using equation below.

$$x\left(\frac{n}{2pF_x}\right) = \frac{1}{T}\sum_{k=-N/2}^{N/2-1} X_k \exp(j2\pi\frac{kn}{pN}) \qquad 0 < n < pN - 1.$$

(2) See Sect. 3.9. If p is an integer, you multiply the sample data by p by adding (p-1) number of zeros between the samples and input it to a lowpass filter with the cutoff frequency F_x.

Chapter 4

1. N complex values (which is equal to $2N$ real values)
2. $jX_n = -I_n + jR_n$
3. If the original sequence is purely real, the real part and the imaginary part of the spectrum are even and odd, respectively. If the original sequence is purely imaginary, the real part and the imaginary part of the spectrum are odd and even, respectively.
4. A complex sequence.

5. Yes. Let DFT's of x_n, y_n and $x_n + jy_n$ be $X_r(k) + jX_i(k)$, $Y_r(k) + jY_i(k)$, and $Z_r(k) + jZ_i(k)$, respectively. Since $Z_r(k) = X_r(k) - Y_i(k)$ and $Z_i(k) = X_i(k) + Y_r(k)$, and $X_r(k)$ and $Y_r(k)$ are even functions and $X_i(k)$ and $Y_i(k)$ are odd functions, $X_r(k)$ and $Y_r(k)$ are obtained by

$$X_r(k) = \{Z_r(k) + Z_r(N-k)\}/2 \qquad 0 \le k < N/2$$

and

$$Y_r(k) = \{Z_i(k) - Z_i(N-k)\}/2 \qquad 0 \le k < N/2$$

respectively.
6. Not necessary.
7. Yes. Let the DFT of real $x(n)$ be $X_r(k) + jX_i(k)$. Since $X_r(k)$ is even, and $X_i(k)$ is odd, the necessary values in the range $N/2 \le k \le N-1$ for IDFT are given by $X_r(N-k) = X_r(k)$ and $X_i(N-k) = -X_i(k)$, where $0 \le k \le N/2$.
8. Impossible.
9. Impossible. However, since the maximum frequency of the spectrum is known, the spectrum in the low frequency region can be recovered.
10. $0.8F_x$.
11. When the sampled sequences are arranged periodically, the discontinuities at the joints in (A) are smaller than those in (B). In order to represent this larger discontinuity, waveform (B) needs higher frequency components than waveform (A).
12. Follow the procedure given in Appendix 5.
13. 14 Follow the procedure used to derive DCT-II (see Sect. 4.6).

Chapter 5

1. $b = k$.
2. $0 \le b, k \le M - 1$.
3. Since $360 = 5 \times 8 \times 9$, write efficient programs for 5-, 8-, and 9-point DFTs and then draw the flow chart similar to Fig. 5.2.

Chapter 6

1. $\cos(2\pi mn/N)$
2. $-j\sin(2\pi mn/N)$
3. $-\cos(2\pi mn/N) - j0.5\sin(2\pi kn/N)$
4. Waveforms with non-integer numbers of sine and cosine waves in the N-point sample sequences.

5. A N-point DFT is a Fourier transform of an infinite periodic series of a sample sequences. If the sample sequence is of a waveform which is composed of non-integer numbers of sine and cosine components in the sequence, there occurs a discontinuity (including the discontinuity of the slope) at the joints between the sequences. The Fourier series requires many components to take care of these discontinuities as well as the original sine and cosine components.
6. See the explanation on Eq. (3.6).
7. When the waveform is periodic and the period of the waveform is k/N, where N is the size of the sequence and k is an integer ($1 \leq k \leq N$).
8. Impossible.
9. Approximately $1/T$ Hz.
10. See Sect. 6.2.
11. Impossible in the strict sense but it is possible to roughly guess, because the 11 wave sinusoidal component produces line spectra at ± 11 frequencies and the 13.5 wave sinusoidal component produces spectral distributions which have peaks at ± 13 and ± 14 frequencies.
12. See the answer 11.
13. When the sample sequence is symmetric with respect to the center of the analysis period.
14. When the sample sequence is neither symmetric nor anti-symmetric.

Chapter 7

1. Replace sine with cosine in Eq. (7.5).
2. The windows such as the Hanning window help prevent or reduce to produce spurious spectrum which is not included in the original waveform by removing abrupt changes from a finite value to zero.
3. The widths of the main lobes of the rectangular and Hanning windows are 2 times and 4 times of the reciprocal of the window length, respectively. Therefore, it becomes impossible to separate each harmonic of waveform if the number of the periods of the waveform in the window length is small.
4. See the explanations of Fig. 7.2.
5. See the explanations of Fig. 7.2.
6. Five. See Fig. 7.11.

Index

K. Kido, *Digital Fourier Analysis: Fundamentals*,
Undergraduate Lecture Notes in Physics, DOI: 10.1007/978-1-4614-9260-3,